QUANTAL DESCRIPTION OF SPINODAL INSTABILITIES IN ASYMMETRIC NUCLEAR MATTER

A THESIS SUBMITTED TO
THE GRADUATE SCHOOL OF NATURAL AND APPLIED SCIENCES
OF
MIDDLE EAST TECHNICAL UNIVERSITY

FATMA ACAR ÇAKIRCA

IN PARTIAL FULFILLMENT OF THE REQUIREMENTS
FOR
THE DEGREE OF DOCTOR OF PHILOSOPHY
IN
PHYSICS

JULY 2017

Approval of the thesis:

QUANTAL DESCRIPTION OF SPINODAL INSTABILITIES IN ASYMMETRIC NUCLEAR MATTER

submitted by **FATMA ACAR ÇAKIRCA** in partial fulfillment of the requirements for the degree of **Doctor of Philosophy in Physics Department, Middle East Technical University** by,

Prof. Dr. Gülbin Dural Ünver
Dean, Graduate School of **Natural and Applied Sciences**　　　　——————

Prof. Dr. Altuğ Özpineci
Head of Department, **Physics**　　　　——————

Prof. Dr. Osman Yılmaz
Supervisor, **Department of Physics, METU**　　　　——————

Prof. Dr. Şakir Ayık
Co-supervisor, **Physics Department, Tennessee Technological** —————
University

Examining Committee Members:

Prof. Dr. Ahmet Gökalp
Department of Physics, Bilkent University　　　　——————

Prof. Dr. Osman Yılmaz
Department of Physics, METU　　　　——————

Prof. Dr. Gürsevil Turan
Department of Physics, METU　　　　——————

Prof. Dr. Bülent Akınoğlu
Department of Physics, METU　　　　——————

Assoc. Prof. Dr. Bülent Yılmaz
Department of Physics, Ankara University　　　　——————

Date:　　　　——————

I hereby declare that all information in this document has been obtained and presented in accordance with academic rules and ethical conduct. I also declare that, as required by these rules and conduct, I have fully cited and referenced all material and results that are not original to this work.

Name, Last Name: FATMA ACAR ÇAKIRCA

Signature   :

ABSTRACT

QUANTAL DESCRIPTION OF SPINODAL INSTABILITIES IN ASYMMETRIC NUCLEAR MATTER

Acar Çakırca, Fatma

Ph.D., Department of Physics

Supervisor   : Prof. Dr. Osman Yılmaz

Co-Supervisor   : Prof. Dr. Şakir Ayık

July 2017, 138 pages

Spinodal instability mechanism and early development of density fluctuations for asymmetric hot nuclear matter produced in heavy-ion collisions are investigated in non-relativistic and relativistic stochastic mean-field approaches. In relativistic approach, a stochastic extension of the relativistic mean-field approximation based on non-linear Walecka model employed in a quantal framework. The mediator rho meson is added to the Walecka model in order to investigate the isospin dependence of the system. The growth rates of the unstable collective modes are calculated and the boundary of the spinodal region is obtained from the phase diagram for different initial conditions at different asymmetries. In general, growth of instabilities becomes slower with increasing charge asmmetry. The baryon density correlation function that includes information about the initial size of the condensing fragments is also calculated for the collective modes.

In the non-relativistic framework, a complete treatment of density correlation functions is presented by including collective modes and non-collective modes as well.

The growth of density fluctuations in the spinodal region of asymmetric nuclear matter is investigated in the stochastic mean-field approach based on Skyrme-type effective interactions. It is possible to derive nearly analytical expression for the density correlation function in the linear response limit of the stochastic mean-field approach, which involves a counter integration over the complex frequency plane. In order to provide a complete description of the correlation function, we evaluate collective and also non-collective poles in numerical calculations. These investigations will allow us to obtain more accurate information about the condensation mechanism and early evolution of liquid-gas phase transformation of nuclear matter.

Keywords: Stochastic Mean Field Approach, Spinodal Instabilities, Nuclear multi-fragmentation, Walecka Model.

ÖZ

ASİMETRİK NÜKLEER MADDENİN SPİNODAL KARARSIZLIKLARININ KUANTAL OLARAK İNCELENMESİ

Acar Çakırca, Fatma

Doktora, Fizik Bölümü

Tez Yöneticisi   : Prof. Dr. Osman Yılmaz

Ortak Tez Yöneticisi   : Prof. Dr. Şakir Ayık

Temmuz 2017 , 138 sayfa

Relativistik ve relativistik olmayan stokastik ortalama alan yaklaşımları kullanılarak ağır iyon çarpışmalarında ortaya çıkan asimetrik sıcak nükleer madde için spinodal kararsızlık mekanizmaları ve yoğunluk dalgalanmalarının erken gelişimi çalışıldı. Bu çalışmada, lineer olmayan Walecka modeline dayalı relativistik ortalama-alan modeli stokastik bir yaklaşımda kuantal bir çerçevede kullanıldı. Sistemin izospin bağımlılığını incelemek için Walecka modeline aracı parçacık olarak rho mesonu eklendi. Baskın kararsız modların büyüme oranları farklı başlangıç koşulları için değişik asimetri değerlerinde hesaplandı ve faz diyagramları kullanılarak spinodal kararsızlık bölgesinin sınırları belirlendi. Asimetri arttıkça kararsızlıkların büyümesinin yavaşladığı gözlemlendi. Ayrıca, yoğunlaşan damlacıkların ilk boyutları hakkında bilgi içeren baryon yoğunluk fonksiyonları kollektif modlar için hesaplandı.

Relativistik olmayan hesaplarda kollektif katkılara ek olarak kollektif olmayan katkılar göz önüne alınarak yoğunluk korelasyon fonksiyonlarının bütün gelişimi incelen-

miştir. Spinodal bölgedeki yoğunluk dalgalanmalarının gelişimi Skyrme tipi etkileşmeye dayanan Stokastik ortalama alan modeli kullanılarak asimetrik nükleer madde için incelendi. Bu modelin lineer limitinde yoğunluk korelasyon fonksiyonları yaklaşık analitik olarak ifade edilebilir. Bu hesaplar kompleks frekans düzleminde kontur integrali içermektedir ve korelasyon fonksiyonlarının nümerik hesapları hem kollektif hem de kollektif olmayan katkılar değerlendirilerek yapılmıştır. Bu araştırma, asimetrik nükleer maddenin yoğunlaşma mekanizması ve sıvı-gaz faz dönüşümünün ilk evreleri hakkında bilgi edinmemizi sağlayacaktır.

Anahtar Kelimeler: Stokastik Ortalama Alan Yaklaşımı, Spinodal Kararsızlıklar, Nükleer Çoklu Parçalanma, Walecka Modeli.

To my daughter, Zeynep Nil

ACKNOWLEDGMENTS

TABLE OF CONTENTS

LIST OF TABLES

TABLES

LIST OF FIGURES

FIGURES

CHAPTER 1

INTRODUCTION

The study of heavy-ion collisions provides opportunities to study the nuclear systems under extreme conditions. Due to the collisions, different states of nuclear matter far from equilibrium may produce. For instance, at high densities and temperatures, the nucleons in the nucleus dissolve into a quark-gluon plasma. At lower temperatures, which are achieved at the intermediate energy heavy-ion collisions with energies in the order of ten MeV, no such exotic states emerge but there is a possibility to observe the liquid-gas phase transition leading to the breakup of the nuclear system into many fragments which is known as multifragmentation process [1].

The possibility of the liquid-gas phase transition is predicted because of the similarity between the nuclear force and the intermolecular forces of classical Van der Waals fluid which are attractive at short range and repulsive at long and intermediate ranges [2]. The classical Van der Waals fluid enters the spinodal instability region at the critical temperatures and the liquid-gas phase transition occurs through the nature of the intermolecular forces [3]. Likewise, at normal density and zero temperature, nuclear matter behaves like Fermi liquid with specific quantum properties thus a change of phase to the gas state is expected at high temperatures. In the recent years, the experimental studies at intermediate energies have displayed the possibility for the decay of highly excited and compressed nuclear matter into many fragments. Such multifragmentation process can be considered as a signal that the nuclear system undergoes a phase transition [4, 5].

Spinodal instability mechanism provides a possible description for the cluster formation in hot nuclear matter occuring just after the heavy-ion collisions [3]. A hot and

compressed nuclear system at temperatures $10 - 15$ MeV is produced during the nuclear collisions at low bombarding energies. This system expands with the effect of thermal pressure, then cools down and enters into the mechanically unstable region at low densities below the density value of nuclear matter at equilibrium which is approximately $\rho_0 = 0.16$ fm^{-3}. This unstable region of hot nuclear matter is named as the spinodal instability region which is the domain of negative incompressibility and of mechanical instability of uniform matter. In the experimental studies based on nuclear multifragmentation, observations of charge correlations for fragments suggest that a possible origin of phase transition and the resulting multifragmentation can be explained through the density fluctuations arising due to the mechanical instabilities in the spinodal region [6, 7]. The spinodal decomposition can be defined as the growth of small density fluctuations in a short time interval around an equilibrium density, that leads to the break up of the nuclear system into an ensemble of various sized fragments [8, 9].

In this study, the spinodal instabilities of infinite asymmetric nuclear matter and the early growth of density fluctuations are investigated. Infinite nuclear systems, where the surface effects can be neglected, provide a theoretical framework for the investigation of nucleon-nucleon interactions. At finite temperatures, this idealized system provides a starting point to study not only many problems in nuclear physics but also for understanding the evolution of early universe and some astrophysical systems such as neutron stars [10]. For instance, it has been suggested that the liquid-gas mixture exists in the crusts of the neutron stars at very low temperatures [11]. The neutron-rich matter with asymmetry $I = 0.8$ at low densities and low temperatures around $T = 1$ MeV corresponds the typical conditions in the crust of the neutron stars therefore the study of spinodal instabilities in asymmetric nuclear systems has great importance in some astrophysical issues as well as nuclear collisions.

The mean field transport theories have been extensively employed to describe the reaction dynamics at low energy nuclear collisions. In order to explain the growth of density fluctuations, one requires a mean field model which includes dissipation and fluctuation mechanisms together. The time dependent Hartree Fock (TDHF) model and the semi-classical simulations based on the nuclear Boltzmann equation give a good description for the average evolution of one-body observables at the initial phase

of the collision, when the system is hot and compressed, but they become inadequate when expansion and cooling drive to the system into the instability region in which density fluctuations emerge [12, 13, 14, 15]. In the framework of these models, limited information about the spinodal instabilities can be obtained such as the growth rates of the unstable modes and the boundary of spinodal region. However, density fluctuation dynamics and condensation mechanism cannot be explained through the standard mean field theories. These models include one-body dissipation mechanism, collision of nucleons with the average nuclear potential, but the related fluctuation mechanism are not incorporated into the description [16]. In order to describe the dynamics of density fluctuations, the mean field approaches should be improved by including dissipation and the resulting fluctuation mechanisms together.

Considerable effort has been made to develop the transport approach for describing the dynamical fluctuation mechanism beyond the mean field approximation [17]. There are basically two different mechanism for density fluctuations; collisional fluctuations arising from two-body collisions and one-body mechanism or mean-field fluctuations. Fluctuations and dissipation due to the collisional mechanism are important at intermediate and high energy nuclear collisions. The extended mean-field theory, known as Boltzmann-Langevin (BL) model, provides a suitable description for density fluctuations at these energy scales [16]. However, the mean field fluctuations at the initial state are the dominant source of density fluctuations at low energies [17]. In order to understand the nuclear spinodal instabilities, extensive studies are carried out based on the semi-classical BL type stochastic transport models [3]. Nevertheless, a large amount of numerical effort is required for the simulations of BL approach and this model provides a framework only for semi-classical description. However, quantum statictical effects are important for spinodal decomposition [16, 18].

Stochastic Mean Field (SMF) approach maintains a suitable basis for description of density fluctuation dynamics at low energy nuclear systems [19]. The SMF approach includes the one-body dissipation and the resulting fluctuation mechanism in accordance with the quantal-dissipation and fluctuation relation, and furthermore the numerical simulations of this model can be performed without much effort [16, 17]. Therefore, the SMF approach provides a useful microscopic tool to describe low en-

ergy nuclear processes such as heavy-ion fusion near barrier energies, deep-inelastic collisions and spinodal decomposition of nuclear matter in which the mean-field fluctuation mechanisms play a dominant role [16].

In previous studies [9, 16, 17, 20], the spinodal dynamics and the early development of density fluctuations are investigated by employing the SMF approach in a nonrelativistic framework based on Skyrme type effective interactions, as well as in a relativistic framework based on Walecka-type effective field theory in the semi-classical and quantal descriptions. In these studies, the early growth of density fluctuations is calculated in the linear response regime of the SMF approach. For nuclear matter, linearizing the equation of motion around a suitable initial state in the spinodal region and using the one-sided Fourier transformation method, it is possible to carry out nearly analytical treatment for the density correlation function in the linear response regime. In these studies, only unstable collective modes are taken into account in the calculations of correlation functions. As indicated in Ref. [21], it is nesessary to include the effect of noncollective poles as well for a complete description of density correlation functions. In this study, our aim is to calculate the correlation functions of density fluctuations exactly by including collective as well as non-collective poles for charge asymmetric nuclear matter. In the first part of this thesis, we investigate the spinodal instabilities and the early growth of density fluctuations in a semi-classical limit of the SMF approach in non-relativistic framework by including the effect of non-collective poles.

In the second part of the thesis, early development of spinodal instabilities and density correlation functions are studied within the stochastic extention of the Walecka-type relativistic mean-field including rho mesons. In the previous investigations [9, 20], the symmetric nuclear matter is studied through the standard Walecka model with point couplings and with the extensions of the Walecka model including non-linear self interaction terms of the scalar meson and density dependent couplings in the semi-classical approximation. Furthermore, in a recent study, a quantal investigation is presented for symmetric nuclear matter to examine the quantal effects on the early growth of spinodal instabilities [17]. However, all these studies are performed for symmetric nuclear matter. On the other hand, recent investigations on collisions of radioactive nuclei and on formation and structure of neutron stars have attracted at-

tention to the charged asymmetric nuclear matter [8]. In this work, we also study the effect of asymmetry on spinodal instabilities of nuclear matter at subsaturation densities. The early development of spinodal instabilities and baryon density correlation functions are investigated for asymmetric nuclear matter by employing the stochastic extension of the relativistic mean field theory in a quantal framework. The isospin asymmetry is included into the system with the addition of rho mesons coupled to baryon fields of Lagrangian density of nonlinear Walecka model.

In chapter 2, we present a brief description of TDHF theory and the stochastic mean-field approach, and then the nearly analytical description of density fluctuations including both collective and noncollective poles is presented for asymmetric nuclear matter in non-relativistic approach. The numerical results of spinodal instabilities are introduced at zero temperature and finite temperatures in chapter 3. We investigate the growth rates of unstable modes and the boundary of the spinodal region for different asymmetry values. Moreover, density correlation functions and the spectral intensity of density correlations are also demonstrated. In chapter 4, the nonlinear Walecka model including rho mesons is introduced and then by employing the stochastic extension of the relativistic mean field approach we develop a linear response treatment for spinodal instabilities in the quantal framework. The results of numerical calculations are demonstrated for early growth of baryon density correlation functions for different initial conditions in different charge-asymmetric nuclear matter in chapter 5. Finally, the conclusion is given in chapter 6.

CHAPTER 2

EARLY GROWTH OF DENSITY FLUCTUATIONS WITHIN A NON-RELATIVISTIC APPROACH

2.1 Mean-field Approach and TDHF

The study of nuclear matter, the theoretical uniform infinite system of nucleons, is an important area of nuclear physics since it forms a starting point for describing more complicated and realistic phenomena in nuclear physics such as the properties of finite nuclei and the dynamics of heavy-ion collisions. The nuclear matter is a many body system of strongly interacting nucleons (neutrons and protons). In describing the many-body nuclear system, the mean field approximations are widely used to describe the many static and dynamical aspects. According to the mean field description, the complex many body problem is replaced with the effective one-body problem by considering an ensemble of independent particles in a self-consistent mean-field [22]. In these approximations, two body collisions are neglected and the nucleons move in a self-consistent potential produced by all other nucleons. The mean field model also known as the time dependent Hartree-Fock (TDHF) has been used to describe the nuclear collision dynamics at low energies (below 10 MeV per nucleon) and also other many body systems [13, 14].

In the mean field description of a many body system, the time-dependent wave function, which is an anti-symmetric wave function, is taken to be a Slater determinant constructed with a number of time dependent single-particle wave functions $\phi_i(\vec{r}, t)$

$$\Phi(\vec{r}_1, ..., \vec{r}_N, t) = \frac{1}{\sqrt{N!}} det \left\{ \phi_i(\vec{r}_j, t) \right\}$$ (2.1)

The single particle wave functions are determined by the time-dependent Hartree-Fock equations with proper initial conditions according to [19, 23]

$$i\hbar\frac{\partial}{\partial t}\phi_j(\vec{r}, t) = h(\rho)\phi_j(\vec{r}, t) , \qquad (2.2)$$

here $h(\rho)$ denotes the Hamiltonian of self-consistent mean-field. However, in many situations, the mean-field approximation is expressed by the single particle density matrix $\rho(\vec{r}, \vec{r}', t)$ instead of the single particle wave functions. The single particle density matrix is defined as

$$\rho(\vec{r}, \vec{r}', t) = \sum_j \phi_j^*(\vec{r}, t)n_j\phi_j(\vec{r}', t) . \qquad (2.3)$$

Here n_j denotes the occupation factor for the single particle states and it is equal to one for occupied and zero for unoccupied states at zero temperature. In the mean field approximation, the single-particle density matrix evolves according to the transport equation

$$i\hbar\frac{\partial}{\partial t}\rho(t) = [h(\rho), \rho(t)] \qquad (2.4)$$

which is known as TDHF equation.

The standard mean-field approach provides a useful description for the average behavior of collective motion of nuclear matter at low energy reactions by including one-body dissipation mechanism. However, it becomes inadequate to describe the fluctuation dynamics of one-body observables [13]. Therefore, we need an approximation beyond the standard mean-field approach to include the fluctuation mechanism. The stochastic mean-field approach (SMF) provides a powerful framework to describe the nuclear collective motion by including one-body dissipation and fluctuation mechanisms [19].

2.2 Stochastic Mean-Field Approach

TDHF maintains a deterministic description for evolution of the single particle density matrix starting from a well-defined initial state and leading to a well-defined final state [14]. We can include the fluctuation mechanism into dynamics by considering the superposition of determinantal wave functions rather than the single Slater determinant description which used in the standard TDHF. In the stochastic mean-field

description, an ensemble of single-particle density matrices as superposition of Slater determinants is obtained by considering only the initial correlations [16, 22]. This way, the zero-point quantal and thermal fluctuations at the initial state are considered in a stochastic manner [14].

The SMF approach introduces a microscopic description for density fluctuations dynamics at low energy nuclear collisions. In the framework of this approach, one can calculate not only the mean value of an observable but also the probability distribution of the observables. In the SMF method, the source of the stochasticity stems from the initial correlations and therefore the initial density fluctuations are simulated by using an ensemble of density matrices instead of a single-particle density matrix [19].

In order to improve a stochastic description, it is needed to determine enough number of occupied and unoccupied single particle states. A member of single particle density matrix represented by the event label λ is written in the form

$$\hat{\rho}_a^\lambda(\vec{r}, \vec{r}', t) = \sum_{ij} \phi_i^*(\vec{r}, t; \lambda) \langle i | \rho_a^\lambda(0) | j \rangle \phi_j(\vec{r}', t; \lambda) . \tag{2.5}$$

Here the label a denotes the proton and neutron species and $\langle i | \rho_a^\lambda(0) | j \rangle$ are the time independent elements of density matrix defined by the initial conditions. According to the basic assumption of this approach, each element of density matrix is assumed to be a Gaussian random number specified by an average value $\overline{\langle i | \rho_a^\lambda(0) | j \rangle} = \delta_{ij} n_a(i)$ and a variance

$$\overline{\langle i | \delta\rho_a^\lambda(0) | j \rangle \langle j' | \delta\rho_b^\lambda(0) | i' \rangle} = \frac{1}{2} \delta_{ab} \delta_{ii'} \delta_{jj'} \{ n_a(i)[1 - n_a(j)] + n_a(j)[1 - n_a(i)] \}. \tag{2.6}$$

In the above expression $\langle i | \delta\rho_a^\lambda(0) | j \rangle$ denotes the fluctuating parts of the initial density matrix and $n_a(i)$ are the average occupation numbers which are one for occupied and zero for unoccupied states at zero temperature, and at finite temperature they are determined by the Fermi-Dirac distribution $n_a(j) = 1/[exp(\varepsilon_j - \mu_a)/T + 1]$, here μ_a is the chemical potential and ε_j is the Fermi energy at the equilibrium density.

In this approach, different from the standard TDHF, the time dependent single particle wave functions of nucleons are evolved by their own self-consistent mean field for each event according to

$$i\hbar \frac{\partial}{\partial t} \phi_j^a(\vec{r}, t; \lambda) = h_a^\lambda \phi_j^a(\vec{r}, t; \lambda) \tag{2.7}$$

where $h_a^\lambda = p^2/2m_a + U_a\left(\rho_p^\lambda, \rho_n^\lambda\right)$ indicates the self-consistent mean-field Hamiltonian and it depends on the proton and neutron local densities $\rho_a^\lambda(\vec{r}, t)$. Similar to Eq. (2.4), the time evolution of the SMF approach in terms of single particle density matrices of nucleons are given as

$$i\hbar\frac{\partial}{\partial t}\hat{\rho}_a^\lambda(t) = [h_a^\lambda(t), \hat{\rho}_a^\lambda(t)] \tag{2.8}$$

where the label $a = p\uparrow, p\downarrow, n\uparrow, n\downarrow$ represents the spin-isospin quantum numbers, and $h_a^\lambda(t)$ is the mean-field Hamiltonian in the event.

The one-body dissipation and fluctuation mechanism is incorporated into the collision dynamics within a stochastic manner by including the initial correlations in the SMF approach. In this thesis, the early growth of density fluctuations is studied within the framework of this approach in the spinodal region.

2.3 Skyrme Interaction

For nuclear matter, the Skyrme potential, which is zero-range, density and momentum dependent, is widely used effective potential in Hartree-Fock calculations. The Hamiltonian density for a system can be expressed as an algebraic function of the nuclear and kinetic energy densities by considering the simple structure of the Skyrme force [24]. In its original form Skyrme's interaction can be written as a potential,

$$V = \sum_{i<j} V(i,j) + \sum_{i<j<k} V(i,j,k) \tag{2.9}$$

with two-body and three-body parts [23]. The range of the nuclear force is rather short and therefore the nuclear potential is written as a zero-range force. Such forces are useful since they are simple and describe many nuclear properties quite well. In the short-range limit, the Skyrme interaction consists of zero-range force with momentum dependent two-body force plus the density dependent two-body force. We have performed the numerical calculations with an effective two-body Skyrme interaction given as [25],

$$V_{1,2} = t_0(1 + x_0 P^\sigma)\delta(\vec{r}_1 - \vec{r}_2) + \frac{1}{6}t_3\left(1 + x_3 P^\sigma\right)\left[\rho\left(\frac{\vec{r}_1 - \vec{r}_2}{2}\right)\right]^\alpha \delta(\vec{r}_1 - \vec{r}_2)$$
$$\tag{2.10}$$

where P^σ is the spin exchange operator and the parameters $t_0 = -2973\ \mathrm{MeV} \cdot \mathrm{fm}^3$, $t_3 = 19034\ \mathrm{MeV} \cdot \mathrm{fm}^{3(\alpha+1)}$, $x_0 = 0.025$, $x_3 = 0$ and $\alpha = 1/6$ give the correct values for saturation density and binding energy of symmetric nuclear matter. The first term is for the long-range attraction ($t_0 < 0$) while the second term provides the short range repulsion ($t_3 > 0$) and this maintains the saturation at a certain density ρ_0 [3].

According to the Skyrme interaction given in Eq. (2.10), the potential energy density is expressed as [8, 25],

$$H_{pot}(\rho_n, \rho_p) = \frac{A}{2} \frac{\rho^2}{\rho_0} + \frac{B}{\alpha+2} \frac{\rho^{\alpha+2}}{\rho_0^{\alpha+1}} + \frac{C(\rho)}{2} \frac{\rho'^2}{\rho_0} + \frac{D}{2}(\vec{\nabla}\rho)^2 - \frac{D'}{2}(\vec{\nabla}\rho')^2 \quad (2.11)$$

where $\rho = \rho_n + \rho_p$ and $\rho' = \rho_n - \rho_p$ are respectively the total and relative densities, and $\rho_0 = 0.16\,fm^{-3}$ is the saturation density of nuclear matter. The coefficients A, B and C are connected to the Skyrme parameters as follows [25]: $A = \frac{3}{4}t_0\rho_0$, $B = \frac{\alpha+2}{16}t_3\rho_0^{\alpha+1}$ and $C(\rho) = -\rho_0\left[\frac{t_0}{2}(x_0 + 1/2) + \frac{t_3}{12}(x_3 + 1/2)\rho^\alpha\right]$.

Consequently, the mean-field potential for neutron and proton is given by

$$U_a(\rho_n, \rho_p) = \frac{\delta H_{pot}(\rho_n, \rho_p)}{\delta \rho_a}$$
$$= A\left(\frac{\rho}{\rho_0}\right) + B\left(\frac{\rho}{\rho_0}\right)^{\alpha+1} + C\left(\frac{\rho'}{\rho_0}\right)\tau_a + \frac{1}{2}\frac{dC}{d\rho}\frac{\rho'^2}{\rho_0} - D\Delta\rho + D'\Delta\rho'\tau_a$$
$$(2.12)$$

where $\tau_a = +1$ for neutrons and $\tau_a = -1$ for protons. The numerical parameters $A = -356.8$ MeV, $B = +303.9$ MeV and $D = +130.0$ MeV fm^5 are fitted to the saturation properties of nuclear matter (the binding energy $\varepsilon_0 = 15.7$ MeV per nucleon at saturation density and compressibility coefficient $K = 201$ MeV) and the surface energy coefficient in the Weizsacker mass formula $a_{surf} = 18.6$ MeV. The numerical value of parameter $D' = +34$ MeV fm^5 is close to the value given by the SkM^* interaction [26]. The symmetry energy coefficient is equal to $C(\rho) = C_1 - C_2(\rho/\rho_0)^\alpha$ with $C_1 = +124.9\ MeV$ and $C_2 = +93.5\ MeV$. At saturation density, the coefficient $C(\rho_0) = 31.4$ gives the symmetry energy coefficient in the Weizsacker mass formula as $a_{sym} = \varepsilon_F(\rho_0)/3 + C(\rho_0)/2 = 28.0\ MeV$ where $\varepsilon_F(\rho_0) = 36.9$ MeV is the Fermi energy for the symmetric system at $\rho = \rho_0$.

Moreover, for symmetric nuclear matter the Eq. (2.12) reduces to

$$U(\rho) = A\left(\frac{\rho}{\rho 0}\right) + B\left(\frac{\rho}{\rho 0}\right)^{\alpha+1} - D\Delta\rho \,. \tag{2.13}$$

2.4 Early Growth of Density Fluctuations

2.4.1 Dispersion Relation

In this part of the thesis, our aim is to investigate the early growth of density fluctuations in spinodal instability region for asymmetric nuclear matter therefore it is sufficient to linearize Eq. (2.8) around a uniform initial state, $\hat{\rho}_a^0$. A perturbation $\delta\hat{\rho}_a^\lambda(t) = \hat{\rho}_a^\lambda(t) - \hat{\rho}_a^0$ of the single particle density matrix away from the initial state are determined by the linearized TDHF equations which are given for fluctuations of neutron and proton density matrices as

$$i\hbar\frac{\partial}{\partial t}\delta\hat{\rho}_a^\lambda(t) = \left[h_a, \delta\hat{\rho}_a^\lambda(t)\right] + \left[\delta U_a^\lambda(t), \hat{\rho}_a^0\right] \tag{2.14}$$

where h_a denotes the mean field Hamiltonian at the initial state and δU_a^λ is the fluctuating part of the mean-field in the event. This response treatment maintains a quantal description for the early development of spinodal instabilities for nuclear matter [3]. We are interested in investigating the growth of spinodal instabilities in nuclear matter around a uniform initial state. In this case, we assume that the mean field Hamiltonian is uniform in the equilibrium state and the single-particle density matrix is diagonal in momentum representation at the equilibrium $\langle\vec{p}|\hat{\rho}_0|\vec{p}'\rangle = \delta(\vec{p} - \vec{p}')\rho_0(\vec{p})$ where $\rho_0(\vec{p})$ is a finite temperature Fermi-Dirac factor. This way, it is possible to provide an almost analytical treatment for the density fluctuations by using the plane wave representations. In the plane wave representation, the linearized TDHF equation can be expressed as

$$i\hbar\frac{\partial}{\partial t}\langle\vec{p_1}|\delta\hat{\rho}_a^\lambda(t)|\vec{p_2}\rangle = \langle\vec{p_1}|\left[h_a, \delta\hat{\rho}_a^\lambda(t)\right]|\vec{p_2}\rangle + \langle\vec{p_1}|\left[\delta U_a^\lambda(t), \hat{\rho}_a^0\right]|\vec{p_2}\rangle \tag{2.15}$$

where

$$
\begin{aligned}
\langle\vec{p_1}|\left[h_a, \delta\hat{\rho}_a^\lambda(t)\right]|\vec{p_2}\rangle &= \langle\vec{p_1}|h_a\delta\hat{\rho}_a^\lambda(t)|\vec{p_2}\rangle - \langle\vec{p_1}|\delta\hat{\rho}_a^\lambda(t)h_a|\vec{p_2}\rangle \\
&= [\varepsilon_a(\vec{p_1}) - \varepsilon_a(\vec{p_2})]\langle\vec{p_1}|\delta\hat{\rho}_a^\lambda(t)|\vec{p_2}\rangle \tag{2.16}
\end{aligned}
$$

and

$$
\begin{aligned}
\langle \vec{p_1}| \left[\delta U_a^\lambda(t), \hat{\rho}_a^0 \right] |\vec{p_2}\rangle &= \langle \vec{p_1}|\delta U_a^\lambda(t) \int d\vec{p'}_2 |\vec{p'}_2\rangle\langle \vec{p'}_2|\hat{\rho}_a^0|\vec{p_2}\rangle \\
&\quad - \langle \vec{p_1}|\hat{\rho}_a^0 \int d\vec{p'}_1 |\vec{p'}_1\rangle\langle \vec{p'}_1|\delta U_a^\lambda(t)|\vec{p_2}\rangle \\
&= \int d\vec{p'}_2 \langle \vec{p_1}|\delta U_a^\lambda(t)|\vec{p'}_2\rangle f_0^a(\vec{p'}_2)\delta(\vec{p_2} - \vec{p'}_2) \\
&\quad - \int d\vec{p'}_1 \langle \vec{p'}_1|\delta U_a^\lambda(t)|\vec{p_2}\rangle f_0^a(\vec{p'}_1)\delta(\vec{p_1} - \vec{p'}_1) \, .
\end{aligned}
$$

(2.17)

Then, the linear response equation is found as

$$
\begin{aligned}
i\hbar \frac{\partial}{\partial t}\langle \vec{p_1}|\delta\hat{\rho}_a^\lambda(t)|\vec{p_2}\rangle &= \left[\varepsilon_a(\vec{p_1}) - \varepsilon_a(\vec{p_2}) \right] \langle \vec{p_1}|\delta\hat{\rho}_a^\lambda(t)|\vec{p_2}\rangle \\
&\quad - \left[f_0^a(\vec{p_1}) - f_0^a(\vec{p_2}) \right] \langle \vec{p_1}|\delta U_a^\lambda(t)|\vec{p_2}\rangle .
\end{aligned}
$$

(2.18)

According to the basic assumption of the SMF approach, the elements of the initial density matrix are uncorrelated Gaussian random numbers with zero mean values and with well-defined variances. In the plane wave representation, their variances are given by [16, 27, 28],

$$
\begin{aligned}
&\overline{\langle \vec{p} + \hbar\vec{k}/2|\delta\hat{\rho}_{a,s}^\lambda(0)|\vec{p} - \hbar\vec{k}/2\rangle\langle \vec{p'} - \hbar\vec{k'}/2|\delta\hat{\rho}_{b,s'}^\lambda(0)|\vec{p'} + \hbar\vec{k'}/2\rangle} \\
&= \delta_{ab}\delta_{ss'}(2\pi\hbar)^3(2\pi)^3\delta(\vec{p} - \vec{p'})\delta(\vec{k} - \vec{k'})f_0^a(\vec{p} + \hbar\vec{k}/2)\left(1 - f_0^a(\vec{p} - \hbar\vec{k}/2) \right) .
\end{aligned}
$$

(2.19)

In this expression, the overline represents the ensemble average and $\delta_{ab}\delta_{ss'}$ reflects the assumption that local density fluctuations are uncorrelated in the initial state. Here $f_0^a(\vec{p})$ is the Fermi-Dirac distribution function, $f_0^a(\vec{p}) = \frac{1}{e^{(\varepsilon - \mu_a)/T} + 1}$, for finite temperatures. At zero temperature, it is zero for unoccupied states and one for occupied states.

We can solve the linear response Eq. (2.18) by employing the method of one-sided Fourier transformation in time [29, 30],

$$
\delta\tilde{\rho}_a^\lambda(\vec{k}, \omega) = \int_0^\infty dt\, e^{i\omega t}\delta\rho_a^\lambda(\vec{k}, t) \, .
$$

(2.20)

After transformation, one-sided Fourier transformed form of the local density fluctuations becomes

$$
\int_0^\infty dt\, e^{i\omega t}\frac{\partial}{\partial t}\langle \vec{p_1}|\delta\tilde{\rho}_a^\lambda(\vec{k}, t)|\vec{p_2}\rangle = -\langle \vec{p_1}|\delta\hat{\rho}_a(0)|\vec{p_2}\rangle - i\omega\langle \vec{p_1}|\delta\tilde{\rho}_a^\lambda(\vec{k}, \omega)|\vec{p_2}\rangle \, .
$$

(2.21)

13

Here $\langle \vec{p_1}|\delta\hat{\rho}_a(0)|\vec{p_2}\rangle$ is the source term arising from the initial conditions. We introduce the Fourier transform of the mean-field potential in time as

$$\int_0^\infty dt e^{i\omega t} \langle \vec{p_1}|\delta U_a^\lambda(t)|\vec{p_2}\rangle = \langle \vec{p_1}|\delta U_a^\lambda(\omega)|\vec{p_2}\rangle . \tag{2.22}$$

Finally, the linearized TDHF equation can be written as follows

$$\langle \vec{p_1}|\delta\tilde{\rho}_a^\lambda(\vec{k},\omega)|\vec{p_2}\rangle = -\frac{f_0^a(\vec{p_1}) - f_0^a(\vec{p_2})}{\hbar\omega - \varepsilon_a(\vec{p_1}) + \varepsilon(\vec{p_2})}\langle \vec{p_1}|\delta U_a^\lambda(\omega)|\vec{p_2}\rangle + i\hbar\frac{\langle \vec{p_1}|\delta\hat{\rho}_a(0)|\vec{p_2}\rangle}{\hbar\omega - \varepsilon_a(\vec{p_1}) + \varepsilon(\vec{p_2})}. \tag{2.23}$$

In this equation, we use the momentum vectors as $\vec{p_1} = \vec{p} + \hbar\vec{k}/2$ and $\vec{p_2} = \vec{p} - \hbar\vec{k}/2$ and introduce the space Fourier transform of nucleon density fluctuations $\delta\rho_a^\lambda(\vec{k},t)$ which is related to the fluctuations of the density matrix according to

$$\delta\rho_a^\lambda(\vec{k},t) = \sum_s \int \frac{d^3p}{(2\pi\hbar)^3} \langle \vec{p} + \hbar\vec{k}/2|\delta\hat{\rho}_{a,s}^\lambda(t)|\vec{p} - \hbar\vec{k}/2\rangle \tag{2.24}$$

where the summation indicates the sum over the spin quantum numbers $s = \uparrow, \downarrow$. Finally, we obtain a coupled algebraic equation for the Fourier transform of the local proton and neutron densities $\delta\rho_a^\lambda(\vec{k},\omega)$:

$$\left(\begin{array}{c} \left[1 + F_0^{nn}\chi_n(\vec{k},\omega)\right]\delta\rho_n^\lambda(\vec{k},\omega) + F_0^{np}\chi_n(\vec{k},\omega)\delta\rho_p^\lambda(\vec{k},\omega) \\ \left[1 + F_0^{pp}\chi_p(\vec{k},\omega)\right]\delta\rho_p^\lambda(\vec{k},\omega) + F_0^{pn}\chi_p(\vec{k},\omega)\delta\rho_n^\lambda(\vec{k},\omega) \end{array} \right) = i \left(\begin{array}{c} S_n^\lambda(\vec{k},\omega) \\ S_p^\lambda(\vec{k},\omega) \end{array} \right). \tag{2.25}$$

The details for the derivation of Eq. (2.25) are presented in Appendix A. In deriving these coupled equations, we consider that the mean-field potential depends only on the local nucleon densities, $U_a^\lambda = U(\rho_p^\lambda, \rho_n^\lambda)$. In the above equation, F_0^{ab} denotes the zeroth-order Landau parameters which defined as the derivative of the mean-field potential energy with respect to the proton and neutron densities evaluated at the initial state, $F_0^{ab} = (\partial U_b/\partial\rho_a)_0$ and the integral $\chi_a(\vec{k},\omega)$ is the Linhard function for protons and neutrons

$$\chi_a(\vec{k},\omega) = -2 \int \frac{d^3p}{(2\pi\hbar)^3} \frac{f_0^a(\vec{p} - \hbar\vec{k}/2) - f_0^a(\vec{p} + \hbar\vec{k}/2)}{\hbar\omega - \vec{p}\cdot\hbar\vec{k}/m}. \tag{2.26}$$

Here the factor 2 comes from spin summation. The source term $S_a^\lambda(\vec{k},\omega)$ is determined by the elements of the initial density fluctuation matrix $\delta\hat{\rho}_{a,s}^\lambda(0)$ in spin-isospin channel as

$$S_a^\lambda(\vec{k},\omega) = \sum_s \hbar \int \frac{d^3p}{(2\pi\hbar)^3} \frac{\langle \vec{p} + \hbar\vec{k}/2|\delta\hat{\rho}_{a,s}^\lambda(0)|\vec{p} - \hbar\vec{k}/2\rangle}{\hbar\omega - \vec{p}\cdot\hbar\vec{k}/m}. \tag{2.27}$$

14

The solution of the coupled algebraic equations in Eq. (2.25) for the Fourier transform of the local density fluctuations are given by

$$\delta\rho_a^\lambda(\vec{k},\omega) = \frac{i}{\varepsilon(\vec{k},\omega)} G_a^\lambda(\vec{k},\omega). \tag{2.28}$$

The quantity $G_a^\lambda(\vec{k},\omega)$ is given for neutrons and protons as

$$\begin{pmatrix} G_n^\lambda(\vec{k},\omega) \\ G_p^\lambda(\vec{k},\omega) \end{pmatrix} = \begin{pmatrix} \left[1 + F_0^{pp}\chi_p(\vec{k},\omega)\right] S_n^\lambda(\vec{k},\omega) - F_0^{np}\chi_n(\vec{k},\omega)S_p^\lambda(\vec{k},\omega) \\ \left[1 + F_0^{nn}\chi_n(\vec{k},\omega)\right] S_p^\lambda(\vec{k},\omega) - F_0^{pn}\chi_p(\vec{k},\omega)S_n^\lambda(\vec{k},\omega) \end{pmatrix},$$
$$\tag{2.29}$$

and $\varepsilon(\vec{k},\omega)$ denotes the susceptibility

$$\varepsilon(\vec{k},\omega) = 1 + F_0^{nn}\chi_n(\vec{k},\omega) + F_0^{pp}\chi_p(\vec{k},\omega) + [F_0^{nn}F_0^{pp} - F_0^{np}F_0^{pn}]\chi_n(\vec{k},\omega)\chi_p(\vec{k},\omega). \tag{2.30}$$

When $\varepsilon(\vec{k},\omega) = 0$, this equation indicates a dispersion relation for the system. In the infinite nuclear matter, collective modes are determined by the wave number. The solution of the dispersion relation gives the characteristic frequencies for the corresponding wave numbers. The frequencies are real in the stable region ($\rho > \rho_{critical}$) and imaginary for the unstable modes ($\rho < \rho_{critical}$). In the following chapter, the growth rates of the unstable modes will be presented as a function of wave number.

2.4.2 Growth of Density Fluctuations

In this part, the time-dependency of density fluctuations is determined by taking the inverse Fourier transform of Eq. (2.28) in time according to the method of one-sided Fourier transformation. The inverse transformation is expressed as a contour integral in the complex ω-plane as [27, 28],

$$\delta\rho_a^\lambda(\vec{k},t) = i \int_{-\infty+i\sigma}^{+\infty+i\sigma} \frac{d\omega}{2\pi} \frac{G_a^\lambda(\vec{k},\omega)}{\varepsilon(\vec{k},\omega)} e^{-i\omega t}, \tag{2.31}$$

here the integration path passes above all singularities as shown in Fig.1 by line C1. This integral can be calculated with the help of the residue theorem by closing the contour in a suitable manner shown in Fig.1. The solutions of the dispersion relation, $\varepsilon(\vec{k},\omega) = 0$, gives the collective poles of the integral. In the spinodal region, we will have two solutions with imaginary frequencies which is given by $\omega = \pm i\Gamma_k$. The collective poles make the dominant contribution to the growth of density fluctuations.

15

However, Bozek pointed out that [21], collective poles are not the only singularities of this integral so the description of the growth of density fluctuations is not fully represented. In fact, the collective poles alone do not even satisfy the initial conditions. Therefore, the effect of non-collective poles should be considered in addition to the collective ones. By calculating the angular integral in the Lindhard function given by Eq. (2.27), it is possible to see that, there is a cut singularity of the integrand in Eq. (2.31) along real axis in the complex ω-plane. Moreover, $G_a(\vec{k}, \omega)$ may also have singularities on the real axis [21]. The non-collective poles appear here as a cut singularity. Since the integrand in complex ω-plane is multivalued, the entire real ω-axis is a brunch cut. To calculate the integral in Eq. (2.31), we choose the contour C, as shown in Fig.1. We exclude the real ω-axis by drawing the contour from $+\infty$ to the origin just above the real ω-axis, and after jumping from the first Riemann sheet to the second at the origin, by drawing contour just below the real ω-axis from origin to $+\infty$. Contour is completed with a large semi-circle and by jumping from the second Riemann surface to the first one at origin, as shown in figure. As a result, we find the integral which can be expressed as [27]

$$\delta \rho_a^\lambda(\vec{k}, t) = \delta \rho_a^\lambda(P; \vec{k}, t) + \delta \rho_a^\lambda(C; \vec{k}, t), \qquad (2.32)$$

where the first term is the pole (P) contribution

$$\delta \rho_a^\lambda(P; \vec{k}, t) = -\sum_{\pm} \frac{G_a^\lambda(\vec{k}, \pm i\Gamma_k)}{\partial \varepsilon(\vec{k}, \omega)/\partial \omega|_{\omega = \pm i\Gamma_k}} e^{\pm \Gamma_k t} \qquad (2.33)$$

and the second term is the cut (C) contribution that is given by

$$\delta \rho_a^\lambda(C; \vec{k}, t) = -i \int_{-\infty}^{+\infty} \frac{d\omega}{2\pi} \left[\frac{G_a^\lambda(\vec{k}, \omega + i\eta)}{\varepsilon(\vec{k}, \omega + i\eta)} - \frac{G_a^\lambda(\vec{k}, \omega - i\eta)}{\varepsilon(\vec{k}, \omega - i\eta)} \right] e^{-i\omega t}. \qquad (2.34)$$

We can obtain the information about the boundary of spinodal region and the growth rates of the unstable modes in the spinodal region by using the dispersion relation. However, our aim is to understand the dynamical evolution of the unstable nuclear system in the instability region which is determined from the equal time correlation function of density fluctuations. Actually, the density correlation function exhibits initial times of the dynamics of liquid-gas phase transformation of nuclear matter. In the Stochastic mean-field approach, the equal time density correlation function
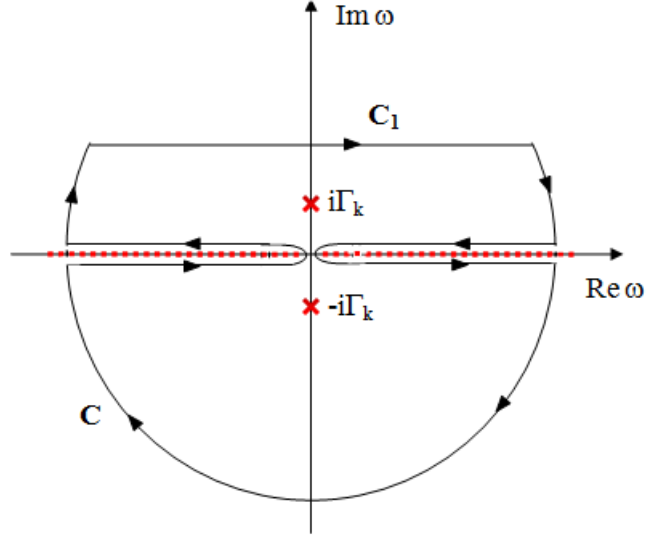
Figure 2.1: The contour chosen to calculate the integral in Eq. (2.31). Crosses $\pm i\Gamma_k$ indicate the collective poles of the integrand, and dotted line along the entire real ω-axis is the branch cut of the integrand.

$\sigma_{ab}(|\vec{r} - \vec{r'}|, t)$ is defined in terms of the density fluctuations as follows

$$\sigma_{ab}(|\vec{r} - \vec{r'}|, t) = \overline{\delta\rho_a^\lambda(\vec{r}, t)\delta\rho_b^\lambda(\vec{r'}, t)} = \int \frac{d^3k}{(2\pi)^3} e^{i\vec{k}\cdot(\vec{r}-\vec{r'})} \sigma_{ab}(\vec{k}, t). \qquad (2.35)$$

Here $|\vec{r} - \vec{r'}|$ is the distance between two space locations and a, b represent the neutron or proton. The local nucleon density fluctuations $\delta\rho_a^\lambda(\vec{r}, t)$ are obtained from the Fourier transformation of $\delta\rho_a^\lambda(\vec{k}, t)$, similarly, the equal time correlation functions $\sigma_{ab}(|\vec{r} - \vec{r'}|, t)$ are determined by the Fourier transform of the spectral intensity functions $\sigma_{ab}(\vec{k}, t)$. In the SMF approach, the spectral intensity of density correlations is related to the variance of the Fourier transform of density fluctuations according to

$$\sigma_{ab}(\vec{k}, t)(2\pi)^3\delta(\vec{k} - \vec{k'}) = \overline{\delta\rho_a^\lambda(\vec{k}, t)\delta\rho_b^\lambda(-\vec{k'}, t)}. \qquad (2.36)$$

In the above expression, the bar represents the average taken over the ensemble produced from the distribution of the initial fluctuations. We calculate the spectral intensity function by using the result in Eq. (2.32) and evaluating the ensemble average as

17

follows

$$\overline{\delta\rho_a^\lambda(\vec{k},t)\delta\rho_b^\lambda(-\vec{k}',t)} =$$
$$\overline{\left[\delta\rho_a^\lambda(P;\vec{k},t) + \delta\rho_a^\lambda(C;\vec{k},t)\right]\left[\delta\rho_b^\lambda(P;-\vec{k}',t) + \delta\rho_b^\lambda(C;-\vec{k}',t)\right]} =$$
$$\overline{\delta\rho_a^\lambda(P;\vec{k},t) + \delta\rho_b^\lambda(P;-\vec{k}',t)} + \overline{\delta\rho_a^\lambda(C;\vec{k},t) + \delta\rho_b^\lambda(C;-\vec{k}',t)}$$
$$+ \overline{\delta\rho_a^\lambda(P;\vec{k},t) + \delta\rho_b^\lambda(C;-\vec{k}',t)} + \overline{\delta\rho_a^\lambda(C;\vec{k},t) + \delta\rho_b^\lambda(P;-\vec{k}',t)}.$$

$$(2.37)$$

Here the last two terms are equal each other. As a result, the spectral intensity is expressed as

$$\sigma_{ab}(\vec{k},t) = \sigma_{ab}(PP;\vec{k},t) + 2\sigma_{ab}(PC;\vec{k},t) + \sigma_{ab}(CC;\vec{k},t), \qquad (2.38)$$

where the first and last term are due to only pole and only cut parts of the spectral intensity respectively and the middle term denotes the cross contribution. The spectral intensity function for neutron and proton can be calculated separately (by taking $a,b = n$ or $a,b = p$). Similarly, the total spectral intensity is obtained by summing over isospin components:

$$\sigma(\vec{k},t) = \sigma_{pp}(\vec{k},t) + 2\sigma_{pn}(\vec{k},t) + \sigma_{nn}(\vec{k},t). \qquad (2.39)$$

In the above expression, each isospin component of the spectral intensity includes both pole and cut contributions given in Eq. (2.38). The expression for the total correlation function of density fluctuations $\sigma(|\vec{r}-\vec{r}'|,t) = \sigma_{pp}(|\vec{r}-\vec{r}'|,t) + \sigma_{nn}(|\vec{r}-\vec{r}'|,t) + 2\sigma_{pn}(|\vec{r}-\vec{r}'|,t)$, which is summed over neutron, proton and cross components, is determined by using the total spectral density $\sigma(\vec{k},t)$ in Eq. (2.39). As mentioned earlier, the standard solution including only the collective poles $\delta\rho_a^\lambda(P;\vec{k},t)$ differs at $t = 0$ from the initial conditions and we need to include the cut contributions. We can determine the initial conditions by using the Eq. (2.19) and the definition of density fluctuations at Eq. (2.24) which must be equal to the initial condition of the spectral density $\sigma(\vec{k},t)$. This leads to a non-trivial sum rule given in the following equation

$$\sum_{p,n} \int 2\frac{d^3p}{(2\pi\hbar)^3} f_0^a(\vec{p})\left(1 - f_0^a(\vec{p})\right) = \sigma_{pp}(\vec{k},0) + 2\sigma_{pn}(\vec{k},0) + \sigma_{nn}(\vec{k},0). \qquad (2.40)$$

In the following subsections, the pole and cut contributions of the spectral intensity function will be given.

18

2.4.3 Pole Contribution to Density Correlations

The collective poles are determined from the roots of the dispersion relation, $\varepsilon(\vec{k}, \omega) = 0$. There are two collective poles namely the growing and decaying poles at $\omega = \pm i\Gamma_k$ shown by cross at Fig. 2.1. In order to calculate the pole contribution, we evaluate the integral in Eq. (2.31) by using the Cauchy-Residue theorem at these two poles. Cauchy-Residue theorem for a counter integral $\int_C f(z)dz \equiv \int_C \frac{g(z)}{h(z)}dz$ with the conditions $g(z_0) \neq 0, h(z_0) = 0$ and $\frac{\partial h}{\partial z}|_{z=z_0} \neq 0$ gives

$$\int_C f(z)dz \equiv \int_C \frac{g(z)}{h(z)}dz = 2\pi i \text{Res}[f(z), z = z_0] = 2\pi i \sum_k \lim_{z \to z_0} \frac{g(z)}{h'(z)} \quad (2.41)$$

Then the pole contribution of the density fluctuation is written as

$$
\begin{aligned}
\delta\rho_a^\lambda(P; \vec{k}, t) &= \frac{i}{2\pi}(2\pi i) \left\{ \frac{G_a^\lambda(\vec{k}, i\Gamma_k)}{\partial\varepsilon(\vec{k}, \omega)/\partial\omega|_{\omega=i\Gamma_k}} e^{\Gamma_k t} + \frac{G_a^\lambda(\vec{k}, i\Gamma_k)}{\partial\varepsilon(\vec{k}, \omega)/\partial\omega|_{\omega=i\Gamma_k}} e^{\Gamma_k t} \right\} \\
&= -\sum_\pm \frac{G_a^\lambda(\vec{k}, \pm i\Gamma_k)}{\partial\varepsilon(\vec{k}, \omega)/\partial\omega|_{\omega=\pm i\Gamma_k}} e^{\pm\Gamma_k t} = \delta\rho_a^+(\vec{k})e^{\Gamma_k t} + \delta\rho_a^-(\vec{k})e^{-\Gamma_k t}
\end{aligned}
$$

$$(2.42)$$

where the growing and decaying parts for neutron and proton are given by

$$
\delta\rho_n^\pm(\vec{k}) = -\left\{ \frac{\left[1 + F_0^{pp}\chi_p(\vec{k}, \omega)\right] S_n^\lambda(\vec{k}, \omega) - F_0^{np}\chi_n(\vec{k}, \omega)S_p^\lambda(\vec{k}, \omega)}{\partial\varepsilon(\vec{k}, \omega)/\partial\omega} \right\}_{\omega=\pm i\Gamma_k}
$$

$$
\delta\rho_p^\pm(\vec{k}) = -\left\{ \frac{\left[1 + F_0^{nn}\chi_n(\vec{k}, \omega)\right] S_p^\lambda(\vec{k}, \omega) - F_0^{pn}\chi_p(\vec{k}, \omega)S_n^\lambda(\vec{k}, \omega)}{\partial\varepsilon(\vec{k}, \omega)/\partial\omega} \right\}_{\omega=\pm i\Gamma_k}
$$

$$(2.43)$$

By using the definition in Eq. (2.36), the pole contribution of the spectral intensity of density correlations can be expressed as

$$
\begin{aligned}
\sigma_{ab}(PP; \vec{k}, t)(2\pi)^3\delta(\vec{k} - \vec{k}') &= \overline{\delta\rho_a^\lambda(P; \vec{k}, t)\delta\rho_b^\lambda(P; -\vec{k}', t)} \\
&= \overline{\delta\rho_a^+(\vec{k})\delta\rho_b^+(-\vec{k}')}e^{2\Gamma_k t} + \overline{\delta\rho_a^-(\vec{k})\delta\rho_b^+(-\vec{k}')} \\
&+ \overline{\delta\rho_a^+(\vec{k})\delta\rho_b^+(-\vec{k}')} + \overline{\delta\rho_a^-(\vec{k})\delta\rho_b^-(-\vec{k}')}e^{-2\Gamma_k t}.
\end{aligned}
$$

$$(2.44)$$

We calculate the neutron-neutron, proton-proton and neutron-proton density correlations to obtain the total spectral intensity of pole contributions. For neutron-neutron

we obtain

$$\overline{\delta\rho_n^\lambda(P;\vec{k},t)\delta\rho_n^\lambda(P;-\vec{k}',t)} =$$

$$\frac{[1+F_0^{pp}\chi_p]^2\overline{S_n^\lambda(\vec{k},i\Gamma)S_n^\lambda(-\vec{k}',i\Gamma)}+[F_0^{np}\chi_n]^2\overline{S_p^\lambda(\vec{k},i\Gamma)S_p^\lambda(-\vec{k}',i\Gamma)}}{[\partial\varepsilon(\vec{k},\omega)/\partial\omega]_{\omega=i\Gamma}[\partial\varepsilon(-\vec{k}',\omega)/\partial\omega]_{\omega=i\Gamma}}e^{2\Gamma_k t}$$

$$+\frac{[1+F_0^{pp}\chi_p]^2\overline{S_n^\lambda(\vec{k},-i\Gamma)S_n^\lambda(-\vec{k}',-i\Gamma)}+[F_0^{np}\chi_n]^2\overline{S_p^\lambda(\vec{k},-i\Gamma)S_p^\lambda(-\vec{k}',-i\Gamma)}}{[\partial\varepsilon(\vec{k},\omega)/\partial\omega]_{\omega=-i\Gamma}[\partial\varepsilon(-\vec{k}',\omega)/\partial\omega]_{\omega=-i\Gamma}}e^{-2\Gamma_k t}$$

$$+2\frac{[1+F_0^{pp}\chi_p]^2\overline{S_n^\lambda(\vec{k},i\Gamma)S_n^\lambda(-\vec{k}',-i\Gamma)}+[F_0^{np}\chi_n]^2\overline{S_p^\lambda(\vec{k},i\Gamma)S_p^\lambda(-\vec{k}',-i\Gamma)}}{[\partial\varepsilon(\vec{k},\omega)/\partial\omega]_{\omega=i\Gamma}[\partial\varepsilon(-\vec{k}',\omega)/\partial\omega]_{\omega=-i\Gamma}}.$$

$$(2.45)$$

For proton-proton

$$\overline{\delta\rho_p^\lambda(P;\vec{k},t)\delta\rho_p^\lambda(P;-\vec{k}',t)} =$$

$$\frac{[1+F_0^{nn}\chi_n]^2\overline{S_p^\lambda(\vec{k},i\Gamma)S_p^\lambda(-\vec{k}',i\Gamma)}+[F_0^{pn}\chi_p]^2\overline{S_n^\lambda(\vec{k},i\Gamma)S_n^\lambda(-\vec{k}',i\Gamma)}}{[\partial\varepsilon(\vec{k},\omega)/\partial\omega]_{\omega=i\Gamma}[\partial\varepsilon(-\vec{k}',\omega)/\partial\omega]_{\omega=i\Gamma}}e^{2\Gamma_k t}$$

$$+\frac{[1+F_0^{nn}\chi_n]^2\overline{S_p^\lambda(\vec{k},-i\Gamma)S_p^\lambda(-\vec{k}',-i\Gamma)}+[F_0^{pn}\chi_p]^2\overline{S_n^\lambda(\vec{k},-i\Gamma)S_n^\lambda(-\vec{k}',-i\Gamma)}}{[\partial\varepsilon(\vec{k},\omega)/\partial\omega]_{\omega=-i\Gamma}[\partial\varepsilon(-\vec{k}',\omega)/\partial\omega]_{\omega=-i\Gamma}}e^{-2\Gamma_k t}$$

$$+2\frac{[1+F_0^{nn}\chi_n]^2\overline{S_p^\lambda(\vec{k},i\Gamma)S_p^\lambda(-\vec{k}',-i\Gamma)}+[F_0^{pn}\chi_p]^2\overline{S_n^\lambda(\vec{k},i\Gamma)S_n^\lambda(-\vec{k}',-i\Gamma)}}{[\partial\varepsilon(\vec{k},\omega)/\partial\omega]_{\omega=i\Gamma}[\partial\varepsilon(-\vec{k}',\omega)/\partial\omega]_{\omega=-i\Gamma}}$$

$$(2.46)$$

For neutron-proton

$$\overline{\delta\rho_n^\lambda(P;\vec{k},t)\delta\rho_p^\lambda(P;-\vec{k}',t)} =$$

$$-\frac{[1+F_0^{pp}\chi_p]F_0^{pn}\chi_p\overline{S_n^\lambda(\vec{k},i\Gamma)S_n^\lambda(-\vec{k}',i\Gamma)}+F_0^{np}\chi_n[1+F_0^{nn}\chi_n]\overline{S_p^\lambda(\vec{k},i\Gamma)S_p^\lambda(-\vec{k}',i\Gamma)}}{[\partial\varepsilon(\vec{k},\omega)/\partial\omega]_{\omega=i\Gamma}[\partial\varepsilon(-\vec{k}',\omega)/\partial\omega]_{\omega=i\Gamma}}e^{2\Gamma_k t}$$

$$-\frac{[1+F_0^{pp}\chi_p]F_0^{pn}\chi_p\overline{S_n^\lambda(\vec{k},-i\Gamma)S_n^\lambda(-\vec{k}',-i\Gamma)}+F_0^{np}\chi_n[1+F_0^{nn}\chi_n]\overline{S_p^\lambda(\vec{k},-i\Gamma)S_p^\lambda(-\vec{k}',-i\Gamma)}}{[\partial\varepsilon(\vec{k},\omega)/\partial\omega]_{\omega=-i\Gamma}[\partial\varepsilon(-\vec{k}',\omega)/\partial\omega]_{\omega=-i\Gamma}}e^{-2\Gamma_k t}$$

$$-2\frac{[1+F_0^{pp}\chi_p]F_0^{pn}\chi_p\overline{S_n^\lambda(\vec{k},i\Gamma)S_n^\lambda(-\vec{k}',-i\Gamma)}+F_0^{np}\chi_n[1+F_0^{nn}\chi_n]\overline{S_p^\lambda(\vec{k},i\Gamma)S_p^\lambda(-\vec{k}',-i\Gamma)}}{[\partial\varepsilon(\vec{k},\omega)/\partial\omega]_{\omega=i\Gamma}[\partial\varepsilon(-\vec{k}',\omega)/\partial\omega]_{\omega=-i\Gamma}}$$

$$(2.47)$$

where the relation between Linhard functions is $\chi_a(\vec{k},i\Gamma) = \chi_a(\vec{k},-i\Gamma) = \chi_a(-\vec{k},i\Gamma) = \chi_a(-\vec{k},-i\Gamma)$ and the correlation between source terms are obtained by using the variance relation given in Eq. (2.19);

$$\overline{S_a^\lambda(\vec{k},i\Gamma)S_a^\lambda(-\vec{k}',i\Gamma)} = \overline{S_a^\lambda(\vec{k},-i\Gamma)S_a^\lambda(-\vec{k}',-i\Gamma)}$$

$$\overline{S_a^\lambda(\vec{k},i\Gamma)S_a^\lambda(-\vec{k}',-i\Gamma)} = \overline{S_a^\lambda(\vec{k},-i\Gamma)S_a^\lambda(-\vec{k}',i\Gamma)} \qquad (2.48)$$

and the cross terms correlations will be zero due to the main assumption of the SMF approach, $\overline{S_p^\lambda(\vec{k},i\Gamma)S_n^\lambda(-\vec{k}',i\Gamma)} = \overline{S_n^\lambda(\vec{k},i\Gamma)S_p^\lambda(-\vec{k}',i\Gamma)} = 0$. The details of the

calculations about the source correlations and the Linhard functions are given in Appendix B. Finally, the pole-pole contribution of the spectral intensity function can be calculated as

$$\tilde{\sigma}_{ab}(PP; \vec{k}, t) = \frac{E_{ab}^+}{\left| \left[\partial \varepsilon(\vec{k}, \omega)/\partial \omega \right]_{\omega = i\Gamma_k} \right|^2} \left(e^{+2\Gamma_k t} + e^{-2\Gamma_k t} \right) + \frac{2E_{ab}^-}{\left| \left[\partial \varepsilon(\vec{k}, \omega)/\partial \omega \right]_{\omega = i\Gamma_k} \right|^2}$$

(2.49)

where the quantities $E_{ab}^{\pm}$ for neutrons and protons are given by

$$E_{nn}^{\mp} = [1 + F_0^{pp} \chi_p]^2 I_n^{\mp} + [F_0^{np} \chi_n]^2 I_p^{\mp}$$

$$E_{pp}^{\mp} = [1 + F_0^{nn} \chi_n]^2 I_p^{\mp} + [F_0^{pn} \chi_p]^2 I_n^{\mp}$$

$$E_{np}^{\mp} = -(1 + F_0^{pp} \chi_p) F_0^{pn} \chi_p I_n^{\mp} - (1 + F_0^{nn} \chi_n) F_0^{np} \chi_n I_p^{\mp}$$

(2.50)

with the following integral

$$I_a^{\mp} = 2\hbar^2 \int \frac{d^3 p}{(2\pi\hbar)^3} \frac{\left[(\hbar\Gamma_k)^2 \mp (\vec{p} \cdot \hbar\vec{k}/m)^2 \right]}{\left[(\hbar\Gamma_k)^2 + (\vec{p} \cdot \hbar\vec{k}/m)^2 \right]^2} f_0^a(\vec{p} + \hbar\vec{k}/2) \left(1 - f_0^a(\vec{p} - \hbar\vec{k}/2) \right).$$

(2.51)

The analytical calculations of density fluctuations are performed in the quantal framework in this chapter. In the following chapter, we produce the numerical calculations in the quantal framework for zero temperature case which is the extreme quantum case; however, the numerical results are obtained in the semi-classical limit for finite temperature case. The expression for the Fermi-Dirac distribution function at the semi-classical limit can be obtained by expanding the function for the condition, $\hbar \to 0$. The expansion gives

$$f_0(\vec{p} \pm \hbar\vec{k}/2) = f_0(\vec{p}) \pm \frac{\partial f_0(\vec{p})}{\partial \varepsilon} \left(\frac{\hbar\vec{k}}{2} \cdot \frac{\vec{p}}{m} \right) + \frac{1}{2} \frac{\partial^2 f_0(\vec{p})}{\partial \varepsilon^2} \left(\frac{\hbar\vec{k}}{2} \cdot \frac{\vec{p}}{m} \right)^2 + \dots$$

(2.52)

Here we take the first two terms of the expansion as the leading terms. This is a good approximation for the long wavelength limit. As a result, semi-classical limit of quantal expressions are obtained by replacing the integrals $I_a^{\mp}$ and $\chi_a(\vec{k}, \omega)$ with following expressions in the long wavelength limit

$$I_a^{\mp}(sc) = 2\hbar^2 \int \frac{d^3 p}{(2\pi\hbar)^3} \frac{\left[(\hbar\Gamma_k)^2 \mp (\vec{p} \cdot \hbar\vec{k}/m)^2 \right]}{\left[(\hbar\Gamma_k)^2 + (\vec{p} \cdot \hbar\vec{k}/m)^2 \right]^2} f_0^a(\vec{p}) \left(1 - f_0^a(\vec{p}) \right)$$

(2.53)

21

and

$$\chi_a^{sc}(\vec{k},\omega) = 2 \int \frac{d^3p}{(2\pi\,\hbar)^3} \frac{\vec{p}\cdot\hbar\vec{k}/m}{\hbar\omega - \vec{p}\cdot\hbar\vec{k}/m} \frac{\partial f_a(p)}{\partial\varepsilon}. \tag{2.54}$$

2.4.4 Cut Contribution to Density Correlations

The cut contribution includes the cut-cut part and the mixed cut-pole parts. To calculate the cut-cut part, i.e. $\sigma_{ab}(CC;\vec{k},t) \sim \overline{\delta\rho_a^\lambda(C;\vec{k},t) + \delta\rho_b^\lambda(C;-\vec{k}',t)}$, we use the cut contribution of the Fourier transform of density fluctuations $\delta\rho_a^\lambda(C;\vec{k},t)$ in the explicit form as follows

$$\delta\rho_a^\lambda(C;\vec{k},t) = -i \int_{-\infty}^{+\infty} \frac{d\omega}{2\pi} e^{-i\omega t}$$

$$\times \left\{ \frac{\left[1 + F_0^{bb}\chi_b(\vec{k},\omega + i\eta)\right] S_a^\lambda(\vec{k},\omega + i\eta) - F_0^{ab}\chi_a(\vec{k},\omega + i\eta) S_b^\lambda(\vec{k},\omega + i\eta)}{\varepsilon(\vec{k},\omega + i\eta)} \right.$$

$$\left. - \frac{\left[1 + F_0^{bb}\chi_b(\vec{k},\omega - i\eta)\right] S_a^\lambda(\vec{k},\omega - i\eta) - F_0^{ab}\chi_a(\vec{k},\omega - i\eta) S_b^\lambda(\vec{k},\omega + i\eta)}{\varepsilon(\vec{k},\omega - i\eta)} \right\}$$

$$\tag{2.55}$$

and

$$\delta\rho_b^\lambda(C;-\vec{k}',t) = -i \int_{-\infty}^{+\infty} \frac{d\omega'}{2\pi} e^{-i\omega' t}$$

$$\times \left\{ \frac{[1 + F_0^{aa}\chi_a^-(\omega' + i\eta)] S_b^\lambda(-\vec{k}',\omega' + i\eta) - F_0^{ba}\chi_b^-(\omega' + i\eta) S_a^\lambda(-\vec{k}',\omega' + i\eta)}{\varepsilon(-\vec{k}',\omega' + i\eta)} \right.$$

$$\left. - \frac{[1 + F_0^{aa}\chi_a^-(\omega' - i\eta)] S_b^\lambda(-\vec{k}',\omega' - i\eta) - F_0^{ba}\chi_b^-(\omega' - i\eta) S_a^\lambda(-\vec{k}',\omega' + i\eta)}{\varepsilon(-\vec{k}',\omega' - i\eta)} \right\}.$$

$$\tag{2.56}$$

where we use the shorthand notation for $\chi^-(\omega' + i\eta) = \chi(-\vec{k}',\omega' + i\eta)$. In this case, the cut-cut part of the spectral intensity contains four terms:

$$\tilde{\sigma}_{ab}(CC;\vec{k},t) = A_{ab}^+(\vec{k},t) + \tilde{A}_{ab}^+(\vec{k},t) + \tilde{A}_{ab}^-(\vec{k},t) + A_{ab}^-(\vec{k},t). \tag{2.57}$$

The first term $A_{ab}^+(\vec{k},t)$ comes from the multiplication of the first terms in the expressions $\delta\rho_a^\lambda(C;\vec{k},t)$ and $\delta\rho_b^\lambda(C;-\vec{k}',t)$, and the last term $A_{ab}^-(\vec{k},t)$ comes from the multiplication of the second terms. After this calculations, the following expressions

are obtained for neutron-neutron and proton-proton

$$
\begin{pmatrix} A_{nn}^{\mp}(\vec{k},t) \\ A_{pp}^{\mp}(\vec{k},t) \end{pmatrix} =
$$

$$
\int\limits_{-\infty}^{+\infty} \frac{d\omega}{2\pi} \int\limits_{-\infty}^{+\infty} \frac{d\omega'}{2\pi} \frac{e^{-i(\omega+\omega')t}}{\omega+\omega'\mp 2i\eta} \begin{pmatrix} W_{nn}^{\mp} & V_{np}^{\mp} \\ V_{pn}^{\mp} & W_{pp}^{\mp} \end{pmatrix} \otimes \begin{pmatrix} \frac{\phi_n(\omega\mp i\eta)+\phi_n(\omega'\mp i\eta)}{\varepsilon(\omega\mp i\eta)\varepsilon(\omega'\mp i\eta)} \\ \frac{\phi_p(\omega\mp i\eta)+\phi_p(\omega'\mp i\eta)}{\varepsilon(\omega\mp i\eta)\varepsilon(\omega'\mp i\eta)} \end{pmatrix}
$$

$$(2.58)$$

and for proton-neutron

$$
A_{pn}^{\mp}(\vec{k},t) = - \int\limits_{-\infty}^{+\infty} \frac{d\omega}{2\pi} \int\limits_{-\infty}^{+\infty} \frac{d\omega'}{2\pi} \frac{e^{-i(\omega+\omega')t}}{\omega+\omega'\mp 2i\eta} \begin{pmatrix} W_{pn}^{\mp} & V_{nn}^{\mp} \end{pmatrix} \otimes \begin{pmatrix} \frac{\phi_n(\omega\mp i\eta)+\phi_n(\omega'\mp i\eta)}{\varepsilon(\omega\mp i\eta)\varepsilon(\omega'\mp i\eta)} \\ \frac{\phi_p(\omega\mp i\eta)+\phi_p(\omega'\mp i\eta)}{\varepsilon(\omega\mp i\eta)\varepsilon(\omega'\mp i\eta)} \end{pmatrix}.
$$

$$(2.59)$$

In these expressions and below, the symbol $\otimes$ denotes the matrix multiplication. The double integrals in $A_{ab}^{\pm}(\vec{k},t)$ can be divided into the principle value and delta function parts by using the identity $1/(\omega+\omega'\mp 2i\eta) = P(1/\omega+\omega') \pm i\pi\delta(\omega+\omega')$. The elements of W and V matrices are given by

$$
\begin{pmatrix} W_{nn}^{\mp} & V_{np}^{\mp} \\ V_{pn}^{\mp} & W_{pp}^{\mp} \end{pmatrix} = \begin{pmatrix} \left(1+F_0^{pp}\chi_p^{\mp}\right)\left(1+F_0^{pp}\chi_p'^{\mp}\right) & (F_0^{np})^2\chi_n^{\mp}\chi_n'^{\mp} \\ (F_0^{pn})^2\chi_p^{\mp}\chi_p'^{\mp} & \left(1+F_0^{nn}\chi_n^{\mp}\right)\left(1+F_0^{nn}\chi_n'^{\mp}\right) \end{pmatrix}
$$

$$(2.60)$$

and

$$
\begin{pmatrix} W_{pn}^{\mp} \\ V_{nn}^{\mp} \end{pmatrix} = \begin{pmatrix} F_0^{pn}\chi_p^{\mp}\left(1+F_0^{pp}\chi_p'^{\mp}\right) \\ \left(1+F_0^{nn}\chi_n^{\mp}\right)F_0^{np}\chi_n'^{\mp} \end{pmatrix}.
$$

$$(2.61)$$

In these expressions and also below, η is an infinitesimal positive number and we use the short hand notation $\chi_a^{\mp} = \chi_a(\vec{k},\omega\mp i\eta)$, $\chi_a'^{\mp} = \chi_a(\vec{k},\omega'\mp i\eta)$, and the quantity $\phi_a(\omega\mp i\eta)$ is defined as

$$
\phi_a(\omega\mp i\eta) = 2 \int\limits_{-\infty}^{+\infty} \frac{d^3p}{(2\pi\,\hbar)^3} f_0^a(\vec{p}+\hbar\vec{k}/2)\left[1-f_0^a(\vec{p}-\hbar\vec{k}/2)\right] \frac{1}{\vec{p}\cdot\vec{k}/m-(\omega\mp i\eta)}.
$$

$$(2.62)$$

The terms $\tilde{A}_{ab}^{+}(\vec{k},t)$ and $\tilde{A}_{ab}^{-}(\vec{k},t)$ involve the product of the cross terms in Eqs. (2.54) and (2.55), i.e. the product of first and second terms; and second and first terms. These terms also involve double integrations over ω and ω' and have similar structure with

23

$A_{ab}^{\pm}(\vec{k}, t)$:

$$
\begin{pmatrix} \tilde{A}_{nn}^{\mp}(\vec{k}, t) \\ \tilde{A}_{pp}^{\mp}(\vec{k}, t) \end{pmatrix} =
$$

$$
- \int\limits_{-\infty}^{+\infty} \frac{d\omega}{2\pi} \int\limits_{-\infty}^{+\infty} \frac{d\omega'}{2\pi} \frac{e^{-i(\omega+\omega')t}}{\omega + \omega'} \begin{pmatrix} \tilde{W}_{nn}^{\mp} & \tilde{V}_{np}^{\mp} \\ \tilde{V}_{pn}^{\mp} & \tilde{W}_{pp}^{\mp} \end{pmatrix} \otimes \begin{pmatrix} \frac{\phi_n(\omega\mp i\eta)+\phi_n(\omega'\pm i\eta)}{\varepsilon(\omega\mp i\eta)\varepsilon(\omega'\pm i\eta)} \\ \frac{\phi_p(\omega\mp i\eta)+\phi_p(\omega'\pm i\eta)}{\varepsilon(\omega\mp i\eta)\varepsilon(\omega'\pm i\eta)} \end{pmatrix}
$$

$$(2.63)$$

and

$$
\tilde{A}_{pn}^{\pm}(\vec{k}, t) = \int\limits_{-\infty}^{+\infty} \frac{dw}{2\pi} \int\limits_{-\infty}^{+\infty} \frac{dw'}{2\pi} \frac{e^{-i(\omega+\omega')t}}{\omega + \omega'} \begin{pmatrix} \tilde{W}_{pn}^{\mp} & \tilde{V}_{nn}^{\mp} \end{pmatrix} \otimes \begin{pmatrix} \frac{\phi_n(\omega\pm i\eta)+\phi_n(\omega'\mp i\eta)}{\varepsilon(\omega\pm i\eta)\varepsilon(\omega'\mp i\eta)} \\ \frac{\phi_p(\omega\pm i\eta)+\phi_p(\omega'\mp i\eta)}{\varepsilon(\omega\pm i\eta)\varepsilon(\omega'\mp i\eta)} \end{pmatrix}.
$$

$$(2.64)$$

Although the denominator in the integrand in $\tilde{A}_{ab}^{\pm}(\vec{k}, t)$ is zero when $\omega'=-\omega$, the ratio $[\phi(\omega \mp i\eta) + \phi(\omega' \pm i\eta)]/(\omega + \omega')$ is finite. Therefore, the integrand is a well-behaved function in contrast to its appearance. The elements of $\tilde{W}$ and $\tilde{V}$ matrices are given by

$$
\begin{pmatrix} \tilde{W}_{nn}^{\mp} & \tilde{V}_{np}^{\mp} \\ \tilde{V}_{pn}^{\mp} & \tilde{W}_{pp}^{\mp} \end{pmatrix} = \begin{pmatrix} \left(1 + F_0^{pp}\chi_p^{\mp}\right)\left(1 + F_0^{pp}\chi_p'^{\pm}\right) & (F_0^{np})^2 \chi_n^{\mp}\chi_n'^{\pm} \\ (F_0^{pn})^2 \chi_p^{\mp}\chi_p'^{\pm} & \left(1 + F_0^{nn}\chi_n^{\mp}\right)\left(1 + F_0^{nn}\chi_n'^{\pm}\right) \end{pmatrix}
$$

$$(2.65)$$

and

$$
\begin{pmatrix} W_{pn}^{\mp} \\ V_{nn}^{\mp} \end{pmatrix} = \begin{pmatrix} F_0^{pn}\chi_p^{\pm}\left(1 + F_0^{pp}\chi_p'^{\mp}\right) \\ \left(1 + F_0^{nn}\chi_p^{\pm}\right)F_0^{np}\chi_n'^{\mp} \end{pmatrix}.
$$

$$(2.66)$$

In a similar way, we can calculate the mixed pole-cut terms in the spectral intensity, i.e. $\sigma_{ab}(PC; \vec{k}, t) \sim \overline{\delta\rho_a^{\lambda}(P; \vec{k}, t) + \delta\rho_b^{\lambda}(C; -\vec{k}', t)} = \overline{\delta\rho_a^{\lambda}(C; \vec{k}, t) + \delta\rho_b^{\lambda}(P; -\vec{k}', t)}$, by using the Eq. (2.42) and Eq. (2.55). In this case, the pole-cut contribution has also four terms:

$$
\tilde{\sigma}_{ab}(PC; \vec{k}, t) = B_{ab}^{+}(\vec{k}, t) + \tilde{B}_{ab}^{+}(\vec{k}, t) + \tilde{B}_{ab}^{-}(\vec{k}, t) + B_{ab}^{-}(\vec{k}, t).
$$

$$(2.67)$$

Here, the first term $B_{ab}^{+}(\vec{k}, t)$ arises from the multiplication of the first terms in the expressions $\delta\rho_a^{\lambda}(P; \vec{k}, t)$ and $\delta\rho_a^{\lambda}(C; -\vec{k}', t)$, and the last term $B_{ab}^{-}(\vec{k}, t)$ comes from the multiplication of the second terms. The second and third terms involve the product of the cross terms. As a result, the following expressions are obtained for neutron-

24

neutron and proton-proton

$$
\begin{pmatrix} B_{nn}^{\mp}(\vec{k},t) \\ B_{pp}^{\mp}(\vec{k},t) \end{pmatrix} =
$$

$$
\frac{\pm i e^{\mp\Gamma t}}{\partial\varepsilon/\partial\omega|_{\omega=\mp i\Gamma}} \int\limits_{-\infty}^{+\infty} \frac{d\omega}{2\pi} \frac{e^{-i\omega t}}{\omega\mp i\Gamma} \begin{pmatrix} X_{nn}^{\mp} & Y_{np}^{\mp} \\ Y_{pn}^{\mp} & X_{pp}^{\mp} \end{pmatrix} \otimes \begin{pmatrix} \frac{\phi_n(\mp i\Gamma)+\phi_n(\omega\mp i\eta)}{\varepsilon(\omega\mp i\eta)} \\ \frac{\phi_p(\mp i\Gamma)+\phi_p(\omega\mp i\eta)}{\varepsilon(\omega\mp i\eta)} \end{pmatrix}
$$

$$(2.68)$$

and for neutron-proton

$$
B_{pn}^{\mp}(\vec{k},t) = \frac{\mp i e^{\mp\Gamma t}}{\partial\varepsilon/\partial\omega|_{\omega=\mp i\Gamma}} \int\limits_{-\infty}^{+\infty} \frac{d\omega}{2\pi} \frac{e^{-i\omega t}}{\omega\mp i\Gamma} \begin{pmatrix} X_{pn}^{\mp} & Y_{nn}^{\mp} \end{pmatrix} \otimes \begin{pmatrix} \frac{\phi_n(\mp i\Gamma_k)+\phi_n(\omega\mp i\eta)}{\varepsilon(\omega\mp i\eta)} \\ \frac{\phi_p(\mp i\Gamma_k)+\phi_p(\omega\mp i\eta)}{\varepsilon(\omega\mp i\eta)} \end{pmatrix}.
$$

$$(2.69)$$

Here , we use the short hand notation $\phi_a(\mp i\Gamma) = \phi_a(\vec{k},\omega = \mp i\Gamma)$ and the elements of X and Y matrices are given by

$$
\begin{pmatrix} X_{nn}^{\mp} & Y_{np}^{\mp} \\ Y_{pn}^{\mp} & X_{pp}^{\mp} \end{pmatrix} = \begin{pmatrix} \left(1+F_0^{pp}\chi_p^{\mp i\Gamma}\right)\left(1+F_0^{pp}\chi_p^{\mp}\right) & (F_0^{np})^2\chi_n^{\mp i\Gamma}\chi_n^{\mp} \\ (F_0^{pn})^2\chi_p^{\mp i\Gamma}\chi_p^{\mp} & \left(1+F_0^{nn}\chi_n^{\mp i\Gamma}\right)\left(1+F_0^{nn}\chi_n^{\mp}\right) \end{pmatrix}
$$

$$(2.70)$$

and

$$
\begin{pmatrix} X_{pn}^{\mp} \\ Y_{nn}^{\mp} \end{pmatrix} = \begin{pmatrix} F_0^{pn}\chi_p^{\mp i\Gamma}\left(1+F_0^{pp}\chi_p^{\mp}\right) \\ \left(1+F_0^{nn}\chi_n^{\mp i\Gamma}\right)F_0^{np}\chi_n^{\mp} \end{pmatrix}.
$$

$$(2.71)$$

where $\chi_a^{\mp i\Gamma} = \chi_a(\vec{k},\omega = \mp i\Gamma)$. Similarly, the second and third terms can be calculated as

$$
\begin{pmatrix} \tilde{B}_{nn}^{\mp}(\vec{k},t) \\ \tilde{B}_{pp}^{\mp}(\vec{k},t) \end{pmatrix} =
$$

$$
\frac{\mp i e^{\mp\Gamma t}}{\partial\varepsilon/\partial\omega|_{\omega=\mp i\Gamma}} \int\limits_{-\infty}^{+\infty} \frac{d\omega}{2\pi} \frac{e^{-i\omega t}}{\omega\mp i\Gamma} \begin{pmatrix} \tilde{X}_{nn}^{\mp} & \tilde{Y}_{np}^{\mp} \\ \tilde{Y}_{pn}^{\mp} & \tilde{X}_{pp}^{\mp} \end{pmatrix} \otimes \begin{pmatrix} \frac{\phi_n(\mp i\Gamma)+\phi_n(\omega\pm i\eta)}{\varepsilon(\omega\pm i\eta)} \\ \frac{\phi_p(\mp i\Gamma)+\phi_p(\omega\pm i\eta)}{\varepsilon(\omega\pm i\eta)} \end{pmatrix}
$$

$$(2.72)$$

and

$$
\tilde{B}_{pn}^{\mp}(\vec{k},t) = \frac{\pm i e^{\mp\Gamma t}}{\partial\varepsilon/\partial\omega|_{\omega=\mp i\Gamma}} \int\limits_{-\infty}^{+\infty} \frac{d\omega}{2\pi} \frac{e^{-i\omega t}}{\omega\mp i\Gamma} \begin{pmatrix} \tilde{X}_{pn}^{\mp} & \tilde{Y}_{nn}^{\mp} \end{pmatrix} \otimes \begin{pmatrix} \frac{\phi_n(\mp i\Gamma)+\phi_n(\omega\pm i\eta)}{\varepsilon(\omega\pm i\eta)} \\ \frac{\phi_p(\mp i\Gamma)+\phi_p(\omega\pm i\eta)}{\varepsilon(\omega\pm i\eta)} \end{pmatrix}.
$$

$$(2.73)$$

The elements of $\tilde{X}$ and $\tilde{Y}$ matrices are given by

$$
\begin{pmatrix} \tilde{X}_{nn}^{\mp} & \tilde{Y}_{np}^{\mp} \\ \tilde{Y}_{pn}^{\mp} & \tilde{X}_{pp}^{\mp} \end{pmatrix} = \begin{pmatrix} \left(1 + F_0^{pp}\chi_p^{\mp i\Gamma}\right)\left(1 + F_0^{pp}\chi_p^{\pm}\right) & (F_0^{np})^2\chi_n^{\mp i\Gamma}\chi_n^{\pm} \\ (F_0^{pn})^2\chi_p^{\mp i\Gamma}\chi_p^{\pm} & \left(1 + F_0^{nn}\chi_n^{\mp i\Gamma}\right)\left(1 + F_0^{nn}\chi_n^{\pm}\right) \end{pmatrix}
$$
(2.74)

and

$$
\begin{pmatrix} \tilde{X}_{pn}^{\mp} \\ \tilde{Y}_{nn}^{\mp} \end{pmatrix} = \begin{pmatrix} F_0^{pn}\chi_p^{\mp i\Gamma}\left(1 + F_0^{pp}\chi_p^{\pm}\right) \\ \left(1 + F_0^{nn}\chi_n^{\mp i\Gamma}\right)F_0^{np}\chi_n^{\pm} \end{pmatrix} .
$$
(2.75)

In the above expressions, we use $\phi_a(\mp i\Gamma)$ which is defined as

$$
\phi_a(\mp i\Gamma) = 2\int_{-\infty}^{+\infty}\frac{d^3p}{(2\pi\hbar)^3}f_0^a(\vec{p} + \hbar\vec{k}/2)\left[1 - f_0^a(\vec{p} - \hbar\vec{k}/2)\right]\frac{1}{\vec{p}\cdot\vec{k}/m \pm i\Gamma}.
$$
(2.76)

Likewise the pole contributions, the semi-classical limit of quantal expressions in cut contribution calculations are obtained by using the Linhard functions given in Eq. (2.53) and replacing the integrals $\phi_a(\omega \mp i\eta)$ and $\phi_a(\mp i\Gamma)$ with the following expressions in the long wavelength limit

$$
\phi_a(\omega \mp i\eta) = 2\int_{-\infty}^{+\infty}\frac{d^3p}{(2\pi\ \hbar)^3}f_0^a(\vec{p})\left[1 - f_0^a(\vec{p})\right]\frac{1}{\vec{p}\cdot\vec{k}/m - (\omega \mp i\eta)}
$$
(2.77)

and

$$
\phi_a(\mp i\Gamma) = 2\int_{-\infty}^{+\infty}\frac{d^3p}{(2\pi\hbar)^3}f_0^a(\vec{p})\left[1 - f_0^a(\vec{p})\right]\frac{1}{\vec{p}\cdot\vec{k}/m \pm i\Gamma} .
$$
(2.78)

26

CHAPTER 3

NUMERICAL CALCULATIONS IN NON-RELATIVISTIC APPROACH

In chapter 2, we present the description of the density correlation functions including collective and noncollective modes in the linear response framework of the Stochastic mean-field approach. The calculations are introduced in the non-relativistic framework for charge asymmetric nuclear matter. Actually, the calculations including collective as well as noncollective modes are performed for both symmetric [27] and asymmetric nuclear matter [28]. However, the numerical calculations for symmetric matter give the same results with the calculations of asymmetric matter when $I = 0.0$. Therefore, the calculations for the symmetric matter are not presented separately. The analytical expressions for symmetric matter including cut contributions are relatively simpler than those for asymmetric matter. We also derived the analytic expressions for symmetric matter in Appendix D by employing the Skyrme potential given in Eq. (2.13).

The early growth of density fluctuations including only the collective poles are studied in a quantal framework for symmetric and asymmetric nuclear matter in Ref. [16]. The description including only the effects of collective poles provides a good approximation for longer wavelengths however it does not satisfy the initial conditions and leads to a singular behavior when the wave numbers approach their upper limits specified by the dispersion relation. As pointed out in Ref. [21], the effect of non-collective poles play an important role for a complete description of density correlation function. In this study, we aim to calculate the correlation function exactly by including the non-collective poles in addition to the collective poles for asymmetric

nuclear matter. However, the evaluation of the cut contributions with the numerical methods is very complicated in a quantal approach for finite temperature case. Therefore in this chapter, we calculate numerically the growth of density fluctuations in a semi-classical approach for finite temperatures and in a quantal description for zero temperature by using the expressions derived in Chapter 2.

3.1   Spinodal Instabilities for Finite Temperature

In this section, the initial development of spinodal instabilities for asymmetric nuclear matter is calculated numerically in the semi-classical approach by employing the expressions derived in the previous sections. The growth rates of the unstable modes and the spinodal region boundary are investigated with the use of the dispersion relation given in Eq. (2.30). Also, the early growth of density correlation functions and the corresponding spectral intensities are examined for temperatures $T = 1$ MeV and $T = 5$ MeV . In the numerical calculations, we employ the effective Skyrme potential given in Eq. (2.12) for asymmetric nuclear matter. The calculations are performed for the initial charge asymmetries $I = 0.0, I = 0.4$ and $I = 0.8$ to observe the isospin dependency of the system. The initial charge asymmetry is defined according to $I = \left(\rho_n^0 - \rho_p^0 \right) / \left(\rho_n^0 + \rho_p^0 \right) .$

3.1.1   Growth Rates of Unstable Modes

The growth rates of the unstable modes are obtained from the roots of the susceptibility, $\varepsilon(\vec{k}, \omega) = 0$. In Fig. 3.1, the growth rates for the unstable modes are presented as a function of wave number for different values of initial asymmetry at temperatures $T = 1$ MeV and $T = 5$ MeV, for the initial baryon density $\rho = 0.3\rho_0$. For each temperature and asymmetry values, the growth rate increases until a maximum at a certain value of the wave number, then reduces to zero. As the asymmetry parameter increases, the wave number associated with the maximum growth rate reduces from 0.8 fm^{-1} to 0.6 fm^{-1} for $T = 1$ MeV and shifts from 0.7 fm^{-1} to 0.5 fm^{-1} for $T = 5$ MeV. Also, the temperature dependency of unstable behaviour of the system can be seen from the graph due to the fact that the growth rates reduce when temperature

28

increases at the same initial density and asymmetry values.
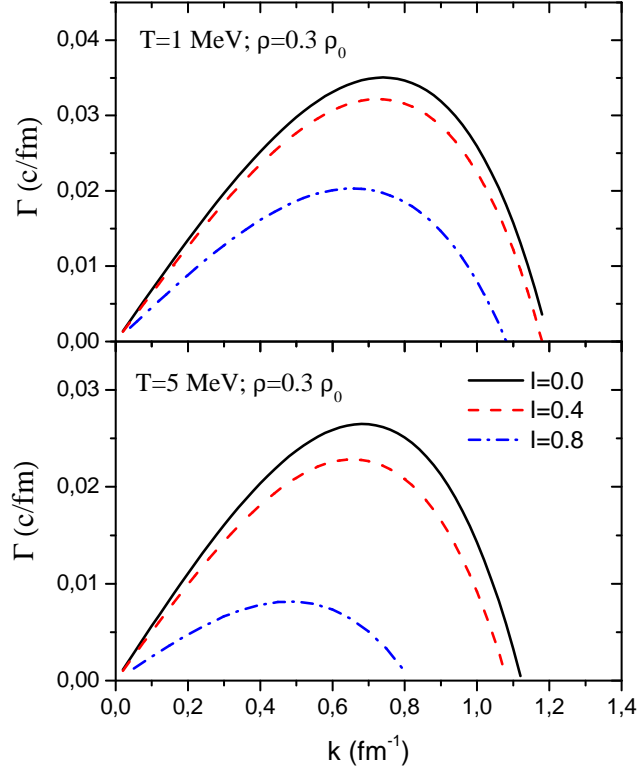
Figure 3.1: Growth rates of unstable modes as a function of wave number with the initial density $\rho = 0.3\rho_0$ for initial charge asymmetries $I = 0.0, I = 0.4$ and $I = 0.8$ at temperatures $T = 1$ MeV and $T = 5$ MeV.

Moreover, the growth time that characterizes the initial growth of density fluctuations can be determined by using the inverse of the growth rate, $\tau = 1/\Gamma_k$. For instance, the shortest growth time is varying $(30-50)$ fm/c for $T = 1$ MeV and $(35-100)$ fm/c for $T = 5$ MeV. It is seen from the graph that when asymmetry increases, the shortest growth time also increases and this reflects the fact that the unstable behaviour of density fluctuations is growing slowly for greater asymmetry values.

The most unstable modes are occurring around the wave numbers $k \approx (0.5-0.8)$ fm^{-1} with the corresponding wavelengths $\lambda \approx (8-12)$ fm and this wavelength values become important to determine the boundary of spinodal region. The asymmetry of the system has a greater effect on the growth rate at the same temperature. In fact, the neutron rich system displays less unstable behaviour than the symmetric system at the same conditions.
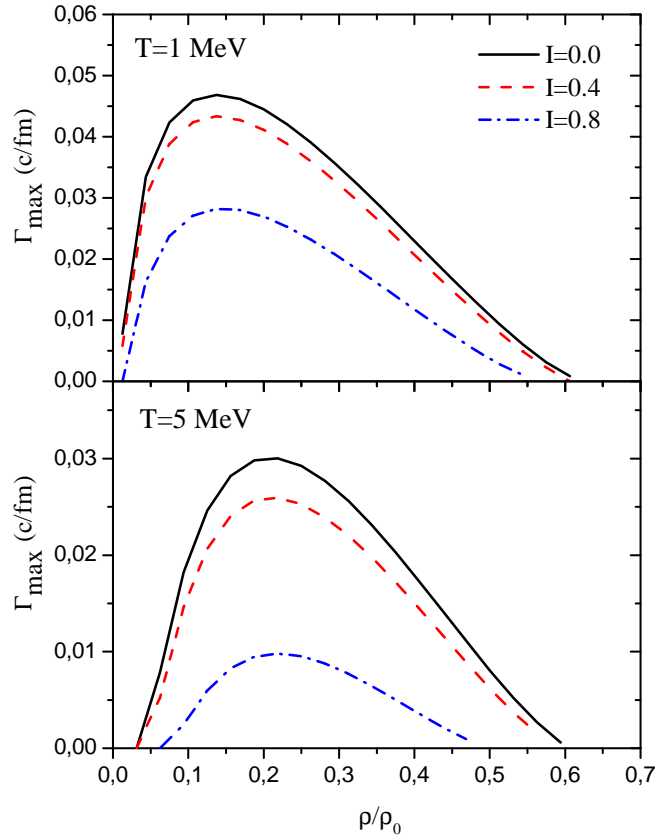
Figure 3.2: Growth rates of the most unstable modes as a function of the initial density for initial charge asymmetries $I = 0.0, I = 0.4$ and $I = 0.8$ at temperatures $T = 1$ MeV and $T = 5$ MeV.

Fig. 3.2 represents the growth rates of the most unstable modes depending on ρ/ρ_0 for asymmetry parameters $I = 0.0, I = 0.4$ and $I = 0.8$ at temperatures $T = 1$ MeV and $T = 5$ MeV. The most unstable behaviour occurs around $\rho = 0.2\rho_0$ and the density values for the most unstable modes do not exhibit any significant difference with increasing asymmetry for each temperature values. Also, it can be observed that the unstable response of the system shifts towards at slightly higher densities with increasing temperature.

3.1.2 Boundary of Spinodal Region

In this section, the boundary of the spinodal instability region is determined from the phase diagrams. Fig. 3.3 represents the phase diagrams corresponding to different

30
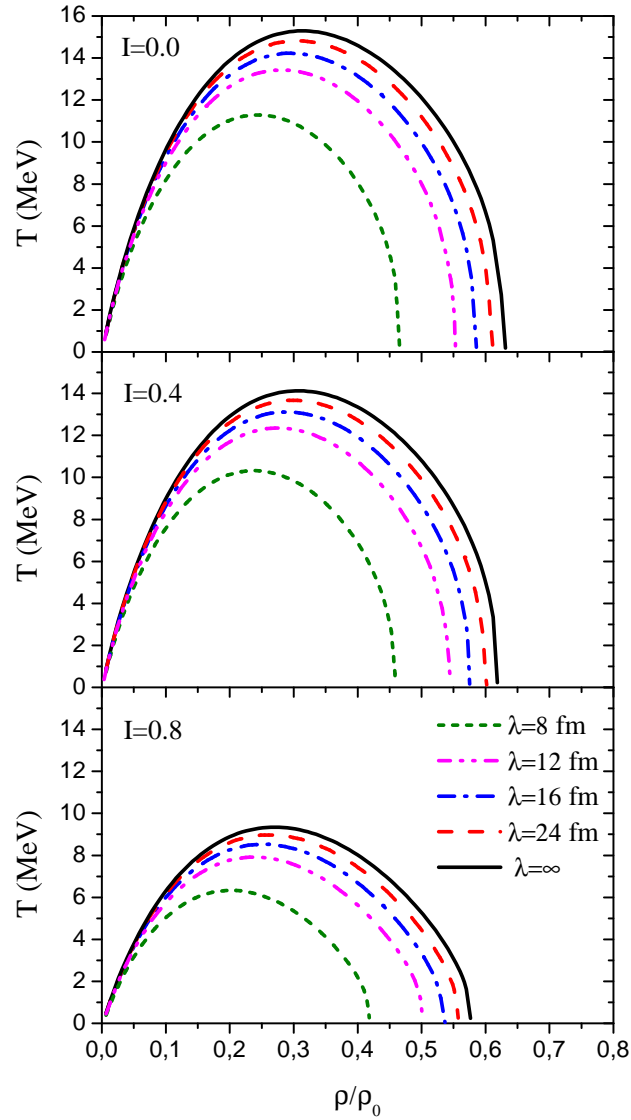
Figure 3.3: Phase diagram in density-temperature plane for different wavelengths corresponding to the potential given by Eq. (2.12).

wavelengths, starting from the uppermost boundary $\lambda = \infty$, in the temperature-density plane. The boundaries of the spinodal region are introduced for the initial asymmetry parameters $I = 0.0$, $I = 0.4$ and $I = 0.8$ to exhibit the isospin dependence of the system. The upper limits of the parabola-like curves show the critical temperatures of the corresponding wavelengths. In the region above the curve, there is uniform nuclear matter which exists in the gas phase. However, the nuclear system exhibits unstable behaviour and exists as a mixture of liquid and gas phases in the area under the curve. In this spinodal region, small amplitude density fluctuations grow

rapidly and lead to the multifragmentation of the system. The critical temperatures increase with the rising wavelengths up to the upper limit $\lambda = \infty$.

The value of the critical temperatures depends on the initial charge asymmetries $I = 0.0, I = 0.4$ and $I = 0.8$, are obtained as almost $T_c = 15$ MeV, $T_c = 14$ MeV and $T_c = 9$ MeV, respectively. The critical temperatures occur approximately at the same initial density $\rho = 0.3\rho_0$. It is observed that with increasing charge asymmetry, the spinodal instability region shrinks to smaller size, consistent with earlier calculations [3]. The limiting phase transition boundary occurs at density value around $\rho = 0.6\rho_0$ for asymmetries $I = 0.0$ and $I = 0.4$. The neutron rich nuclear matter with $I = 0.8$ and $T = 1$ MeV have importance since it corresponds to the structure of crust of neutron stars. The nucleon density which restricts the spinodal boundary under these conditions occurs around $\rho = 0.55\rho_0$ and it is consistent with earlier results in literature [31].

We choose a reference state from the spinodal region with an initial density $\rho = 0.3\rho_0$, at which the critical temperatures occur, in order to calculate the density correlation functions and we make our calculations at two different temperatures $T = 1$ MeV and $T = 5$ MeV.

3.1.3 Spectral Intensity of Density Correlations

In order to investigate the unstable dynamics of the nuclear matter in the spinodal region, the behaviour of the density correlation functions carries valuable information. According to the expression in Eq. (2.38), the total spectral intensity $\tilde{\sigma}(\vec{k}, t)$ of density correlation functions is illustrated in Figs. 3.4 and 3.5 as a function of wave number k at time $t = 40$ fm/c for two different temperatures and three different initial charge asymmetries. At each initial charge asymmetry and temperature value, the upper limit of the wave number range k_{max} is specified from the condition that the growth rate of the unstable modes become zero ($\Gamma_k = 0$) which can be seen from Fig. 3.1. In the spectral intensity graphs, the largest growth occurs at the wave numbers which encounter with those obtained in Fig. 3.1 for the most unstable modes. When the initial charge asymmetry of the system increases, the growth rates decrease for both temperature cases. Also, we deduce that the growth rate of the spectral intensity

function is larger at high temperature case.
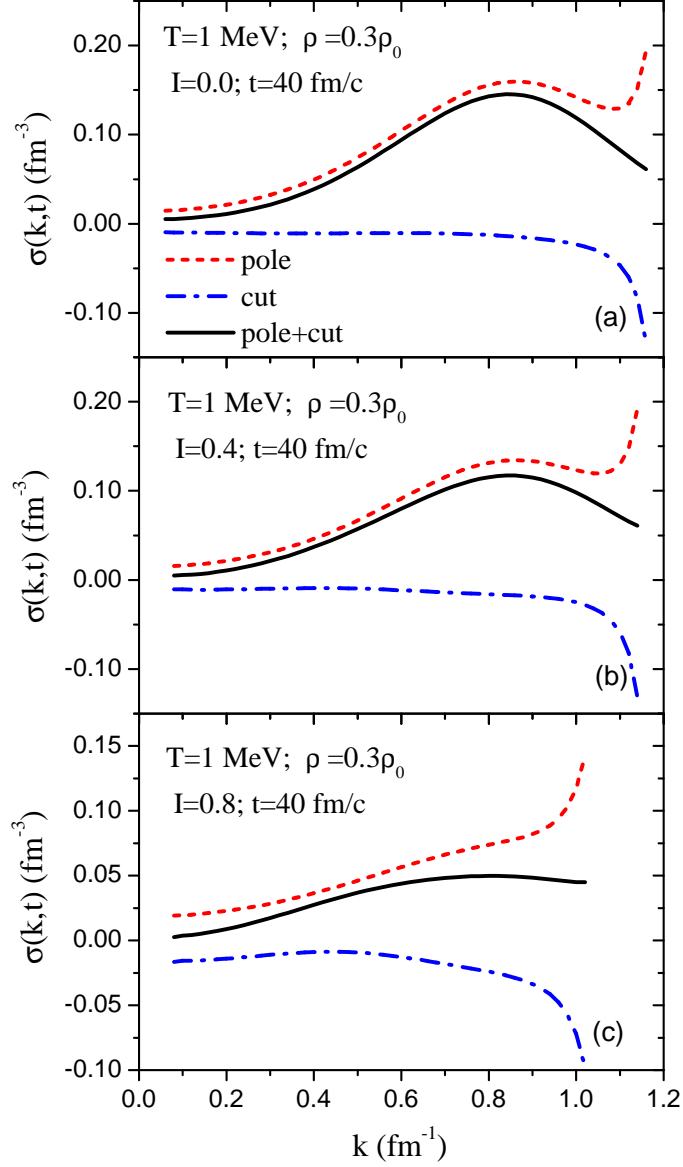
Figure 3.4: Spectral intensity of the correlation function as a function of wave number at initial density $\rho = 0.3\rho_0$ at time $t = 40$ fm/c at temperature $T = 1$ MeV for three different charge asymmetries. Dotted, dashed-dotted and solid lines are results of pole, cut and total contributions, respectively.

In Figs. 3.4 and 3.5, dashed, dash-dotted and solid lines represent the result of calculations in Eq. (2.38) with pole contributions $\sigma_{ab}(PP; \vec{k}, t)$ only, with cut contributions only and the total of all terms, respectively. The cut part contains cut-cut contribution $\sigma_{ab}(CC; \vec{k}, t)$ and the mixed terms due to pole and cut parts $2\sigma_{ab}(PC; \vec{k}, t)$. From
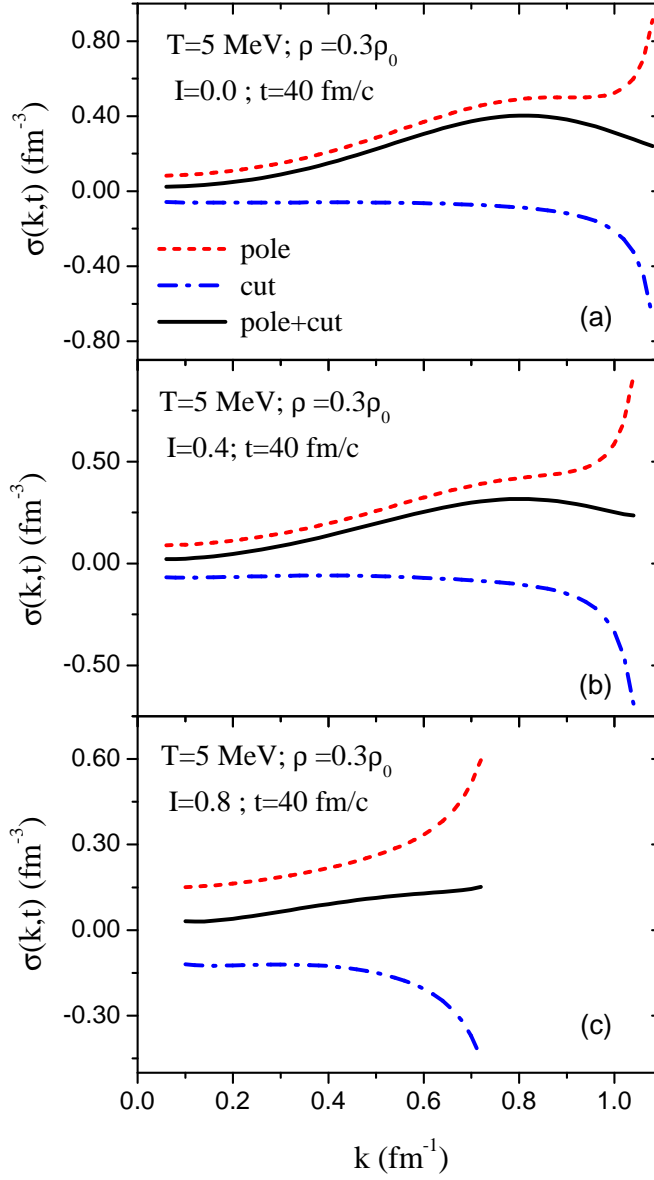
Figure 3.5: Spectral intensity of the correlation function as a function of wave number at initial density $\rho = 0.3\rho_0$ at time $t = 40$ fm$/c$ at temperature $T = 5$ MeV for three different charge asymmetries. Dotted, dashed-dotted and solid lines are results of pole, cut and total contributions, respectively.

these figures, we make two significant investigations for each value of temperature and asymmetry parameter. The first one is that the cut terms make a significant negative contribution in the early stages of growth, as a consequence slowing down the growth of instabilities in the spinodal region. Collective poles presented by pole contributions dominate the growth of density fluctuations during later times, and the cut

terms representing the effects of non-collective poles do not evolve in time [3, 27, 28]. The second point is that both pole and cut contributions have divergent behavior with opposite signs for higher wave number values. Consequently, these divergent behaviors cancel out each other to produce a nice regular behavior of the spectral intensity as a function of wave number.
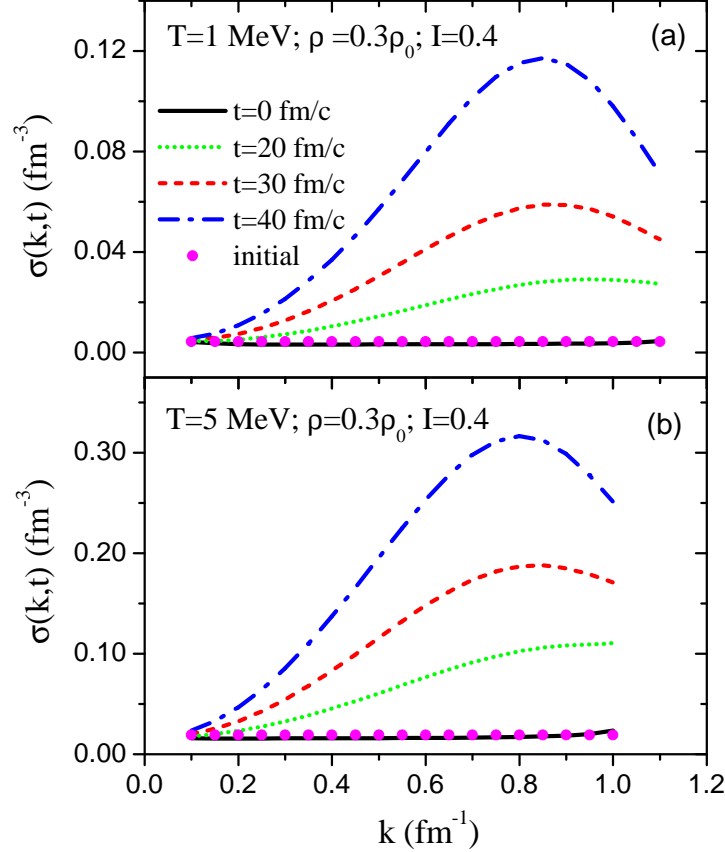
Figure 3.6: Spectral intensity of the correlation function as a function of wave number at initial density $\rho = 0.3\rho_0$ and charge asymmetry $I = 0.4$ for different times at temperature $T = 1$ MeV (a) and $T = 5$ MeV (b). Dots on the solid lines at times $t = 0$ represent the initial conditions.

Fig. 3.6 indicates the total spectral intensity of density correlation function as a function of wave number k for charge asymmetry $I = 0.4$ at different times for initial temperatures $T = 1$ MeV and $T = 5$ MeV. We notice that the total spectral intensity including pole and cut contributions demonstrates the growth of the initial density fluctuations clearly. The curves representing the spectral intensity function show more and more peaked-like behavior around the most unstable modes with increasing
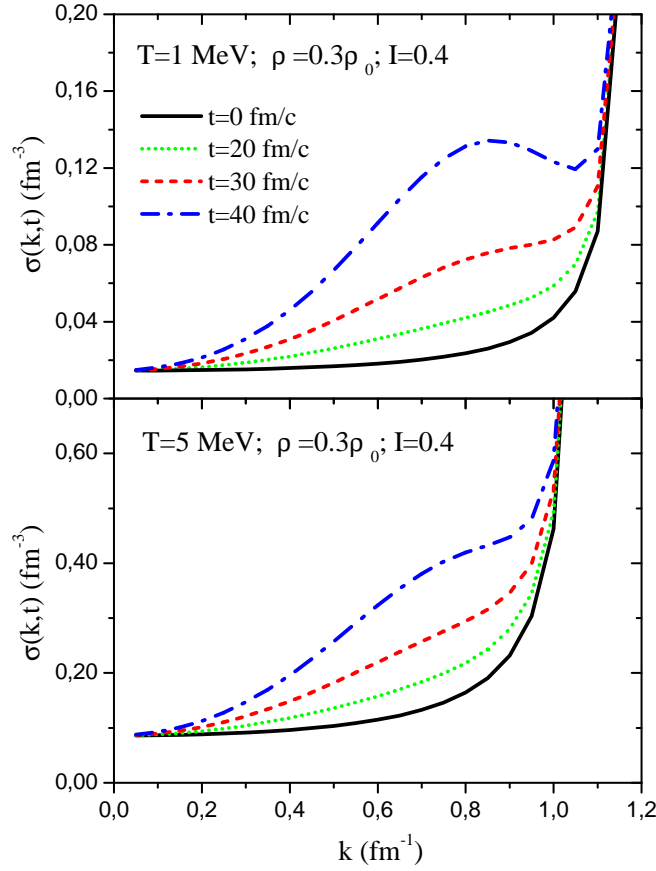
Figure 3.7: Spectral intensity of the correlation function as a function of wave number due to the pole contributions only at initial density $\rho = 0.3\rho_0$ and charge asymmetry $I = 0.4$ for different times at temperature $T = 1$ MeV (a) and $T = 5$ MeV (b).

time. Moreover, the initial value of the spectral intensity at time $t = 0$ demonstrated by the black solid line is calculated as the sum of the pole-pole terms, $\sigma_{ab}(PP; \vec{k}, t)$, cut-cut terms $\sigma_{ab}(CC; \vec{k}, t)$ and pole-cut terms $2\sigma_{ab}(PC; \vec{k}, t)$. Otherwise, the solid circles on this line are obtained from the initial conditions given in the left hand side of Eq. (2.40). It can be seen that both calculations are compatible and this shows the validity of the nontrivial sum-rule presented by Eq. (2.40). As a result, the exact calculation of the correlation functions with the additional cut contribution satisfies the initial conditions. However, if only the collective poles are considered then the initial fluctuations cannot be fully expressed. For instance, Fig. 3.7 indicates the spectral intensity function calculated according to the pole contributions only. It appears from the figure that the results at time $t = 0$ does not match the initial conditions given in

36

Fig. 3.6. and a slight growth is observed at that time which is not concluded from the results of the exact calculations. In addition, the singular behaviour is observed at higher wave numbers for both temperatures. Although the collective poles play dominant role in early growth of density fluctuations, they do not give the full description of the growth of instabilities. Therefore, we also include the cut contributions which reflect the effect of non-collective poles in order to calculate the density correlation functions precisely.

3.1.4 Density Correlation Functions

The expression of the total density correlation function is obtained in the previous chapter as a sum over neutron, proton and cross components by using the total spectral intensity function. In this section, the numerical calculations of the equal time density correlation functions, including collective and non-collective modes are presented in the linear response framework in the semi-classical limit.

Fig. 3.8 indicates the equal time correlation functions $\sigma(|\vec{r}-\vec{r'}|, t)$ of the total density fluctuations in terms of distance between two space locations $x = |\vec{r}-\vec{r'}|$ at $T = 1$ MeV with the initial density $\rho = 0.3\rho_0$ for three different times $t = 20, 30, 40$ fm$/c$. The density correlation functions are calculated by using the full spectral intensities which are given by solid lines in Fig. 3.4 and the graphs are plotted for three different charge asymmetries to illustrate the asymmetry dependence of the system. The time evolution of density fluctuations is faster for symmetric matter and decreases as the matter becomes neutron-rich. In Fig. 3.9, the correlation functions are plotted for the same initial conditions with Fig. 3.8 but at a higher temperature $T = 5$ MeV. The growth of density fluctuations can be observed obviously from these figures. In addition, we can obtain information about the typical size of condensing fragments arising at the initial stages of spinodal decomposition. For this aim, we define the correlation length x_C as the width of the correlation function at half maximum. The correlation length characterizes the size of the initial condensation regions throughout the growth of fluctuations. The variance of the local density fluctuations $\delta\rho_a^\lambda(\vec{r}, t)$ is approximately specified by $\sigma(x_C, t)$ in the correlation volume which is defined as $\Delta V_C = 4\pi x_C^3/3$. The number of nucleons in each correlation volume fluctuates with
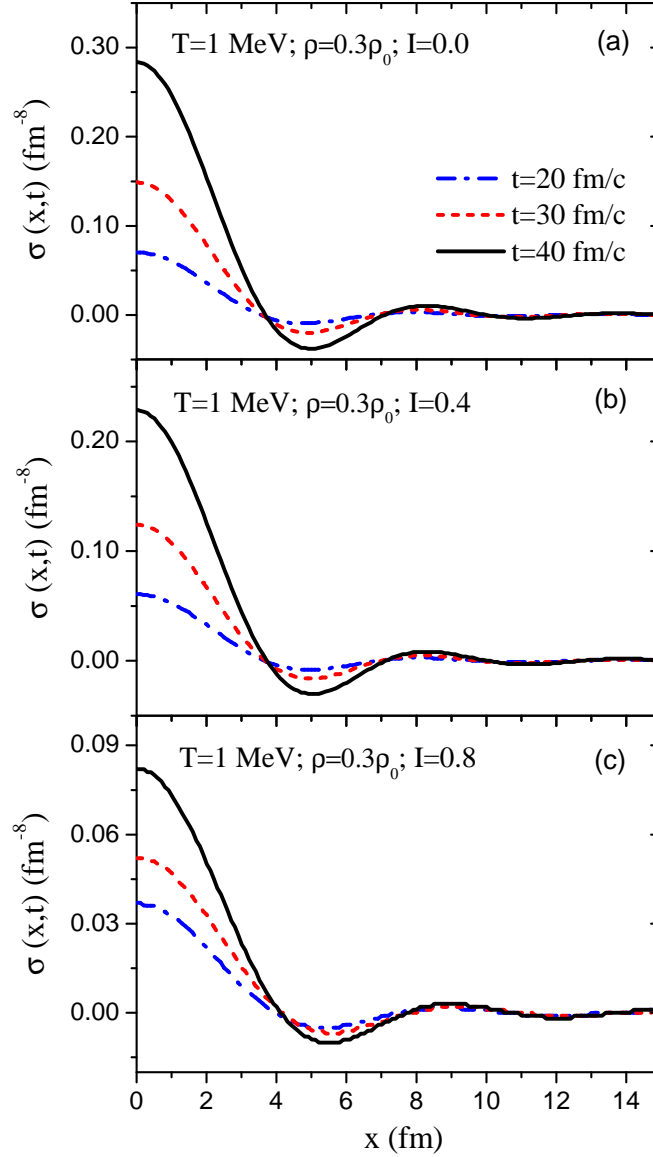
Figure 3.8: Density correlation function as a function of distance between two space points for initial density $\rho = 0.3\rho_0$, at temperature $T = 1$ MeV at different charge asymmetries $I = 0.0, 0.4, 0.8$ in sections (a), (b) and (c), respectively.

a dispersion $\Delta A_C = \Delta V_C \sqrt{\sigma(x_C, t)}$. Consequently, the total nucleon number in each correlation volume varies approximately within the interval $\Delta A_0 - \Delta A_C \leq \Delta A \leq \Delta A_0 + \Delta A_C$, where we use $\Delta A_0 = \Delta V_C \rho_0$ that is the number of nucleons at the initial uniform state. From this analysis we can deduce that the spinodal decomposition mechanism does not give rise to equal sized fragments. On the contrary, it leads to a

mixture of different sized clusters.

From Figs. 3.8 and 3.9, it is observed that the correlation length is not very sensitive to the time evolution and temperature but depends on the initial charge asymmetry. As an example, at temperature $T = 5$ MeV and the initial charge asymmetry $I = 0.4$, the correlation length is approximately $x_C = 3.0$ fm. In this case, the magnitude of dispersion of density fluctuations is about $\sqrt{\sigma(x_C, t)} = 0.04$ fm^{-3} at time $t = 30$ fm/c and this result gives the number of nucleons in the correlation volume approximately in the range of $1 \leq \Delta A \leq 9$. For temperature $T = 5$ MeV and asymmetry $I = 0.8$, the correlation length is approximately $x_C = 3.0$ fm and the magnitude of dispersion of density fluctuations is about $\sqrt{\sigma(x_C, t)} = 0.02$ fm^{-3} at time $t = 30$ fm/c. This gives us the number of nucleons fluctuating in the correlation volume in the range of $8 \leq \Delta A \leq 16$.

From the above discussion, we conclude that the spinodal decomposition provides a dynamical mechanism for the liquid-gas phase transition. The linear response approach describes only the early phase of the transition inside the spinodal region. For describing whole phase transition, we need to study nonlinear evolution of the density fluctuations. Since the density fluctuations grow nearly exponentially in time, the linear response treatment of fluctuations over a limiting time does not give a realistic description for instabilities. To exclude this undesirable result we can constraint the linear response approach by the condition that the dispersion on the nucleon density fluctuations keeps below the average nucleon density in the correlation volume, i.e. $\sqrt{\sigma(x_C, t)} \leq \rho$. This condition is satisfied for all the cases represented by Figs. 3.8 and 3.9 for the given times.

In the previous studies [9, 16, 17, 20], only the contributions of the collective poles were included in the calculations of the density correlation functions. However, as seen from Figs. 3.4 and 3.5, we encounter the problem that pole contributions have divergent behavior as wave numbers approach its upper limit, $k \to k_{\max}$. Therefore, we cut the spectral intensity graph at a suitable cut-off wave number value to cure this problem. At the initial charge asymmetry $I = 0.4$, the cutoff value is taken $k_{cut} = 1.05$ fm^{-1} (that is the local minimum point) for $T = 1$ MeV and $k_{cut} = 0.9$ fm^{-1} for $T = 5$ MeV, then we plotted the equal time correlation functions graph after this
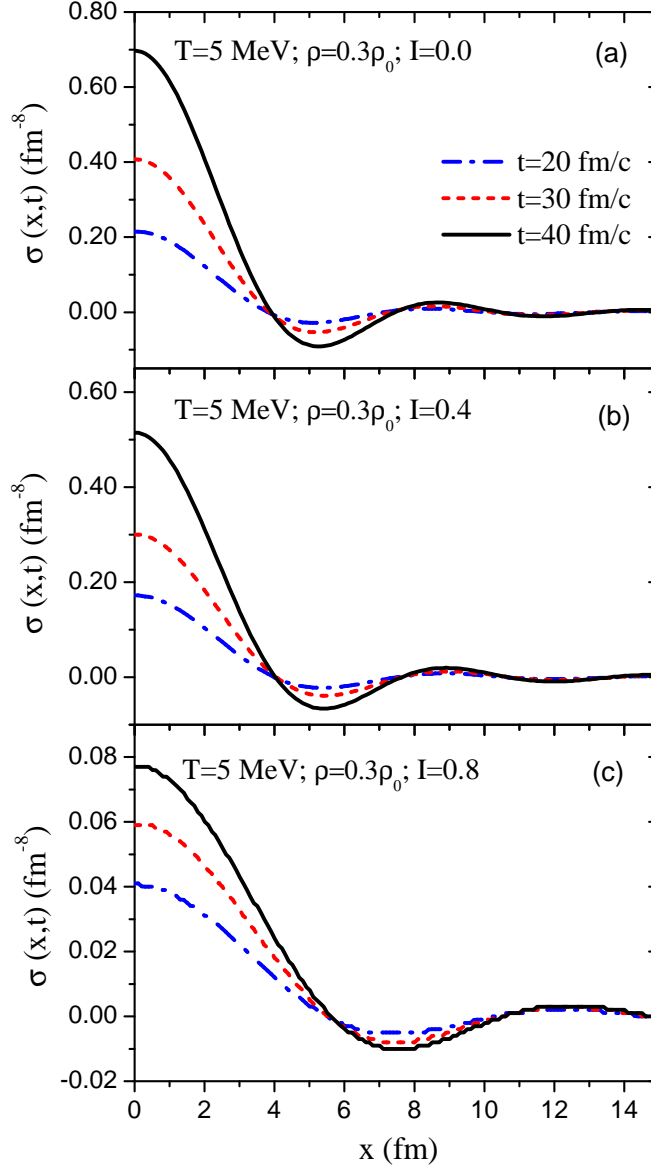
Figure 3.9: Density correlation function as a function of distance between two space points for initial density $\rho = 0.3\rho_0$, at temperature $T = 5$ MeV at different charge asymmetries $I = 0.0, 0.4, 0.8$ in sections (a), (b) and (c), respectively.

cut-off approximation. In Fig. 3.10, calculations with cut-off are compared with the complete calculations of the density correlation function at temperatures $T = 1$ MeV and $T = 5$ MeV. Solid lines represent the total density correlation function whereas the dashed lines show the pole contribution of correlation functions obtained from the cut-off values. As seen from the graph, we can say that the cut-off provides a

good approximation. However, the cut contributions are important for a complete description. Moreover, we observe that the results obtained with pole approximations are rather sensitive to the cut-off wave number at higher temperature case, since there is no visible local minimum of the spectral intensity.

Figure 3.10: Density correlation function as a function of distance between two space points at initial density $\rho = 0.3\rho_0$ and charge asymmetry $I = 0.4$, at temperatures $T = 1$ MeV and $T = 5$ MeV.

3.2 Spinodal Instabilities for Zero Temperature Case

In this section, the numerical calculations of the early growth of density fluctuations are presented for asymmetric nuclear matter at zero temperature case by using the expressions given in Chapter 2. For zero temperature case, the momentum integral is restricted to the Fermi surface since $\partial_\varepsilon f_0 = -\delta(\varepsilon - \varepsilon_F)$, so the integrals $I_a^\pm$ in the pole contribution expressions; and $\phi_a(i\Gamma)$ and $\phi_a(\omega \pm i\eta)$ in the cut contribution

expressions give zero in the semi-classical limit. Consequently, there is no semi-classical contribution at zero temperature and the calculations are performed in a quantal framework.

In the quantal framework, the Linhard functions and the integral $I_a^{\pm}$ at zero temperature can be expressed as

$$\chi_a(\vec{k}, \omega) = -2 \int \frac{d^3p}{(2\pi\hbar)^3} \frac{\theta(p_F - |\vec{p} - \hbar\vec{k}/2|) - \theta(p_F - |\vec{p} + \hbar\vec{k}/2|)}{\hbar\omega - \vec{p} \cdot \hbar\vec{k}/m}. \quad (3.1)$$

and

$$I_a^{\mp} = 2\hbar^2 \int \frac{d^3p}{(2\pi\hbar)^3} \frac{\left[(\hbar\Gamma_k)^2 \mp (\vec{p} \cdot \hbar\vec{k}/m)^2\right]}{\left[(\hbar\Gamma_k)^2 + (\vec{p} \cdot \hbar\vec{k}/m)^2\right]^2}$$
$$\times \theta(p_F - |\vec{p} + \hbar\vec{k}/2|) \left(1 - \theta(p_F - |\vec{p} - \hbar\vec{k}/2|)\right). \quad (3.2)$$

In addition, the integral $\phi_a(\omega \pm i\eta)$ in the cut contributions is given by

$$\phi_a(\omega \mp i\eta) = 2 \int \frac{d^3p}{(2\pi\hbar)^3} \frac{\theta(p_F - |\vec{p} + \hbar\vec{k}/2|) \left(1 - \theta(p_F - |\vec{p} - \hbar\vec{k}/2|)\right)}{\vec{p} \cdot \vec{k}/m - (\omega \mp i\eta)}. \quad (3.3)$$

In the above expressions, $\theta(p_F - p)$ is the step function. The polar parts of these integrals are evaluated analytically and then the numerical methods are applied in the evaluation of the resultant integrals.

3.2.1 Growth Rates of Unstable Modes at Zero Temperature

The growth rates of the unstable modes are obtained from the dispersion relation at $T = 0$ MeV within the quantal approach. In Fig. 3.11, the growth rates for the unstable modes are given as a function of wave number for different values of initial asymmetry for the initial density $\rho = 0.3\rho_0$. For each asymmetry values, the growth rates show the similar behavior to the finite temperature case, increasing until a maximum at a certain value of the wave number, then reduces to zero. The wave number corresponding to the maximum growth rate decreases from 0.65 fm^{-1} to 0.5 fm^{-1} with the increasing values of asymmetry. In addition, the most unstable modes are found to occur approximately between the wavelengths $\lambda \approx (10 - 12)$ fm.

The shortest growth time of primary density fluctuations can be obtained from the inverse of the growth rate. As an example, the shortest growth time is about 30 fm$/c$ for symmetric matter and close to 65 fm$/c$ when asymmetry $I = 0.8$. The results again show the fact that the unstable behaviour of density fluctuations is growing slowly for neutron rich systems.
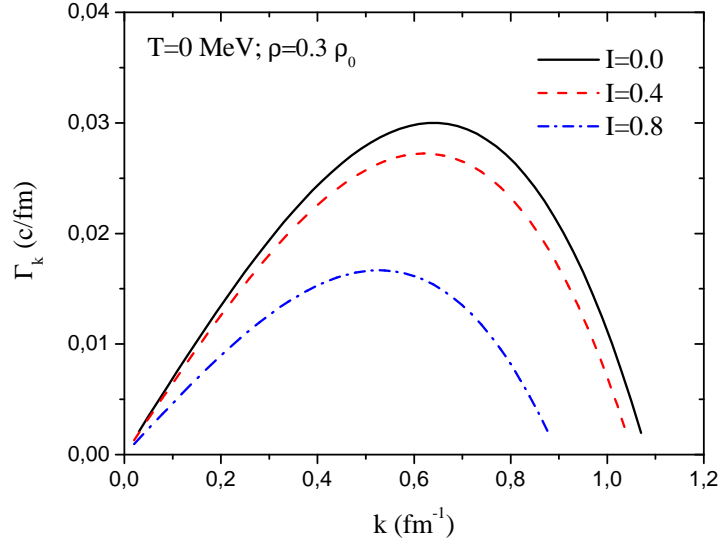
Figure 3.11: Growth rates of unstable modes as a function of wave number with the initial density $\rho = 0.3\rho_0$ for initial charge asymmetries $I = 0.0, I = 0.4$ and $I = 0.8$ at temperature $T = 0$ MeV.

3.2.2 Quantal Correlation Functions

Fig. 3.12 shows the total spectral intensity $\sigma(\vec{k}, t)$ of density correlation functions as a function of wave number k at time $t = 40$ fm$/c$ at $T = 0$ MeV for three different initial charge asymmetries. In this figure similar to the Figs. 3.4 and 3.5, dashed, dash-dotted and solid lines demonstrate the result of calculations in Eq. (2.38) with pole contributions $\sigma_{ab}(PP; \vec{k}, t)$ only, with cut contributions only and the total of all terms, respectively. The cut part contains cut-cut contribution $\sigma_{ab}(CC; \vec{k}, t)$ and the mixed terms due to pole and cut parts $2\sigma_{ab}(PC; \vec{k}, t)$. The cut contributions slow down the growth of instabilities in the spinodal region as expected; however the cut terms become more significant at higher values of asymmetry at $T = 0$ MeV in the quantal framework. In addition, the cut and pole contributions have not a divergent

43

behavior in the higher wave numbers, which occurred at finite temperature case, at these calculations.
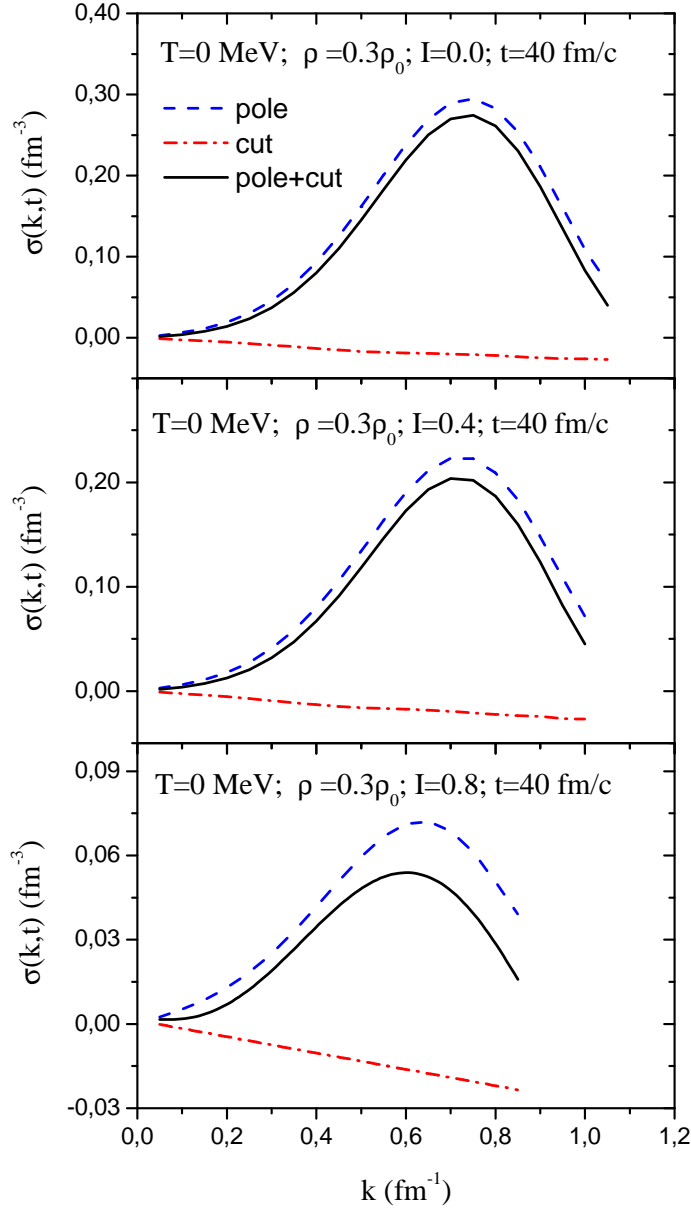
Figure 3.12: Spectral intensity of the correlation function as a function of wave number at initial density $\rho = 0.3\rho_0$ at time $t = 40$ fm/c at zero temperature for three different charge asymmetries. Dotted, dashed-dotted and solid lines are results of pole, cut and total contributions, respectively.

Fig. 3.13 represents the total spectral intensity of the correlation function $\sigma(\vec{k}, t)$ for charge asymmetry $I = 0.4$ as a function of wave number at different times for the

44

temperature $T = 0$ MeV. The total spectral intensity includes pole and cut contributions of density fluctuations. Similar to the finite temperature case, the initial value of the spectral intensity at time $t = 0$ represented by the black solid line is obtained by numerical calculations of the pole-pole terms, $\sigma_{ab}(PP; \vec{k}, t = 0)$, cut-cut terms $\sigma_{ab}(CC; \vec{k}, t = 0)$ and pole-cut terms $2\sigma_{ab}(PC; \vec{k}, t = 0)$. Moreover, the solid circles on this line are calculated by the initial conditions given in the left hand side of Eq. (2.40). Eventually, the nice agreement of both calculations shows the validity of the nontrivial sum-rule presented by Eq. (2.40) in the quantal framework for zero temperature case.
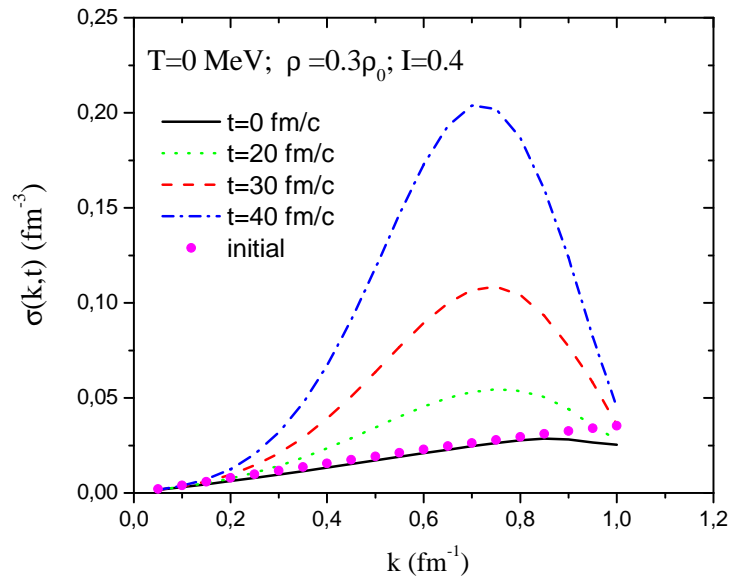
Figure 3.13: Spectral intensity of the correlation function as a function of wave number at initial density $\rho = 0.3\rho_0$ and charge asymmetry $I = 0.4$ for different times at zero temperature. Dots on the solid lines at time $t = 0$ represent the initial conditions.

Fig. 3.14 indicates the equal time correlation functions $\sigma(|\vec{r} - \vec{r}'|, t)$ of the total density fluctuations in terms of distance between two space locations $x = |\vec{r} - \vec{r}'|$ at $T = 0$ MeV with the initial density $\rho = 0.3\rho_0$ for three different charge asymmetries corresponding to Fig. 3.12. The density correlation functions are calculated by using the full spectral intensities which are given by solid lines in Fig. 3.12 and the graphs are plotted at three different times $t = 20, 30, 40$ fm/c . From this graph, we can obtain information about the size of the condensation regions during the initial growth of fluctuations by using the correlation length at $T = 0$ MeV . For example, the

45

correlation length is about $x_C = 2.0$ fm at the initial charge asymmetry $I = 0.4$ and in this case, the magnitude of dispersion of density fluctuations at $t = 40$ fm/c is nearly $\sqrt{\sigma(x_C, t)} = 0.05$ fm^{-3}. As a result, the number of nucleons fluctuating in the correlation volume occurs in the range $3 \leq \Delta A \leq 7$. For $I = 0.8$, the correlation length is nearly $x_C = 3.0$ fm and the initial size of the condensing droplets in the correlation volume gets bigger for the same time.
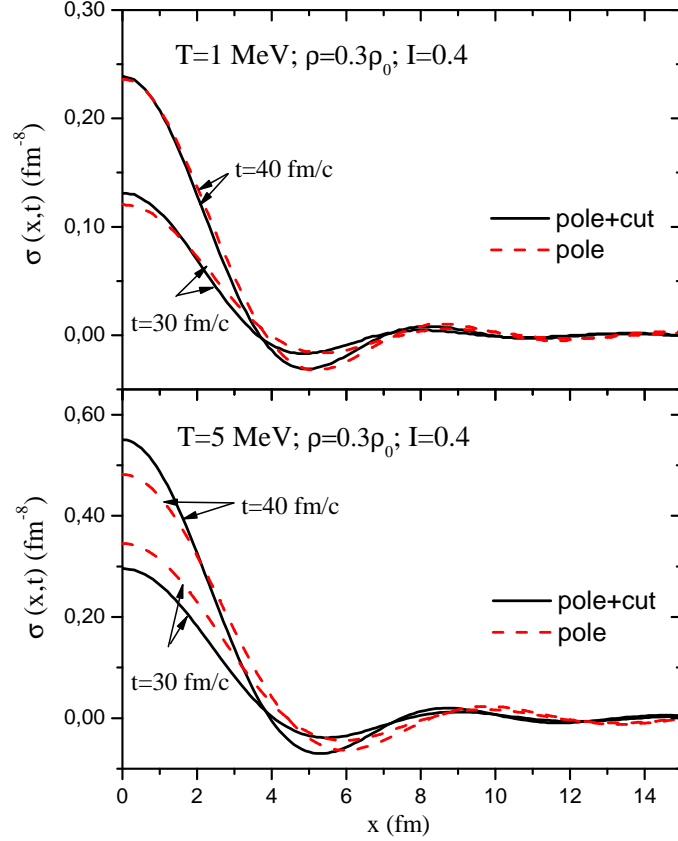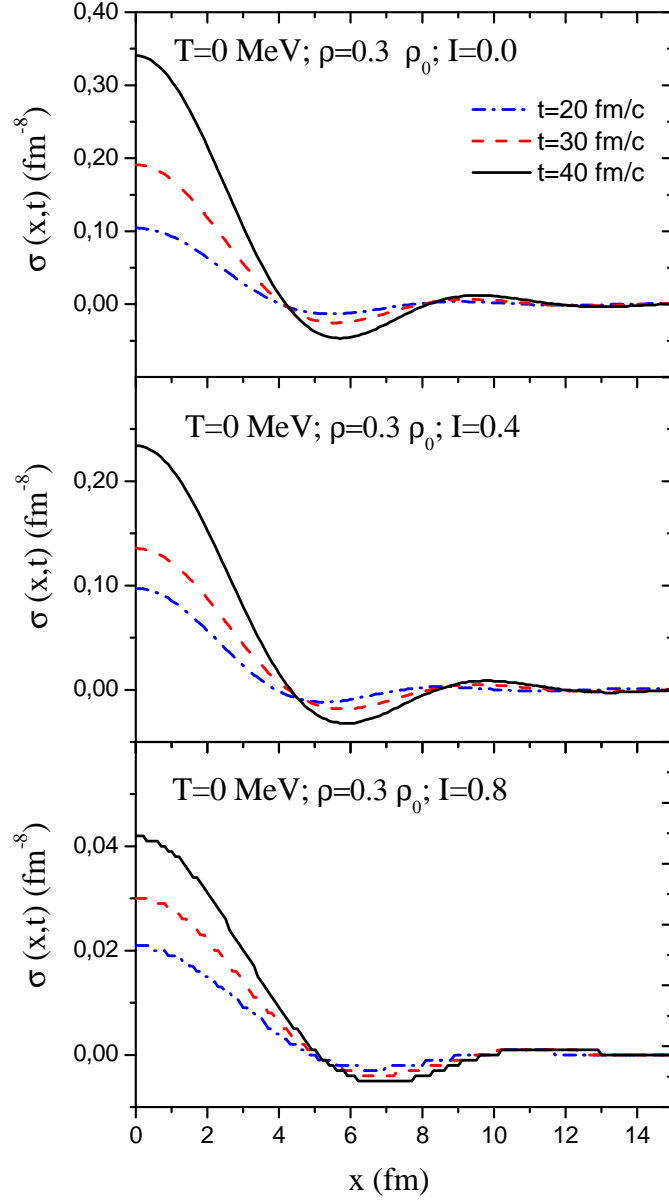
Figure 3.14: Density correlation function as a function of distance between two space points for initial density $\rho = 0.3\rho_0$, at zero temperature and at different charge asymmetries $I = 0.0, 0.4, 0.8$ in sections (a), (b) and (c), respectively.

CHAPTER 4

GROWTH OF DENSITY FLUCTUATIONS IN ASYMMETRIC NUCLEAR MATTER WITHIN A RELATIVISTIC MEAN-FIELD APPROACH

In the previous sections, the spinodal instabilities and early development of density fluctuations are investigated in the framework of the non-relativistic approach since the nuclear spinodal fragmentation occurs at low energies to permit the use of non-relativistic kinematics [3]. However, it has been shown in the recent decades that the nuclear many-body system is in principle a relativistic system of baryons and mesons. Relativistic models have been employed with a great success to describe various aspects of the nuclear structure and nuclear dynamics [32, 33]. A number of investigations on spinodal instabilities in nuclear matter have been carried out by employing the relativistic mean-field models [20].

In this part of the thesis, early development of spinodal instabilities and density fluctuations are investigated for asymmetric nuclear matter by employing the stochastic relativistic mean-field approach in the quantal framework.

4.1 Nonlinear Walecka Model including rho mesons

Quantum Hadrodynamics (QHD) is a general name for the relativistic quantum field theories based on hadronic (baryon and meson) degrees of freedom and it gives a theoretical framework for describing the relativistic nuclear many-body problem. It was introduced by J. D. Walecka in early seventies. The strong interaction between

the nucleons is analyzed in terms of meson exchanges in QHD formalism [10, 32]. The analysis based on QHD provide a suitable description for many baryon systems at low energy scales [10].

In the original Walecka model, also known as QHD-I, the interaction between nucleons are mediated by neutral scalar σ meson and neutral vector ω meson. In the literature, there are several extensions of the standard Walecka model and different parameter sets obtained by fitting the properties of many nuclei. QHD-I describes well the bulk properties of nuclear matter and provides the main feature of the nucleon-nucleon interaction: short range repulsion coming from vector meson exchange while the long-range attraction coming from scalar meson exchange [34]. However, this model does not contain the isospin dependence and can only present a description for the symmetric nuclear matter.

The presence of the isospin degree of freedom enriches the Walecka model and we can examine the effect of asymmetry on the nuclear spinodal instabilities. Therefore, a more realistic model can be obtained by inserting the coupling of charged rho mesons to the Lagrangian of the original model. This extended model known as QHD-II contains the nucleons, neutral scalar σ, neutral vector ω and isovector vector ρ mesons [10].

The effective Lagrangian density of QHD-II including the baryon field $\psi = \begin{pmatrix} \psi_p \\ \psi_n \end{pmatrix}$ with mass M, the scalar meson field ϕ with mass m_s, the vector meson field $V_\mu \equiv (V_0, \vec{V})$ with mass m_v, the isovector field $b_\mu \equiv (b_0, \vec{b})$ with mass m_ρ and the massless photon field $A_\mu \equiv (V_0, \vec{V})$ is given by

$$
\begin{aligned}
L =\ & \overline{\psi}[\gamma^\mu i\hbar\partial_\mu - Mc^2]\psi + \frac{1}{2}\partial_\mu\phi\partial^\mu\phi + g_s\overline{\psi}\psi\phi - U(\phi) \\
& -\frac{1}{4}\Omega_{\mu\nu}\Omega^{\mu\nu} + \frac{1}{2}\mu_v^2 V_\mu V^\mu - g_v\overline{\psi}\gamma^\mu\psi V_\mu \\
& -\frac{1}{4}\vec{G}_{\mu\nu}\vec{G}^{\mu\nu} + \frac{1}{2}\mu_\rho^2 \vec{b}_\mu \vec{b}^\mu - \frac{1}{2}g_\rho\overline{\psi}\gamma^\mu\vec{\tau}\vec{b}_\mu\psi \\
& -\frac{1}{4}F_{\mu\nu}F^{\mu\nu} - \frac{e}{2}(1+\tau_3)\overline{\psi}\gamma^\mu A_\mu\psi
\end{aligned}
\tag{4.1}
$$

where , $\mu_v \equiv m_v c/\hbar$ and $\mu_\rho \equiv m_\rho c/\hbar$ are the mass parameters of vector and isovector meson fields. The related field tensors are represented as $\Omega_{\mu\nu} = \partial_\mu V_\nu - \partial_\nu V_\mu$,

$\vec{G}_{\mu\nu} = \partial_\mu \vec{b}_\nu - \partial_\nu \vec{b}_\mu$ and $F_{\mu\nu} = \partial_\mu A_\nu - \partial_\nu A_\mu$ for the vector, isovector and photon fields, respectively. $\vec{\tau}$ indicates the Pauli isospin matrices and $\frac{1}{2}(1 + \tau_3)$ is the isospin projection operator with the values $\tau_3 = 1$ for proton and $\tau_3 = -1$ for neutron [10]. The neutron and proton form an isospin doublet with total isospin 1/2 and third component $\pm 1/2$.

In the Lagrangian, the mass parameters and the strong coupling constants g_s, g_v and g_ρ for the scalar, vector and isovector fields are phenomenological constants usually determined by a fitting procedure to some properties of a set of spherical nuclei [35]. While the scalar meson potential is $U(\phi) = \frac{1}{2}\mu_s^2\phi^2$ in the standard Walecka model, it is given by $U(\phi) = \frac{1}{2}\mu_s^2\phi^2 + \frac{\kappa}{3!}\phi^3 + \frac{\lambda}{4!}\phi^4$ in the nonlinear Walecka model, where κ and λ are the self-coupling constants and $\mu_s \equiv (m_s c/\hbar)$. In this work, the nonlinear Walecka model is used with the NL3 parameter set which provides a better description for the nuclear structure properties and giant monopole excitations in medium weight and heavy nuclei [20]. The original Walecka model gives nuclear compressibility much higher than the experimental value and leads to a smaller effective nucleon mass [9]. However, the nonlinear Walecka model which includes the nonlinear self-interaction terms of the scalar meson field allows a more accurate value of nuclear compressibility and the nucleon effective mass. In the NL3 parameter set given in Ref. [35], the nucleon mass is taken to be 939 MeV and the other parameters are determined by fitting the predicted values of different nuclear properties such as binding energy, charge radii, and neutron radii of several spherical nuclei. The parameters in the NL3 set are given in Table 4.1 with the corresponding nuclear properties.

The meson field equations can be found from the Lagrangian given in Eq. (4.1) by applying the Euler-Lagrange equation as follows;

$$(\partial_\mu \partial^\mu + \mu_s^2)\phi + \frac{\kappa}{2}\phi^2 + \frac{\lambda}{6}\phi^3 = g_s\bar{\psi}\psi \ , \tag{4.2}$$

$$(\partial_\mu \partial^\mu + \mu_v^2)V^\nu = g_v\bar{\psi}\gamma^\nu\psi, \tag{4.3}$$

$$(\partial_\mu \partial^\mu + \mu_\rho^2)\vec{b}^\nu = \frac{1}{2}g_\rho\overline{\psi}\gamma^\nu\vec{\tau}\psi \ . \tag{4.4}$$

These are the usual Klein-Gordon equations with the source terms $g_s\bar{\psi}\psi$, $g_v\bar{\psi}\gamma^\nu\psi$ and $\frac{1}{2}g_\rho\overline{\psi}\gamma^\nu\vec{\tau}\psi$. The field equation for the electromagnetic field is

$$\partial_\mu \partial^\mu A^\nu = e\left[\overline{\psi}\gamma^\nu\frac{1}{2}(1 + \tau_3)\psi\right] \ . \tag{4.5}$$

Table4.1: The NL3 parameter set and the predictions for the nuclear matter properties

The NL3 Parameter Set	
$m_s(MeV)$	508.194
$m_v(MeV)$	782.501
$m_\rho(MeV)$	763.000
g_s	10.217
g_v	12.868
g_ρ	4.474
$\kappa(fm^{-1})$	10.431
λ	-28.885
Nuclear Matter Properties	
$\rho_0(fm^{-3})$	0.148
E/A (MeV)	-16.299
K (MeV)	271.76
M^*/M	0.60

Similarly, the Dirac equation for the baryon fields including the meson fields and photon field interactions can be obtained as

$$\left[\gamma^\mu(i\hbar\partial_\mu - g_v V_\mu - \frac{1}{2}g_\rho\vec{\tau}\cdot\vec{b_\mu} - e\frac{1}{2}(1+\tau_3)A_\mu) - (Mc^2 - g_s\phi)\right]\psi = 0 \ . \quad (4.6)$$

The field equations, Eqs. (4.2-4.6), are nonlinear coupled equations and the exact solutions are very complicated. Therefore, the mean field approach (MFT) can be applied as an approximate nonperturbative method at high baryon densities. In the relativistic mean-field approximation, the meson field operators are replaced by their ground state expectation values and the meson fields are treated as classical fields

$$\begin{aligned}
\phi &\rightarrow \langle\phi\rangle \equiv \phi_0 \\
V^\mu &\rightarrow \langle V^\mu\rangle \equiv V_0 g^{\mu 0} \\
b_a^\mu &\rightarrow \langle b_a^\mu\rangle \equiv g^{\mu 0}\delta_{a3}b_0 \\
A^\mu &\rightarrow \langle A^\mu\rangle \equiv g^{\mu 0}A_0 \ .
\end{aligned} \quad (4.7)$$

Since nuclear system has well defined electric charge, only the neutral component of the ρ meson field appears in the equation of motion, which is indicated by $b_{3,\mu}(\vec{r},t) \equiv [b_{3,0}(\vec{r},t), \vec{b_3}(\vec{r},t)]$. For a static uniform system at equilibrium, the quantities ϕ_0, V_0, b_0 and A_0 are constants and the expectation values of vector components of the vector,

isovector and photon fields vanish. Similarly, the ground state expectation values are also substituted for the baryon sources in the meson field equations;

$$
\begin{aligned}
\overline{\psi}\psi &\rightarrow \langle\overline{\psi}\psi\rangle = \rho_s \\
\overline{\psi}\gamma^\mu\psi &\rightarrow \langle\overline{\psi}\gamma^\mu\psi\rangle = g^{\mu 0}\rho_{\mathsf{b}} \\
\overline{\psi}\gamma^\mu\tau_a\psi &\rightarrow \langle\overline{\psi}\gamma^\mu\tau_a\psi\rangle = g^{\mu 0}\delta_{a3}\rho_3 \\
\overline{\psi}\gamma^\mu\frac{1}{2}(1+\tau_3)\psi &\rightarrow \langle\overline{\psi}\gamma^\mu\frac{1}{2}(1+\tau_3)\psi\rangle = g^{\mu 0}\rho_p
\end{aligned}
\tag{4.8}
$$

where the densities can be written in terms of proton and neutron densities as; $\rho_{\mathrm{s}} = \rho_{\mathrm{s},p} + \rho_{\mathrm{s},n}$, $\rho_B = \rho_{\mathrm{b},p} + \rho_{\mathrm{b},n}$, $\vec{\rho}_{\mathrm{v}} = \vec{\rho}_{\mathrm{v},p} + \vec{\rho}_{\mathrm{v},n}$ and $\rho_3 = \rho_{\mathrm{b},p} - \rho_{\mathrm{b},n}$. The field equations are exactly solvable in the mean-field limit, thus MFT provides a meaningful starting point to describe the relativistic nuclear many body system [10]. In our investigation of spinodal instabilities, we use time-dependent Hartree Fock (TDHF) model as a mean field approach in a quantal framework.

4.2 Stochastic Extension of Relativistic Mean Field Theory

The mean-field theory in terms of TDHF equations has been widely used to describe the reaction dynamics in nuclear collisions at low energies. At this energy scales, one-body dissipation mechanism plays a dominant role in nuclear dynamics and short range two-body collisions can be neglected [13, 17]. The mean field description gives a good approximation for average evolution of the collective motion. However, it is completely inadequate to describe the fluctuation dynamics of one-body observables. It is demonstrated that the stochastic mean field approach provides a useful description for the dynamics of density fluctuations at low energies [19].

In the SMF approach, different from the standard mean field theory, the initial quantal zero-point and thermal fluctuations are incorporated into the calculations in a stochastic manner. The initial fluctuations are simulated by considering an ensemble of initial single-particle density matrices according to the self-consistent mean-field evolution of each event [17, 36]. Each member of the relativistic single-particle density matrix is developed in time with respect to its own self consistent mean-field hamiltonian

53

$h_a(\rho^{(\lambda)})$ [37],

$$i\hbar\frac{\partial}{\partial t}\rho_a^{(\lambda)}(t) = [h_a(\rho^{(\lambda)}),\ \rho_a^{(\lambda)}(t)]\ . \tag{4.9}$$

where $a = p, n$ denotes the neutron or proton and λ is the event label. This equation is same as the non-relativistic TDHF equation given in Eq. (2.8). However, it should be noted that $h_a(\rho^{(\lambda)})$ represents the relativistic mean-field Hamiltonian in the event λ and $\rho_a(t)$ is a 4×4 matrix in the spinor space whose elements are random Gaussian numbers. For clarity of presentation, the event label is ignored in the rest of the chapter.

In the Walecka model, the relativistic mean field theory is based on an effective interaction Lagrangian given in Eq. (4.1). By using the QHD-II Lagrangian, the relativistic mean-field Hamiltonians are obtained for proton and neutron,

$$h_p(\rho) = \vec{\alpha}\cdot[c\vec{p} - g_v\vec{V} - \frac{1}{2}g_\rho\vec{b}_3 - e\vec{A}] + \beta(Mc^2 - g_s\phi) + g_vV_0 + \frac{1}{2}g_\rho b_{3,0} + eA_0 \tag{4.10}$$

and

$$h_n(\rho) = \vec{\alpha}\cdot[c\vec{p} - g_v\vec{V} + \frac{1}{2}g_\rho\vec{b}_3] + \beta(Mc^2 - g_s\phi) + g_vV_0 - \frac{1}{2}g_\rho b_{3,0}\ . \tag{4.11}$$

where $\vec{\alpha}$ and β are Dirac matrices. Fluctuating meson fields are determined in terms of the fluctuating densities from the usual Klein-Gordon equations as,

$$(\partial_\mu\partial^\mu + \mu_s^2)\phi(\vec{r}, t) = g_s\rho_s(\vec{r}, t) - \frac{\kappa}{2}\phi^2 - \frac{\lambda}{6}\phi^3\ , \tag{4.12}$$

$$(\partial_\mu\partial^\mu + \mu_v^2)V_\mu(\vec{r}, t) = g_v\rho_\mu(\vec{r}, t), \tag{4.13}$$

$$(\partial_\mu\partial^\mu + \mu_\rho^2)\vec{b}_{3,\mu}(\vec{r}, t) = \frac{1}{2}g_\rho\rho_{3,\mu}(\vec{r}, t)\ , \tag{4.14}$$

$$\partial_\mu\partial^\mu A_\mu(\vec{r}, t) = e\rho_\mu^{em}(\vec{r}, t)\ . \tag{4.15}$$

The fluctuating scalar $\rho_a^s(\vec{r}, t)$, baryon $\rho_a^b(\vec{r}, t)$ and current $\vec{\rho}_a^v(\vec{r}, t)$ densities for protons and neutrons are defined according to

$$\begin{pmatrix} \vec{\rho}_a^v(\vec{r}, t) \\ \rho_a^b(\vec{r}, t) \\ \rho_a^s(\vec{r}, t) \end{pmatrix} = \sum_{ij}\Psi_{a,j}^\dagger(\vec{r}, t)\begin{pmatrix} c\vec{\alpha} \\ 1 \\ \beta \end{pmatrix}\Psi_{a,i}(\vec{r}, t)\rho_{ij}(a)\ . \tag{4.16}$$

where summations i, j run over a complete set of spinors $\Psi_{a,i}(\vec{r}, t)$ and $\rho_{ij}(a)$ represents the time-independent elements of the single particle density matrix.

4.3 Linear Response Treatment of Density Fluctuations

The linear response analysis of dynamical evolution is considered in order to investigate the initial growth of density fluctuations in the spinodal region. The small amplitude fluctuations of the single particle density matrix around an equilibrium initial state with proton and neutron densities, $(\rho_p^0, \rho_n^0) \equiv \rho_0$, are obtained by considering the linear limit of Eq. (4.9). For the fluctuating density matrices, $\delta\rho_a(t) = \rho_a(t) - \rho_a^0$, the linearized TDHF equation becomes

$$i\hbar\frac{\partial}{\partial t}\delta\rho_a(t) = [h_a(\rho_0),\ \delta\rho(t)] + [\delta h(t),\ \rho_a^0] \ . \tag{4.17}$$

Here $h_a(\rho_0)$ represents the mean-field Hamiltonian for protons and neutrons in the initial reference state given by

$$h_p(\rho_0) = \vec{\alpha}\cdot c\vec{p} + \beta(Mc^2 - g_s\phi_0) + g_vV_0 + \frac{1}{2}g_\rho b_{3,0} + eA_0 \tag{4.18}$$

and

$$h_n(\rho_0) = \vec{\alpha}\cdot c\vec{p} + \beta(Mc^2 - g_s\phi_0) + g_vV_0 - \frac{1}{2}g_\rho b_{3,0} \ . \tag{4.19}$$

In the initial state, average baryon and scalar densities are assumed to be uniform. Therefore, the meson field equations for asymmetric infinite nuclear matter in terms of initial densities are written as

$$
\begin{aligned}
\phi_0 &= \frac{1}{\mu_s^2}\left[g_s(\rho_{s,p}^0 + \rho_{s,n}^0) - \frac{\kappa}{2}\phi_0^2 - \frac{\lambda}{6}\phi_0^3\right] \\
V_0^0 &= \frac{g_v}{\mu_v^2}(\rho_{b,p}^0 + \rho_{b,n}^0) \\
\vec{V}_0 &= 0 \\
b_3^0 &= \frac{1}{2}\frac{g_\rho}{\mu_\rho^2}(\rho_{b,p}^0 - \rho_{b,n}^0) \\
\vec{b}_3 &= 0 \\
A_0^0 &= 0 \\
\vec{A}_0 &= 0
\end{aligned}
\tag{4.20}
$$

where $\rho_{s,p}^0$, $\rho_{s,n}^0$, $\rho_{b,p}^0$ and $\rho_{b,n}^0$ are scalar and baryon densities for protons and neutrons in the initial state, respectively. The small amplitude fluctuations of the meson fields are determined from the linearized Klein-Gordon equations. Meson fields are

linearized around their initial values as $\phi = \phi_0 + \delta\phi(\vec{r}, t)$, $V^\mu = V_0^\mu + \delta V^\mu(\vec{r}, t)$, $b^\mu = b_0^\mu + \delta b^\mu(\vec{r}, t)$ and $A^\mu = A_0^\mu + \delta A^\mu(\vec{r}, t)$. The meson field fluctuations depends on $(\vec{r}, t)$, however, their initial values ϕ_0, V_0^μ and b_3^μ are constants. Although the vector components of the fields $\vec{V}$, $\vec{b}$, $\vec{A}$ are zero at the initial equilibrium state, the corresponding fluctuations $\delta\vec{V}$, $\delta\vec{b}$ and $\delta\vec{A}$ are non-zero. Then, we obtain the linearized equation for the scalar meson field as

$$\left(\partial_\mu \partial^\mu + \mu_s^2 + \kappa\phi_0(\vec{r}, t) + \frac{\lambda}{2}\phi_0^2 \right) \delta\phi = g_s \delta\rho_s(\vec{r}, t) . \tag{4.21}$$

Similarly, the linearized field equations for the vector meson, charged rho meson and electromagnetic fields are obtained for the space and time components separately, which are given as

$$\begin{aligned}
\left(\partial_\mu \partial^\mu + \mu_v^2 \right) \delta V_0(\vec{r}, t) &= g_v \left(\delta\rho_{b,p}(\vec{r}, t) + \delta\rho_{b,n}(\vec{r}, t) \right) \\
\left(\partial_\mu \partial^\mu + \mu_v^2 \right) \delta\vec{V}(\vec{r}, t) &= g_v \left(\delta\vec{\rho}_{v,p}(\vec{r}, t) + \delta\vec{\rho}_{v,n}(\vec{r}, t) \right) ,
\end{aligned} \tag{4.22}$$

$$\begin{aligned}
\left(\partial_\mu \partial^\mu + \mu_\rho^2 \right) \delta b_0(\vec{r}, t) &= \frac{1}{2}g_\rho \left(\delta\rho_{b,p}(\vec{r}, t) - \delta\rho_{b,n}(\vec{r}, t) \right) \\
\left(\partial_\mu \partial^\mu + \mu_\rho^2 \right) \delta\vec{b}(\vec{r}, t) &= \frac{1}{2}g_\rho \left(\delta\vec{\rho}_{v,p}(\vec{r}, t) - \delta\vec{\rho}_{v,n}(\vec{r}, t) \right)
\end{aligned} \tag{4.23}$$

and

$$\begin{aligned}
\partial_\mu \partial^\mu \delta A_0(\vec{r}, t) &= \delta\rho_{b,p}(\vec{r}, t) \\
\partial_\mu \partial^\mu \delta\vec{A}(\vec{r}, t) &= \delta\vec{\rho}_{v,p}(\vec{r}, t)
\end{aligned} \tag{4.24}$$

Consequently, the fluctuating parts of the mean-field Hamiltonian for protons and neutrons in the linearized TDHF equation are given in terms of meson field fluctuations,

$$\begin{aligned}
\delta h_a &= \left(\frac{\partial h_a}{\partial V_i} \right)_0 \delta V_i + \left(\frac{\partial h_a}{\partial V_0} \right)_0 \delta V_0 + \left(\frac{\partial h_a}{\partial \phi} \right)_0 \delta\phi \\
&+ \left(\frac{\partial h_a}{\partial b_{3,i}} \right)_0 \delta b_{3,i} + \left(\frac{\partial h_a}{\partial b_{3,0}} \right)_0 \delta b_0 + \left(\frac{\partial h_a}{\partial A_i} \right)_0 \delta A_i + \left(\frac{\partial h_a}{\partial A_0} \right)_0 \delta A_0
\end{aligned} \tag{4.25}$$

where $(\ )_0$ denotes the corresponding values at the initial state. The derivatives can simply be evaluated from Eqs. (4.10) and (4.11), then δh_p and δh_n can be found as

$$\begin{aligned}
\delta h_p(t) &= -\vec{\alpha} \cdot [g_v \delta\vec{V}(\vec{r}, t) + \frac{1}{2}g_\rho \delta\vec{b}_3(\vec{r}, t) + e\delta\vec{A}(\vec{r}, t)] - \beta g_s \delta\phi(\vec{r}, t) + g_v \delta V_0(\vec{r}, t) \\
&+ \frac{1}{2}g_\rho \delta b_{3,0}(\vec{r}, t) + e\delta A_0(\vec{r}, t)
\end{aligned} \tag{4.26}$$

56

and

$$\delta h_n(t) = -\vec{\alpha} \cdot [g_v \delta \vec{V}(\vec{r}, t) - \frac{1}{2} g_\rho \delta \vec{b}_3(\vec{r}, t)] - \beta g_s \delta \phi(\vec{r}, t) + g_v \delta V_0(\vec{r}, t) - \frac{1}{2} g_\rho \delta b_{3,0}(\vec{r}, t) \ .$$

(4.27)

The linear response analysis for the instabilities in nuclear matter can be carried out in an almost analytical framework by using the plane wave representation. In this case, the plane wave representation of spinors for protons and neutrons ($a = p, n$) maintains an appropriate description for the quantal investigation of the instabilities. Positive energy ($\lambda = +1$) and negative energy ($\lambda = -1$) plane wave spinors with spin quantum number $s = \pm 1/2$ can be expressed as [38],

$$| \psi_{a,\lambda}(\vec{p}, s)\rangle = N_{a,\lambda}(\vec{p}) \begin{pmatrix} \chi_{a,s} \\ \frac{\vec{\sigma} \cdot c\vec{p}}{Mc^2 + \lambda \varepsilon^*(p)} \chi_{a,s} \end{pmatrix} | e^{i\vec{p} \cdot \vec{r}/\hbar}\rangle \ .$$

(4.28)

Here, $\chi_{\alpha,s} = \begin{pmatrix} 1 \\ 0 \end{pmatrix}, \begin{pmatrix} 0 \\ 1 \end{pmatrix}$ denote spin states for protons and neutrons, $N_{a,\lambda}(\vec{p}) = \sqrt{[Mc^2 + \lambda \varepsilon^*(\vec{p})]/2\lambda \varepsilon^*(p)}$ is the normalization factor and $\varepsilon^*(p) = \sqrt{\vec{p}^2 c^2 + M^{*2} c^4}$ indicates the effective single-particle energies in the initial state which is determined by the effective nucleon mass $M^* c^2 = Mc^2 - g_s \phi_0$. These plane wave spinors are eigenstates of mean-field Hamiltonian in the uniform initial state, $h_a(\rho_0) | \psi_{a,\lambda}(\vec{p}, s)\rangle = E_{a,\lambda}(\vec{p}) | \psi_{a,\lambda}(\vec{p}, s)\rangle$ with the eigenvalues $E_{p,\lambda}(p) = g_v V_0 + \Delta E + \lambda \varepsilon^*(\vec{p})$ for protons and $E_{n,\lambda}(p) = g_v V_0 - \Delta E + \lambda \varepsilon^*(\vec{p})$ for neutrons, where $\Delta E = (g_\rho/2m_\rho)^2 (\rho_{B,p}^0 - \rho_{B,n}^0)$ denotes the single-particle energy shift due to the asymmetry energy. It is possible to express the fluctuating density matrix $\delta \rho_a(t)$ in terms of plane wave spinor representation as follows,

$$\delta \rho_a(t) = \sum_{\lambda \lambda' s_2 s_1} \int \frac{d^3 p_1 d^3 p_2}{(2\pi\hbar)^6} | \Psi_{a,\lambda'}(\vec{p}_2, s_2)\rangle \delta \rho_{a,\lambda'\lambda}^{s_2 s_1}(\vec{p}_2, \vec{p}_1, t)\langle \Psi_{a,\lambda}(\vec{p}_1, s_1) | \ .$$

(4.29)

In this study, the density fluctuations are analyzed in the no-sea approximation. In this expansion, there are four different energy sectors $(\lambda, \lambda') = (+, +), (-, +), (+, -)$ and $(-, -)$ corresponding to positive-energy particle-hole excitations above the Fermi level, negative-energy particle positive-energy hole, negative-energy hole positive-energy particle and particle-hole excitations within the Dirac sea, respectively [37] . The occupation numbers of unoccupied states are zero at zero temperature and very

small at low temperatures in the no-sea approximation, therefore the contributions coming from the sector $(-,-)$ can be ignored in the calculations. According to ref. [37], the particle-hole excitations corresponding to $(+,-)$ and $(-,+)$ sectors make sizable contributions on the excitation strength of giant collective vibrations. However, it was found that contributions of these particle-hole sectors in the development of unstable collective modes are less than 10% for symmetric nuclear matter [17]. In our calculations, we include $(+,-)$ and $(-,+)$ sectors because the magnitude of these contributions tends to increase with increasing charge asymmetry of the system. We consider the spin-averaged matrix elements of the fluctuating single-particle density matrix, $\delta\rho_{a,\lambda'\lambda}(\vec{p}_2,\vec{p}_1,t) = \frac{1}{2}\sum_s \delta\rho_{a,\lambda'\lambda}^{ss}(\vec{p}_2,\vec{p}_1,t)$, to simplify the description. The linearized TDHF equation is obtained in the plane wave representation by calculating the matrix element $\delta\rho_a(t)$ between the spinors as follows,

$$i\hbar\frac{\partial}{\partial t}\langle\Psi_{a,\lambda'}(\vec{p}_2,s_2)\mid\delta\rho_a(t)\mid\Psi_{a,\lambda}(\vec{p}_1,s_1)\rangle =$$
$$[E_{a,\lambda'}(p_2) - E_{a,\lambda}(p_1)]\langle\Psi_{a,\lambda'}(\vec{p}_2,s_2)\mid\delta\rho_a(t)\mid\Psi_{a,\lambda}(\vec{p}_1,s_1)\rangle$$
$$- [n_{a,\lambda'}(p_2) - n_{a,\lambda}(p_1)]\langle\Psi_{a,\lambda'}(\vec{p}_2,s_2)\mid\delta h_a(t)\mid\Psi_{a,\lambda}(\vec{p}_1,s_1)\rangle \quad (4.30)$$

where we use $\rho_a^0\psi_{a,\lambda}(\vec{p},s) = n_{a,\lambda}(p)\psi_{a,\lambda}(\vec{p},s)$. The matrix elements for the fluctuating part of the Hamiltonian for proton and neutron becomes,

$$\langle\Psi_{p,\lambda'}(\vec{p}_2,s_2)\mid\delta h_p(t)\mid\Psi_{p,\lambda}(\vec{p}_1,s_1)\rangle = \int d^3x e^{-i\vec{k}\cdot\vec{x}} u_{\lambda'}^\dagger(\vec{p}_2,s_2)$$
$$\times\left\{-\vec{\alpha}\cdot[g_v\delta\vec{V} + \frac{1}{2}g_\rho\delta\vec{b}_3 + e\delta\vec{A}] - \beta g_s\delta\phi + g_v\delta V_0 + \frac{1}{2}g_\rho\delta b_{3,0} + e\delta A_0\right\}u_\lambda(\vec{p}_1,s_1)$$
$$(4.31)$$

and

$$\langle\Psi_{n,\lambda'}(\vec{p}_2,s_2)\mid\delta h_n(t)\mid\Psi_{n,\lambda}(\vec{p}_1,s_1)\rangle = \int d^3x e^{-i\vec{k}\cdot\vec{x}} u_{\lambda'}^\dagger(\vec{p}_2,s_2)$$
$$\times\left\{-\vec{\alpha}\cdot[g_v\delta\vec{V} + \frac{1}{2}g_\rho\delta\vec{b}_3] - \beta g_s\delta\phi + g_v\delta V_0 + \frac{1}{2}g_\rho\delta b_{3,0}\right\}u_\lambda(\vec{p}_1,s_1)\,.$$
$$(4.32)$$

Here $u_\lambda(\vec{p},s)$ denotes the column vector,

$$u_\lambda(\vec{p},s) = N_\lambda(\vec{p})\begin{pmatrix}\chi_s \\ \frac{\vec{\sigma}\cdot c\vec{p}}{Mc^2+\lambda\varepsilon^*(p)}\chi_s\end{pmatrix}, \qquad (4.33)$$

where χ_s is spin wave function and $u_\lambda^\dagger(\vec{p}, s)$ is transpose of the column vector. In the above expressions, we use the momentum vectors as $\vec{p}_2 = \vec{p} + \hbar\vec{k}/2$ and $\vec{p}_1 = \vec{p} - \hbar\vec{k}/2$. We also introduce $\langle \Psi_{a,\lambda'}(\vec{p}_2, s_2) \mid \delta\rho_a(t) \mid \Psi_{a,\lambda}(\vec{p}_1, s_1) \rangle = \delta\rho_{a,\lambda'\lambda}(\vec{p}_2, \vec{p}_1, t)$, then the linearized TDHF equations for proton and neutron becomes

$$
i\hbar\frac{\partial}{\partial t}\delta\rho_{p,\lambda'\lambda}(\vec{p}_2, \vec{p}_1, t) = [\lambda'\varepsilon^*(p_2) - \lambda\varepsilon^*(p_1)]\delta\rho_{p,\lambda'\lambda}(\vec{p}_2, \vec{p}_1, t)
$$
$$
- [n_{p,\lambda'}(p_2) - n_{p,\lambda}(p_1)]\left\{-u_{\lambda'}^\dagger(\vec{p}_2, s_2)\beta g_s\delta\phi(\vec{k}, t)u_\lambda(\vec{p}_1, s_1)\right.
$$
$$
- u_{\lambda'}^\dagger(\vec{p}_2, s_2)\vec{\alpha}\cdot[g_v\delta\vec{V}(\vec{k}, t) + \frac{1}{2}g_\rho\delta\vec{b}_3(\vec{k}, t) + e\delta\vec{A}(\vec{k}, t)]u_\lambda(\vec{p}_1, s_1)
$$
$$
\left. + u_{\lambda'}^\dagger(\vec{p}_2, s_2)[g_v\delta V_0(\vec{k}, t) + \frac{1}{2}g_\rho\delta b_{3,0}(\vec{k}, t) + e\delta A_0(\vec{k}, t)]u_\lambda(\vec{p}_1, s_1)\right\}
$$
$$
(4.34)
$$

and

$$
i\hbar\frac{\partial}{\partial t}\delta\rho_{n,\lambda'\lambda}(\vec{p}_2, \vec{p}_1, t) = [\lambda'\varepsilon^*(p_2) - \lambda\varepsilon^*(p_1)]\delta\rho_{n,\lambda'\lambda}(\vec{p}_2, \vec{p}_1, t)
$$
$$
- [n_{n,\lambda'}(p_2) - n_{n,\lambda}(p_1)]\left\{-u_{\lambda'}^\dagger(\vec{p}_2, s_2)\vec{\alpha}\cdot[g_v\delta\vec{V}(\vec{k}, t) + \frac{1}{2}g_\rho\delta\vec{b}_3(\vec{k}, t)]u_\lambda(\vec{p}_1, s_1)\right.
$$
$$
- u_{\lambda'}^\dagger(\vec{p}_2, s_2)\beta g_s\delta\phi(\vec{k}, t)u_\lambda(\vec{p}_1, s_1)
$$
$$
\left. + u_{\lambda'}^\dagger(\vec{p}_2, s_2)[g_v\delta V_0(\vec{k}, t) + \frac{1}{2}g_\rho\delta b_{3,0}(\vec{k}, t)]u_\lambda(\vec{p}_1, s_1)\right\}
$$
$$
(4.35)
$$

In these expressions, $n_{a,\lambda}(p) = 1/[exp(\varepsilon^* - \lambda\mu_a^*)/T + 1]$ denotes baryon occupation factors for positive and negative energy states. Here, the reduced chemical potential for proton is $\mu_p^* = \mu_p^0 - \left[g_v V_0 + \frac{1}{2}g_\rho b_{3,0} + eA_0\right]$ and it is $\mu_n^* = \mu_n^0 - \left[g_v V_0 + \frac{1}{2}g_\rho b_{3,0}\right]$ for neutron where μ_a^0 is the chemical potential for protons and neutrons at the initial state. The quantities $\delta\vec{V}(\vec{k}, t)$, $\delta V_0(\vec{k}, t)$, $\delta\vec{A}(\vec{k}, t)$, $\delta A_0(\vec{k}, t)$, $\delta\phi(\vec{k}, t)$, $\delta\vec{b}_3(\vec{k}, t)$, and $\delta b_{3,0}(\vec{k}, t)$ represent the space Fourier transforms of fluctuating vector and meson fields, respectively, with $\hbar\vec{k} = \vec{p}_2 - \vec{p}_1$. For a short hand notation, we define the following quantities,

$$
\begin{aligned}
\xi_{\lambda'\lambda}^b(\vec{p}_2, \vec{p}_1) &= u_{\lambda'}^\dagger(\vec{p}_2, s_2)u_\lambda(\vec{p}_1, s_1) \\
\xi_{\lambda'\lambda}^s(\vec{p}_2, \vec{p}_1) &= u_{\lambda'}^\dagger(\vec{p}_2, s_2)\beta u_\lambda(\vec{p}_1, s_1) \\
\vec{\xi}_{\lambda'\lambda}^v(\vec{p}_2, \vec{p}_1) &= u_{\lambda'}^\dagger(\vec{p}_2, s_2)\vec{\alpha} u_\lambda(\vec{p}_1, s_1)
\end{aligned}
\qquad (4.36)
$$

Consequently, the Eqs. (4.34-4.35) can be expressed as

$$i\hbar\frac{\partial}{\partial t}\delta\rho_{p,\lambda'\lambda}(\vec{p}_2,\vec{p}_1,t) = [\lambda'\varepsilon^*(p_2) - \lambda\varepsilon^*(p_1)]\delta\rho_{p,\lambda'\lambda}(\vec{p}_2,\vec{p}_1,t)$$

$$+[n_{p\lambda}(p_1) - n_{p\lambda'}(p_2)]\left\{-\vec{\xi}^{v}_{\lambda'\lambda}\cdot[g_v\delta\vec{V}(\vec{k},t) + \frac{1}{2}g_\rho\delta\vec{b}_3(\vec{k},t) + e\delta\vec{A}(\vec{k},t)]\right.$$

$$\left.-\xi^{s}_{\lambda'\lambda}g_s\delta\phi(\vec{k},t) + \xi^{b}_{\lambda'\lambda}[g_v\delta V_0(\vec{k},t) + \frac{1}{2}g_\rho\delta b_{3,0}(\vec{k},t) + e\delta A_0(\vec{k},t)]\right\}$$

(4.37)

and

$$i\hbar\frac{\partial}{\partial t}\delta\rho_{n,\lambda'\lambda}(\vec{p}_2,\vec{p}_1,t) = [\lambda'\varepsilon^*(p_2) - \lambda\varepsilon^*(p_1)]\delta\rho_{n,\lambda'\lambda}(\vec{p}_2,\vec{p}_1,t)$$

$$+[n_{n\lambda}(p_1) - n_{n\lambda'}(p_2)]\left\{-\vec{\xi}^{v}_{\lambda'\lambda}\cdot[g_v\delta\vec{V}(\vec{k},t) - \frac{1}{2}g_\rho\delta\vec{b}_3(\vec{k},t)]\right.$$

$$\left.-\xi^{s}_{\lambda'\lambda}g_s\delta\phi(\vec{k},t) + \xi^{b}_{\lambda'\lambda}[g_v\delta V_0(\vec{k},t) - \frac{1}{2}g_\rho\delta b_{3,0}(\vec{k},t)]\right\} .$$

(4.38)

The space Fourier transformation of the meson field fluctuations and the derivation of the quantities $\xi^{b}_{\lambda'\lambda}(\vec{p}_2,\vec{p}_1)$, $\xi^{s}_{\lambda'\lambda}(\vec{p}_2,\vec{p}_1)$ and $\vec{\xi}^{v}_{\lambda'\lambda}(\vec{p}_2,\vec{p}_1)$ are given in Appendix E. We neglect the slight difference of these quantities for proton and neutron due to their effective masses. Moreover, it is possible to express the space Fourier transforms of spin-isospin averaged baryon density, scalar density and vector density fluctuations for protons and neutrons in terms of the fluctuating density matrix as

$$\begin{pmatrix} \delta\vec{\rho}^{v}_a(\vec{k},t) \\ \delta\rho^{s}_a(\vec{k},t) \\ \delta\rho^{b}_a(\vec{k},t) \end{pmatrix} = \gamma\sum_{\lambda\lambda'}\int\frac{d^3p}{(2\pi\hbar)^3}\begin{pmatrix} \vec{\xi}^{v}_{\lambda'\lambda}(\vec{p}_2,\vec{p}_1) \\ \xi^{s}_{\lambda'\lambda}(\vec{p}_2,\vec{p}_1) \\ \xi^{b}_{\lambda'\lambda}(\vec{p}_2,\vec{p}_1) \end{pmatrix}\delta\rho_{a,\lambda'\lambda}(\vec{p}_2,\vec{p}_1,t)$$

(4.39)

where $\gamma = 2$ is the spin factor. The derivation of the above equation is also given in Appendix E in detail.

4.4 Dispersion Relation

The solution for the linear response equations given in Eqs. (4.37-4.38) can be obtained by employing the one-sided Fourier transformation method in time, $\delta\tilde{\rho}_a(\vec{k},\omega) = \int_0^\infty dt e^{i\omega t}\delta\rho_a(\vec{k},t)$. After transformation, the linearized TDHF equations for protons

60

and neutrons becomes

$$i\hbar[\delta\rho_{p,\lambda'\lambda}(\vec{p}_2,\vec{p}_1,0) - i\omega\delta\tilde{\rho}_{p,\lambda'\lambda}(\vec{p}_2,\vec{p}_1,\omega) = [\lambda'\varepsilon^*(p_2) - \lambda\varepsilon^*(p_1)]\delta\rho_{p,\lambda'\lambda}(\vec{p}_2,\vec{p}_1,\omega)$$

$$+[n_{p\lambda}(p_1) - n_{p\lambda'}(p_2)]\left\{-\vec{\xi}_{\lambda'\lambda}^{\mathrm{v}} \cdot [g_{\mathrm{v}}\delta\vec{V}(\vec{k},\omega) + \frac{1}{2}g_\rho\delta\vec{b}_3(\vec{k},\omega) + e\delta\vec{A}(\vec{k},\omega)]\right.$$

$$\left.-\xi_{\lambda'\lambda}^{\mathrm{s}}g_{\mathrm{s}}\delta\phi(\vec{k},\omega) + \xi_{\lambda'\lambda}^{\mathrm{b}}[g_{\mathrm{v}}\delta V_0(\vec{k},\omega) + \frac{1}{2}g_\rho\delta b_{3,0}(\vec{k},\omega) + e\delta A_0(\vec{k},\omega)]\right\} \qquad (4.40)$$

and

$$i\hbar[\delta\rho_{n,\lambda'\lambda}(\vec{p}_2,\vec{p}_1,0) - i\omega\delta\tilde{\rho}_{n,\lambda'\lambda}(\vec{p}_2,\vec{p}_1,\omega) = [\lambda'\varepsilon^*(p_2) - \lambda\varepsilon^*(p_1)]\delta\rho_{n,\lambda'\lambda}(\vec{p}_2,\vec{p}_1,\omega)$$

$$+[n_{n\lambda}(p_1) - n_{n\lambda'}(p_2)]\left\{-\vec{\xi}_{\lambda'\lambda}^{\mathrm{v}} \cdot [g_{\mathrm{v}}\delta\vec{V}(\vec{k},\omega) - \frac{1}{2}g_\rho\delta\vec{b}_3(\vec{k},\omega)]\right.$$

$$\left.-\xi_{\lambda'\lambda}^{\mathrm{s}}g_{\mathrm{s}}\delta\phi(\vec{k},\omega) + \xi_{\lambda'\lambda}^{\mathrm{b}}[g_{\mathrm{v}}\delta V_0(\vec{k},\omega) - \frac{1}{2}g_\rho\delta b_{3,0}(\vec{k},\omega)]\right\}. \qquad (4.41)$$

In these expressions, $\delta\rho_{a,\lambda'\lambda}(\vec{p}_2,\vec{p}_1,0)$ represents fluctuations of proton and neutron density matrices in the initial state. It is possible to express the Fourier transformed forms of the fluctuating meson fields in terms of fluctuating scalar, baryon and current density fluctuations by applying one-sided Fourier transformation to the linearized meson field equations. The solution of the free particle Klein-Gordon equations is taken in the form of the plane wave function, $\phi(x^\mu) \approx e^{i(\vec{k}\cdot\vec{x}-wt)} = e^{i(k_\mu x^\mu)}$. Consequently, the Fourier transforms of the fluctuating meson fields become

$$\delta\phi(\vec{k},\omega) = \left[\frac{g_s}{-w^2 + k^2 + {\mu_s}^2 + \kappa\phi_0 + \frac{\lambda}{2}\phi_0^2}\right]\delta\rho_s(\vec{k},\omega)$$

$$\delta V_0(\vec{k},\omega) = \frac{g_{\mathrm{v}}}{-w^2 + k^2 + {\mu_{\mathrm{v}}}^2}\delta\rho_{\mathrm{b}}(\vec{k},\omega)$$

$$\delta\vec{V}(\vec{k},\omega) = \frac{g_{\mathrm{v}}}{-w^2 + k^2 + {\mu_{\mathrm{v}}}^2}\delta\vec{\rho}_{\mathrm{v}}(\vec{k},\omega)$$

$$\delta b_0(\vec{k},\omega) = \frac{g_\rho}{-w^2 + k^2 + {\mu_\rho}^2}\frac{1}{2}\delta\rho_{3,0}(\vec{k},\omega)$$

$$\delta\vec{b}(\vec{k},\omega) = \frac{g_\rho}{-w^2 + k^2 + {\mu_\rho}^2}\frac{1}{2}\delta\vec{\rho}_3(\vec{k},\omega)$$

$$\delta A_0(\vec{k},\omega) = \frac{e}{-w^2 + k^2}\delta\rho_{\mathrm{b},p}(\vec{k},\omega)$$

$$\delta\vec{A}(\vec{k},\omega) = \frac{e}{-w^2 + k^2}\delta\vec{\rho}_{\mathrm{b},p}(\vec{k},\omega). \qquad (4.42)$$

As a result, the Fourier transforms of the linear response equations for protons and

neutrons in terms of density fluctuations can be obtained as

$$\delta\tilde{\rho}_{p,\lambda'\lambda}(\vec{p}_2,\vec{p}_1,\omega) - X_{p,\lambda'\lambda}(\vec{k},\omega)\left[\frac{n_{p,\lambda'}(\vec{p}_2) - n_{p,\lambda}(\vec{p}_1)}{\hbar\omega - [\lambda'\varepsilon^*(p_2) - \lambda\varepsilon^*(p_1)]}\right]$$
$$= i\hbar\frac{\delta\rho_{p,\lambda'\lambda}(\vec{p}_2,\vec{p}_1,0)}{\hbar\omega - [\lambda'\varepsilon^*(p_2) - \lambda\varepsilon^*(p_1)]} \quad (4.43)$$

and

$$\delta\tilde{\rho}_{n,\lambda'\lambda}(\vec{p}_2,\vec{p}_1,\omega) - X_{n,\lambda'\lambda}(\vec{k},\omega)\left[\frac{n_{n,\lambda'}(\vec{p}_2) - n_{n,\lambda}(\vec{p}_1)}{\hbar\omega - [\lambda'\varepsilon^*(p_2) - \lambda\varepsilon^*(p_1)]}\right]$$
$$= i\hbar\frac{\delta\rho_{n,\lambda'\lambda}(\vec{p}_2,\vec{p}_1,0)}{\hbar\omega - [\lambda'\varepsilon^*(p_2) - \lambda\varepsilon^*(p_1)]} \ . \quad (4.44)$$

where the quantities $X_{p,\lambda'\lambda}(\vec{k},\omega)$ and $X_{n,\lambda'\lambda}(\vec{k},\omega)$ are given by

$$\begin{aligned}
X_{p,\lambda'\lambda}(\vec{k},\omega) &= G_s^2\xi_{\lambda'\lambda}^s\delta\tilde{\rho}_s(\vec{k},\omega) - G_v^2[\xi_{\lambda'\lambda}^b\delta\tilde{\rho}_b(\vec{k},\omega) - \vec{\xi}_{\lambda'\lambda}^v \cdot \delta\vec{\tilde{\rho}}_v(\vec{k},\omega)] \\
&\quad - G_\rho^2[\xi_{\lambda'\lambda}^b\delta\tilde{\rho}_{3,0}(\vec{k},\omega) - \vec{\xi}_{\lambda'\lambda}^v \cdot \delta\vec{\tilde{\rho}}_3(\vec{k},\omega)] \\
&\quad - G_\gamma^2[\xi_{\lambda'\lambda}^b\delta\tilde{\rho}_{p,b}(\vec{k},\omega) - \vec{\xi}_{\lambda'\lambda}^v \cdot \delta\vec{\tilde{\rho}}_{p,v}(\vec{k},\omega)] \quad (4.45)
\end{aligned}$$

and

$$\begin{aligned}
X_{n,\lambda'\lambda}(\vec{k},\omega) &= G_s^2\xi_{\lambda'\lambda}^s\delta\tilde{\rho}_s(\vec{k},\omega) - G_v^2[\xi_{\lambda'\lambda}^b\delta\tilde{\rho}_b(\vec{k},\omega) - \vec{\xi}_{\lambda'\lambda}^v \cdot \delta\vec{\tilde{\rho}}_v(\vec{k},\omega)] \\
&\quad - G_\rho^2[\xi_{\lambda'\lambda}^b\delta\tilde{\rho}_{3,0}(\vec{k},\omega) - \vec{\xi}_{\lambda'\lambda}^v \cdot \delta\vec{\tilde{\rho}}_3(\vec{k},\omega)] \ . \quad (4.46)
\end{aligned}$$

In these expressions, the effective coupling constants are defined in terms of the point coupling constants as

$$\begin{pmatrix} G_v^2 \\ G_s^2 \\ G_\rho^2 \\ G_\gamma^2 \end{pmatrix} = \begin{pmatrix} g_v^2/[-(\omega/c)^2 + k^2 + \mu_v^2] \\ g_s^2/[-(\omega/c)^2 + k^2 + \mu_v^2 - 2g_2\phi_0 - 3g_3\phi_0^2] \\ g_\rho^2/4[-(\omega/c)^2 + k^2 + \mu_\rho^2] \\ e^2/[-(\omega/c)^2 + k^2] \end{pmatrix} \ . \quad (4.47)$$

Multiplying both sides of Eqs. (4.43) and (4.44) by $\xi_{\lambda'\lambda}^b(\vec{p}_2,\vec{p}_1)$ and integrating over the momentum $\vec{p}$ and using the definitions given in Eq. (4.39) for baryon density fluctuations, we obtain the following equations for the Fourier transforms of the baryon density fluctuations for protons and neutrons as follows;

62

$$\delta\tilde{\rho}_p^{\rm b}(\vec{k},\omega) = \gamma\sum_{\lambda\lambda'}\int\frac{d^3p}{(2\pi\hbar)^3}\left[\frac{n_{p,\lambda'}(\vec{p}_2)-n_{p,\lambda}(\vec{p}_1)}{\hbar\omega-[\lambda'\varepsilon^*(p_2)-\lambda\varepsilon^*(p_1)]}\right]\left\{\xi_{\lambda'\lambda}^{\rm b}\xi_{\lambda'\lambda}^{\rm s}G_{\rm s}^2(\delta\tilde{\rho}_p^{\rm s}+\delta\tilde{\rho}_n^{\rm s})\right.$$
$$+\xi_{\lambda'\lambda}^{\rm b}\vec{\xi}_{\lambda'\lambda}^{\rm v}\cdot[(G_{\rm v}^2+G_\rho^2+G_\gamma^2)\delta\vec{\tilde{\rho}}_p^{\rm v}+(G_{\rm v}^2-G_\rho^2)\delta\vec{\tilde{\rho}}_n^{\rm v}]$$
$$-\xi_{\lambda'\lambda}^{\rm b}\xi_{\lambda'\lambda}^{\rm b}[(G_{\rm v}^2+G_\rho^2+G_\gamma^2)\delta\tilde{\rho}_p^{\rm b}+(G_{\rm v}^2-G_\rho^2)\delta\tilde{\rho}_n^{\rm b}]\right\}$$
$$+i\hbar\gamma\sum_{\lambda\lambda'}\int\frac{d^3p}{(2\pi\hbar)^3}\xi_{\lambda'\lambda}^{\rm b}\frac{\delta\rho_{p,\lambda'\lambda}(\vec{p}_2,\vec{p}_1,0)}{\hbar\omega-[\lambda'\varepsilon^*(p_2)-\lambda\varepsilon^*(p_1)]}\qquad(4.48)$$

and

$$\delta\tilde{\rho}_n^{\rm b}(\vec{k},\omega) = \gamma\sum_{\lambda\lambda'}\int\frac{d^3p}{(2\pi\hbar)^3}\left[\frac{n_{n,\lambda'}(\vec{p}_2)-n_{n,\lambda}(\vec{p}_1)}{\hbar\omega-[\lambda'\varepsilon^*(p_2)-\lambda\varepsilon^*(p_1)]}\right]\left\{\xi_{\lambda'\lambda}^{\rm b}\xi_{\lambda'\lambda}^{\rm s}G_{\rm s}^2(\delta\tilde{\rho}_p^{\rm s}+\delta\tilde{\rho}_n^{\rm s})\right.$$
$$+\xi_{\lambda'\lambda}^{\rm b}\vec{\xi}_{\lambda'\lambda}^{\rm v}\cdot[(G_{\rm v}^2-G_\rho^2)\delta\vec{\tilde{\rho}}_p^{\rm v}+(G_{\rm v}^2+G_\rho^2)\delta\vec{\tilde{\rho}}_n^{\rm v}]$$
$$-\xi_{\lambda'\lambda}^{\rm b}\xi_{\lambda'\lambda}^{\rm b}[(G_{\rm v}^2-G_\rho^2)\delta\tilde{\rho}_p^{\rm b}+(G_{\rm v}^2+G_\rho^2)\delta\tilde{\rho}_n^{\rm b}]\right\}$$
$$+i\hbar\gamma\sum_{\lambda\lambda'}\int\frac{d^3p}{(2\pi\hbar)^3}\xi_{\lambda'\lambda}^{\rm b}\frac{\delta\rho_{n,\lambda'\lambda}(\vec{p}_2,\vec{p}_1,0)}{\hbar\omega-[\lambda'\varepsilon^*(p_2)-\lambda\varepsilon^*(p_1)]}\;.\qquad(4.49)$$

Similarly, we can obtain equations for the Fourier transforms of the fluctuating vector density of protons and neutrons after multiplication of Eqs. (4.43) and (4.44) by $\vec{\xi}_{\lambda'\lambda}^{\rm v}(\vec{p}_2,\vec{p}_1)$ and integrating over the momentum, which can be expressed as

$$\delta\vec{\tilde{\rho}}_p^{\rm v} = \gamma\sum_{\lambda\lambda'}\int\frac{d^3p}{(2\pi\hbar)^3}\left[\frac{n_{p,\lambda'}(\vec{p}_2)-n_{p,\lambda}(\vec{p}_1)}{\hbar\omega-[\lambda'\varepsilon^*(p_2)-\lambda\varepsilon^*(p_1)]}\right]\left\{\xi_{\lambda'\lambda}^{\rm v}\xi_{\lambda'\lambda}^{\rm s}G_{\rm s}^2(\delta\tilde{\rho}_p^{\rm s}+\delta\tilde{\rho}_n^{\rm s})\right.$$
$$+\vec{\xi}_{\lambda'\lambda}^{\rm v}\vec{\xi}_{\lambda'\lambda}^{\rm v}\cdot[(G_{\rm v}^2+G_\rho^2+G_\gamma^2)\delta\vec{\tilde{\rho}}_p^{\rm v}+(G_{\rm v}^2-G_\rho^2)\delta\vec{\tilde{\rho}}_n^{\rm v}]$$
$$-\xi_{\lambda'\lambda}^{\rm b}\xi_{\lambda'\lambda}^{\rm b}[(G_{\rm v}^2+G_\rho^2+G_\gamma^2)\delta\tilde{\rho}_p^{\rm b}+(G_{\rm v}^2-G_\rho^2)\delta\tilde{\rho}_n^{\rm b}]\right\}$$
$$+i\hbar\gamma\sum_{\lambda\lambda'}\int\frac{d^3p}{(2\pi\hbar)^3}\vec{\xi}_{\lambda'\lambda}^{\rm v}\frac{\delta\rho_{p,\lambda'\lambda}(\vec{p}_2,\vec{p}_1,0)}{\hbar\omega-[\lambda'\varepsilon^*(p_2)-\lambda\varepsilon^*(p_1)]}\qquad(4.50)$$

and

$$\delta\vec{\tilde{\rho}}_n^{\rm v}(\vec{k},\omega) = \gamma\sum_{\lambda\lambda'}\int\frac{d^3p}{(2\pi\hbar)^3}\left[\frac{n_{n,\lambda'}(\vec{p}_2)-n_{n,\lambda}(\vec{p}_1)}{\hbar\omega-[\lambda'\varepsilon^*(p_2)-\lambda\varepsilon^*(p_1)]}\right]\left\{\vec{\xi}_{\lambda'\lambda}^{\rm v}\xi_{\lambda'\lambda}^{\rm s}G_{\rm s}^2(\delta\tilde{\rho}_p^{\rm s}+\delta\tilde{\rho}_n^{\rm s})\right.$$
$$+\vec{\xi}_{\lambda'\lambda}^{\rm v}\vec{\xi}_{\lambda'\lambda}^{\rm v}\cdot[(G_{\rm v}^2-G_\rho^2)\delta\vec{\tilde{\rho}}_p^{\rm v}+(G_{\rm v}^2+G_\rho^2)\delta\vec{\tilde{\rho}}_n^{\rm v}]$$
$$-\vec{\xi}_{\lambda'\lambda}^{\rm v}\xi_{\lambda'\lambda}^{\rm b}[(G_{\rm v}^2-G_\rho^2)\delta\tilde{\rho}_p^{\rm b}+(G_{\rm v}^2+G_\rho^2)\delta\tilde{\rho}_n^{\rm b}]\right\}$$
$$+i\hbar\gamma\sum_{\lambda\lambda'}\int\frac{d^3p}{(2\pi\hbar)^3}\vec{\xi}_{\lambda'\lambda}^{\rm v}\frac{\delta\rho_{n,\lambda'\lambda}(\vec{p}_2,\vec{p}_1,0)}{\hbar\omega-[\lambda'\varepsilon^*(p_2)-\lambda\varepsilon^*(p_1)]}\;.\qquad(4.51)$$

63

Finally, the last two equations for the proton and neutron scalar density fluctuations can be obtained by multiplying the Eqs. (4.43) and (4.44) by $\xi^{\rm s}_{\lambda'\lambda}(\vec{p}_2, \vec{p}_1)$ and evaluating in a similar procedure presented above. Consequently, we can find

$$
\begin{aligned}
\delta\tilde{\rho}^{\rm s}_p &= \gamma \sum_{\lambda\lambda'} \int \frac{d^3p}{(2\pi\hbar)^3} \left[\frac{n_{p,\lambda'}(\vec{p}_2) - n_{p,\lambda}(\vec{p}_1)}{\hbar\omega - [\lambda'\varepsilon^*(p_2) - \lambda\varepsilon^*(p_1)]} \right] \left\{ \xi^{\rm s}_{\lambda'\lambda}\xi^{\rm s}_{\lambda'\lambda}G_{\rm s}^2(\delta\tilde{\rho}^{\rm s}_p + \delta\tilde{\rho}^{\rm s}_n) \right. \\
&\quad + \xi^{\rm s}_{\lambda'\lambda}\vec{\xi}^{\,\rm v}_{\lambda'\lambda} \cdot [(G_{\rm v}^2 + G_\rho^2 + G_\gamma^2)\delta\vec{\tilde{\rho}}^{\rm v}_p + (G_{\rm v}^2 - G_\rho^2)\delta\vec{\tilde{\rho}}^{\rm v}_n] \\
&\quad \left. - \xi^{\rm s}_{\lambda'\lambda}\xi^{\rm b}_{\lambda'\lambda}[(G_{\rm v}^2 + G_\rho^2 + G_\gamma^2)\delta\tilde{\rho}^{\rm b}_p + (G_{\rm v}^2 - G_\rho^2)\delta\tilde{\rho}^{\rm b}_n] \right\} \\
&\quad + i\hbar\gamma \sum_{\lambda\lambda'} \int \frac{d^3p}{(2\pi\hbar)^3} \xi^{\rm s}_{\lambda'\lambda} \frac{\delta\rho_{p,\lambda'\lambda}(\vec{p}_2, \vec{p}_1, 0)}{\hbar\omega - [\lambda'\varepsilon^*(p_2) - \lambda\varepsilon^*(p_1)]} \quad\quad (4.52)
\end{aligned}
$$

and

$$
\begin{aligned}
\delta\tilde{\rho}^{\rm s}_n(\vec{k}, \omega) &= \gamma \sum_{\lambda\lambda'} \int \frac{d^3p}{(2\pi\hbar)^3} \left[\frac{n_{n,\lambda'}(\vec{p}_2) - n_{n,\lambda}(\vec{p}_1)}{\hbar\omega - [\lambda'\varepsilon^*(p_2) - \lambda\varepsilon^*(p_1)]} \right] \left\{ \xi^{\rm s}_{\lambda'\lambda}\xi^{\rm s}_{\lambda'\lambda}G_{\rm s}^2(\delta\tilde{\rho}^{\rm s}_p + \delta\tilde{\rho}^{\rm s}_n) \right. \\
&\quad + \xi^{\rm s}_{\lambda'\lambda}\vec{\xi}^{\,\rm v}_{\lambda'\lambda} \cdot [(G_{\rm v}^2 - G_\rho^2)\delta\vec{\tilde{\rho}}^{\rm v}_p + (G_{\rm v}^2 + G_\rho^2)\delta\vec{\tilde{\rho}}^{\rm v}_n] \\
&\quad \left. - \xi^{\rm s}_{\lambda'\lambda}\xi^{\rm b}_{\lambda'\lambda}[(G_{\rm v}^2 - G_\rho^2)\delta\tilde{\rho}^{\rm b}_p + (G_{\rm v}^2 + G_\rho^2)\delta\tilde{\rho}^{\rm b}_n] \right\} \\
&\quad + i\hbar\gamma \sum_{\lambda\lambda'} \int \frac{d^3p}{(2\pi\hbar)^3} \xi^{\rm s}_{\lambda'\lambda} \frac{\delta\rho_{n,\lambda'\lambda}(\vec{p}_2, \vec{p}_1, 0)}{\hbar\omega - [\lambda'\varepsilon^*(p_2) - \lambda\varepsilon^*(p_1)]} . \quad\quad (4.53)
\end{aligned}
$$

We have found six coupled algebraic equations represented above, which contain the relations between the Fourier transforms of the small amplitude fluctuations for the baryon density, the scalar density and the vector density of protons and neutrons. These equations can be expressed as a matrix equation in the following form:

$$
\begin{pmatrix}
A_1^p & A_2^p & A_3^p & A_1^n & A_2^n & A_3^n \\
B_1^p & B_2^p & B_3^p & B_1^n & B_2^n & B_3^n \\
C_1^p & C_2^p & C_3^p & C_1^n & C_2^n & C_3^n \\
D_1^p & D_2^p & D_3^p & D_1^n & D_2^n & D_3^n \\
E_1^p & E_2^p & E_3^p & E_1^n & E_2^n & E_3^n \\
F_1^p & F_2^p & F_3^p & F_1^n & F_2^n & F_3^n
\end{pmatrix}
\begin{pmatrix}
\delta\tilde{\rho}^{\rm v}_p(\vec{k}, \omega) \\
\delta\tilde{\rho}^{\rm s}_p(\vec{k}, \omega) \\
\delta\tilde{\rho}^{\rm b}_p(\vec{k}, \omega) \\
\delta\tilde{\rho}^{\rm v}_n(\vec{k}, \omega) \\
\delta\tilde{\rho}^{\rm s}_n(\vec{k}, \omega) \\
\delta\tilde{\rho}^{\rm b}_n(\vec{k}, \omega)
\end{pmatrix}
= i\hbar
\begin{pmatrix}
\tilde{S}^{\rm b}_p(\vec{k}, \omega) \\
\tilde{S}^{\rm s}_p(\vec{k}, \omega) \\
\tilde{S}^{\rm v}_p(\vec{k}, \omega) \\
\tilde{S}^{\rm b}_n(\vec{k}, \omega) \\
\tilde{S}^{\rm s}_n(\vec{k}, \omega) \\
\tilde{S}^{\rm v}_n(\vec{k}, \omega)
\end{pmatrix} . \quad (4.54)
$$

The elements of the coefficient matrix is given by

$$
\begin{pmatrix} A_1^p \\ B_1^p \\ C_1^p \\ D_1^p \\ E_1^p \\ F_1^p \end{pmatrix}
=
\begin{pmatrix} -\left(G_{\mathrm{v}}^2 + G_{\rho}^2 + G_{\gamma}^2\right)\chi_p^{\mathrm{v}} \\ -\left(G_{\mathrm{v}}^2 + G_{\rho}^2 + G_{\gamma}^2\right)\tilde{\chi}_p^{\mathrm{v}} \\ 1-\left(G_{\mathrm{v}}^2 + G_{\rho}^2 + G_{\gamma}^2\right)\tilde{\chi}_p^{b} \\ -\left(G_{\mathrm{v}}^2 - G_{\rho}^2\right)\chi_n^{\mathrm{v}} \\ -\left(G_{\mathrm{v}}^2 - G_{\rho}^2\right)\tilde{\chi}_n^{\mathrm{v}} \\ -\left(G_{\mathrm{v}}^2 - G_{\rho}^2\right)\tilde{\chi}_n^{b} \end{pmatrix}
\qquad
\begin{pmatrix} A_2^p \\ B_2^p \\ C_2^p \\ D_2^p \\ E_2^p \\ F_2^p \end{pmatrix}
=
\begin{pmatrix} -G_{\mathrm{s}}^2\chi_p^{\mathrm{s}} \\ 1-G_{\mathrm{s}}^2\tilde{\chi}_p^{\mathrm{s}} \\ -G_{\mathrm{s}}^2\tilde{\chi}_p^{\mathrm{v}} \\ -G_{\mathrm{s}}^2\chi_n^{\mathrm{s}} \\ -G_{\mathrm{s}}^2\tilde{\chi}_n^{\mathrm{s}} \\ -G_{\mathrm{s}}^2\tilde{\chi}_n^{\mathrm{v}} \end{pmatrix}
$$

$$
\begin{pmatrix} A_3^p \\ B_3^p \\ C_3^p \\ D_3^p \\ E_3^p \\ F_3^p \end{pmatrix}
=
\begin{pmatrix} 1+\left(G_{\mathrm{v}}^2 + G_{\rho}^2 + G_{\gamma}^2\right)\chi_p^{b} \\ \left(G_{\mathrm{v}}^2 + G_{\rho}^2 + G_{\gamma}^2\right)\chi_p^{\mathrm{s}} \\ \left(G_{\mathrm{v}}^2 + G_{\rho}^2 + G_{\gamma}^2\right)\chi_p^{\mathrm{v}} \\ \left(G_{\mathrm{v}}^2 - G_{\rho}^2\right)\chi_n^{b} \\ \left(G_{\mathrm{v}}^2 - G_{\rho}^2\right)\chi_n^{\mathrm{s}} \\ \left(G_{\mathrm{v}}^2 - G_{\rho}^2\right)\chi_n^{\mathrm{v}} \end{pmatrix}
\qquad
\begin{pmatrix} A_1^n \\ B_1^n \\ C_1^n \\ D_1^n \\ E_1^n \\ F_1^n \end{pmatrix}
=
\begin{pmatrix} -\left(G_{\mathrm{v}}^2 - G_{\rho}^2\right)\chi_p^{\mathrm{v}} \\ -\left(G_{\mathrm{v}}^2 - G_{\rho}^2\right)\tilde{\chi}_p^{\mathrm{v}} \\ -\left(G_{\mathrm{v}}^2 - G_{\rho}^2\right)\tilde{\chi}_p^{b} \\ -\left(G_{\mathrm{v}}^2 + G_{\rho}^2\right)\chi_n^{\mathrm{v}} \\ -\left(G_{\mathrm{v}}^2 + G_{\rho}^2\right)\tilde{\chi}_p^{\mathrm{v}} \\ 1-\left(G_{\mathrm{v}}^2 + G_{\rho}^2\right)\tilde{\chi}_n^{b} \end{pmatrix}
$$

$$
\begin{pmatrix} A_2^n \\ B_2^n \\ C_2^n \\ D_2^n \\ E_2^n \\ F_2^n \end{pmatrix}
=
\begin{pmatrix} -G_{\mathrm{s}}^2\chi_p^{\mathrm{s}} \\ -G_{\mathrm{s}}^2\tilde{\chi}_p^{\mathrm{s}} \\ -G_{\mathrm{s}}^2\tilde{\chi}_p^{\mathrm{v}} \\ -G_{\mathrm{s}}^2\chi_n^{\mathrm{s}} \\ 1-G_{\mathrm{s}}^2\tilde{\chi}_n^{\mathrm{s}} \\ -G_{\mathrm{s}}^2\tilde{\chi}_n^{\mathrm{v}} \end{pmatrix}
\qquad
\begin{pmatrix} A_3^n \\ B_3^n \\ C_3^n \\ D_3^n \\ E_3^n \\ F_3^n \end{pmatrix}
=
\begin{pmatrix} \left(G_{\mathrm{v}}^2 - G_{\rho}^2\right)\chi_p^{b} \\ \left(G_{\mathrm{v}}^2 - G_{\rho}^2\right)\chi_p^{s} \\ \left(G_{\mathrm{v}}^2 - G_{\rho}^2\right)\chi_p^{\mathrm{v}} \\ 1+\left(G_{\mathrm{v}}^2 + G_{\rho}^2\right)\chi_n^{b} \\ \left(G_{\mathrm{v}}^2 + G_{\rho}^2\right)\tilde{\chi}_n^{s} \\ \left(G_{\mathrm{v}}^2 + G_{\rho}^2\right)\tilde{\chi}_n^{\mathrm{v}} \end{pmatrix}.
$$

$$(4.55)$$

In the above expressions, the quantities χ's and $\tilde{\chi}$'s are the relativistic quantal Lindhard functions associated with baryon, scalar and vector densities. In our analysis of spinodal instabilities in the relativistic mean field approximation, we consider the longitudinal unstable collective modes. Hence, only the component along the propagation direction are taken into account for the vector density fluctuations and we use the notation $\delta\tilde{\rho}_a^{\mathrm{v}}(\vec{k},\omega) = \delta\vec{\rho}_a^{\mathrm{v}}(\vec{k},\omega)\cdot\vec{k}$ and $\tilde{\xi}_a^{\mathrm{v}} = \vec{\xi}_a^{\mathrm{v}}\cdot\vec{k}$ in the following expressions. For the longitudinal modes, the Linhard functions for charge asymmetric nuclear matter are given by

$$
\begin{pmatrix} \chi_a^{\mathrm{v}}(\vec{k},\omega) \\ \chi_a^{\mathrm{s}}(\vec{k},\omega) \\ \chi_a^{\mathrm{b}}(\vec{k},\omega) \end{pmatrix} = \gamma \sum_{\lambda\lambda'} \int \frac{d^3p}{(2\pi\hbar)^3} \begin{pmatrix} \xi_{\lambda'\lambda}^{\mathrm{b}} \xi_{\lambda'\lambda}^{\mathrm{v}} \\ \xi_{\lambda'\lambda}^{\mathrm{b}} \xi_{\lambda'\lambda}^{\mathrm{s}} \\ \xi_{\lambda'\lambda}^{\mathrm{b}} \xi_{\lambda'\lambda}^{\mathrm{b}} \end{pmatrix}
$$

$$
\times \frac{n_{a,\lambda'}(\vec{p}+\hbar\vec{k}/2) - n_{a,\lambda}(\vec{p}-\hbar\vec{k}/2)}{\hbar\omega - [\lambda'\varepsilon^*(\vec{p}+\hbar\vec{k}/2) - \lambda\varepsilon^*(\vec{p}-\hbar\vec{k}/2)]} \quad (4.56)
$$

and

$$
\begin{pmatrix} \tilde{\chi}_a^{\mathrm{v}}(\vec{k},\omega) \\ \tilde{\chi}_a^{\mathrm{s}}(\vec{k},\omega) \\ \tilde{\chi}_a^{\mathrm{b}}(\vec{k},\omega) \end{pmatrix} = \gamma \sum_{\lambda\lambda'} \int \frac{d^3p}{(2\pi\hbar)^3} \begin{pmatrix} \xi_{\lambda'\lambda}^{\mathrm{s}} \xi_{\lambda'\lambda}^{\mathrm{v}} \\ \xi_{\lambda'\lambda}^{\mathrm{s}} \xi_{\lambda'\lambda}^{\mathrm{s}} \\ \xi_{\lambda'\lambda}^{\mathrm{v}} \xi_{\lambda'\lambda}^{\mathrm{v}} \end{pmatrix}
$$

$$
\times \frac{n_{a,\lambda'}(\vec{p}+\hbar\vec{k}/2) - n_{a,\lambda}(\vec{p}-\hbar\vec{k}/2)}{\hbar\omega - [\lambda'\varepsilon^*(\vec{p}+\hbar\vec{k}/2) - \lambda\varepsilon^*(\vec{p}-\vec{k}/2)]} \; . \quad (4.57)
$$

The stochastic source terms in Eq. (4.54) are given by,

$$
\begin{pmatrix} \tilde{S}_a^{\mathrm{v}}(\vec{k},\omega) \\ \tilde{S}_a^{\mathrm{s}}(\vec{k},\omega) \\ \tilde{S}_a^{\mathrm{b}}(\vec{k},\omega) \end{pmatrix} = \gamma \sum_{\lambda\lambda'} \int \frac{d^3p}{(2\pi\hbar)^3} \begin{pmatrix} \xi_{\lambda'\lambda}^{\mathrm{v}} \\ \xi_{\lambda'\lambda}^{\mathrm{s}} \\ \xi_{\lambda'\lambda}^{\mathrm{b}} \end{pmatrix} \frac{\delta\rho_{a,\lambda'\lambda}(\vec{p}+\hbar\vec{k}/2, \vec{p}-\hbar\vec{k}/2)}{\hbar\omega - [\lambda'\varepsilon^*(\vec{p}+\hbar\vec{k}/2) - \lambda\varepsilon^*(\vec{p}-\hbar\vec{k}/2)]}
$$

$$
(4.58)
$$

where $\delta\rho_{a,\lambda'\lambda}(\vec{p}+\hbar\vec{k}/2, \vec{p}-\hbar\vec{k}/2) = \delta\rho_{a,\lambda'\lambda}(\vec{p}+\hbar\vec{k}/2, \vec{p}-\hbar\vec{k}/2, 0)$ represents the single-particle density matrix fluctuation in the initial state. We can solve the algebraic equation given in Eq. (4.54) for the proton and neutron baryon density fluctuations by applying the Cramer's rule. The proton density fluctuation $\delta\tilde{\rho}_p^{\mathrm{b}}(\vec{k},\omega)$ is found as

$$
\delta\tilde{\rho}_p^{\mathrm{b}}(\vec{k},\omega) = \frac{1}{\varepsilon(\vec{k},\omega)} \begin{vmatrix} A_1^p & A_2^p & i\hbar\tilde{S}_p^{\mathrm{b}} & A_1^n & A_2^n & A_3^n \\ B_1^p & B_2^p & i\hbar\tilde{S}_p^{\mathrm{s}} & B_1^n & B_2^n & B_3^n \\ C_1^p & C_2^p & i\hbar\tilde{S}_p^{\mathrm{v}} & C_1^n & C_2^n & C_3^n \\ D_1^p & D_2^p & i\hbar\tilde{S}_n^{\mathrm{b}} & D_1^n & D_2^n & D_3^n \\ E_1^p & E_2^p & i\hbar\tilde{S}_n^{\mathrm{s}} & E_1^n & E_2^n & E_3^n \\ F_1^p & F_2^p & i\hbar\tilde{S}_n^{\mathrm{v}} & F_1^n & F_2^n & F_3^n \end{vmatrix} \quad (4.59)
$$

where $\varepsilon(\vec{k},\omega)$ denotes the susceptibility. If we expand this equation with respect to the third column, we get

66

$$\delta\tilde{\rho}_p^{\mathrm{b}}(\vec{k},\omega) =$$

$$+ \frac{i\hbar\tilde{S}_p^{\mathrm{v}}}{\varepsilon(\vec{k},\omega)} \begin{vmatrix} B_1^p & B_2^p & B_1^n & B_2^n & B_3^n \\ C_1^p & C_2^p & C_1^n & C_2^n & C_3^n \\ D_1^p & D_2^p & D_1^n & D_2^n & D_3^n \\ E_1^p & E_2^p & E_1^n & E_2^n & E_3^n \\ F_1^p & F_2^p & F_1^n & F_2^n & F_3^n \end{vmatrix} - \frac{i\hbar\tilde{S}_p^{\mathrm{s}}}{\varepsilon(\vec{k},\omega)} \begin{vmatrix} A_1^p & A_2^p & A_1^n & A_2^n & A_3^n \\ C_1^p & C_2^p & C_1^n & C_2^n & C_3^n \\ D_1^p & D_2^p & D_1^n & D_2^n & D_3^n \\ E_1^p & E_2^p & E_1^n & E_2^n & E_3^n \\ F_1^p & F_2^p & F_1^n & F_2^n & F_3^n \end{vmatrix}$$

$$+ \frac{i\hbar\tilde{S}_p^{\mathrm{b}}}{\varepsilon(\vec{k},\omega)} \begin{vmatrix} A_1^p & A_2^p & A_1^n & A_2^n & A_3^n \\ B_1^p & B_2^p & B_1^n & B_2^n & B_3^n \\ D_1^p & D_2^p & D_1^n & D_2^n & D_3^n \\ E_1^p & E_2^p & E_1^n & E_2^n & E_3^n \\ F_1^p & F_2^p & F_1^n & F_2^n & F_3^n \end{vmatrix} - \frac{i\hbar\tilde{S}_n^{\mathrm{v}}}{\varepsilon(\vec{k},\omega)} \begin{vmatrix} A_1^p & A_2^p & A_1^n & A_2^n & A_3^n \\ B_1^p & B_2^p & B_1^n & B_2^n & B_3^n \\ C_1^p & C_2^p & C_1^n & C_2^n & C_3^n \\ E_1^p & E_2^p & E_1^n & E_2^n & E_3^n \\ F_1^p & F_2^p & F_1^n & F_2^n & F_3^n \end{vmatrix}$$

$$+ \frac{i\hbar\tilde{S}_n^{\mathrm{s}}}{\varepsilon(\vec{k},\omega)} \begin{vmatrix} A_1^p & A_2^p & A_1^n & A_2^n & A_3^n \\ B_1^p & B_2^p & B_1^n & B_2^n & B_3^n \\ C_1^p & C_2^p & C_1^n & C_2^n & C_3^n \\ D_1^p & D_2^p & D_1^n & D_2^n & D_3^n \\ F_1^p & F_2^p & F_1^n & F_2^n & F_3^n \end{vmatrix} - \frac{i\hbar\tilde{S}_n^{\mathrm{b}}}{\varepsilon(\vec{k},\omega)} \begin{vmatrix} A_1^p & A_2^p & A_1^n & A_2^n & A_3^n \\ B_1^p & B_2^p & B_1^n & B_2^n & B_3^n \\ C_1^p & C_2^p & C_1^n & C_2^n & C_3^n \\ D_1^p & D_2^p & D_1^n & D_2^n & D_3^n \\ E_1^p & E_2^p & E_1^n & E_2^n & E_3^n \end{vmatrix}$$

$$(4.60)$$

where the five by five matrices are defined as N_1^p, N_2^p, N_3^p, N_4^p, N_5^p, N_6^p respectively. By using these definitions, the baryon density fluctuations for proton can be expressed as

$$\delta\tilde{\rho}_p^{b}(\vec{k},\omega) = \frac{i\hbar}{\varepsilon(\vec{k},\omega)}[N_1^p\tilde{S}_p^{\mathrm{b}} - N_2^p\tilde{S}_p^{\mathrm{s}} + N_3^p\tilde{S}_p^{\mathrm{v}} - N_4^p\tilde{S}_n^{\mathrm{b}} + N_5^p\tilde{S}_n^{\mathrm{s}} - N_6^p\tilde{S}_n^{\mathrm{v}}]. \quad (4.61)$$

By the same way, the neutron density fluctuations $\delta\tilde{\rho}_n^{b}(\vec{k},\omega)$ is obtained as

$$\delta\tilde{\rho}_n^{b}(\vec{k},\omega) = \frac{i\hbar}{\varepsilon(\vec{k},\omega)}[-N_1^n\tilde{S}_p^{\mathrm{b}} + N_2^n\tilde{S}_p^{\mathrm{s}} - N_3^p\tilde{S}_p^{\mathrm{v}} + N_4^n\tilde{S}_n^{\mathrm{b}} - N_5^n\tilde{S}_n^{\mathrm{s}} + N_6^n\tilde{S}_n^{\mathrm{v}}]. \quad (4.62)$$

67

Here the expansion coefficients N_j^n, for $j = 1, ..., 6$ are given by

$$
N_1^n = \begin{vmatrix} B_1^p & B_2^p & B_3^p & B_1^n & B_2^n \\ C_1^p & C_2^p & C_3^p & C_1^n & C_2^n \\ D_1^p & D_2^p & D_3^p & D_1^n & D_2^n \\ E_1^p & E_2^p & E_3^p & E_1^n & E_2^n \\ F_1^p & F_2^p & F_3^p & F_1^n & F_2^n \end{vmatrix} \quad
N_2^n = \begin{vmatrix} A_1^p & A_2^p & A_3^p & A_1^n & A_2^n \\ C_1^p & C_2^p & C_3^p & C_1^n & C_2^n \\ D_1^p & D_2^p & D_3^p & D_1^n & D_2^n \\ E_1^p & E_2^p & E_3^p & E_1^n & E_2^n \\ F_1^p & F_2^p & F_3^p & F_1^n & F_2^n \end{vmatrix}
$$

$$
N_3^n = \begin{vmatrix} A_1^p & A_2^p & A_3^p & A_1^n & A_2^n \\ B_1^p & B_2^p & B_3^p & B_1^n & B_2^n \\ D_1^p & D_2^p & D_3^p & D_1^n & D_2^n \\ E_1^p & E_2^p & E_3^p & E_1^n & E_2^n \\ F_1^p & F_2^p & F_3^p & F_1^n & F_2^n \end{vmatrix} \quad
N_4^n = \begin{vmatrix} A_1^p & A_2^p & A_3^p & A_1^n & A_2^n \\ B_1^p & B_2^p & B_3^p & B_1^n & B_2^n \\ C_1^p & C_2^p & C_3^p & C_1^n & C_2^n \\ E_1^p & E_2^p & E_3^p & E_1^n & E_2^n \\ F_1^p & F_2^p & F_3^p & F_1^n & F_2^n \end{vmatrix}
$$

$$
N_5^n = \begin{vmatrix} A_1^p & A_2^p & A_3^p & A_1^n & A_2^n \\ B_1^p & B_2^p & B_3^p & B_1^n & B_2^n \\ C_1^p & C_2^p & C_3^p & C_1^n & C_2^n \\ D_1^p & D_2^p & D_3^p & D_1^n & D_2^n \\ F_1^p & F_2^p & F_3^p & F_1^n & F_2^n \end{vmatrix} \quad
N_6^n = \begin{vmatrix} A_1^p & A_2^p & A_3^p & A_1^n & A_2^n \\ B_1^p & B_2^p & B_3^p & B_1^n & B_2^n \\ C_1^p & C_2^p & C_3^p & C_1^n & C_2^n \\ D_1^p & D_2^p & D_3^p & D_1^n & D_2^n \\ E_1^p & E_2^p & E_3^p & E_1^n & E_2^n \end{vmatrix} .
$$

$$(4.63)$$

Furthermore, the susceptibility is defined as the determinant of the coefficient matrix in Eq. (4.54),

$$
\varepsilon(\vec{k}, \omega) = \begin{vmatrix} A_1^p & A_2^p & A_3^p & A_1^n & A_2^n & A_3^n \\ B_1^p & B_2^p & B_3^p & B_1^n & B_2^n & B_3^n \\ C_1^p & C_2^p & C_3^p & C_1^n & C_2^n & C_3^n \\ D_1^p & D_2^p & D_3^p & D_1^n & D_2^n & D_3^n \\ E_1^p & E_2^p & E_3^p & E_1^n & E_2^n & E_3^n \\ F_1^p & F_2^p & F_3^p & F_1^n & F_2^n & F_3^n \end{vmatrix} .
\qquad (4.64)
$$

The condition $\varepsilon(\vec{k}, \omega) = 0$ gives the dispersion relation. The boundary of the spinodal region and the growth rates for the unstable collective modes in the spinodal region can be calculated from the dispersion relation.

4.5 Growth of Baryon Density Fluctuations

The time development of baryon density fluctuations is determined by taking the inverse Fourier transform of $\delta\tilde{\rho}_a^B(\vec{k}, \omega)$ in time as $\delta\tilde{\rho}_a^B(\vec{k}, t) = \int \frac{\omega}{2\pi} \delta\tilde{\rho}_a^B(\vec{k}, \omega) e^{-i\omega t}$. We can evaluate this integral with the help of residue theorem. When using the residue theorem, we need to consider the poles arising from the susceptibility and source terms $\tilde{S}_a^b$, $\tilde{S}_a^s$ and $\tilde{S}_a^v$ in Eqs. (4.61) and (4.62). As mentioned in Chapter 2, non-collective poles are important for specifying density fluctuations at the initial state, however the resulting density fluctuations do not grow in time [21]. Moreover, it is known from the previous analysis that the contributions of the non-collective poles are effective for higher wave numbers. Therefore, we neglect non-collective poles of the susceptibility and poles of the source terms in this analysis. In the calculation of density fluctuations, we keep only the collective poles of the susceptibility which give the dominant contribution. There are two collective poles at $\omega = \mp i\Gamma_k$ in the spinodal region and by evaluating these poles according to the Cauchy-Residue theorem, we find

$$\delta\tilde{\rho}_a^B(\vec{k}, t) = \delta\rho_a^+(\vec{k}) e^{+\Gamma_k t} + \delta\rho_a^-(\vec{k}) e^{-\Gamma_k t} \tag{4.65}$$

where the growing and decaying parts of neutron and proton baryon density fluctuations given as

$$\delta\rho_n^\mp(\vec{k}) = -\hbar \left\{ \frac{-N_1^n \tilde{S}_p^b + N_2^n \tilde{S}_p^s - N_3^n \tilde{S}_p^v + N_4^n \tilde{S}_n^b - N_5^n \tilde{S}_n^s + N_6^n \tilde{S}_n^v}{\partial\varepsilon(\vec{k}, \omega)/\partial\omega} \right\}_{\omega = \mp i\Gamma_k} \tag{4.66}$$

and

$$\delta\rho_p^\mp(\vec{k}) = -\hbar \left\{ \frac{N_1^p \tilde{S}_p^b - N_2^p \tilde{S}_p^s + N_3^p \tilde{S}_p^v - N_4^p \tilde{S}_n^b + N_5^p \tilde{S}_n^s - N_6^p \tilde{S}_n^v}{\partial\varepsilon(\vec{k}, \omega)/\partial\omega} \right\}_{\omega = \mp i\Gamma_k}. \tag{4.67}$$

The derivative of the susceptibility $\frac{\partial\varepsilon(\vec{k}, \omega)}{\partial\omega}$ are presented in Appendix F.

By using the time development of density fluctuations, we can calculate the correlation function of density fluctuations and obtain useful information about dynamical evolution of the unstable nuclear system in the spinodal region. Here we consider only the baryon density correlation function. The equal time baryon density correla-

tion function can be defined as

$$\sigma_{ab}(|\vec{r} - \vec{r}'|, t) = \overline{\delta\rho_a^B(\vec{r}, t)\delta\rho_b^B(\vec{r}', t)} = \int \frac{d^3k}{(2\pi)^3} e^{i\vec{k}\cdot\vec{x}} \tilde{\sigma}_{ab}(\vec{k}, t) \qquad (4.68)$$

where a and b represent the neutron or proton. Here $x = \vec{r} - \vec{r}'$ denotes distance between two space locations and $\tilde{\sigma}_{ab}(\vec{k}, t)$ is the spectral intensity of the baryon density correlation functions. In the SMF approach, spectral intensities are defined as the second moment of the Fourier transform of the baryon density fluctuations according to,

$$\overline{\delta\tilde{\rho}_a^B(\vec{k}, t)(\delta\tilde{\rho}_b^B(\vec{k}', t))^*} = (2\pi)^3 \delta(\vec{k} - \vec{k}')\tilde{\sigma}_{ab}(\vec{k}, t) \qquad (4.69)$$

where the overline denotes the average over the ensemble produced at the initial state. In order to calculate the total spectral intensity function, we consider all the contributions arising from protons, neutrons and cross terms as $\tilde{\sigma}(\vec{k}, t) = \tilde{\sigma}_{pp}(\vec{k}, t) + \tilde{\sigma}_{np}(\vec{k}, t) + \tilde{\sigma}_{pn}(\vec{k}, t) + \tilde{\sigma}_{nn}(\vec{k}, t)$. By using the growing and decaying parts of the density fluctuations, the spectral intensity of baryon density correlations can be expressed as

$$\tilde{\sigma}_{ab}^{BB}(\vec{k}, t)(2\pi)^3\delta^3(\vec{k} - \vec{k}') = \overline{\delta\rho_a^{B+}(\vec{k})(\delta\rho_b^{B+}(\vec{k}))^*}e^{2\Gamma_k t} + \overline{\delta\rho_a^{B-}(\vec{k})(\delta\rho_b^{B-}(\vec{k}))^*}e^{-2\Gamma_k t}$$
$$+\overline{\delta\rho_a^{B+}(\vec{k})(\delta\rho_b^{B-}(\vec{k}))^*} + \overline{\delta\rho_a^{B-}(\vec{k})(\delta\rho_b^{B+}(\vec{k}))^*} .$$
$$(4.70)$$

According to the main assumption of the Stochastic mean-field approach, the variance of the initial density fluctuations in the plane wave representation can be expressed in the following form:

$$\overline{\delta\rho_{\lambda\mu}^a(\vec{p}_2, \vec{p}_1, 0)\delta\rho_{\lambda'\mu'}^b(\vec{p}_2, \vec{p}_1, 0)} = \delta_{ab}\delta_{\lambda\lambda'}\delta_{\mu\mu'}(2\pi\hbar)^6\delta(\vec{p}_1 - \vec{p}_1')\delta(\vec{p}_2 - \vec{p}_2')$$
$$\times \frac{1}{2}\left[n_\lambda(\vec{p}_2)(1 - n_\mu(\vec{p}_1)) + n_\mu(\vec{p}_1)(1 - n_\lambda(\vec{p}_2))\right]$$
$$(4.71)$$

where the factor $(2\pi\hbar)^6$ emerges due to the normalization in the plane wave representation. Each term in Eq. (4.70) is calculated by employing this result. For instance, we obtain the first and second terms for proton-proton spectral intensity function by

taking $a = b = p$ as

$$\overline{\left(\delta\rho_p^B(\vec{k})\right)^{\pm}\left[\left(\delta\rho_p^B(\vec{k})\right)^{\pm}\right]^*} = \frac{(2\pi)^3\delta(\vec{k}-\vec{k}')\hbar^2}{\left|\left(\frac{\partial\varepsilon(k,\omega)}{\partial\omega}\right)_{\omega=i\Gamma}\right|^2}$$

$$\times \left\{ K_{BB}^{+p}|N_{1p}^+|^2 - K_{BS}^{+p}(N_{1p}^{+*}N_{2p}^+ + N_{2p}^+N_{1p}^{+*}) + K_{SS}^{+p}|N_{2p}^+|^2 + K_{VV}^{+p}|N_{3p}^+|^2 \right.$$

$$+K_{BB}^{+n}|N_{4p}^+|^2 - K_{BS}^{+n}(N_{4p}^+N_{5p}^{+*} + N_{5p}^+N_{4p}^{+*}) + K_{SS}^{+n}|N_{5p}^+|^2 + K_{VV}^{+n}|N_{6p}^+|^2$$

$$+ K_{BV}^{+p}(N_{1p}^+N_{3p}^{+*} + N_{3p}^+N_{1p}^{+*}) - K_{SV}^{+p}(N_{2p}^+N_{3p}^{+*} + N_{3p}^+N_{2p}^{+*})$$

$$\left. + K_{BV}^{+n}(N_{4p}^+N_{6p}^{+*} + N_{6p}^+N_{4p}^{+*}) - K_{SV}^{+n}(N_{5p}^+N_{6p}^{+*} + N_{6p}^+N_{5p}^{+*}) \right\} \qquad (4.72)$$

The third and fourth terms can be written as,

$$\overline{\left(\delta\rho_p^B(\vec{k})\right)^{+}\left[\left(\delta\rho_p^B(\vec{k})\right)^{-}\right]^*} = \frac{(2\pi)^3\delta(\vec{k}-\vec{k}')\hbar^2}{\left[\left(\frac{\partial\varepsilon(k,\omega)}{\partial\omega}\right)_{\omega=i\Gamma}\right]\left[\left(\frac{\partial\varepsilon(k,\omega)}{\partial\omega}\right)_{\omega=-i\Gamma}\right]^*}$$

$$\times \left\{ K_{BB}^{-p}N_{1p}^+N_{1p}^{-*} - K_{BS}^{-p}(N_{1p}^+N_{2p}^{-*} + N_{2p}^+N_{1p}^{-*}) + K_{SS}^{-p}N_{2p}^+N_{2p}^{-*} + K_{VV}^{-p}N_{3p}^+N_{3p}^{-*} \right.$$

$$+K_{BB}^{-n}N_{4p}^+N_{4p}^{-*} - K_{BS}^{-n}(N_{4p}^+N_{5p}^{-*} + N_{5p}^+N_{4p}^{-*}) + K_{SS}^{-n}N_{5p}^+N_{5p}^{-*} + K_{VV}^{-n}N_{6p}^+N_{6p}^{-*}$$

$$+K_{BV}^{-p}(N_{1p}^+N_{3p}^{-*} + N_{3p}^+N_{1p}^{-*}) - K_{SV}^{-p}(N_{2p}^+N_{3p}^{-*} + N_{3p}^+N_{2p}^{-*})$$

$$\left. + K_{BV}^{-n}(N_{4p}^+N_{6p}^{-*} + N_{6p}^+N_{4p}^{-*}) - K_{SV}^{-n}(N_{5p}^+N_{6p}^{-*} + N_{6p}^+N_{5p}^{-*}) \right\}$$

$$(4.73)$$

and

$$\overline{\left(\delta\rho_p^B(\vec{k})\right)^{-}\left[\left(\delta\rho_p^B(\vec{k})\right)^{+}\right]^*} = \frac{(2\pi)^3\delta(\vec{k}-\vec{k}')\hbar^2}{\left[\left(\frac{\partial\varepsilon(k,\omega)}{\partial\omega}\right)_{\omega=-i\Gamma}\right]\left[\left(\frac{\partial\varepsilon(k,\omega)}{\partial\omega}\right)_{\omega=i\Gamma}\right]^*}$$

$$\times \left\{ K_{BB}^{-p}N_{1p}^-N_{1p}^{+*} - K_{BS}^{-p}(N_{1p}^-N_{2p}^{+*} + N_{2p}^-N_{1p}^{+*}) + K_{SS}^{-p}N_{2p}^-N_{2p}^{+*} + K_{VV}^{-p}N_{3p}^-N_{3p}^{+*} \right.$$

$$+K_{BB}^{-n}N_{4p}^-N_{4p}^{+*} - K_{BS}^{-n}(N_{4p}^-N_{5p}^{+*} + N_{5p}^-N_{4p}^{+*}) + K_{SS}^{-n}N_{5p}^-N_{5p}^{+*} + K_{VV}^{-n}N_{6p}^-N_{6p}^{+*}$$

$$+K_{BV}^{-p}(N_{1p}^-N_{3p}^{+*} + N_{3p}^-N_{1p}^{+*}) - K_{SV}^{-p}(N_{2p}^-N_{3p}^{+*} + N_{3p}^-N_{2p}^{+*})$$

$$\left. + K_{BV}^{-n}(N_{4p}^-N_{6p}^{+*} + N_{6p}^-N_{4p}^{+*}) - K_{SV}^{-n}(N_{5p}^-N_{6p}^{+*} + N_{6p}^-N_{5p}^{+*}) \right\} \ .$$

$$(4.74)$$

In the above expressions, N_{ia}^+ factors are evaluated at $\omega = +i\Gamma_k$ and N_{ia}^- factors are evaluated at $\omega = -i\Gamma_k$ for $i = 1, ..., 6$. According to the numerical calculations, $N_{1a}^\pm, N_{2a}^\pm, N_{4a}^\pm$ and $N_{5a}^\pm$ are found as real and $N_{3a}^\pm, N_{6a}^\pm$ are imaginary. There is a relation between them, that can be written as $N_{ia}^- = N_{ia}^+$ for $i = 1, 2, 4, 5$ and $N_{ia}^- = -N_{ia}^+$

71

for $i = 3, 6$. Consequently, if we write the spectral intensity function as

$$\tilde{\sigma}_{pp}(\vec{k}, t) = \hbar^2 \frac{E_{pp}^+}{\left|\left(\frac{\partial \varepsilon(k,\omega)}{\partial \omega}\right)_{\omega=i\Gamma}\right|^2} (e^{2\Gamma t} + e^{-2\Gamma t}) + \hbar^2 \frac{E_{pp}^{+-} + E_{pp}^{-+}}{\left[\left(\frac{\partial \varepsilon(k,\omega)}{\partial \omega}\right)_{\omega=i\Gamma}\right]\left[\left(\frac{\partial \varepsilon(k,\omega)}{\partial \omega}\right)_{\omega=-i\Gamma}\right]^*}$$
(4.75)

where the short-hand notation E are used for the terms in parenthesis in Eqs. (4.72-4.74), the contributions coming from K_{BV}^{-a} and K_{SV}^{-a} terms cancelled each other.

The spectral intensities $\tilde{\sigma}_{nn}(\vec{k}, t)$, $\tilde{\sigma}_{pn}(\vec{k}, t)$ and $\tilde{\sigma}_{np}(\vec{k}, t)$ can also be determined by following the same steps. The detailed calculations are given in Appendix G. As a result, the spectral intensity of density correlation functions can be written in a general form as

$$\tilde{\sigma}_{ab}(\vec{k}, t) = \hbar^2 \frac{E_{ab}^+(\vec{k})}{|[\partial \varepsilon(\vec{k},\omega)/\partial \omega]_{\omega=i\Gamma_k}|^2} (e^{+2\Gamma_k t} + e^{-2\Gamma_k t}) + \frac{2\hbar^2 E_{ab}^-(\vec{k})}{|[\partial \varepsilon(\vec{k},\omega)/\partial \omega]_{\omega=i\Gamma_k}|^2}$$
(4.76)

where the quantities $E_{ab}^{\pm}$ for neutrons, protons and cross terms are given by

$$
\begin{aligned}
E_{pp}^{\pm} &= K_{BB}^{\pm p}|N_{1p}^+|^2 - 2K_{BS}^{\pm p}(N_{1p}^+ N_{2p}^+) + K_{SS}^{\pm p}|N_{2p}^+|^2 + K_{VV}^{\pm p}|N_{3p}^+|^2 \\
&\quad + K_{BB}^{\pm n}|N_{4p}^+|^2 - 2K_{BS}^{\pm n}(N_{4p}^+ N_{5p}^+) + K_{SS}^{\pm n}|N_{5p}^+|^2 + K_{VV}^{\pm n}|N_{6p}^+|^2
\end{aligned}
$$

$$
\begin{aligned}
E_{nn}^{\pm} &= K_{BB}^{\pm p}|N_{1n}^+|^2 - 2K_{BS}^{\pm p}(N_{1n}^+ N_{2n}^+) + K_{SS}^{\pm p}|N_{2n}^+|^2 + K_{VV}^{\pm p}|N_{3n}^+|^2 \\
&\quad + K_{BB}^{\pm n}|N_{4n}^+|^2 - 2K_{BS}^{\pm n}(N_{4n}^+ N_{5n}^+) + K_{SS}^{\pm n}|N_{5n}^+|^2 + K_{VV}^{\pm n}|N_{6n}^+|^2
\end{aligned}
$$

$$
\begin{aligned}
E_{pn}^{\pm} &= E_{np}^{\pm} = -K_{BB}^{\pm p}(N_{1p}^+ N_{1n}^+) + K_{BS}^{\pm p}(N_{2p}^+ N_{1n}^+ + N_{1p}^+ N_{2n}^+) - K_{SS}^{\pm p}(N_{2p}^+ N_{2n}^+) \\
&\quad - K_{VV}^{\pm p}(N_{3p}^+ N_{3n}^+) - K_{BB}^{\pm n}(N_{4p}^+ N_{4n}^+) + K_{BS}^{\pm n}(N_{4p}^+ N_{5n}^+ + N_{5p}^+ N_{4n}^+) \\
&\quad - K_{SS}^{\pm n}(N_{5p}^+ N_{5n}^+) - K_{VV}^{\pm n}(N_{6p}^+ N_{6n}^+) .
\end{aligned}
$$
(4.77)

The quantities $K^{\pm a}$ including the source term correlations are defined as

$$
\begin{pmatrix} K_{BB}^{\pm a} \\ K_{ss}^{\pm a} \\ K_{vv}^{\pm a} \\ K_{Bs}^{\pm a} \end{pmatrix} = \gamma^2 \sum_{\lambda\lambda'} \int \frac{d^3p}{(2\pi\hbar)^3} \begin{pmatrix} \xi_{\lambda'\lambda}^B \xi_{\lambda'\lambda}^B \\ \xi_{\lambda'\lambda}^s \xi_{\lambda'\lambda}^s \\ \xi_{\lambda'\lambda}^v \xi_{\lambda'\lambda}^v \\ \xi_{\lambda'\lambda}^B \xi_{\lambda'\lambda}^s \end{pmatrix}
$$

$$
\times \frac{(\hbar\Gamma_k)^2 \pm [\lambda'\varepsilon^*(\vec{p}_2) - \lambda\varepsilon^*(\vec{p}_1)]^2}{\{(\hbar\Gamma_k)^2 + [\lambda'\varepsilon^*(\vec{p}_2) - \lambda\varepsilon^*(\vec{p}_1)]^2\}^2} n_{a\lambda'}(\vec{p}_2)[1 - n_{a\lambda}(\vec{p}_1).
$$
(4.78)

In this chapter, we consider only the pole contributions arising from the collective poles and neglect the cut contributions due to the non-collective poles in the relativistic calculations. Therefore, the initial value of the density correlation function does not match the initial condition given in Eq. (4.71) and the initial value of the expression obtained by pole approximation diverges as Γ_k goes to zero for short wavelengths. In order to cancel out this divergent behaviour, we carry out the integration in Eq. (4.68) up to a k_{cut}. This cut-off value is taken sufficiently below the singular behavior of $\tilde{\sigma}_{ab}(\vec{k}, t = 0)$.

Consequently, the total baryon density correlation function is expressed as the sum of proton and neutron correlation functions and the cross-correlations according to,

$$\sigma(|\vec{r} - \vec{r}'|, t) = \sigma_{pp}(|\vec{r} - \vec{r}'|, t) + \sigma_{nn}(|\vec{r} - \vec{r}'|, t) + 2\sigma_{pn}(|\vec{r} - \vec{r}'|, t). \quad (4.79)$$

CHAPTER 5

NUMERICAL RESULTS IN RELATIVISTIC APPROACH

In chapter 4, early development of spinodal instabilities and density fluctuations are investigated in the stochastic extension of the nonlinear Walecka model for asymmetric nuclear matter. In this section, the numerical calculations are performed by using the expressions evaluated in the previous chapter. We calculate essentially the growth rates and phase diagrams of the unstable collective modes in the spinodal region, and early growth of the baryon density correlation functions. In the calculations, we employ the NL3 parameter set given in Table 4.1 which includes the non-linear self-interactions of the scalar meson. All of the calculations are performed for temperatures $T = 1$ MeV and $T = 5$ MeV at two different initial densities $\rho_B = 0.2\rho_0$ and $\rho_B = 0.4\rho_0$ in order to observe the unstable behaviour of nuclear matter in the spinodal region. Also the results are implemented for the initial charge asymmetries $I = 0.0, \ 0.5$ and 0.8.

Furthermore, we compare the quantal calculations with the semi-classical results given in Ref. [36, 39] for asymmetries $I = 0.5$ and 0.8 to examine the quantal effects. In the semi-classical description [39], time evolution of density fluctuations are given by the relativistic Vlasov equation instead of TDHF equation.

5.1 Growth Rates of the Unstable Collective Modes

By using the dispersion relation given in Eq. (4.62), we can obtain the growth rates of the unstable collective modes characterized by the wave number. Fig. 5.1 represents the growth rates of unstable modes as a function of wave number for temperature

75

$T = 1$ MeV at the initial densities $\rho_B = 0.2\rho_0$ and $\rho_B = 0.4\rho_0$ for different initial asymmetries. We observe that the behavior of the dispersion relation of the unstable collective modes is similar to those obtained in non-relativistic calculations. The wave number around the maximum growth rate shifts approximately from 0.7 fm^{-1} to 0.5 fm^{-1} when the asymmetry parameter increases. For smaller densities, $\rho_B = 0.2\rho_0$, unstable modes extend over a broader range of wave number compared to the density $\rho_B = 0.4\rho_0$. In order to observe the temperature dependence of the dispersion relation Fig. 5.2 is introduced at temperature $T = 5$ MeV under the similar conditions of Fig. 5.1. It can be seen from the graphs that the growth rates reduce as temperature increases at the same initial density and asymmetry values. For different asymmetry values, the wave numbers associated with the maximum growth rates change between 0.45 fm^{-1} to 0.6 fm^{-1} with the corresponding wavelengths $\lambda = (10 - 14)$ fm for density $\rho_B = 0.2\rho_0$, and 0.3 fm^{-1} to 0.6 fm^{-1} for density $\rho_B = 0.4\rho_0$. As a result, the range of unstable modes reduces with increasing temperature, initial density and asymmetry parameters. The unstable behaviour of the system have a strong isospin dependence, therefore the neutron rich system displays less unstable activity under the same conditions with symmetric matter.

Figure 5.1: Growth rates of the unstable collective modes as a function of wave number at initial baryon densities $\rho_B = 0.2\rho_0$ and $\rho_B = 0.4\rho_0$ for asymmetry parameters $I = 0.0, 0.5, 0.8$ at $T = 1\ MeV$. The solid lines indicate the presence of the Coulomb interaction.

In both graphs, the effects of the Coulomb interaction are also presented with the separate curves. The solid lines indicate the calculations including the Coulomb in-

Figure 5.2: Growth rates of the unstable collective modes as a function of wave number at initial baryon densities $\rho_B = 0.2\rho_0$ and $\rho_B = 0.4\rho_0$ for asymmetry parameters $I = 0.0$, 0.5, 0.8 at $T = 5$ MeV. The solid lines indicate the presence of the Coulomb interaction.

teraction while the dashed lines are drawn for the systems without the electromagnetic interaction. It can be observed that there is a small cut-off at the long wavelength edge at each graphs due to the electromagnetic interaction. Except this cut-off value, the contribution of the Coulomb interaction does not change the behaviour of the dispersion relation and growth rates of unstable collective modes especially at the lower densities.

Fig. 5.3 denotes the comparison of the quantal and semi-classical dispersion relations for initial baryon densities $\rho_B = 0.2\rho_0$ and $\rho_B = 0.4\rho_0$ at $T = 1$ MeV and $T = 5$ MeV for two different asymmetry parameters $I = 0.5$ and 0.8. In the figure, the solid lines represent the quantal calculations while the dashed lines are the results of semi-classical calculations. The semi-classical results are also obtained in the framework of the relativistic Walecka model with NL3 parameter set [39]. In semi-classical results, the range of unstable modes are larger than the results of quantal calculations at smaller densities, $\rho_B = 0.2\rho_0$, for both temperature and asymmetry values. On the other hand, quantal and semi-classical calculations yield almost the same results at density $\rho_B = 0.4\rho_0$. As a result, the quantum statistical effects are important at lower densities. The maximum of dispersion relation is reduced due to quantal effects at the initial state therefore fluctuations take more time to develop in
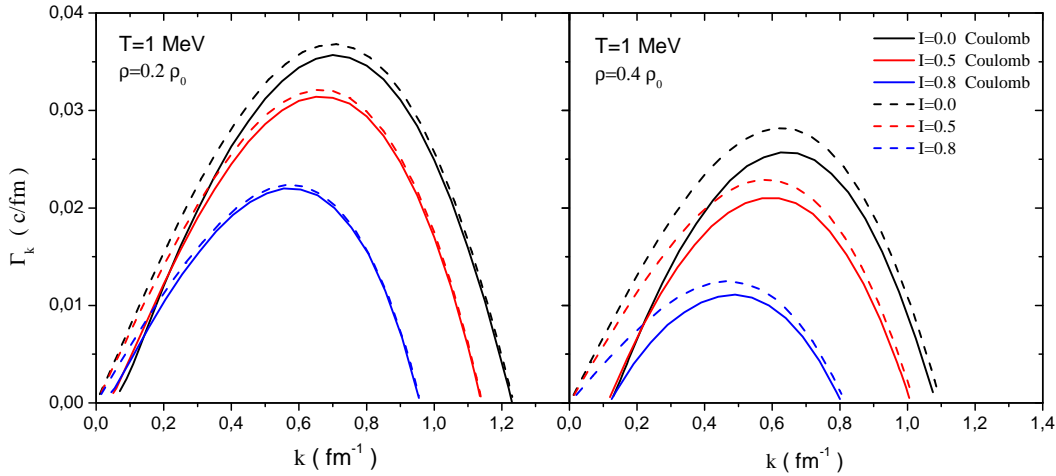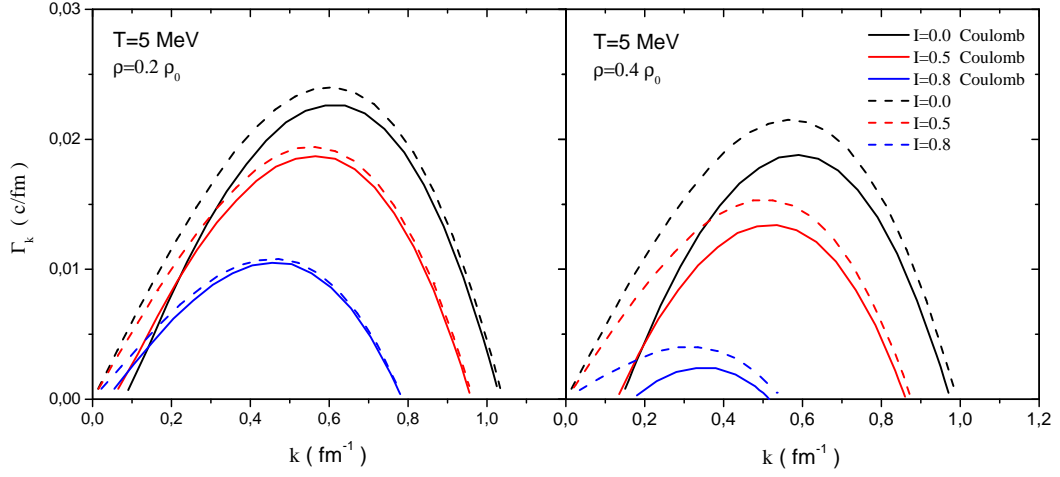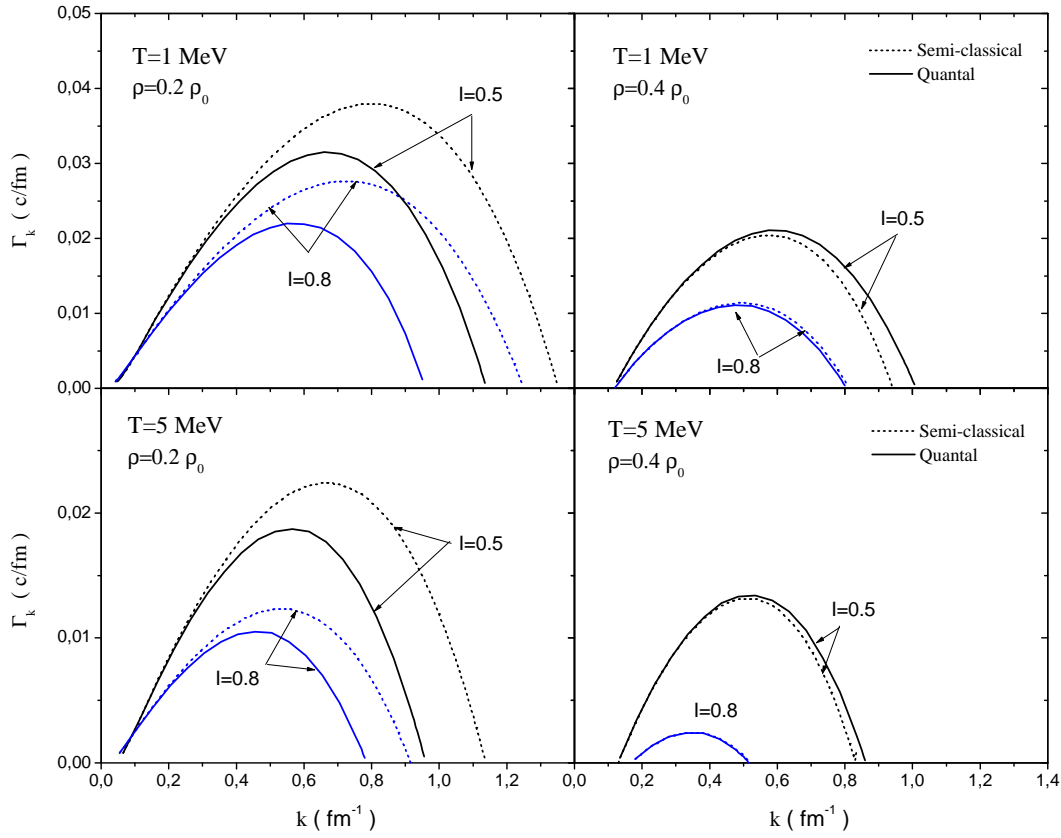
Figure 5.3: Growth rates of the unstable collective modes as a function of wave number at initial baryon densities $\rho_B = 0.2\rho_0$ and $\rho_B = 0.4\rho_0$ for asymmetry parameters $I = 0.5$ and 0.8 at $T = 1\,\mathrm{MeV}$ and $T = 5\,\mathrm{MeV}$. The solid and dashed lines are results of quantal and semi-classical calculations, respectively.

the case of quantal calculations as in Ref. [16, 18].

Fig. 5.4 illustrates the growth rates of the most unstable collective modes depending on the initial baryon density in asymmetric matter with $I = 0.0,\ 0.5$ and 0.8 at two different temperatures $T = 1\,\mathrm{MeV}$ and $T = 5\,\mathrm{MeV}$. The figure represents the effect of Coulomb interaction and the isospin dependence of unstable behavior of the system. The most unstable behavior of the system occurs around $\rho_B = 0.2\rho_0$ at temperature $T = 1\,\mathrm{MeV}$. At higher temperature of $T = 5\,\mathrm{MeV}$, the most unstable modes shift toward slightly higher densities around $\rho_B = 0.3\rho_0$. Furthermore, the density values at which the most unstable modes occurs do not change significantly with increasing asymmetry values. The contribution of electromagnetic interaction becomes observable at higher densities. It can be seen from Figs. 5.1, 5.2 and 5.4 that

the Coulomb force has little influence on the instabilities. Therefore, this influence do not presented separately in the rest of the chapter and all the figures include the Coulomb effect.
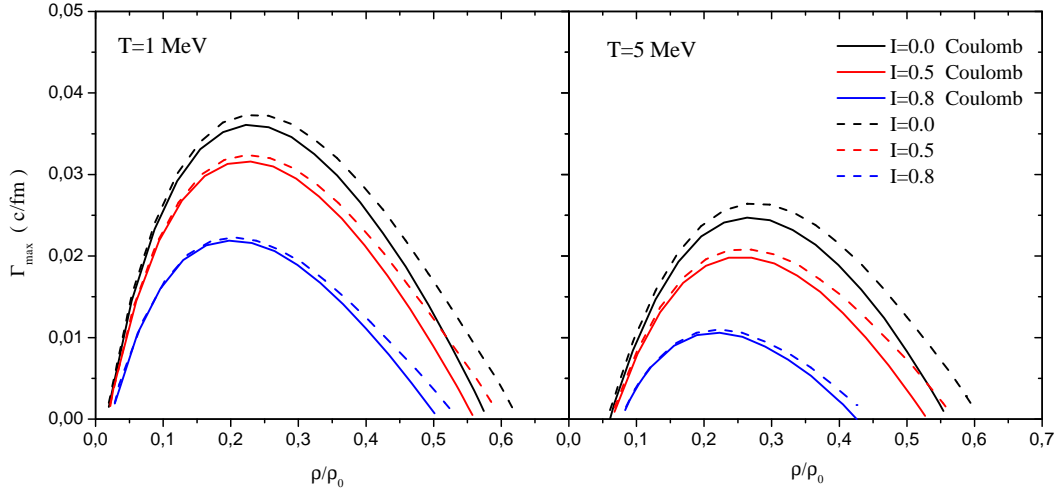
Figure 5.4: Growth rates of the most unstable collective modes as a function of initial baryon density in asymmetric matter with $I = 0.0,\ 0.5$ and 0.8 at temperature $T = 1$ MeV and $T = 5$ MeV. The solid lines indicate the presence of the Coulomb interaction.

In Fig. 5.5, the comparison of the most unstable modes as a result of quantal and semi-classical calculations are presented. Solid lines indicates the quantal results when the dashed lines are drawn for the semi-classical calculations. At temperature $T = 1$ MeV, the growth rates of the most unstable modes are higher in the semi-classical calculations. However, quantal and semi-classical results display similar behaviour at higher temperature. The density values corresponding to the most unstable modes are approximately same for each calculations. As a result, we can say that quantal dispersion relation are very close to that found in the semi-classical calculations. Therefore, we conclude that the particle-hole excitations resulting from $(-, +)$ and $(+, -)$ sectors, that do not have a counterpart in the semi-classical calculations, do not give any significant addition to the dispersion relation and growth rates of the unstable collective modes.
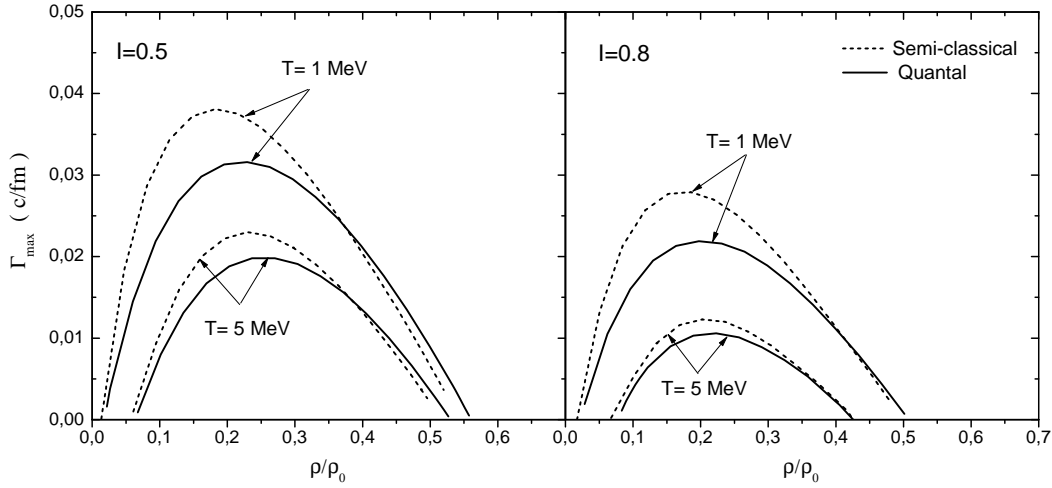
Figure 5.5: Growth rates of the most unstable collective modes as a function of initial baryon density in asymmetric matter with $I = 0.5$ and 0.8 at temperature $T = 1$ MeV and $T = 5$ MeV. The solid and dashed lines are results of quantal and semi-classical calculations, respectively.

5.2 Boundary of Spinodal Region

The boundary of the spinodal instability region can be determined through the phase diagrams. In Fig. 5.6, the phase diagrams for asymmetric nuclear matter are given as temperature versus density graphs for different wavelength values. The graphs are introduced for initial asymmetries $I = 0.0,\ 0.5$ and 0.8 for comparison. The peaks of each curve specify the critical temperatures for corresponding wavelengths. As mentioned earlier, the nuclear system is in equilibrium above the critical temperature while the system becomes unstable and exists as a mixture of liquid and gas phases in the regions under the curves. The value of the critical temperature increases with increasing wavelengths up to a saturation point. In this case, T_C does not change with the wavelengths above $\lambda = 18$ fm.

Furthermore, similar to the non-relativistic case, the critical temperature has a strong dependence on the initial asymmetry value in the relativistic calculations. We conclude again that the spinodal instability region and also the critical temperature reduce with increasing value of asymmetry parameter. The value of critical temperatures are read as approximately $T_c = 12$ MeV, $T_c = 11$ MeV and $T_c = 9$ MeV for the corresponding asymmetry values $I = 0.0,\ 0.5$ and $I = 0.8$. These critical temperatures

occurs at density $\rho = 0.3\rho_0$ for $I = 0.0$ and 0.5, and at $\rho = 0.2\rho_0$ for $I = 0.8$.
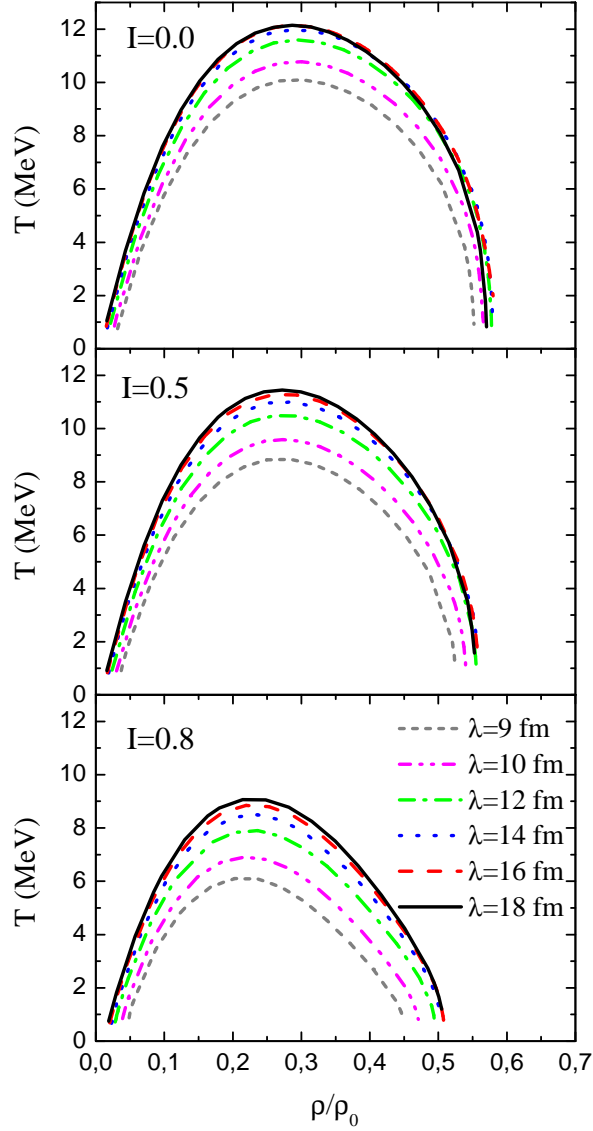
Figure 5.6: Phase diagram in density-temperature plane for a set of wavelengths with asymmetries $I = 0.0, \ 0.5$ and 0.8 .

From the lowest panel of Fig. 5.6, we can obtain the limiting density value for phase transition for neutron-rich matter at temperature $T = 1$ MeV with asymmetry $I = 0.8$ that are consistent with the conditions in the crusts of the neutron stars. In this case, the phase transition takes place up to the limiting density value $\rho_B = 0.5\rho_0$. For asymmetries $I = 0.0$ and 0.5, the spinodal region are bounded with the value $\rho_B = 0.55\rho_0$.

5.3 Spectral Intensity of Density Correlations

For the investigation of initial growth of baryon density fluctuations the density correlation functions are defined in Eq. (4.68) in terms of spectral intensity $\sigma(\vec{k}, t)$ of density correlations. In Fig. 5.7, the total spectral intensity of density correlation functions is illustrated as a function of wave number at temperature $T = 1$ MeV for varying asymmetry parameters at initial baryon densities $\rho_B = 0.2\rho_0$ and $\rho_B = 0.4\rho_0$. In the spectral intensity graphs, it is observed that the maximum growth takes place over the wave numbers corresponding to the range of dominant unstable modes obtained in Fig. 5.1. The growth of the spectral intensities depend strongly on the initial charge asymmetry; the growth rates reduce for both density cases with increasing asymmetry value. By comparing the spectral intensities with densities $\rho_B = 0.2\rho_0$ and $\rho_B = 0.4\rho_0$, we deduce that the spectral intensities grow faster at lower densities for temperature $T = 1$ MeV.

Fig. 5.8 are given for the system at $T = 5$ MeV with same conditions of Fig. 5.7. The asymmetric nuclear matter with $I = 0.8$ and density $\rho_B = 0.4\rho_0$ does not enter the spinodal region at this temperature which can be observed from the phase diagram. Therefore, this figure is drawn up to the asymmetry $I = 0.5$. Again, the range for maximum growth match with the range of wave number for the most unstable collective modes. As the temperature increases, the growth of spectral intensities becomes slower at lower densities, $\rho_B = 0.2\rho_0$, while the growth becomes faster at higher densities, $\rho_B = 0.4\rho_0$. In addition, the range for the unstable collective modes decreases with increasing temperature and initial density values.

In Figs. 5.7 and 5.8, the spectral intensities of density correlations are calculated for only the collective poles. However, we know that there are also non-collective poles arising from the susceptibility and source terms. The density fluctuations due to non-collective poles do not grow in time and these poles are effective at higher wave numbers. Therefore, we consider only the long wavelength regions in which the dominant contribution comes from the collective poles. Consequently, spectral intensity graphs are drawn up to a cut-off wave number between the values $k_{cut} = 0.7 - 1.15$ fm^{-1}. This cut-off value is determined due to the singular behavior of pole contributions. The calculation of correlation functions up to the cut-off value is

Figure 5.7: Spectral intensity of baryon density correlation function as a function of wave number at initial baryon densities $\rho_B = 0.2\rho_0$ and $\rho_B = 0.4\rho_0$ for asymmetry parameters $I = 0.0, 0.5$ and 0.8 at $T = 1$ MeV.

a good approximation but it is necessary to include the cut contributions come from the non-collective poles to satisfy the initial conditions accurately.

Figure 5.8: Spectral intensity of baryon density correlation function as a function of wave number at initial baryon densities $\rho_B = 0.2\rho_0$ and $\rho_B = 0.4\rho_0$ for asymmetry parameters $I = 0.0$ and 0.5 at $T = 5$ MeV.

5.4 Density Correlation Functions

The total correlation function of baryon density fluctuations is expressed as the sum of proton and neutron correlation functions and the cross-correlations in Eq. (4.79). The numerical calculation of baryon density correlation function gives a measure about the typical size of primary condensed regions and time scale of condensation mechanism. Fig. 5.9 illustrates the equal time baryon density correlation functions as a function of distance between two space locations $x = |\vec{r} - \vec{r}'|$ at $T = 1$ MeV with initial densities $\rho = 0.2\rho_0$ and $\rho = 0.4\rho_0$. The density correlation functions are evaluated by using the total spectral intensities given in Fig. 5.7 and the graphs are plotted for three different charge asymmetries. The time evolution of density fluctuations is faster for symmetric matter and decreases as the matter becomes

84

neutron-rich. At lower density case, $\sigma_{bb}(x = 0, \, t = 50\text{fm}/c) = 0.018$ fm^{-6} for symmetric matter while $\sigma_{bb}(x = 0, \, t = 50 \text{ fm}/c) = 0.003$ fm^{-6} for asymmetric matter with $I = 0.8$. The baryon density fluctuations grow six times slower in neutron-rich matter than in symmetric matter. From Fig. 5.9, we can also observe the change in density correlations due to varying initial densities. At the higher density of $\rho_B = 0.4\rho_0$, $\sigma_{bb}(x = 0, \, t = 50 \text{ fm}/c) = 0.0095$ fm^{-6} for $I = 0.0$ and $\sigma_{bb}(x = 0, \, t = 50 \text{ fm}/c) = 0.001$ fm^{-6} for asymmetry parameter $I = 0.8$. At lower densities, the time development of baryon density correlation function is faster at temperature $T = 1$ MeV.

Furthermore, valuable information related to the approximate size of clusters formed during the initial time of spinodal decomposition is obtained from these graphs. The correlation length x_c, which provide a measure for radius of correlation volume, is defined as the width of the correlation function at half maximum. The correlation length is about $x_c = 2.2$ fm for symmetric matter and increases to $x_c = 2.7$ fm for asymmetric matter with $I = 0.8$ at density $\rho = 0.2\rho_0$. At the higher density of $\rho_B = 0.4\rho_0$, it increases from about 2.5 fm to 3.3 fm when the matter becomes neutron-rich. The nuclear matter with $I = 0.8$ at low temperature around $T = 1$ MeV reflects the typical conditions in the crust of neutron stars and the correlation length at this condition gives the number of nucleons fluctuating in the correlation volume in the range of $17 \leq \Delta A \leq 27$.

In Fig. 5.10, the same graphs are given but at a higher temperature $T = 5$ MeV. At this temperature, baryon density fluctuations grow slower than $T = 1$ MeV case at both densities. For all asymmetry parameters, the growth rates decrease and the correlation lengths increase as the temperature increases. For instance, in asymmetric matter with $I = 0.5$ the correlation length increases from about $x_c = 2.8$ fm at temperature $T = 1$ MeV to about $x_c = 3.3$ fm at temperature $T = 5$ MeV for density $\rho_B = 0.4\rho_0$. From Figs. 5.9 and 5.10, we can conclude that the correlation length depends on the initial charge asymmetry, temperature and the initial baryon density. Besides, we note that the radius of the correlation volume calculated from density correlation functions is consistent with the quarter wavelengths of the dominant unstable modes obtained from the dispersion relations for the corresponding temperature, initial density and charge asymmetries.
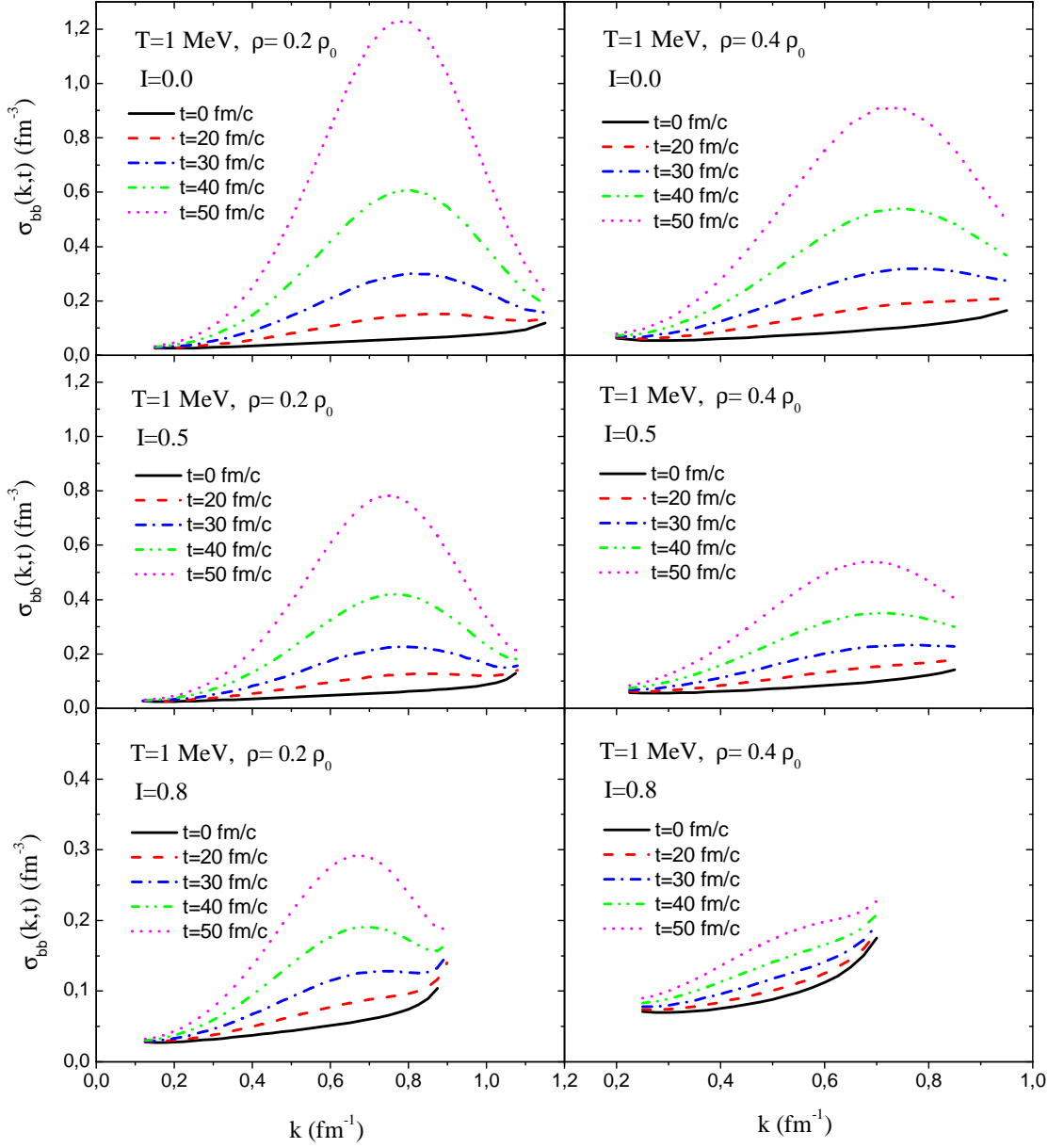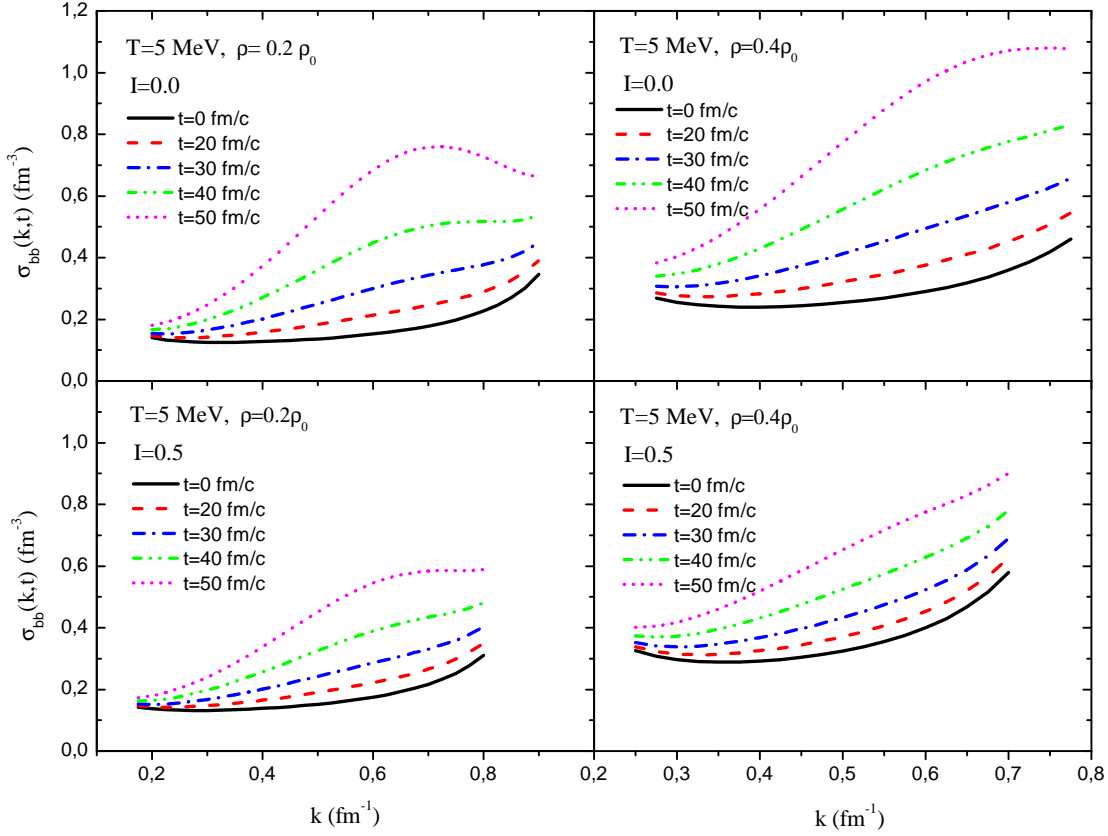
Figure 5.9: Baryon density correlation functions as a function of distance at initial baryon densities $\rho_B = 0.2\rho_0$ and $\rho_B = 0.4\rho_0$ for asymmetry parameters $I = 0.0, 0.5$ and 0.8 at temperature $T = 1$ MeV.

In Fig. 5.11, the baryon density correlation functions of quantal and semi-classical calculations are compared for asymmetric nuclear matter with $I = 0.5$ at densities $\rho_B = 0.2\rho_0$ and $\rho_B = 0.4\rho_0$ for temperatures $T = 1$ MeV and $T = 5$ MeV at times $t = 0$ and $t = 50$ fm/c. The solid and dashed lines denote the results of quan-
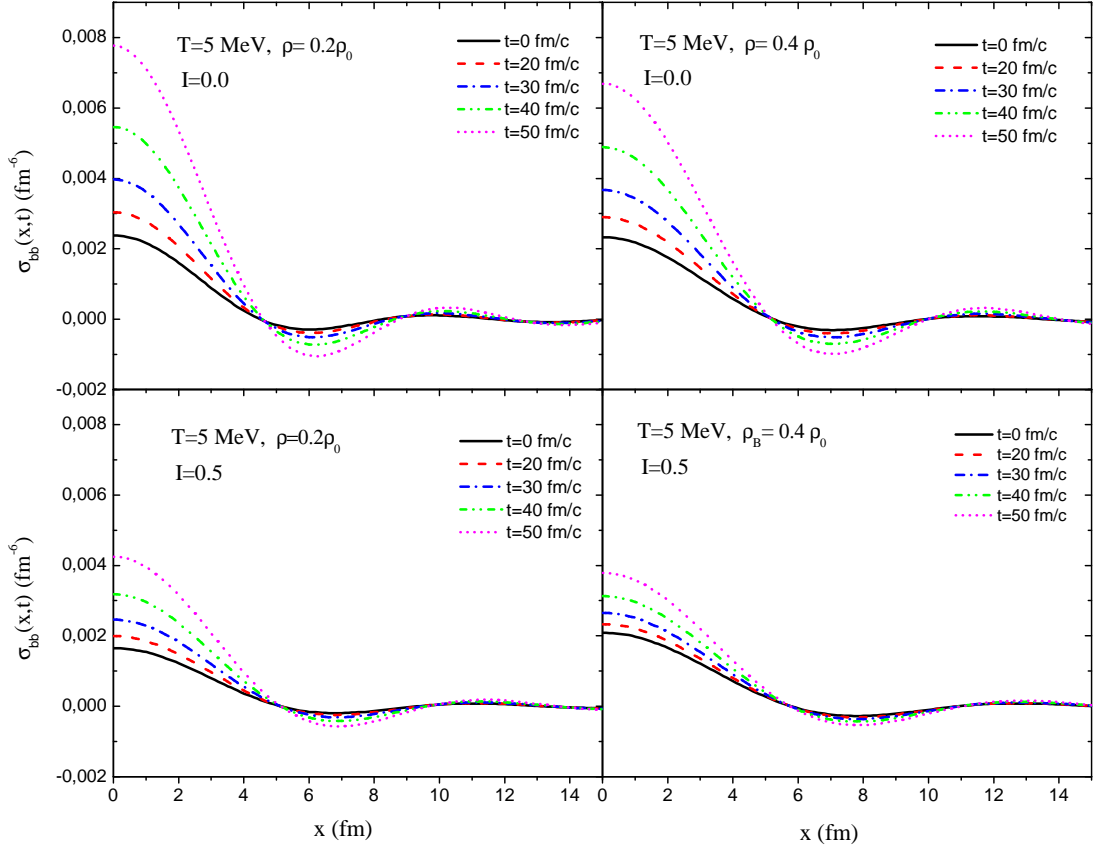
Figure 5.10: Baryon density correlation functions as a function of distance at initial baryon densities $\rho_B = 0.2\rho_0$ and $\rho_B = 0.4\rho_0$ for asymmetry parameters $I = 0.0$ and 0.5 at temperature $T = 5$ MeV.

tal and semi-classical calculations, respectively. At lower temperature $T = 1$ MeV, the growth of density correlation functions is larger in quantal calculations compared to the semi-classical results due to the large quantal effects. On the other hand, the baryon density correlation functions for semi-classical limit grow faster at temperature $T = 5$ MeV since the quantal effects are not important for higher temperatures. From Fig. 5.11, we observe that at $T = 5$ MeV, the semi-classical calculations provide a good approximation for density correlation functions particularly at higher densities. The correlation lengths are found nearly same for quantal and semi-classical calculations hence we can conclude that the correlation length is not very sensitive to the quantal effects.
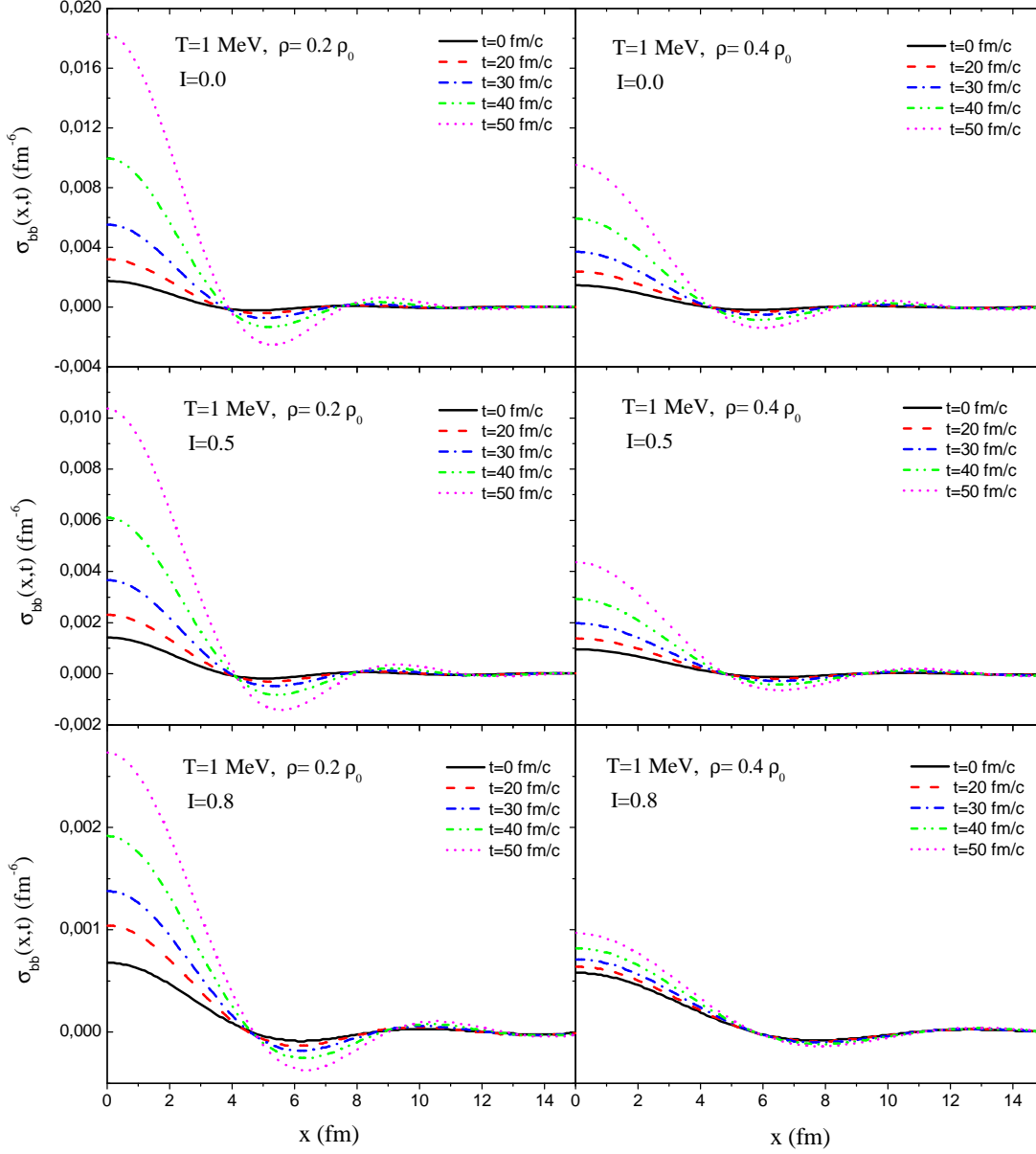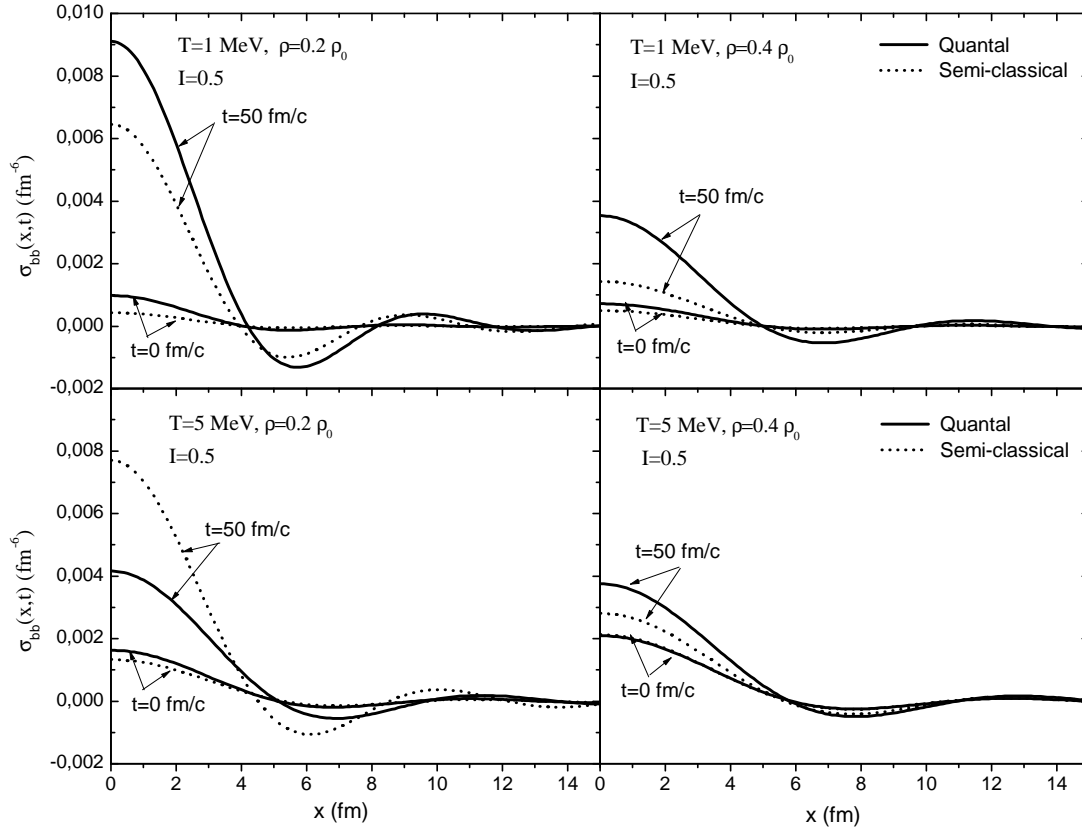
Figure 5.11: Baryon density correlation functions as a function of distance at initial baryon densities $\rho_B = 0.2\rho_0$ and $\rho_B = 0.4\rho_0$ at temperatures $T = 1$ MeV and $T = 5$ MeV for asymmetry $I = 0.5$. The solid and dashed lines are results of quantal and semi-classical calculations, respectively.

88

CHAPTER 6

CONCLUSION

In this thesis, early development of density fluctuations in the spinodal region are investigated for asymmetric nuclear matter in both the non-relativistic and relativistic frameworks by employing the stochastic mean-field approach. The SMF approach in either non-relativistic or relativistic frameworks goes beyond the standard mean field theory by incorporating quantal and thermal fluctuations at the initial state in a stochastic manner. The stochastic mean field approach includes the one-body dissipation and the associated fluctuation mechanism in accordance with the fluctuation-dissipation relation, and it introduces an effective description for the dynamics of density fluctuations in low energy nuclear reactions. In our study, we investigate the early growth of spinodal instabilities employing the SMF approach in the linear response regime.

In the first part, we investigate the early growth of density fluctuations for charge asymmetric nuclear matter in non-relativistic framework by including collective and non-collective poles into the description. In the linear limit of SMF approach, we can carry out an almost analytical treatment for the correlation functions of density fluctuations by applying the one-sided Fourier transformation method. The density correlation function provides a typical measure for the condensation regions during the initial stages of the liquid-gas phase transition of the system. The one-sided Fourier transformation offers a contour integration in the complex frequency plane including collective and non-collective poles. In the standard treatment, this contour integral is evaluated due to the two pole contributions from the zeros of the susceptibility associated with unstable collective poles, and non-collective poles were ignored. Although

this standard approach provides a satisfactory description for the growth of density fluctuations, it is inadequate in two points. It does not satisfy the initial conditions and moreover leads to a divergent behaviour when the wave numbers close to their upper limits. In this study, the density correlation functions are calculated including the effects of collective poles as well as non-collective poles in terms of the cut contribution in the complex frequency plane. The cut contribution also exhibits a divergent behavior approaching to the upper limits of wave numbers but with the opposite sign. As a consequence, these divergent behaviors with opposite signs cancel out each other to generate a nice regular behavior of the spectral intensity function. A complete calculation of density correlation functions are carried out by including both pole and cut contributions in the linear response regime. Besides, the exact calculations of the correlation functions satisfy the initial conditions, which reflects the validity of the highly nontrivial sum rule.

The numerical results of spinodal instabilities and density fluctuations for asymmetric nuclear matter is presented in a semi-classical approach for finite temperatures and in a quantal framework for zero temperature. The calculations are carried out for initial density $\rho = 0.3 \, \rho_0$, at the critical temperatures occur, for different asymmetry parameters $I = 0.0, \, 0.4$ and 0.8. The growth rates of the unstable modes are investigated and the boundary of the spinodal region is determined. The system displays less unstable behavior with increasing asymmetry. Moreover, the asymmetry leads to shrinking of the spinodal region, decreasing the critical temperature and density. Furthermore, we can obtain information about the initial size of the condensing fragments from the density correlation function. The correlation length characterizes the size of the initial condensation regions during the growth of fluctuations. From our results, it is observed that the correlation length is not very sensitive to the time evolution and temperature but depends on the initial charge asymmetry. We also observe that the spinodal instabilities are reduced by charge asymmetry, leading to larger sized fragments.

In the second part of the thesis, we employ the stochastic extension of the Walecka-type relativistic mean field model in order to examine the spinodal instabilities and early development of condensation mechanism in the quantal framework. In the calculations, the nonlinear Walecka model including the coupling of baryon fields to

rho meson is utilized with the NL3 parameter set. We consider the linear response analysis of dynamical evolution for the investigation of the early growth of density fluctuations, thus the meson field equations are linearized around their initial equilibrium state. The quantal dispersion relation is obtained by retaining only the collective poles. The growth rates of unstable collective modes are determined for two different initial densities, $\rho_B = 0.2\rho_0$ and $\rho_B = 0.4\rho_0$, at temperatures $T = 1$ MeV and $T = 5$ MeV for asymmetric nuclear matter with $I = 0.0,\ 0.5$ and 0.8. We observe that the range of unstable modes reduces with increasing values of temperature, initial density and asymmetry parameters. As a result, the most unstable behavior of the system exhibits at lower temperatures around the initial density $\rho_B = 0.2\rho_0$. The quantal results are compared with the calculations in the semi-classical framework under the same conditions [39]. We have found that at low densities, most unstable collective modes shift towards relatively longer wavelengths and concentrated over a narrower range in quantal calculations whereas the range of the unstable modes are broader in the semi-classical results. On the other hand, at higher densities, $\rho_B = 0.4\rho_0$, the unstable response of the system nearly coincide in both calculations for all values of temperatures and asymmetry parameters. Furthermore, the boundary of the spinodal region is obtained from the phase diagram of nuclear matter. The liquid-gas phase transition is expected below this boundary specified with the critical temperatures and densities.

Within the framework of the stochastic mean field approach we are able to calculate the growth of baryon density correlation function which provides further information about the condensation mechanism throughout the initial time of phase transition. We observe that the growth of baryon density correlation functions are relatively faster in quantal calculations than in the semi-classical approach, except at higher temperature $T = 5$ MeV with density $\rho_B = 0.2\rho_0$ where the quantal growth occurs at a slower range. We also note that the early size of primary clusters that is calculated from the baryon density correlation functions are consistent with those extracted from the dispersion relation.

In this work, the growth of density fluctuations is examined for asymmetric nuclear matter in the linear response framework of SMF approach therefore we obtain only the information about the early stages of the liquid-gas phase transition in the spin-

odal region. For describing whole phase transition, we need to study the nonlinear evolution of the density fluctuations by carrying out the long time simulations of the SMF method. We also note that the relativistic calculations of this thesis are carried out by including only the pole contributions and the cut contributions are neglected. Although this approach gives satisfactory results, the complete treatment is always desirable. Therefore, it is important to include the non-collective poles for a complete description of baryon density correlation functions.

REFERENCES

[1] H. Jaqaman, A.Z. Mekjian, and L.Zamick, Phys. Rev. **C 27** (1983) 2782.

[2] C. Wu and Z. Ren, Phys. Rev. **C 83** (2011) 044605.

[3] Ph. Chomaz, M. Colonna and J. Randrup, Phys. Rep. **389** (2004) 263.

[4] N. Le Neindre et al. (INDRA and ALADIN Collaborations), Nucl Phys. **795** (2007) 47.

[5] E. Bonnet, et al. (INDRA and ALADIN Collaborations), Phys. Rev. Lett. **105** (2010) 142701.

[6] B. Borderie et al. (INDRA Collaboration), Phys. Rev. Lett. **86** (2001) 3252.

[7] L. Beaulieu et al., Phys. Rev. Lett. **84** (2000) 5971.

[8] V. Baran, M. Colonna, M. Di Toro, A.B. Larionov, Nucl. Phys. **A 632** (1998) 287.

[9] S. Ayik, O. Yilmaz, N. Er, A. Gokalp, P. Ring, Phys. Rev. **C 80** (2009) 034613.

[10] J. D. Walecka, Ann. Phys. **83** (1974) 491; B. D. Serot, J. D. Walecka, "Advances in Nuclear Physics Vol.16", Plenium Press, New York, 1997.

[11] G. Hua, L. Bo, M. Di Toro, Phys. Rev. **C 62** (2000) 035203.

[12] J. D. Frankland et al. (INDRA Collaboration), Nucl. Phys. **A 689** (2001) 940.

[13] K. Washiyama, S. Ayik and D. Lacroix, Phys. Rev. **C 80** (2009) 031602(R).

[14] S. Ayik, K. Washiyama and D. Lacroix, Phys. Rev. **C 79** (2009) 054606.

[15] B. Borderie, et al., Nucl. Phys. **A 734** (2004) 495.

[16] S. Ayik, N. Er, O. Yilmaz and A. Gokalp, Nucl. Phys. **A 812** (2008) 44.

[17] O. Yilmaz, S. Ayik and A. Gokalp, Eur. Phys. J. **A 47** (2011) 123.

[18] S. Ayik, M. Colonna and Ph. Chomaz, Phys. Lett. **B 353** (1995) 417.

[19] S. Ayik, Phys. Lett. **B 658** (2008) 174.

[20] S. Ayik, O. Yilmaz, F. Acar, B. Danisman, N. Er and A. Gokalp, Nucl. Phys. **A 859** (2011) 73.

[21] P. Bozek, Phys. Lett. **B 383** (1996) 121.

[22] D. Lacroix and S. Ayik, Eur. Phys. J. **A 50** (2014) 95.

[23] P. Ring and P. Schuck, "The Nuclear Many-Body Problem", Springer, New York, 1980.

[24] D. Vautherin, D. M. Brink, Phys. Rev. **C 5** (1972) 626.

[25] M. Colonna, M. Di Toro, A. B. Larionov, Phys. Lett. **B 428** (1998) 1.

[26] H. Krivine, J. Trainer and O. Bohigas, Nucl. Phys. **A 336** (1990) 155.

[27] O. Yilmaz, S. Ayik, F. Acar and A. Gokalp, Phys. Rev. **C 91** (2015) 014605.

[28] F. Acar, S. Ayik, O. Yilmaz and A. Gokalp, Phys. Rev. **C 92** (2015) 034605.

[29] E. M. Lifshitz and L. P. Pitaevskii, "Physical Kinetics", Pergamon, Oxford, 1981.

[30] H.Heiselberg, C. J. Pethick and D. G. Ravenhall, Phys. Rev. Lett. **61** (1988) 818.

[31] J. Xu and C. M. Ko, Phys. Rev. **C 82** (2010) 044311.

[32] B. D. Serot, J. D. Walecka, Int. J. Mod. Phys. **E6** (1997) 515.

[33] P. Ring, Prog. Part. Nucl. Phys. **37** (1996) 193.

[34] J.D. Walecka, "Theoretical Nuclear and Subnuclear Physics", Imperial College Press, 2004.

[35] G. A. Lalazissis, J. Konig and P.Ring, Phys. Rev. **C 55** (1997) 540.

[36] O. Yilmaz, S. Ayik, F. Acar, S. Saatci, A. Gokalp, Eur. Phys. **J A 49** (2013) 33.

[37] P. Ring et al., Nucl. Phys. **A 694** (2001) 249.

[38] W. Greiner, "Relativistic Quantum Mechanics", Springer-Verlag, 1987.

[39] Selen Saatci, "Semi-Classical Descrition of Spinodal Instabilities of Asymmetric Nuclear Matter In a Relativistic Stochastic Model", MS Thesis, METU, 2013.

APPENDIX A

DERIVATION OF NON-RELATIVISTIC DISPERSION RELATION

The linearized TDHF equation after transformation is given in Eq. (2.23) as

$$\langle \vec{p}_1 | \delta\tilde{\rho}_a^\lambda(\omega) | \vec{p}_2 \rangle = -\frac{f_0^a(\vec{p}_1) - f_0^a(\vec{p}_2)}{\hbar\omega - \varepsilon_a(\vec{p}_1) + \varepsilon(\vec{p}_2)} \langle \vec{p}_1 | \delta U_a^\lambda(\omega) | \vec{p}_2 \rangle + i\hbar \frac{\langle \vec{p}_1 | \delta\hat{\rho}_a(0) | \vec{p}_2 \rangle}{\hbar\omega - \varepsilon_a(\vec{p}_1) + \varepsilon(\vec{p}_2)}.$$
(A.1)

In this equation, we use the momentum vectors as $\vec{p}_1 = \vec{p} + \hbar\vec{k}/2$ and $\vec{p}_2 = \vec{p} - \hbar\vec{k}/2$ and the equation becomes

$$\langle \vec{p} + \frac{\hbar\vec{k}}{2} | \delta\tilde{\rho}_a^\lambda(\omega) | \vec{p} - \frac{\hbar\vec{k}}{2} \rangle$$
$$= \frac{-[f_0^a(\vec{p} + \hbar\vec{k}/2) - f_0^a(\vec{p} - \hbar\vec{k}/2)]}{\hbar\omega - \varepsilon_a(\vec{p} + \hbar\vec{k}/2) + \varepsilon(\vec{p} - \hbar\vec{k}/2)} \langle \vec{p} + \frac{\hbar\vec{k}}{2} | \delta U_a^\lambda(\omega) | \vec{p} - \frac{\hbar\vec{k}}{2} \rangle$$
$$+ i\hbar \frac{\langle \vec{p} + \hbar\vec{k}/2 | \delta\hat{\rho}_a(0) | \vec{p} - \hbar\vec{k}/2 \rangle}{\hbar\omega - \varepsilon_a(\vec{p} + \hbar\vec{k}/2) + \varepsilon(\vec{p} - \hbar\vec{k}/2)}.$$
(A.2)

Here we use the following one-sided Fourier transformation in time,

$$\langle \vec{p} + \frac{\hbar\vec{k}}{2} | \delta\tilde{\rho}_a^\lambda(\omega) | \vec{p} - \frac{\hbar\vec{k}}{2} \rangle = \int_0^\infty dt e^{i\omega t} \langle \vec{p} + \frac{\hbar\vec{k}}{2} | \delta\tilde{\rho}_a^\lambda(t) | \vec{p} - \frac{\hbar\vec{k}}{2} \rangle.$$
(A.3)

By using the position and momentum space representations which are given as

$$\langle \vec{r} | \vec{p} \rangle = \frac{1}{(2\pi\hbar)^{3/2}} e^{\frac{i}{\hbar}\vec{p}\cdot\vec{r}}$$

$$\langle \vec{p} + \frac{\hbar\vec{k}}{2} | \vec{r} \rangle = \frac{1}{(2\pi\hbar)^{3/2}} e^{-\frac{i}{\hbar}(\vec{p} + \frac{\hbar\vec{k}}{2})\cdot\vec{r}}$$
(A.4)

we obtain the relation

$$\langle \vec{p} + \frac{\hbar\vec{k}}{2} | \delta\tilde{\rho}_a^\lambda(\omega) | \vec{p} - \frac{\hbar\vec{k}}{2} \rangle = \int_0^\infty dt e^{i\omega t} \int_{-\infty}^\infty d^3r \int_{-\infty}^\infty d^3r' \langle \vec{p} + \frac{\hbar\vec{k}}{2} | \vec{r} \rangle \langle \vec{r} | \delta\tilde{\rho}_a^\lambda(t) | \vec{r}' \rangle \langle \vec{r}' | \vec{p} - \frac{\hbar\vec{k}}{2} \rangle.$$
(A.5)

Then by evaluating $\int d^3p$ integral of both sides and using the orthonormality relation given by $\int\limits_{-\infty}^{\infty} d^3p\, e^{-\frac{i}{\hbar}\vec{p}\cdot(\vec{r}-\vec{r}')} = (2\pi\hbar)^3\delta(\vec{r}-\vec{r}')$, we obtain

$$\int d^3p\langle\vec{p}+\frac{\hbar\vec{k}}{2}|\delta\tilde{\rho}_a^\lambda(\omega)|\vec{p}-\frac{\hbar\vec{k}}{2}\rangle$$

$$= \int\limits_0^\infty dt e^{i\omega t} \int\limits_{-\infty}^\infty d^3r \int\limits_{-\infty}^\infty d^3r' \int \frac{d^3p}{(2\pi\hbar)^3} e^{-\frac{i}{\hbar}\vec{p}\cdot(\vec{r}-\vec{r}')} e^{-\frac{i}{2}\vec{k}\cdot(\vec{r}+\vec{r}')}\langle\vec{r}|\delta\tilde{\rho}_a^\lambda(t)|\vec{r}'\rangle$$

$$= \int\limits_0^\infty dt e^{i\omega t} \int\limits_{-\infty}^\infty d^3r e^{-i\vec{k}\cdot\vec{r}}\delta\rho_a^\lambda(\vec{r},t) = (2\pi\hbar)^3\delta\tilde{\rho}_a^\lambda(\vec{k},\omega).$$

(A.6)

By the similar way, the Fourier transform of the mean-field potential fluctuation becomes

$$\langle\vec{p}+\frac{\hbar\vec{k}}{2}|\delta U_a^\lambda(\omega)|\vec{p}-\frac{\hbar\vec{k}}{2}\rangle$$

$$= \int\limits_0^\infty dt e^{i\omega t} \int\limits_{-\infty}^\infty d^3r \int\limits_{-\infty}^\infty d^3r'\langle\vec{p}+\frac{\hbar\vec{k}}{2}|\vec{r}\rangle\langle\vec{r}|\delta U_a^\lambda(t)|\vec{r}'\rangle\langle\vec{r}'|\vec{p}-\frac{\hbar\vec{k}}{2}\rangle$$

$$= \int\limits_0^\infty dt e^{i\omega t} \int\limits_{-\infty}^\infty \frac{d^3r}{(2\pi\hbar)^3} \int\limits_{-\infty}^\infty d^3r' e^{-\frac{i}{\hbar}\left(\vec{p}+\frac{\hbar\vec{k}}{2}\right)\cdot\vec{r}} e^{\frac{i}{\hbar}\left(\vec{p}-\frac{\hbar\vec{k}}{2}\right)\cdot\vec{r}'} \delta U_a^\lambda(t)\delta(\vec{r}-\vec{r}')$$

$$= \int\limits_0^\infty dt e^{i\omega t} \int\limits_{-\infty}^\infty \frac{d^3r}{(2\pi\hbar)^3} e^{-i\vec{k}\cdot\vec{r}}U_a^\lambda(t) = U_a^\lambda(\vec{k},\omega).$$

(A.7)

where we use the relation $\langle\vec{r}|\delta U_a^\lambda(t)|\vec{r}'\rangle = \delta U_a^\lambda(t)\delta(\vec{r}-\vec{r}')$. Then, by evaluating $\int \frac{d^3p}{(2\pi\hbar)^3}$ integral of both sides of Eq. (A.2) and using the space Fourier transform of nucleon density fluctuations which is given in Eq. (2.24),

$$\delta\rho_a^\lambda(\vec{k},\omega) = \sum_s \int \frac{d^3p}{(2\pi\hbar)^3}\langle\vec{p}+\hbar\vec{k}/2|\delta\hat{\rho}_{a,s}^\lambda(\omega)|\vec{p}-\hbar\vec{k}/2\rangle \qquad (A.8)$$

we obtain the following equation

$$\tilde{\rho}_a^\lambda(\vec{k},\omega) = \sum_s \int \frac{d^3p}{(2\pi\hbar)^3}\frac{f_0^a(\vec{p}-\hbar\vec{k}/2) - f_0^a(\vec{p}+\hbar\vec{k}/2)}{\hbar\omega - \vec{p}\cdot\hbar\vec{k}/m}\delta U_a^\lambda(\vec{k},\omega)$$

$$+ i\hbar \sum_s \int \frac{d^3p}{(2\pi\hbar)^3}\frac{\langle\vec{p}+\hbar\vec{k}/2|\delta\hat{\rho}_{a,s}^\lambda(0)|\vec{p}-\hbar\vec{k}/2\rangle}{\hbar\omega - \vec{p}\cdot\hbar\vec{k}/m}. \qquad (A.9)$$

Here we use $\varepsilon_a(\vec{p} + \hbar\vec{k}/2) - \varepsilon(\vec{p} - \hbar\vec{k}/2) = \vec{p} \cdot \hbar\vec{k}/m$ in the denominator. The fluctuation of the mean-field potential depends on both neutron and proton density fluctuations.

$$
\delta U_n^\lambda(\vec{k}, \omega) = \left(\frac{\delta U_n}{\delta \rho_n}\right)_0 \delta \rho_n^\lambda(\vec{k}, \omega) + \left(\frac{\delta U_n}{\delta \rho_p}\right)_0 \delta \rho_p^\lambda(\vec{k}, \omega)
$$

$$
\delta U_p^\lambda(\vec{k}, \omega) = \left(\frac{\delta U_p}{\delta \rho_n}\right)_0 \delta \rho_n^\lambda(\vec{k}, \omega) + \left(\frac{\delta U_p}{\delta \rho_p}\right)_0 \delta \rho_p^\lambda(\vec{k}, \omega) \tag{A.10}
$$

where the equilibrium densities of neutron and proton has the same value $\rho_0 = 0.16$ fm^{-3}. If we define the zeroth-order Landau parameters, $F_0^{ab} = (\partial U_b / \partial \rho_a)_0$, and use the definition given in Eqs. (2.26-2.27), we obtain the following equations for neutron and proton density fluctuations respectively

$$
\delta \rho_n^\lambda(\vec{k}, \omega) = -\chi_n(\vec{k}, \omega)[F_0^{nn}\delta\rho_n^\lambda(\vec{k}, \omega) + F_0^{pn}\delta\rho_p^\lambda(\vec{k}, \omega)] + iS_n^\lambda(\vec{k}, \omega)
$$

$$
\delta \rho_p^\lambda(\vec{k}, \omega) = -\chi_p(\vec{k}, \omega)[F_0^{np}\delta\rho_n^\lambda(\vec{k}, \omega) + F_0^{pp}\delta\rho_p^\lambda(\vec{k}, \omega)] + iS_p^\lambda(\vec{k}, \omega) \tag{A.11}
$$

and these equations can also be written in the following form

$$
\begin{pmatrix} \left[1 + F_0^{nn}\chi_n(\vec{k}, \omega)\right]\delta\rho_n^\lambda(\vec{k}, \omega) + F_0^{np}\chi_n(\vec{k}, \omega)\delta\rho_p^\lambda(\vec{k}, \omega) \\ \left[1 + F_0^{pp}\chi_p(\vec{k}, \omega)\right]\delta\rho_p^\lambda(\vec{k}, \omega) + F_0^{pn}\chi_p(\vec{k}, \omega)\delta\rho_n^\lambda(\vec{k}, \omega) \end{pmatrix} = i \begin{pmatrix} S_n^\lambda(\vec{k}, \omega) \\ S_p^\lambda(\vec{k}, \omega) \end{pmatrix}.
\tag{A.12}
$$

APPENDIX B

POLE CONTRIBUTION TO DENSITY CORRELATIONS

By using the definition of quantal Linhard function given in Eq. (2.26) for $\omega = \mp i\Gamma$, we get

$$\chi_a(\vec{k}, i\Gamma) = 2 \int \frac{d^3p}{(2\pi\hbar)^3} \frac{i\Gamma\hbar + \vec{p} \cdot \hbar\vec{k}/m}{(\Gamma\hbar)^2 + (\vec{p} \cdot \hbar\vec{k}/m)^2} [f_0^a(\vec{p} - \hbar\vec{k}/2) - f_0^a(\vec{p} + \hbar\vec{k}/2)] \quad \text{(B.1)}$$

where the term with $i\Gamma\hbar$ gives zero, then we obtain

$$\begin{aligned}
\chi_a(\vec{k}, i\Gamma) &= \chi_a(\vec{k}, -i\Gamma) \\
&= 2 \int \frac{d^3p}{(2\pi\hbar)^3} \frac{\vec{p} \cdot \hbar\vec{k}/m}{(\Gamma\hbar)^2 + (\vec{p} \cdot \hbar\vec{k}/m)^2} [f_0^a(\vec{p} - \hbar\vec{k}/2) - f_0^a(\vec{p} + \hbar\vec{k}/2)].
\end{aligned}$$

$$\text{(B.2)}$$

Then the relation between the Linhard functions becomes

$$\chi_a(\vec{k}, i\Gamma) = \chi_a(\vec{k}, -i\Gamma) = \chi_a(-\vec{k}, i\Gamma) = \chi_a(-\vec{k}, -i\Gamma). \quad \text{(B.3)}$$

In order to find the derivative of susceptibility at $\omega = \mp i\Gamma$, we should calculate the derivative of Linhard functions and the relation between them.

$$\begin{aligned}
\frac{\partial \chi_a(\vec{k}, i\Gamma)}{\partial \omega} &= 2\hbar \int \frac{d^3p}{(2\pi\hbar)^3} \frac{1}{(i\Gamma\hbar - \vec{p} \cdot \hbar\vec{k}/m)^2} [f_0^a(\vec{p} - \frac{\hbar\vec{k}}{2}) - f_0^a(\vec{p} + \frac{\hbar\vec{k}}{2})] \\
&= 2\hbar \int \frac{d^3p}{(2\pi\hbar)^3} \frac{-(\Gamma\hbar)^2 + (\vec{p} \cdot \hbar\vec{k}/m)^2 + 2i\Gamma\hbar\vec{p} \cdot \hbar\vec{k}/m}{((\Gamma\hbar)^2 + (\vec{p} \cdot \hbar\vec{k}/m)^2)^2} \\
&\qquad\qquad\qquad\qquad\qquad \times [f_0^a(\vec{p} - \frac{\hbar\vec{k}}{2}) - f_0^a(\vec{p} + \frac{\hbar\vec{k}}{2})]
\end{aligned}$$

$$\text{(B.4)}$$

In this equation, the following integral gives zero

$$\int \frac{d^3p}{(2\pi\hbar)^3} \frac{-(\Gamma\hbar)^2 + (\vec{p} \cdot \hbar\vec{k}/m)^2}{((\Gamma\hbar)^2 + (\vec{p} \cdot \hbar\vec{k}/m)^2)^2} [f_0^a(\vec{p} - \hbar\vec{k}/2) - f_0^a(\vec{p} + \hbar\vec{k}/2)] = 0. \quad \text{(B.5)}$$

Then,

$$\frac{\partial \chi_a(\vec{k}, i\Gamma)}{\partial \omega} = 2\hbar \int \frac{d^3p}{(2\pi\hbar)^3} \frac{2i\Gamma\hbar\vec{p}\cdot\hbar\vec{k}/m}{((\Gamma\hbar)^2 + (\vec{p}\cdot\hbar\vec{k}/m)^2)^2}$$
$$\times [f_0^a(\vec{p} - \hbar\vec{k}/2) - f_0^a(\vec{p} + \hbar\vec{k}/2)]. \quad \text{(B.6)}$$

This result gives us the following relations

$$\left.\frac{\partial \chi_a(\vec{k}, \omega)}{\partial \omega}\right|_{\omega=-i\Gamma} = -\left.\frac{\partial \chi_a(\vec{k}, \omega)}{\partial \omega}\right|_{\omega=i\Gamma}$$
$$\left.\frac{\partial \chi_a(-\vec{k}, \omega)}{\partial \omega}\right|_{\omega=i\Gamma} = \left.\frac{\partial \chi_a(\vec{k}, \omega)}{\partial \omega}\right|_{\omega=i\Gamma} = -\left.\frac{\partial \chi_a(-\vec{k}, \omega)}{\partial \omega}\right|_{\omega=-i\Gamma} \quad \text{(B.7)}$$

with the resultant relations for the derivative of the susceptibility

$$\left.\frac{\partial \varepsilon_a(\vec{k}, \omega)}{\partial \omega}\right|_{\omega=-i\Gamma} = -\left.\frac{\partial \varepsilon_a(\vec{k}, \omega)}{\partial \omega}\right|_{\omega=i\Gamma}$$
$$\left.\frac{\partial \varepsilon_a(-\vec{k}, \omega)}{\partial \omega}\right|_{\omega=i\Gamma} = \left.\frac{\partial \varepsilon_a(\vec{k}, \omega)}{\partial \omega}\right|_{\omega=i\Gamma} = -\left.\frac{\partial \varepsilon_a(-\vec{k}, \omega)}{\partial \omega}\right|_{\omega=-i\Gamma}. \quad \text{(B.8)}$$

In order to calculate the pole contribution of the spectral intensity function, we need the source term correlations. The definition of the source terms given in Eq. (2.27) as

$$S_a^\lambda(\vec{k}, \omega) = \sum_s \hbar \int \frac{d^3p}{(2\pi\hbar)^3} \frac{\langle \vec{p} + \hbar\vec{k}/2|\delta\hat{\rho}_{a,s}^\lambda(0)|\vec{p} - \hbar\vec{k}/2\rangle}{\hbar\omega - \vec{p}\cdot\hbar\vec{k}/m}. \quad \text{(B.9)}$$

If we use $-\vec{k}$ instead of $\vec{k}$, the equation becomes

$$S_a^\lambda(-\vec{k}, \omega) = \sum_s \hbar \int \frac{d^3p}{(2\pi\hbar)^3} \frac{\langle \vec{p} - \hbar\vec{k}/2|\delta\hat{\rho}_{a,s}^\lambda(0)|\vec{p} + \hbar\vec{k}/2\rangle}{\hbar\omega + \vec{p}\cdot\hbar\vec{k}/m}. \quad \text{(B.10)}$$

Therefore, the correlations in Eqs. (2.45-2.47) can be calculated as

$$\overline{S_a^\lambda(\vec{k}, i\Gamma)S_a^\lambda(-\vec{k}', i\Gamma)} = \sum_{s,s'} \hbar^2 \int_{-\infty}^{\infty}\int_{-\infty}^{\infty} \frac{d^3p}{(2\pi\hbar)^3} \frac{d^3p'}{(2\pi\hbar)^3}$$
$$\overline{\frac{\langle \vec{p} + \hbar\vec{k}/2|\delta\hat{\rho}_{a,s}^\lambda(0)|\vec{p} - \hbar\vec{k}/2\rangle\langle \vec{p'} - \hbar\vec{k'}/2|\delta\hat{\rho}_{a,s'}^\lambda(0)|\vec{p'} + \hbar\vec{k'}/2\rangle}{(i\Gamma\hbar - \vec{p}\cdot\hbar\vec{k}/m)(i\Gamma\hbar + \vec{p'}\cdot\hbar\vec{k'}/m)}}$$
$$= -2\hbar^2(2\pi)^3\delta(\vec{k} - \vec{k}') \int \frac{d^3p}{(2\pi\hbar)^3} \frac{f_{0+}^a(1 - f_{0-}^a)}{(\Gamma\hbar)^2 + (\vec{p}\cdot\hbar\vec{k}/m)^2}$$

$$\text{(B.11)}$$

$$\overline{S_a^\lambda(\vec{k}, -i\Gamma)S_a^\lambda(-\vec{k}', -i\Gamma)} = \sum_{s,s'} \hbar^2 \int\limits_{-\infty}^{\infty}\int\limits_{-\infty}^{\infty} \frac{d^3p}{(2\pi\hbar)^3}\frac{d^3p'}{(2\pi\hbar)^3}$$

$$\frac{\overline{\langle\vec{p}+\hbar\vec{k}/2|\delta\hat{\rho}_{a,s}^\lambda(0)|\vec{p}-\hbar\vec{k}/2\rangle\langle\vec{p}'-\hbar\vec{k}'/2|\delta\hat{\rho}_{a,s'}^\lambda(0)|\vec{p}'+\hbar\vec{k}'/2\rangle}}{(-i\Gamma\hbar - \vec{p}\cdot\hbar\vec{k}/m)(-i\Gamma\hbar + \vec{p}'\cdot\hbar\vec{k}'/m)}$$

$$= -2\hbar^2(2\pi)^3\delta(\vec{k}-\vec{k}')\int \frac{d^3p}{(2\pi\hbar)^3}\frac{f_{0+}^a(1-f_{0-}^a)}{(\Gamma\hbar)^2 + (\vec{p}\cdot\hbar\vec{k}/m)^2}$$

(B.12)

$$\overline{S_a^\lambda(\vec{k}, i\Gamma)S_a^\lambda(-\vec{k}', -i\Gamma)} = \sum_{s,s'} \hbar^2 \int\limits_{-\infty}^{\infty}\int\limits_{-\infty}^{\infty} \frac{d^3p}{(2\pi\hbar)^3}\frac{d^3p'}{(2\pi\hbar)^3}$$

$$\frac{\overline{\langle\vec{p}+\hbar\vec{k}/2|\delta\hat{\rho}_{a,s}^\lambda(0)|\vec{p}-\hbar\vec{k}/2\rangle\langle\vec{p}'-\hbar\vec{k}'/2|\delta\hat{\rho}_{a,s'}^\lambda(0)|\vec{p}'+\hbar\vec{k}'/2\rangle}}{(i\Gamma\hbar - \vec{p}\cdot\hbar\vec{k}/m)(-i\Gamma\hbar + \vec{p}'\cdot\hbar\vec{k}'/m)}$$

$$= 2\hbar^2(2\pi)^3\delta(\vec{k}-\vec{k}')\int \frac{d^3p}{(2\pi\hbar)^3}\frac{(\Gamma\hbar)^2 - (\vec{p}\cdot\hbar\vec{k}/m)^2}{\left[(\Gamma\hbar)^2 + (\vec{p}\cdot\hbar\vec{k}/m)^2\right]^2}f_{0+}^a(1-f_{0-}^a)$$

(B.13)

$$\overline{S_a^\lambda(\vec{k}, -i\Gamma)S_a^\lambda(-\vec{k}', i\Gamma)} = \sum_{s,s'} \hbar^2 \int\limits_{-\infty}^{\infty}\int\limits_{-\infty}^{\infty} \frac{d^3p}{(2\pi\hbar)^3}\frac{d^3p'}{(2\pi\hbar)^3}$$

$$\frac{\overline{\langle\vec{p}+\hbar\vec{k}/2|\delta\hat{\rho}_{a,s}^\lambda(0)|\vec{p}-\hbar\vec{k}/2\rangle\langle\vec{p}'-\hbar\vec{k}'/2|\delta\hat{\rho}_{a,s'}^\lambda(0)|\vec{p}'+\hbar\vec{k}'/2\rangle}}{(-i\Gamma\hbar - \vec{p}\cdot\hbar\vec{k}/m)(i\Gamma\hbar + \vec{p}'\cdot\hbar\vec{k}'/m)}$$

$$= 2\hbar^2(2\pi)^3\delta(\vec{k}-\vec{k}')\int \frac{d^3p}{(2\pi\hbar)^3}\frac{(\Gamma\hbar)^2 - (\vec{p}\cdot\hbar\vec{k}/m)^2}{\left[(\Gamma\hbar)^2 + (\vec{p}\cdot\hbar\vec{k}/m)^2\right]^2}f_{0+}^a(1-f_{0-}^a)$$

(B.14)

where we use the shorthand notation $f_{0+}^a(1-f_{0-}^a) = f_0^a(\vec{p}+\hbar\vec{k}/2)\left(1 - f_0^a(\vec{p}-\hbar\vec{k}/2)\right)$. In order to evaluate the above correlations, we use the variance relation for initial density matrix correlations given in Eq. (2.19) as

$$\overline{\langle\vec{p}+\hbar\vec{k}/2|\delta\hat{\rho}_{a,s}^\lambda(0)|\vec{p}-\hbar\vec{k}/2\rangle\langle\vec{p}'-\hbar\vec{k}'/2|\delta\hat{\rho}_{b,s'}^\lambda(0)|\vec{p}'+\hbar\vec{k}'/2\rangle}$$

$$= \delta_{ab}\delta_{ss'}(2\pi\hbar)^3(2\pi)^3\delta(\vec{p}-\vec{p}')\delta(\vec{k}-\vec{k}')f_0^a(\vec{p}+\hbar\vec{k}/2)\left(1 - f_0^a(\vec{p}-\hbar\vec{k}/2)\right)$$

(B.15)

The factor δ_{ab} gives the cross terms of the source term correlations as zero, i.e. $\overline{S_p^\lambda(\vec{k}, i\Gamma)S_n^\lambda(-\vec{k}', i\Gamma)} = \overline{S_p^\lambda(\vec{k}, i\Gamma)S_n^\lambda(-\vec{k}', i\Gamma)} = 0$. Finally, the following relations

between the source correlations are found;

$$
\begin{aligned}
\overline{S_a^\lambda(\vec{k}, i\Gamma)S_a^\lambda(-\vec{k}', i\Gamma)} &= \overline{S_a^\lambda(\vec{k}, -i\Gamma)S_a^\lambda(-\vec{k}', -i\Gamma)} \\
\overline{S_a^\lambda(\vec{k}, i\Gamma)S_a^\lambda(-\vec{k}', -i\Gamma)} &= \overline{S_a^\lambda(\vec{k}, -i\Gamma)S_a^\lambda(-\vec{k}', i\Gamma)}
\end{aligned}
\tag{B.16}
$$

For the integrals in the above expressions, we use the following definition

$$
I_a^\mp = 2\hbar^2 \int \frac{d^3p}{(2\pi\hbar)^3} \frac{\left[(\hbar\Gamma)^2 \mp (\vec{p}\cdot\hbar\vec{k}/m)^2\right]}{\left[(\hbar\Gamma)^2 + (\vec{p}\cdot\hbar\vec{k}/m)^2\right]^2} f_0^a(\vec{p}+\hbar\vec{k}/2)\left(1 - f_0^a(\vec{p}-\hbar\vec{k}/2)\right)
\tag{B.17}
$$

then the correlations of source terms can be written in terms of $I_a^\mp$

$$
\begin{aligned}
\overline{S_a^\lambda(\vec{k}, i\Gamma)S_a^\lambda(-\vec{k}', i\Gamma)} &= \overline{S_a^\lambda(\vec{k}, -i\Gamma)S_a^\lambda(-\vec{k}', -i\Gamma)} = -I_a^+ (2\pi)^3 \\
\overline{S_a^\lambda(\vec{k}, i\Gamma)S_a^\lambda(-\vec{k}', -i\Gamma)} &= \overline{S_a^\lambda(\vec{k}, -i\Gamma)S_a^\lambda(-\vec{k}', i\Gamma)} = I_a^- (2\pi)^3
\end{aligned}
\tag{B.18}
$$

By using these relations in Eqs. (2.45-2.47), we obtain the expressions in Eqs. (2.49-2.50). In the numerical calculations of the spectral intensity function, we firstly evaluate the polar parts of the integrals $\chi_a(\vec{k}, \omega)$, $\frac{\partial \chi_a(\vec{k},\omega)}{\partial \omega}$ and $I_a^\mp$, then the numerical methods are used in the evaluation of the resultant integrals.

APPENDIX C

CUT CONTRIBUTION TO DENSITY CORRELATIONS

In order to calculate the cut-cut part of spectral intensity of density correlations, we use the relation $\tilde{\sigma}_{ab}(CC; \vec{k}, t)(2\pi)^3 \delta(\vec{k} - \vec{k}') = \overline{\delta\rho_a^\lambda(C; \vec{k}, t) + \delta\rho_b^\lambda(C; -\vec{k}', t)}$ and obtain four terms for each isospin components;

$$\tilde{\sigma}_{ab}(CC; \vec{k}, t) = A_{ab}^+(\vec{k}, t) + \tilde{A}_{ab}^+(\vec{k}, t) + \tilde{A}_{ab}^-(\vec{k}, t) + A_{ab}^-(\vec{k}, t). \qquad \text{(C.1)}$$

The first term $A_{ab}^+(\vec{k}, t)$ is obtained from the correlations of the first terms in the expressions $\delta\rho_a^\lambda(C; \vec{k}, t)$ and $\delta\rho_b^\lambda(C; -\vec{k}', t)$. In the calculations, the Eq. (2.19) is used and the cross term correlations of source terms $S_a^\lambda(\pm\vec{k}, \omega \mp i\eta))$ will be zero due to the factor δ_{ab}. Therefore, we obtain the following expressions for neutron-neutron, proton-proton and neutron-proton;

$$A_{nn}^+(\vec{k}, t) = -\int\limits_{-\infty}^{\infty} \frac{d\omega}{2\pi} \int\limits_{-\infty}^{\infty} \frac{d\omega'}{2\pi} e^{-i(\omega+\omega')t}$$

$$\left\{ \frac{\left[1 + F_0^{pp}\chi_p(\vec{k}, \omega + i\eta)\right]\left[1 + F_0^{pp}\chi_p(\vec{k}', \omega' + i\eta)\right]\overline{S_n^\lambda(\vec{k}, \omega + i\eta)S_n^\lambda(-\vec{k}', \omega' + i\eta)}}{\varepsilon(\vec{k}, \omega + i\eta)\varepsilon(-\vec{k}', \omega' + i\eta)} \right.$$

$$\left. + \frac{(F_0^{np})^2\chi_n(\vec{k}, \omega + i\eta)\chi_n(\vec{k}', \omega' + i\eta)\overline{S_p^\lambda(\vec{k}, \omega + i\eta)S_p^\lambda(-\vec{k}', \omega' + i\eta)}}{\varepsilon(\vec{k}, \omega + i\eta)\varepsilon(-\vec{k}', \omega' + i\eta)} \right\}$$

$$\text{(C.2)}$$

$$A_{pp}^+(\vec{k},t) = -\int\limits_{-\infty}^{\infty}\frac{d\omega}{2\pi}\int\limits_{-\infty}^{\infty}\frac{d\omega'}{2\pi}e^{-i(\omega+\omega')t}$$

$$\left\{\frac{\left[1+F_0^{nn}\chi_n(\vec{k},\omega+i\eta)\right]\left[1+F_0^{nn}\chi_n(\vec{k'},\omega'+i\eta)\right]\overline{S_p^\lambda(\vec{k},\omega+i\eta)S_p^\lambda(-\vec{k'},\omega'+i\eta)}}{\varepsilon(\vec{k},\omega+i\eta)\varepsilon(-\vec{k'},\omega'+i\eta)}\right.$$

$$\left.+\frac{(F_0^{pn})^2\chi_p(\vec{k},\omega+i\eta)\chi_p(\vec{k'},\omega'+i\eta)\overline{S_n^\lambda(\vec{k},\omega+i\eta)S_n^\lambda(-\vec{k'},\omega'+i\eta)}}{\varepsilon(\vec{k},\omega+i\eta)\varepsilon(-\vec{k'},\omega'+i\eta)}\right\}$$

(C.3)

and

$$A_{pn}^+(\vec{k},t) = -\int\limits_{-\infty}^{\infty}\frac{d\omega}{2\pi}\int\limits_{-\infty}^{\infty}\frac{d\omega'}{2\pi}e^{-i(\omega+\omega')t}$$

$$\left\{\frac{\left[1+F_0^{nn}\chi_n(\vec{k},\omega+i\eta)\right]F_0^{np}\chi_n(\vec{k'},\omega'+i\eta)\overline{S_p^\lambda(\vec{k},\omega+i\eta)S_p^\lambda(-\vec{k'},\omega'+i\eta)}}{\varepsilon(\vec{k},\omega+i\eta)\varepsilon(-\vec{k'},\omega'+i\eta)}\right.$$

$$\left.+\frac{F_0^{np}\chi_p(\vec{k},\omega+i\eta)\left[1+F_0^{pp}\chi_p(\vec{k'},\omega'+i\eta)\right]\overline{S_n^\lambda(\vec{k},\omega+i\eta)S_n^\lambda(-\vec{k'},\omega'+i\eta)}}{\varepsilon(\vec{k},\omega+i\eta)\varepsilon(-\vec{k'},\omega'+i\eta)}\right\}$$

(C.4)

In these expressions, the correlations of source terms can be obtained according to the SMF approach,

$$\overline{S_a^\lambda(\vec{k},\omega+i\eta)S_a^\lambda(-\vec{k'},\omega'+i\eta)} = \sum_{s,s'}\hbar^2\int\limits_{-\infty}^{\infty}\frac{d^3p}{(2\pi\hbar)^3}\int\limits_{-\infty}^{\infty}\frac{d^3p'}{(2\pi\hbar)^3}$$

$$\frac{\langle\vec{p}+\hbar\vec{k}/2|\delta\hat{\rho}_{a,s}^\lambda(0)|\vec{p}-\hbar\vec{k}/2\rangle}{\hbar(\omega+i\eta)-\vec{p}\cdot\hbar\vec{k}/m}\frac{\langle\vec{p'}-\hbar\vec{k'}/2|\delta\hat{\rho}_{a,s'}^\lambda(0)|\vec{p'}+\hbar\vec{k'}/2\rangle}{(\hbar(\omega'+i\eta)+\vec{p'}\cdot\hbar\vec{k'}/m}$$

$$= 2(2\pi)^3\delta(\vec{k}-\vec{k'})\int\frac{d^3p}{(2\pi\hbar)^3}\frac{f_0^a(\vec{p}+\hbar\vec{k}/2)\left(1-f_0^a(\vec{p}-\hbar\vec{k}/2)\right)}{\left[\omega+i\eta-\vec{p}\cdot\vec{k}/m\right]\left[\omega'+i\eta+\vec{p}\cdot\vec{k}/m\right]}$$

(C.5)

where we use

$$\left(\frac{1}{\omega+i\eta-\vec{p}\cdot\vec{k}/m}\right)\left(\frac{1}{\omega'+i\eta+\vec{p}\cdot\vec{k}/m}\right)$$

$$= \frac{-1}{\omega+\omega'+2i\eta}\left[\frac{1}{\vec{p}\cdot\vec{k}/m-\omega-i\eta}-\frac{1}{\vec{p}\cdot\vec{k}/m+\omega'+i\eta}\right]$$

(C.6)

104

and the correlation of source terms becomes

$$
\overline{S_a^\lambda(\vec{k}, \omega + i\eta) S_a^\lambda(-\vec{k}', \omega' + i\eta)} = 2(2\pi)^3 \delta(\vec{k} - \vec{k}') \int \frac{d^3 p}{(2\pi\hbar)^3} \frac{-1}{\omega + \omega' + 2i\eta}
$$

$$
\times \left[\frac{1}{\vec{p} \cdot \vec{k}/m - \omega - i\eta} - \frac{1}{\vec{p} \cdot \vec{k}/m + \omega' + i\eta} \right] f_0^a(\vec{p} + \hbar\vec{k}/2) \left(1 - f_0^a(\vec{p} - \hbar\vec{k}/2) \right)
$$

(C.7)

Here the following definition $\phi_a(\omega \mp i\eta)$ will be employed

$$
\phi_a(\omega \mp i\eta) = 2 \int_{-\infty}^{+\infty} \frac{d^3 p}{(2\pi\,\hbar)^3} f_0^a(\vec{p} + \hbar\vec{k}/2) \left[1 - f_0^a(\vec{p} - \hbar\vec{k}/2) \right] \frac{1}{\vec{p} \cdot \vec{k}/m - (\omega \mp i\eta)}.
$$
(C.8)

By applying the transition $\vec{p} \to -\vec{p}$ in this definition, the following relations will be found, $\phi_a(-\omega - i\eta) = -\phi_a(\omega + i\eta)$ and $\phi_a(-\omega + i\eta) = -\phi_a(\omega - i\eta)$. In this way, the correlation of source terms can be expressed by

$$
\overline{S_a^\lambda(\vec{k}, \omega + i\eta) S_a^\lambda(-\vec{k}', \omega' + i\eta)} = -(2\pi)^3 \delta(\vec{k} - \vec{k}') \frac{1}{\omega + \omega' + 2i\eta}
$$

$$
\times \left[\phi_a(\omega + i\eta) + \phi_a(\omega' + i\eta) \right] \quad \text{(C.9)}
$$

Finally, $A_{nn}^+(\vec{k}, t)$, $A_{pp}^+(\vec{k}, t)$ and $A_{pn}^+(\vec{k}, t)$ can be written as

$$
A_{nn}^+(\vec{k}, t) = \int_{-\infty}^{\infty} \frac{d\omega}{2\pi} \int_{-\infty}^{\infty} \frac{d\omega'}{2\pi} \frac{e^{-i(\omega + \omega')t}}{\omega + \omega' + 2i\eta}
$$

$$
\left\{ \frac{\left[1 + F_0^{pp} \chi_p(\vec{k}, \omega + i\eta) \right] \left[1 + F_0^{pp} \chi_p(\vec{k}, \omega' + i\eta) \right] \left[\phi_n(\omega + i\eta) + \phi_n(\omega' + i\eta) \right]}{\varepsilon(\vec{k}, \omega + i\eta) \varepsilon(-\vec{k}', \omega' + i\eta)} \right.
$$

$$
+ \frac{(F_0^{np})^2 \chi_n(\vec{k}, \omega + i\eta) \chi_n(\vec{k}, \omega' + i\eta) \left[\phi_p(\omega + i\eta) + \phi_p(\omega' + i\eta) \right]}{\varepsilon(\vec{k}, \omega + i\eta) \varepsilon(-\vec{k}', \omega' + i\eta)} \left. \right\}
$$

(C.10)

$$
A_{pp}^+(\vec{k}, t) = \int_{-\infty}^{\infty} \frac{d\omega}{2\pi} \int_{-\infty}^{\infty} \frac{d\omega'}{2\pi} \frac{e^{-i(\omega + \omega')t}}{\omega + \omega' + 2i\eta}
$$

$$
\left\{ \frac{\left[1 + F_0^{nn} \chi_n(\vec{k}, \omega + i\eta) \right] \left[1 + F_0^{nn} \chi_n(\vec{k}, \omega' + i\eta) \right] \left[\phi_p(\omega + i\eta) + \phi_p(\omega' + i\eta) \right]}{\varepsilon(\vec{k}, \omega + i\eta) \varepsilon(-\vec{k}', \omega' + i\eta)} \right.
$$

$$
+ \frac{(F_0^{pn})^2 \chi_p(\vec{k}, \omega + i\eta) \chi_p(\vec{k}, \omega' + i\eta) \left[\phi_n(\omega + i\eta) + \phi_n(\omega' + i\eta) \right]}{\varepsilon(\vec{k}, \omega + i\eta) \varepsilon(-\vec{k}', \omega' + i\eta)} \left. \right\}
$$

(C.11)

and

$$
A_{pn}^+(\vec{k}, t) = - \int\limits_{-\infty}^{\infty} \frac{d\omega}{2\pi} \int\limits_{-\infty}^{\infty} \frac{d\omega'}{2\pi} \frac{e^{-i(\omega+\omega')t}}{\omega + \omega' + 2i\eta}
$$

$$
\left\{ \frac{\left[1 + F_0^{nn}\chi_n(\vec{k}, \omega + i\eta)\right] F_0^{np}\chi_n(\vec{k}, \omega' + i\eta) \left[\phi_p(\omega + i\eta) + \phi_p(\omega' + i\eta)\right]}{\varepsilon(\vec{k}, \omega + i\eta)\varepsilon(-\vec{k}', \omega' + i\eta)} \right.
$$

$$
\left. + \frac{F_0^{np}\chi_p(\vec{k}, \omega + i\eta) \left[1 + F_0^{pp}\chi_p(\vec{k}, \omega' + i\eta)\right] \left[\phi_n(\omega + i\eta) + \phi_n(\omega' + i\eta)\right]}{\varepsilon(\vec{k}, \omega + i\eta)\varepsilon(-\vec{k}', \omega' + i\eta)} \right\}.
$$

(C.12)

The other terms in Eq. (C.1) also obtained for each isospin components as follows

$$
A_{nn}^-(\vec{k}, t) = \int\limits_{-\infty}^{\infty} \frac{d\omega}{2\pi} \int\limits_{-\infty}^{\infty} \frac{d\omega'}{2\pi} \frac{e^{-i(\omega+\omega')t}}{\omega + \omega' - 2i\eta}
$$

$$
\left\{ \frac{\left[1 + F_0^{pp}\chi_p(\vec{k}, \omega - i\eta)\right] \left[1 + F_0^{pp}\chi_p(\vec{k}, \omega' - i\eta)\right] \left[\phi_n(\omega - i\eta) + \phi_n(\omega' - i\eta)\right]}{\varepsilon(\vec{k}, \omega - i\eta)\varepsilon(\vec{k}, \omega' - i\eta)} \right.
$$

$$
\left. + \frac{(F_0^{np})^2\chi_n(\vec{k}, \omega - i\eta)\chi_n(\vec{k}, \omega' - i\eta) \left[\phi_p(\omega - i\eta) + \phi_p(\omega' - i\eta)\right]}{\varepsilon(\vec{k}, \omega - i\eta)\varepsilon(\vec{k}, \omega' - i\eta)} \right\}
$$

(C.13)

$$
A_{pp}^-(\vec{k}, t) = \int\limits_{-\infty}^{\infty} \frac{d\omega}{2\pi} \int\limits_{-\infty}^{\infty} \frac{d\omega'}{2\pi} \frac{e^{-i(\omega+\omega')t}}{\omega + \omega' - 2i\eta}
$$

$$
\left\{ \frac{\left[1 + F_0^{nn}\chi_n(\vec{k}, \omega - i\eta)\right] \left[1 + F_0^{nn}\chi_n(\vec{k}, \omega' - i\eta)\right] \left[\phi_p(\omega - i\eta) + \phi_p(\omega' - i\eta)\right]}{\varepsilon(\vec{k}, \omega - i\eta)\varepsilon(\vec{k}, \omega' - i\eta)} \right.
$$

$$
\left. + \frac{(F_0^{pn})^2\chi_p(\vec{k}, \omega - i\eta)\chi_p(\vec{k}, \omega' - i\eta) \left[\phi_n(\omega - i\eta) + \phi_n(\omega' - i\eta)\right]}{\varepsilon(\vec{k}, \omega - i\eta)\varepsilon(\vec{k}, \omega' - i\eta)} \right\}
$$

(C.14)

$$
A_{pn}^-(\vec{k}, t) = -\int\limits_{-\infty}^{\infty} \frac{d\omega}{2\pi} \int\limits_{-\infty}^{\infty} \frac{d\omega'}{2\pi} \frac{e^{-i(\omega+\omega')t}}{\omega + \omega' - 2i\eta}
$$

$$
\left\{ \frac{\left[1 + F_0^{nn}\chi_n(\vec{k}, \omega - i\eta)\right] F_0^{np}\chi_n(\vec{k}, \omega' - i\eta) \left[\phi_p(\omega - i\eta) + \phi_p(\omega' - i\eta)\right]}{\varepsilon(\vec{k}, \omega - i\eta)\varepsilon(\vec{k}, \omega' - i\eta)} \right.
$$

$$
\left. + \frac{F_0^{np}\chi_p(\vec{k}, \omega - i\eta)\left[1 + F_0^{pp}\chi_p(\vec{k}, \omega' - i\eta)\right]\left[\phi_n(\omega - \eta) + \phi_n(\omega' - i\eta)\right]}{\varepsilon(\vec{k}, \omega - i\eta)\varepsilon(\vec{k}, \omega' - i\eta)} \right\}
$$

$$(\text{C.15})$$

$$
\tilde{A}_{nn}^+(\vec{k}, t) = -\int\limits_{-\infty}^{\infty} \frac{d\omega}{2\pi} \int\limits_{-\infty}^{\infty} \frac{d\omega'}{2\pi} \frac{e^{-i(\omega+\omega')t}}{\omega + \omega'}
$$

$$
\left\{ \frac{\left[1 + F_0^{pp}\chi_p(\vec{k}, \omega + i\eta)\right]\left[1 + F_0^{pp}\chi_p(\vec{k}, \omega' - i\eta)\right]\left[\phi_n(\omega + i\eta) + \phi_n(\omega' - i\eta)\right]}{\varepsilon(\vec{k}, \omega + i\eta)\varepsilon(\vec{k}, \omega' - i\eta)} \right.
$$

$$
\left. + \frac{(F_0^{np})^2\chi_n(\vec{k}, \omega + i\eta)\chi_n(\vec{k}, \omega' - i\eta)\left[\phi_p(\omega + i\eta) + \phi_p(\omega' - i\eta)\right]}{\varepsilon(\vec{k}, \omega + i\eta)\varepsilon(\vec{k}, \omega' - i\eta)} \right\}
$$

$$(\text{C.16})$$

$$
\tilde{A}_{pp}^+(\vec{k}, t) = -\int\limits_{-\infty}^{\infty} \frac{d\omega}{2\pi} \int\limits_{-\infty}^{\infty} \frac{d\omega'}{2\pi} \frac{e^{-i(\omega+\omega')t}}{\omega + \omega'}
$$

$$
\left\{ \frac{\left[1 + F_0^{nn}\chi_n(\vec{k}, \omega + i\eta)\right]\left[1 + F_0^{nn}\chi_n(\vec{k}, \omega' - i\eta)\right]\left[\phi_p(\omega + i\eta) + \phi_p(\omega' - i\eta)\right]}{\varepsilon(\vec{k}, \omega + i\eta)\varepsilon(\vec{k}, \omega' - i\eta)} \right.
$$

$$
\left. + \frac{(F_0^{pn})^2\chi_p(\vec{k}, \omega + i\eta)\chi_p(\vec{k}, \omega' - i\eta)\left[\phi_n(\omega + i\eta) + \phi_n(\omega' - i\eta)\right]}{\varepsilon(\vec{k}, \omega + i\eta)\varepsilon(\vec{k}, \omega' - i\eta)} \right\}
$$

$$(\text{C.17})$$

$$
\tilde{A}_{pn}^+(\vec{k}, t) = \int\limits_{-\infty}^{\infty} \frac{d\omega}{2\pi} \int\limits_{-\infty}^{\infty} \frac{d\omega'}{2\pi} \frac{e^{-i(\omega+\omega')t}}{\omega + \omega'}
$$

$$
\left\{ \frac{\left[1 + F_0^{nn}\chi_n(\vec{k}, \omega + i\eta)\right] F_0^{np}\chi_n(\vec{k}, \omega' - i\eta) \left[\phi_p(\omega + i\eta) + \phi_p(\omega' - i\eta)\right]}{\varepsilon(\vec{k}, \omega + i\eta)\varepsilon(\vec{k}, \omega' - i\eta)} \right.
$$

$$
\left. + \frac{F_0^{np}\chi_p(\vec{k}, \omega + i\eta)\left[1 + F_0^{pp}\chi_p(\vec{k}, \omega' - i\eta)\right]\left[\phi_n(\omega + i\eta) + \phi_n(\omega' - i\eta)\right]}{\varepsilon(\vec{k}, \omega + i\eta)\varepsilon(\vec{k}, \omega' - i\eta)} \right\}
$$

$$(\text{C.18})$$

$$\tilde{A}_{nn}^{-}(\vec{k},t) = -\int\limits_{-\infty}^{\infty}\frac{d\omega}{2\pi}\int\limits_{-\infty}^{\infty}\frac{d\omega'}{2\pi}\frac{e^{-i(\omega+\omega')t}}{\omega+\omega'}$$

$$\left\{\frac{\left[1+F_0^{pp}\chi_p(\vec{k},\omega-i\eta)\right]\left[1+F_0^{pp}\chi_p(\vec{k},\omega'+i\eta)\right][\phi_n(\omega-i\eta)+\phi_n(\omega'+i\eta)]}{\varepsilon(\vec{k},\omega-i\eta)\varepsilon(\vec{k},\omega'+i\eta)}\right.$$

$$\left.+\frac{(F_0^{np})^2\chi_n(\vec{k},\omega-i\eta)\chi_n(\vec{k},\omega'+i\eta)\left[\phi_p(\omega-i\eta)+\phi_p(\omega'+i\eta)\right]}{\varepsilon(\vec{k},\omega-i\eta)\varepsilon(\vec{k},\omega'+i\eta)}\right\}$$

(C.19)

$$\tilde{A}_{pp}^{-}(\vec{k},t) = -\int\limits_{-\infty}^{\infty}\frac{d\omega}{2\pi}\int\limits_{-\infty}^{\infty}\frac{d\omega'}{2\pi}\frac{e^{-i(\omega+\omega')t}}{\omega+\omega'}$$

$$\left\{\frac{\left[1+F_0^{nn}\chi_n(\vec{k},\omega-i\eta)\right]\left[1+F_0^{nn}\chi_n(\vec{k},\omega'+i\eta)\right][\phi_p(\omega-i\eta)+\phi_p(\omega'+i\eta)]}{\varepsilon(\vec{k},\omega-i\eta)\varepsilon(\vec{k},\omega'+i\eta)}\right.$$

$$\left.+\frac{(F_0^{pn})^2\chi_p(\vec{k},\omega-i\eta)\chi_p(\vec{k},\omega'+i\eta)\left[\phi_n(\omega-i\eta)+\phi_n(\omega'+i\eta)\right]}{\varepsilon(\vec{k},\omega-i\eta)\varepsilon(\vec{k},\omega'+i\eta)}\right\}$$

(C.20)

$$\tilde{A}_{pn}^{-}(\vec{k},t) = \int\limits_{-\infty}^{\infty}\frac{d\omega}{2\pi}\int\limits_{-\infty}^{\infty}\frac{d\omega'}{2\pi}\frac{e^{-i(\omega+\omega')t}}{\omega+\omega'}$$

$$\left\{\frac{\left[1+F_0^{nn}\chi_n(\vec{k},\omega-i\eta)\right]F_0^{np}\chi_n(\vec{k},\omega'+i\eta)[\phi_p(\omega-i\eta)+\phi_p(\omega'+i\eta)]}{\varepsilon(\vec{k},\omega-i\eta)\varepsilon(\vec{k},\omega'+i\eta)}\right.$$

$$\left.+\frac{F_0^{np}\chi_p(\vec{k},\omega-i\eta)\left[1+F_0^{pp}\chi_p(\vec{k},\omega'+i\eta)\right][\phi_n(\omega-i\eta)+\phi_n(\omega'+i\eta)]}{\varepsilon(\vec{k},\omega-i\eta)\varepsilon(\vec{k},\omega'+i\eta)}\right\}$$

(C.21)

To calculate the pole-cut contributions in the spectral intensity of density correlations, we use the relation $\tilde{\sigma}_{ab}(PC;\vec{k},t)(2\pi)^3\delta(\vec{k}-\vec{k}') = \overline{\delta\rho_a^\lambda(P;\vec{k},t)+\delta\rho_b^\lambda(C;-\vec{k}',t)}$ and obtain four terms for each isospin components;

$$\tilde{\sigma}_{ab}(PC;\vec{k},t) = B_{ab}^{+}(\vec{k},t) + \tilde{B}_{ab}^{+}(\vec{k},t) + \tilde{B}_{ab}^{-}(\vec{k},t) + B_{ab}^{-}(\vec{k},t). \qquad \text{(C.22)}$$

The first term $B_{ab}^{+}(\vec{k},t)$ is obtained from the correlations of the first terms in the

expressions $\delta\rho_a^\lambda(P; \vec{k}, t)$ and $\delta\rho_b^\lambda(C; -\vec{k'}, t)$. We obtain $B_{nn}^+(\vec{k}, t)$ for neutron-neutron

$$B_{nn}^+(\vec{k}, t) = \frac{ie^{\Gamma t}}{\partial \varepsilon(\vec{k}, \omega)/\partial \omega \big|_{\omega = i\Gamma}} \int_{-\infty}^{\infty} \frac{d\omega}{2\pi} e^{-i\omega t}$$

$$\left\{ \frac{\left[1 + F_0^{pp}\chi_p(\vec{k}, i\Gamma)\right]\left[1 + F_0^{pp}\chi_p(-\vec{k'}, \omega + i\eta)\right] \overline{S_n^\lambda(\vec{k}, i\Gamma)S_n^\lambda(-\vec{k'}, \omega + i\eta)}}{\varepsilon(-\vec{k'}, \omega + i\eta)} \right.$$

$$\left. + \frac{(F_0^{np})^2 \chi_n(\vec{k}, i\Gamma)\chi_n(-\vec{k'}, \omega + i\eta) \overline{S_p^\lambda(\vec{k}, i\Gamma)S_p^\lambda(-\vec{k'}, \omega + i\eta)}}{\varepsilon(-\vec{k'}, \omega + i\eta)} \right\}.$$

(C.23)

Here we use the following expression for the source term correlations

$$\overline{S_a^\lambda(\vec{k}, i\Gamma)S_a^\lambda(-\vec{k'}, \omega' + i\eta)} =$$

$$2(2\pi)^3 \delta(\vec{k} - \vec{k'}) \int \frac{d^3p}{(2\pi\hbar)^3} \frac{f_0^a(\vec{p} + \hbar\vec{k}/2)\left[1 - f_0^a(\vec{p} - \hbar\vec{k}/2)\right]}{\left(i\Gamma - \vec{p}\cdot\vec{k}/m\right)\left(\omega + i\eta + \vec{p}\cdot\vec{k}/m\right)} \quad \text{(C.24)}$$

with the definition

$$\phi_a(\mp i\Gamma) = 2 \int_{-\infty}^{\infty} \frac{d^3p}{(2\pi\hbar)^3} f_0^a(\vec{p} + \hbar\vec{k}/2)\left[1 - f_0^a(\vec{p} - \hbar\vec{k}/2)\right] \frac{1}{\vec{p}\cdot\vec{k}/m \mp i\Gamma}. \quad \text{(C.25)}$$

Then, the correlation of the source terms becomes

$$\overline{S_a^\lambda(\vec{k}, i\Gamma)S_a^\lambda(-\vec{k'}, \omega' + i\eta)} = -(2\pi)^3 \delta(\vec{k} - \vec{k'}) \frac{1}{\omega + i\Gamma}\left[\phi_a(i\Gamma) - \phi_a(-\omega - i\eta)\right].$$

(C.26)

By using the expressions above B_{nn}^+ is given by

$$B_{nn}^+(\vec{k}, t) = \frac{-ie^{\Gamma t}}{\partial \varepsilon(\vec{k}, \omega)/\partial \omega \big|_{\omega = i\Gamma}} \int_{-\infty}^{\infty} \frac{d\omega}{2\pi} \frac{e^{-i\omega t}}{\omega + i\Gamma}$$

$$\left\{ \frac{\left[1 + F_0^{pp}\chi_p(\vec{k}, i\Gamma)\right]\left[1 + F_0^{pp}\chi_p(\vec{k}, \omega + i\eta)\right]\left[\phi_n(i\Gamma) - \phi_n(-\omega - i\eta)\right]}{\varepsilon(\vec{k}, \omega + i\eta)} \right.$$

$$\left. + \frac{(F_0^{np})^2 \chi_n(\vec{k}, i\Gamma)\chi_n(\vec{k}, \omega + i\eta)\left[\phi_p(i\Gamma) - \phi_p(-\omega - i\eta)\right]}{\varepsilon(\vec{k}, \omega + i\eta)} \right\}.$$

(C.27)

109

Similarly, B_{pp}^+ and B_{pn}^+ are obtained as

$$
B_{pp}^+(\vec{k}, t) = \frac{-ie^{\Gamma t}}{\partial \varepsilon(\vec{k}, \omega)/\partial \omega\big|_{\omega=i\Gamma}} \int_{-\infty}^{\infty} \frac{d\omega}{2\pi} \frac{e^{-i\omega t}}{\omega + i\Gamma}
$$

$$
\left\{ \frac{\left[1 + F_0^{nn}\chi_n(\vec{k}, i\Gamma)\right]\left[1 + F_0^{nn}\chi_n(\vec{k}, \omega + i\eta)\right]\left[\phi_p(i\Gamma) - \phi_p(-\omega - i\eta)\right]}{\varepsilon(\vec{k}, \omega + i\eta)} \right.
$$

$$
\left. + \frac{(F_0^{pn})^2 \chi_p(\vec{k}, i\Gamma)\chi_p(\vec{k}, \omega + i\eta)\left[\phi_n(i\Gamma) - \phi_n(-\omega - i\eta)\right]}{\varepsilon(\vec{k}, \omega + i\eta)} \right\}
$$

$$ \tag{C.28} $$

and

$$
B_{pn}^+(\vec{k}, t) = \frac{ie^{\Gamma t}}{\partial \varepsilon(\vec{k}, \omega)/\partial \omega\big|_{\omega=i\Gamma}} \int_{-\infty}^{\infty} \frac{d\omega}{2\pi} \frac{e^{-i\omega t}}{\omega + i\Gamma}
$$

$$
\left\{ \frac{\left[1 + F_0^{nn}\chi_n(\vec{k}, i\Gamma)\right] F_0^{np}\chi_n(\vec{k}, \omega + i\eta)\left[\phi_p(i\Gamma) + \phi_p(\omega + i\eta)\right]}{\varepsilon(\vec{k}, \omega + i\eta)} \right.
$$

$$
\left. + \frac{F_0^{pn}\chi_p(\vec{k}, i\Gamma)\left[1 + F_0^{pp}\chi_p(\vec{k}, \omega + i\eta)\right]\left[\phi_n(i\Gamma) + \phi_n(\omega + i\eta)\right]}{\varepsilon(\vec{k}, \omega + i\eta)} \right\}.
$$

$$ \tag{C.29} $$

Likewise, the other terms in Eq. (C.22) also obtained for each isospin case as follows

$$
B_{nn}^-(\vec{k}, t) = \frac{ie^{-\Gamma t}}{\partial \varepsilon(\vec{k}, \omega)/\partial \omega\big|_{\omega=-i\Gamma}} \int_{-\infty}^{\infty} \frac{d\omega}{2\pi} \frac{e^{-i\omega t}}{\omega - i\Gamma}
$$

$$
\left\{ \frac{\left[1 + F_0^{pp}\chi_p(\vec{k}, -i\Gamma)\right]\left[1 + F_0^{pp}\chi_p(\vec{k}, \omega - i\eta)\right]\left[\phi_n(-i\Gamma) - \phi_n(-\omega + i\eta)\right]}{\varepsilon(\vec{k}, \omega - i\eta)} \right.
$$

$$
\left. + \frac{(F_0^{np})^2 \chi_n(\vec{k}, -i\Gamma)\chi_n(\vec{k}, \omega - i\eta)\left[\phi_p(-i\Gamma) - \phi_p(-\omega + i\eta)\right]}{\varepsilon(\vec{k}, \omega - i\eta)} \right\},
$$

$$ \tag{C.30} $$

$$B_{pp}^-(\vec{k},t) = \frac{ie^{-\Gamma t}}{\partial\varepsilon(\vec{k},\omega)/\partial\omega\big|_{\omega=-i\Gamma}} \int\limits_{-\infty}^{\infty} \frac{d\omega}{2\pi}\frac{e^{-i\omega t}}{\omega - i\Gamma}$$

$$\left\{ \frac{\left[1 + F_0^{nn}\chi_n(\vec{k},-i\Gamma)\right]\left[1 + F_0^{nn}\chi_n(\vec{k},\omega - i\eta)\right]\left[\phi_p(-i\Gamma) - \phi_p(-\omega + i\eta)\right]}{\varepsilon(\vec{k},\omega - i\eta)} \right.$$

$$\left. + \frac{(F_0^{pn})^2\chi_p(\vec{k},-i\Gamma)\chi_p(\vec{k},\omega - i\eta)\left[\phi_n(-i\Gamma) - \phi_n(-\omega + i\eta)\right]}{\varepsilon(\vec{k},\omega - i\eta)} \right\},$$

$$\text{(C.31)}$$

$$B_{pn}^-(\vec{k},t) = \frac{-ie^{-\Gamma t}}{\partial\varepsilon(\vec{k},\omega)/\partial\omega\big|_{\omega=-i\Gamma}} \int\limits_{-\infty}^{\infty} \frac{d\omega}{2\pi}\frac{e^{-i\omega t}}{\omega - i\Gamma}$$

$$\left\{ \frac{\left[1 + F_0^{nn}\chi_n(\vec{k},-i\Gamma)\right]F_0^{np}\chi_n(\vec{k},\omega - i\eta)\left[\phi_p(-i\Gamma) + \phi_p(\omega - i\eta)\right]}{\varepsilon(\vec{k},\omega - i\eta)} \right.$$

$$\left. + \frac{F_0^{pn}\chi_p(\vec{k},-i\Gamma)\left[1 + F_0^{pp}\chi_p(\vec{k},\omega - i\eta)\right]\left[\phi_n(-i\Gamma) + \phi_n(\omega - i\eta)\right]}{\varepsilon(\vec{k},\omega - i\eta)} \right\},$$

$$\text{(C.32)}$$

$$\tilde{B}_{nn}^+(\vec{k},t) = \frac{ie^{\Gamma t}}{\partial\varepsilon(\vec{k},\omega)/\partial\omega\big|_{\omega=i\Gamma}} \int\limits_{-\infty}^{\infty} \frac{d\omega}{2\pi}\frac{e^{-i\omega t}}{\omega + i\Gamma}$$

$$\left\{ \frac{\left[1 + F_0^{pp}\chi_p(\vec{k},i\Gamma)\right]\left[1 + F_0^{pp}\chi_p(\vec{k},\omega - i\eta)\right]\left[\phi_n(i\Gamma) - \phi_n(-\omega + i\eta)\right]}{\varepsilon(\vec{k},\omega - i\eta)} \right.$$

$$\left. + \frac{(F_0^{np})^2\chi_n(\vec{k},i\Gamma)\chi_n(\vec{k},\omega - i\eta)\left[\phi_p(i\Gamma) - \phi_p(-\omega + i\eta)\right]}{\varepsilon(\vec{k},\omega - i\eta)} \right\},$$

$$\text{(C.33)}$$

$$\tilde{B}_{pp}^+(\vec{k},t) = \frac{ie^{\Gamma t}}{\partial\varepsilon(\vec{k},\omega)/\partial\omega\big|_{\omega=i\Gamma}} \int\limits_{-\infty}^{\infty} \frac{d\omega}{2\pi}\frac{e^{-i\omega t}}{\omega + i\Gamma}$$

$$\left\{ \frac{\left[1 + F_0^{nn}\chi_n(\vec{k},i\Gamma)\right]\left[1 + F_0^{nn}\chi_n(\vec{k},\omega - i\eta)\right]\left[\phi_p(i\Gamma) - \phi_p(-\omega + i\eta)\right]}{\varepsilon(\vec{k},\omega - i\eta)} \right.$$

$$\left. + \frac{(F_0^{pn})^2\chi_p(\vec{k},i\Gamma)\chi_p(\vec{k},\omega - i\eta)\left[\phi_n(i\Gamma) - \phi_n(-\omega + i\eta)\right]}{\varepsilon(\vec{k},\omega - i\eta)} \right\},$$

$$\text{(C.34)}$$

$$\tilde{B}_{pn}^+(\vec{k}, t) = \frac{-ie^{\Gamma t}}{\partial \varepsilon(\vec{k}, \omega)/\partial \omega\big|_{\omega=i\Gamma}} \int\limits_{-\infty}^{\infty} \frac{d\omega}{2\pi} \frac{e^{-i\omega t}}{\omega + i\Gamma}$$

$$\left\{ \frac{\left[1 + F_0^{nn}\chi_n(\vec{k}, i\Gamma)\right] F_0^{np}\chi_n(\vec{k}, \omega - i\eta) \left[\phi_p(i\Gamma) + \phi_p(\omega - i\eta)\right]}{\varepsilon(\vec{k}, \omega - i\eta)} \right.$$

$$\left. + \frac{F_0^{pn}\chi_p(\vec{k}, i\Gamma) \left[1 + F_0^{pp}\chi_p(\vec{k}, \omega - i\eta)\right] \left[\phi_n(i\Gamma) + \phi_n(\omega - i\eta)\right]}{\varepsilon(\vec{k}, \omega - i\eta)} \right\},$$

(C.35)

$$\tilde{B}_{nn}^-(\vec{k}, t) = \frac{-ie^{-\Gamma t}}{\partial \varepsilon(\vec{k}, \omega)/\partial \omega\big|_{\omega=-i\Gamma}} \int\limits_{-\infty}^{\infty} \frac{d\omega}{2\pi} \frac{e^{-i\omega t}}{\omega - i\Gamma}$$

$$\left\{ \frac{\left[1 + F_0^{pp}\chi_p(\vec{k}, -i\Gamma)\right] \left[1 + F_0^{pp}\chi_p(\vec{k}, \omega + i\eta)\right] \left[\phi_n(-i\Gamma) - \phi_n(-\omega - i\eta)\right]}{\varepsilon(\vec{k}, \omega + i\eta)} \right.$$

$$\left. + \frac{(F_0^{np})^2\chi_n(\vec{k}, -i\Gamma)\chi_n(\vec{k}, \omega + i\eta) \left[\phi_p(-i\Gamma) - \phi_p(-\omega - i\eta)\right]}{\varepsilon(\vec{k}, \omega + i\eta)} \right\},$$

(C.36)

$$\tilde{B}_{pp}^-(\vec{k}, t) = \frac{-ie^{-\Gamma t}}{\partial \varepsilon(\vec{k}, \omega)/\partial \omega\big|_{\omega=-i\Gamma}} \int\limits_{-\infty}^{\infty} \frac{d\omega}{2\pi} \frac{e^{-i\omega t}}{\omega - i\Gamma}$$

$$\left\{ \frac{\left[1 + F_0^{nn}\chi_n(\vec{k}, -i\Gamma)\right] \left[1 + F_0^{nn}\chi_n(\vec{k}, \omega + i\eta)\right] \left[\phi_p(-i\Gamma) - \phi_p(-\omega - i\eta)\right]}{\varepsilon(\vec{k}, \omega + i\eta)} \right.$$

$$\left. + \frac{(F_0^{pn})^2\chi_p(\vec{k}, -i\Gamma)\chi_p(\vec{k}, \omega + i\eta) \left[\phi_n(-i\Gamma) - \phi_n(-\omega - i\eta)\right]}{\varepsilon(\vec{k}, \omega + i\eta)} \right\},$$

(C.37)

and

$$\tilde{B}_{pn}^-(\vec{k}, t) = \frac{ie^{-\Gamma t}}{\partial \varepsilon(\vec{k}, \omega)/\partial \omega\big|_{\omega=-i\Gamma}} \int\limits_{-\infty}^{\infty} \frac{d\omega}{2\pi} \frac{e^{-i\omega t}}{\omega - i\Gamma}$$

$$\left\{ \frac{\left[1 + F_0^{nn}\chi_n(\vec{k}, -i\Gamma)\right] F_0^{np}\chi_n(\vec{k}, \omega + i\eta) \left[\phi_p(-i\Gamma) + \phi_p(\omega + i\eta)\right]}{\varepsilon(\vec{k}, \omega + i\eta)} \right.$$

$$\left. + \frac{F_0^{pn}\chi_p(\vec{k}, -i\Gamma) \left[1 + F_0^{pp}\chi_p(\vec{k}, \omega + i\eta)\right] \left[\phi_n(-i\Gamma) + \phi_n(\omega + i\eta)\right]}{\varepsilon(\vec{k}, \omega + i\eta)} \right\}.$$

(C.38)

112

In numerical calculations, the real and imaginary parts of the expressions $\phi_a(\omega \pm i\eta)$ and $\chi_a(\omega \pm i\eta)$ are evaluated separately. In the semi-classical limit, the integral $\phi_a(\omega + i\eta)$ is calculated as

$$
\phi_a(\omega + i\eta) = 2 \int_{-\infty}^{\infty} \frac{d^3p}{(2\pi\hbar)^3} f_0^a(\vec{p}) \left[1 - f_0^a(\vec{p})\right] \frac{1}{\vec{p}\cdot\vec{k}/m - (\omega + i\eta)}
$$

$$
= 2 \int_0^{\infty} \frac{p^2 dp}{(2\pi\hbar)^3} f_0^a(\vec{p}) \left[1 - f_0^a(\vec{p})\right] \frac{2\pi m}{pk} \int_{-1}^{1} dz \left[P\left(\frac{1}{z - \frac{m\omega}{pk}}\right) + i\pi\delta\left(z - \frac{m\omega}{pk}\right) \right]
$$

$$
= -2T \int_0^{\infty} \frac{p^2 dp}{4\pi^2\hbar^3} \frac{\partial f_0^a(p)}{\partial\varepsilon} \frac{m}{pk} \left[P \int_{-1}^{1} \frac{dz}{z - z_0} + i\pi \int_{-1}^{1} dz\delta(z - z_0) \right]
$$

$$\tag{C.39}$$

where we use $f_0^a(\vec{p})\left[1 - f_0^a(\vec{p})\right] = -T\frac{\partial f_0^a(p)}{\partial\varepsilon}$ and $z_0 = \frac{m\omega}{pk}$. Then the real and imaginary parts of $\phi_a(\omega + i\eta)$ becomes

$$
\operatorname{Re} \phi_a(\omega + i\eta) = -\frac{T}{2\pi^2\hbar^3} \frac{m}{k} \int_0^{\infty} p\,dp \frac{\partial f_0^a(p)}{\partial\varepsilon} \ln\left|\frac{z_0 - 1}{z_0 + 1}\right| \tag{C.40}
$$

and

$$
\operatorname{Im} \phi_a(\omega + i\eta) = \begin{cases} T\frac{m^2}{2\pi\hbar^3 k} f_0^a\left(p = \frac{m|\omega|}{k}\right) & \text{if } -1 < z_0 < 1 \\ 0 & else \end{cases} . \tag{C.41}
$$

Similarly, the Linhard function given by

$$
\chi_a(\omega \pm i\eta) = 2 \int_{-\infty}^{\infty} \frac{d^3p}{(2\pi\hbar)^3} \frac{\vec{p}\cdot\vec{k}/m}{(\omega \pm i\eta) - \vec{p}\cdot\vec{k}/m} \frac{\partial f_0^a}{\partial\varepsilon}
$$

$$
= -\frac{1}{2\pi^2\hbar^3} \int_0^{\infty} p^2 dp \frac{\partial f_0^a}{\partial\varepsilon} \int_{-1}^{1} z\,dz \left[P\left\{\frac{1}{z - \frac{m\omega}{pk}}\right\} \pm i\pi\delta\left(z - \frac{m\omega}{pk}\right) \right\}
$$

$$\tag{C.42}$$

can be divided into real and imaginary parts as

$$
\operatorname{Re} \chi_a(\omega + i\eta) = -\frac{1}{2\pi^2\hbar^3} \int_0^{\infty} p^2 dp \frac{\partial f_0^a(p)}{\partial\varepsilon} \left[2 + \ln\left|\frac{z_0 - 1}{z_0 + 1}\right| \right] \tag{C.43}
$$

and

$$
\operatorname{Im} \chi_a(\omega + i\eta) = \begin{cases} \frac{m^2}{2\pi\hbar^3 k} \frac{\omega}{k} f_0^a\left(p = \frac{m|\omega|}{k}\right) & \text{if } -1 < z_0 < 1 \\ 0 & else \end{cases} . \tag{C.44}
$$

113

APPENDIX D

POLE AND CUT CONTRIBUTIONS FOR SYMMETRIC NUCLEAR MATTER

Similar to the asymmetric matter case, we can solve the linear response Eq. (2.18) for the symmetric matter by employing the one-sided Fourier transformation method in time given in Eq. (2.20). This yields an algebraic equation for the Fourier transform of the local density fluctuations, which can be solved to obtain

$$\delta\tilde{\rho}^\lambda(\vec{k},\omega) = \frac{i}{\varepsilon(\vec{k},\omega)} G^\lambda(\vec{k},\omega) \tag{D.1}$$

where $\varepsilon(\vec{k},\omega) = 1 + F_0 \chi(\vec{k},\omega)$ is the susceptibility with $F_0 = (\partial U/\partial\rho)_0$ as the zeroth order Landau parameter, and $\chi(\vec{k},\omega)$ denotes the Lindhard function for symmetric matter. The semi-classical expression of the Lindhard function is given by

$$\chi(\vec{k},\omega) = 4 \int \frac{d^3p}{(2\pi\hbar)^3} \frac{\vec{p}\cdot\hbar\vec{k}/m}{\hbar\omega - \vec{p}\cdot\hbar\vec{k}/m} \frac{\partial f_0}{\partial\varepsilon}. \tag{D.2}$$

The quantity $G^\lambda(\vec{k},\omega)$ for symmetric matter is determined by the initial conditions

$$G^\lambda(\vec{k},\omega) = \sum_s \hbar \int \frac{d^3p}{(2\pi\hbar)^3} \frac{\langle\vec{p}+\hbar\vec{k}/2|\delta\hat{\rho}_s^\lambda(0)|\vec{p}-\hbar\vec{k}/2\rangle}{\hbar\omega - \vec{p}\cdot\hbar\vec{k}/m}. \tag{D.3}$$

According to the stochastic mean-field approach, the variances of the elements of initial density matrix in semi-classical limit are given by

$$\overline{< \vec{p}+\hbar\vec{k}/2|\delta\hat{\rho}_s^\lambda(0)|\vec{p}-\hbar\vec{k}/2 >< \vec{p}'-\hbar\vec{k}'/2|\delta\hat{\rho}_{s'}^\lambda(0)|\vec{p}'+\hbar\vec{k}'/2 >}$$
$$= \delta_{ss'}(2\pi\hbar)^6 \delta(\vec{p}-\vec{p}')\delta(\vec{k}-\vec{k}')\left[f(\vec{p})\left(1-f(\vec{p})\right)\right]. \tag{D.4}$$

We can evaluate the total spectral intensity $\tilde{\sigma}(\vec{k},t)$ by evaluating the ensemble average using the Eqs. (2.33) and (2.34) for pole $\delta\tilde{\rho}^\lambda(P;\vec{k},t)$ and cut $\delta\tilde{\rho}^\lambda(C;\vec{k},t)$ part of the

115

Fourier transform of density fluctuations and the Eq. (D.4) for the correlation of initial fluctuations. As a result, the total spectral intensity for symmetric matter is expressed as,

$$\tilde{\sigma}(\vec{k}, t) = \tilde{\sigma}(PP; \vec{k}, t) + 2\tilde{\sigma}(PC; \vec{k}, t) + \tilde{\sigma}(CC; \vec{k}, t), \qquad \text{(D.5)}$$

where the first and last term are due to pole-pole and cut-cut parts of the spectral intensity and the middle term denotes the mixed pole-cut contribution. The pole-pole part is

$$\tilde{\sigma}(PP; \vec{k}, t) = \frac{E_+}{\left| \left[\partial \varepsilon(\vec{k}, \omega)/\partial \omega \right]_{\omega = i\Gamma_k} \right|^2} \left(e^{+2\Gamma_k t} + e^{-2\Gamma_k t} \right) - \frac{2E_-}{\left| \left[\partial \varepsilon(\vec{k}, \omega)/\partial \omega \right]_{\omega = i\Gamma_k} \right|^2}$$
(D.6)

where the quantity $E_\pm$ is given by

$$E_\pm = 4 \int \frac{d^3 p}{(2\pi\hbar)^3} f(\vec{p}) \left(1 - f(\vec{p})\right) \frac{(\vec{p} \cdot \vec{k}/m)^2 \pm \Gamma_k^2}{\left[(\vec{p} \cdot \vec{k}/m)^2 + \Gamma_k^2 \right]^2}. \qquad \text{(D.7)}$$

The cut-cut contribution has four terms

$$\tilde{\sigma}(CC; \vec{k}, t) = A_0(\vec{k}, t) + \tilde{A}_+(\vec{k}, t) + \tilde{A}_-(\vec{k}, t) + A_-(\vec{k}, t), \qquad \text{(D.8)}$$

with

$$A_\mp(\vec{k}, t) = \int\limits_{-\infty}^{\infty} \frac{d\omega}{2\pi} \int\limits_{-\infty}^{\infty} \frac{d\omega'}{2\pi} \frac{\phi(\omega \mp i\eta) + \phi(\omega' \mp i\eta)}{\varepsilon(\vec{k}, \omega \mp i\eta)\varepsilon(\vec{k}, \omega' \mp i\eta)} \frac{1}{\omega + \omega' \mp 2i\eta} e^{-i(\omega+\omega')t}, \quad \text{(D.9)}$$

and

$$\tilde{A}_\mp(\vec{k}, t) = -\int\limits_{-\infty}^{\infty} \frac{d\omega}{2\pi} \int\limits_{-\infty}^{\infty} \frac{d\omega'}{2\pi} \frac{\phi(\omega \mp i\eta) + \phi(\omega' \pm i\eta)}{\varepsilon(\vec{k}, \omega \mp i\eta)\varepsilon(\vec{k}, \omega' \pm i\eta)} \frac{1}{\omega + \omega'} e^{-i(\omega+\omega')t}. \quad \text{(D.10)}$$

In the above expressions η is an infinitesimal positive number, and quantity $\phi(\omega + i\eta)$ is given for symmetric matter in the semi-classical limit as

$$\phi(\omega + i\eta) = 4 \int \frac{d^3 p}{(2\pi\hbar)^3} f(\vec{p}) \left(1 - f(\vec{p})\right) \frac{1}{\vec{p} \cdot \vec{k}/m - \omega - i\eta}. \qquad \text{(D.11)}$$

The double integral in $A_\mp(\vec{k}, t)$ can be divided into principle value and delta function parts by using the identity $1/(\omega + \omega' \mp i\eta) = P(1/\omega + \omega') \pm i\eta\delta(\omega + \omega')$. The integrand of $\tilde{A}_\mp(\vec{k}, t)$, in contrast to its appearance, is well behaved function, because when $\omega' = \omega$, the nominator is also zero therefore the following ratio becomes finite: $(\phi(\omega \mp i\eta) + \phi(\omega' \pm i\eta))/(\omega + \omega')$.

116

The mixed pole-cut term in the spectral intensity has also four terms;

$$\tilde{\sigma}(PC; \vec{k}, t) = B_+(\vec{k}, t) + \tilde{B}_+(\vec{k}, t) + \tilde{B}_-(\vec{k}, t) + B_-(\vec{k}, t), \qquad \text{(D.12)}$$

with

$$B_\mp(\vec{k}, t) = \pm i \frac{e^{\mp \Gamma_k t}}{\partial \varepsilon(\vec{k}, \omega)/\partial \omega \big|_{\omega = \mp i\Gamma_k}} \int_{-\infty}^{\infty} \frac{d\omega}{2\pi} \frac{\phi(\mp i\Gamma_k) + \phi(\omega \mp i\eta)}{\varepsilon(\vec{k}, \omega \mp i\eta)} \frac{1}{\omega \mp i\Gamma_k} e^{-i\omega t},$$

$$\text{(D.13)}$$

and

$$\tilde{B}_\mp(\vec{k}, t) = \mp i \frac{e^{\mp \Gamma_k t}}{\partial \varepsilon(\vec{k}, \omega)/\partial \omega \big|_{\omega = \mp i\Gamma_k}} \int_{-\infty}^{\infty} \frac{d\omega}{2\pi} \frac{\phi(\mp i\Gamma_k) + \phi(\omega \pm i\eta)}{\varepsilon(\vec{k}, \omega \pm i\eta)} \frac{1}{\omega \mp i\Gamma_k} e^{-i\omega t}.$$

$$\text{(D.14)}$$

Here the quantity $\phi(\mp i\Gamma_k)$ is given by

$$\phi(\mp i\Gamma_k) = 4 \int \frac{d^3 p}{(2\pi\hbar)^3} f(\vec{p}) \left(1 - f(\vec{p})\right) \frac{1}{\vec{p} \cdot \vec{k}/m \pm i\Gamma_k}. \qquad \text{(D.15)}$$

APPENDIX E

FOURIER TRANSFORM OF THE MESON FIELD FLUCTUATIONS

By applying the space Fourier transformation method, the Fourier transform of the fluctuating meson fields are written as

$$
\begin{pmatrix}
\delta\vec{V}(\vec{k},t) \\
\delta V_0(\vec{k},t) \\
\delta\phi_0(\vec{k},t) \\
\delta\vec{A}(\vec{k},t) \\
\delta A_0(\vec{k},t) \\
\delta\vec{b}_3(\vec{k},t)
\end{pmatrix}
= \int d^3 r e^{-i\vec{k}\cdot\vec{r}}
\begin{pmatrix}
\delta\vec{V}(\vec{r},t) \\
\delta V_0(\vec{r},t) \\
\delta\phi_0(\vec{r},t) \\
\delta\vec{A}(\vec{r},t) \\
\delta A_0(\vec{r},t) \\
\delta\vec{b}_3(\vec{r},t)
\end{pmatrix} .
\tag{E.1}
$$

The quantities $\xi_{\lambda'\lambda}^{\mathrm{b}}(\vec{p}_2,\vec{p}_1)$, $\xi_{\lambda'\lambda}^{\mathrm{s}}(\vec{p}_2,\vec{p}_1)$ and $\vec{\xi}_{\lambda'\lambda}^{\mathrm{v}}(\vec{p}_2,\vec{p}_1)$ defined in Eq.(4.39) can be calculated as follows,

$$
\begin{aligned}
\xi_{\lambda'\lambda}^{B}(\vec{p}_2,\vec{p}_1) &= u_{\lambda'}^{\dagger}(\vec{p}_2,s_2)u_\lambda(\vec{p}_1,s_1) \\
&= N_{\lambda'}(\vec{p}_2)N_\lambda(\vec{p}_1)\left(1+\frac{c\vec{p}_1\cdot c\vec{p}_2}{[\lambda'\varepsilon^*(p_2)+M^*c^2][\lambda\varepsilon^*(p_1)+M^*c^2]}\right)
\end{aligned}
\tag{E.2}
$$

$$
\begin{aligned}
\xi_{\lambda'\lambda}^{s}(\vec{p}_2,\vec{p}_1) &= u_{\lambda'}^{\dagger}(\vec{p}_2,s_2)\beta u_\lambda(\vec{p}_1,s_1) \\
&= N_{\lambda'}(\vec{p}_2)N_\lambda(\vec{p}_1)\left(1-\frac{c\vec{p}_1\cdot c\vec{p}_2}{[\lambda'\varepsilon^*(p_2)+M^*c^2][\lambda\varepsilon^*(p_1)+M^*c^2]}\right)
\end{aligned}
\tag{E.3}
$$

and

$$\vec{\xi}^{v}_{\lambda'\lambda}(\vec{p}_2, \vec{p}_1) = u^{\dagger}_{\lambda'}(\vec{p}_2, s_2)\vec{\alpha}u_{\lambda}(\vec{p}_1, s_1)$$

$$= N_{\lambda'}(\vec{p}_2)N_{\lambda}(\vec{p}_1)\left(\frac{c\vec{p}_1 \cdot \hat{k}}{[\lambda'\varepsilon^*(p_2) + M^*c^2]} + \frac{c\vec{p}_2 \cdot \hat{k}}{[\lambda\varepsilon^*(p_1) + M^*c^2]}\right)$$

(E.4)

where the column vector is $u_{\lambda}(\vec{p}, s) = N_{\lambda}(\vec{p})\begin{pmatrix} \chi_s \\ \frac{\vec{\sigma}\cdot c\vec{p}}{Mc^2 + \lambda\varepsilon^*(p)}\chi_s \end{pmatrix}$ and the transpose

of the column vector is $u^{\dagger}_{\lambda}(\vec{p}, s) = N_{\lambda}(\vec{p})\begin{pmatrix} \chi^{\dagger}_s & \chi^{\dagger}_s\frac{\vec{\sigma}\cdot c\vec{p}}{Mc^2 + \lambda\varepsilon^*(p)} \end{pmatrix}$.

By using the definition of fluctuating densities given in Eq.(4.16) and the plane wave representation of density fluctuation matrix given in Eq.(4.29), the spin averaged density fluctuations are defined according to

$$\begin{pmatrix} \delta\vec{\rho}_{a,\mathrm{v}}(\vec{r}, t) \\ \delta\rho_{a,\mathrm{s}}(\vec{r}, t) \\ \delta\rho_{a,\mathrm{b}}(\vec{r}, t) \end{pmatrix} = \gamma\sum_{\lambda\lambda'}\int\frac{d^3p_2 d^3p_1}{(2\pi\hbar)^6} < \vec{r}|\Psi^{\dagger}_{a,\lambda}(\vec{p}_2) > \begin{pmatrix} \vec{\alpha} \\ \beta \\ 1 \end{pmatrix} < \Psi_{a,\lambda'}(\vec{p}_1)|\vec{r} > .$$

(E.5)

Substituting the expression (4.28) for the plane wave spinors, we find

$$\begin{pmatrix} \delta\vec{\rho}_{a,\mathrm{v}}(\vec{r}, t) \\ \delta\rho_{a,\mathrm{s}}(\vec{r}, t) \\ \delta\rho_{a,\mathrm{b}}(\vec{r}, t) \end{pmatrix} = \gamma\sum_{\lambda\lambda'}\int\frac{d^3p_2 d^3p_1}{(2\pi\hbar)^6}e^{-i\vec{r}\cdot(\vec{p}_2-\vec{p}_1)/\hbar}u^{\dagger}_{a,\lambda}(\vec{p}_2, s)$$

$$\times \begin{pmatrix} \vec{\alpha} \\ \beta \\ 1 \end{pmatrix} u_{a,\lambda'}(\vec{p}_1, s)\delta\rho_{a,\lambda'\lambda}(\vec{p}_2, \vec{p}_1, t) .$$

(E.6)

By taking the space Fourier transforms of the fluctuating densities, we obtain the following equation

$$\begin{pmatrix} \delta\vec{\rho}_{a,\mathrm{v}}(\vec{k}, t) \\ \delta\rho_{a,\mathrm{s}}(\vec{k}, t) \\ \delta\rho_{a,\mathrm{b}}(\vec{k}, t) \end{pmatrix} = \gamma\sum_{\lambda\lambda'}\int\frac{d^3p}{(2\pi\hbar)^3}\begin{pmatrix} \vec{\xi}^{\mathrm{v}}_{\lambda'\lambda}(\vec{p}_2, \vec{p}_1) \\ \xi^{\mathrm{s}}_{\lambda'\lambda}(\vec{p}_2, \vec{p}_1) \\ \xi^{\mathrm{b}}_{\lambda'\lambda}(\vec{p}_2, \vec{p}_1) \end{pmatrix}\delta\rho_{a,\lambda'\lambda}(\vec{p}_2, \vec{p}_1, t) .$$

(E.7)

APPENDIX F

RELATIVISTIC LINHARD FUNCTIONS AND DERIVATIVE
OF THE SUSCEPTIBILITY

In order to evaluate the Linhard functions, we consider $(+,+), (+,-)$ and $(-,+)$ sectors. In the calculations, we use only the particle contributions and neglect the anti-particle contributions since the anti-particle contributions is approximately zero for low temperatures, $n_{a,-} = \frac{1}{[e^{(\varepsilon^* + \mu_a^*)/T} + 1]} \approx 0$. Consequently, the relativistic quantal Linhard functions can be written as follows,

$$
\begin{aligned}
\chi_a^{\mathrm{b}}(\vec{k}, \omega) &= \gamma \int \frac{d^3 p}{(2\pi\hbar)^3} \xi_{\mathrm{b}}^{++} \xi_{\mathrm{b}}^{++} \frac{n_{a+}(\vec{p} + \hbar\vec{k}/2) - n_{a+}(\vec{p} - \hbar\vec{k}/2)}{\hbar\omega - [\varepsilon_+^*(\vec{p} + \hbar\vec{k}/2) - \varepsilon_+^*(\vec{p} - \hbar\vec{k}/2)]} \\
&+ \gamma \int \frac{d^3 p}{(2\pi\hbar)^3} \xi_{\mathrm{b}}^{+-} \xi_{\mathrm{b}}^{+-} \frac{n_{a+}(\vec{p} + \hbar\vec{k}/2)}{\hbar\omega - [\varepsilon_+^*(\vec{p} + \hbar\vec{k}/2) - \varepsilon_-^*(\vec{p} - \hbar\vec{k}/2)]} \\
&+ \gamma \int \frac{d^3 p}{(2\pi\hbar)^3} \xi_{\mathrm{b}}^{-+} \xi_{\mathrm{b}}^{-+} \frac{-n_{a+}(\vec{p} + \hbar\vec{k}/2)}{\hbar\omega - [\varepsilon_-^*(\vec{p} + \hbar\vec{k}/2) - \varepsilon_+^*(\vec{p} - \hbar\vec{k}/2)]} ,
\end{aligned}
\tag{F.1}
$$

$$
\begin{aligned}
\chi_a^{\mathrm{s}}(\vec{k}, \omega) &= \gamma \int \frac{d^3 p}{(2\pi\hbar)^3} \xi_{\mathrm{b}}^{++} \xi_{\mathrm{s}}^{++} \frac{n_{a+}(\vec{p} + \hbar\vec{k}/2) - n_{a+}(\vec{p} - \hbar\vec{k}/2)}{\hbar\omega - [\varepsilon_+^*(\vec{p} + \hbar\vec{k}/2) - \varepsilon_+^*(\vec{p} - \hbar\vec{k}/2)]} \\
&+ \gamma \int \frac{d^3 p}{(2\pi\hbar)^3} \xi_{\mathrm{b}}^{+-} \xi_{\mathrm{s}}^{+-} \frac{n_{a+}(\vec{p} + \hbar\vec{k}/2)}{\hbar\omega - [\varepsilon_+^*(\vec{p} + \hbar\vec{k}/2) - \varepsilon_-^*(\vec{p} - \hbar\vec{k}/2)]} \\
&+ \gamma \int \frac{d^3 p}{(2\pi\hbar)^3} \xi_{\mathrm{b}}^{-+} \xi_{\mathrm{s}}^{-+} \frac{-n_{a+}(\vec{p} + \hbar\vec{k}/2)}{\hbar\omega - [\varepsilon_-^*(\vec{p} + \hbar\vec{k}/2) - \varepsilon_+^*(\vec{p} - \hbar\vec{k}/2)]} ,
\end{aligned}
\tag{F.2}
$$

$$\chi_a^{\rm v}(\vec{k},\omega) = \gamma \int \frac{d^3p}{(2\pi\hbar)^3} \xi_{\rm b}^{++} \xi_{\rm v}^{++} \frac{n_{a+}(\vec{p}+\hbar\vec{k}/2) - n_{a+}(\vec{p}-\hbar\vec{k}/2)}{\hbar\omega - [\varepsilon_+^*(\vec{p}+\hbar\vec{k}/2) - \varepsilon_+^*(\vec{p}-\hbar\vec{k}/2)]}$$

$$+ \ \gamma \int \frac{d^3p}{(2\pi\hbar)^3} \xi_{\rm b}^{+-} \xi_{\rm v}^{+-} \frac{n_{a+}(\vec{p}+\hbar\vec{k}/2)}{\hbar\omega - [\varepsilon_+^*(\vec{p}+\hbar\vec{k}/2) - \varepsilon_-^*(\vec{p}-\hbar\vec{k}/2)]}$$

$$+ \ \gamma \int \frac{d^3p}{(2\pi\hbar)^3} \xi_{\rm b}^{-+} \xi_{\rm v}^{-+} \frac{-n_{a+}(\vec{p}+\hbar\vec{k}/2)}{\hbar\omega - [\varepsilon_-^*(\vec{p}+\hbar\vec{k}/2) - \varepsilon_+^*(\vec{p}-\hbar\vec{k}/2)]} \ ,$$

<div align="right">(F.3)</div>

$$\tilde{\chi}_a^{\rm b}(\vec{k},\omega) = \gamma \int \frac{d^3p}{(2\pi\hbar)^3} \xi_{\rm v}^{++} \xi_{\rm v}^{++} \frac{n_{a+}(\vec{p}+\hbar\vec{k}/2) - n_{a+}(\vec{p}-\hbar\vec{k}/2)}{\hbar\omega - [\varepsilon_+^*(\vec{p}+\hbar\vec{k}/2) - \varepsilon_+^*(\vec{p}-\hbar\vec{k}/2)]}$$

$$+ \ \gamma \int \frac{d^3p}{(2\pi\hbar)^3} \xi_{\rm v}^{+-} \xi_{\rm v}^{+-} \frac{n_{a+}(\vec{p}+\hbar\vec{k}/2)}{\hbar\omega - [\varepsilon_+^*(\vec{p}+\hbar\vec{k}/2) - \varepsilon_-^*(\vec{p}-\hbar\vec{k}/2)]}$$

$$+ \ \gamma \int \frac{d^3p}{(2\pi\hbar)^3} \xi_{\rm v}^{-+} \xi_{\rm v}^{-+} \frac{-n_{a+}(\vec{p}+\hbar\vec{k}/2)}{\hbar\omega - [\varepsilon_-^*(\vec{p}+\hbar\vec{k}/2) - \varepsilon_+^*(\vec{p}-\hbar\vec{k}/2)]} \ ,$$

<div align="right">(F.4)</div>

$$\tilde{\chi}_a^{\rm s}(\vec{k},\omega) = \gamma \int \frac{d^3p}{(2\pi\hbar)^3} \xi_{\rm s}^{++} \xi_{\rm s}^{++} \frac{n_{a+}(\vec{p}+\hbar\vec{k}/2) - n_{a+}(\vec{p}-\hbar\vec{k}/2)}{\hbar\omega - [\varepsilon_+^*(\vec{p}+\hbar\vec{k}/2) - \varepsilon_+^*(\vec{p}-\hbar\vec{k}/2)]}$$

$$+ \ \gamma \int \frac{d^3p}{(2\pi\hbar)^3} \xi_{\rm s}^{+-} \xi_{\rm s}^{+-} \frac{n_{a+}(\vec{p}+\hbar\vec{k}/2)}{\hbar\omega - [\varepsilon_+^*(\vec{p}+\hbar\vec{k}/2) - \varepsilon_-^*(\vec{p}-\hbar\vec{k}/2)]}$$

$$+ \ \gamma \int \frac{d^3p}{(2\pi\hbar)^3} \xi_{\rm s}^{-+} \xi_{\rm s}^{-+} \frac{-n_{a+}(\vec{p}+\hbar\vec{k}/2)}{\hbar\omega - [\varepsilon_-^*(\vec{p}+\hbar\vec{k}/2) - \varepsilon_+^*(\vec{p}-\hbar\vec{k}/2)]} \ ,$$

<div align="right">(F.5)</div>

and

$$\tilde{\chi}_a^{\rm v}(\vec{k},\omega) = \gamma \int \frac{d^3p}{(2\pi\hbar)^3} \xi_{\rm s}^{++} \xi_{\rm v}^{++} \frac{n_{a+}(\vec{p}+\hbar\vec{k}/2) - n_{a+}(\vec{p}-\hbar\vec{k}/2)}{\hbar\omega - [\varepsilon_+^*(\vec{p}+\hbar\vec{k}/2) - \varepsilon_+^*(\vec{p}-\hbar\vec{k}/2)]}$$

$$+ \ \gamma \int \frac{d^3p}{(2\pi\hbar)^3} \xi_{\rm s}^{+-} \xi_{\rm v}^{+-} \frac{n_{a+}(\vec{p}+\hbar\vec{k}/2)}{\hbar\omega - [\varepsilon_+^*(\vec{p}+\hbar\vec{k}/2) - \varepsilon_-^*(\vec{p}-\hbar\vec{k}/2)]}$$

$$+ \ \gamma \int \frac{d^3p}{(2\pi\hbar)^3} \xi_{\rm s}^{-+} \xi_{\rm v}^{-+} \frac{-n_{a+}(\vec{p}+\hbar\vec{k}/2)}{\hbar\omega - [\varepsilon_-^*(\vec{p}+\hbar\vec{k}/2) - \varepsilon_+^*(\vec{p}-\hbar\vec{k}/2)]}$$

<div align="right">(F.6)</div>

where $\varepsilon_+^*(p) = +\sqrt{\vec{p}^2 c^2 + M_0^{*2} c^4}$ and $\varepsilon_-^*(p) = -\sqrt{\vec{p}^2 c^2 + M_0^{*2} c^4}$. In the spinodal region, we calculate the Linhard functions at $\omega = i\Gamma$ and we obtain

$$
\begin{aligned}
\chi_a^{\mathrm{b}}(\vec{k}, i\Gamma) = {} & \gamma \int \frac{d^3 p}{(2\pi\hbar)^3} \xi_{\mathrm{b}}^{++} \xi_{\mathrm{b}}^{++} [n_{a+}(\vec{p}_2) - n_{a+}(\vec{p}_1)] \frac{-i\hbar\Gamma - [\varepsilon^*(\vec{p}_2) - \varepsilon^*(\vec{p}_1)]}{(\hbar\Gamma)^2 + [\varepsilon^*(\vec{p}_2) - \varepsilon^*(\vec{p}_1)]^2} \\
& + \gamma \int \frac{d^3 p}{(2\pi\hbar)^3} \xi_{\mathrm{b}}^{+-} \xi_{\mathrm{b}}^{+-} n_{a+}(\vec{p}_2) \frac{-i\hbar\Gamma - [\varepsilon^*(\vec{p}_2) + \varepsilon^*(\vec{p}_1)]}{(\hbar\Gamma)^2 + [\varepsilon^*(\vec{p}_2) + \varepsilon^*(\vec{p}_1)]^2} \\
& + \gamma \int \frac{d^3 p}{(2\pi\hbar)^3} \xi_{\mathrm{b}}^{-+} \xi_{\mathrm{b}}^{-+} [-n_{a+}(\vec{p}_1)] \frac{-i\hbar\Gamma - [-\varepsilon^*(\vec{p}_2) - \varepsilon^*(\vec{p}_1)]}{(\hbar\Gamma)^2 + [-\varepsilon^*(\vec{p}_2) - \varepsilon^*(\vec{p}_1)]^2} \,,
\end{aligned}
$$
(F.7)

$$
\begin{aligned}
\chi_a^{\mathrm{s}}(\vec{k}, i\Gamma) = {} & \gamma \int \frac{d^3 p}{(2\pi\hbar)^3} \xi_{\mathrm{b}}^{++} \xi_{\mathrm{s}}^{++} [n_{a+}(\vec{p}_2) - n_{a+}(\vec{p}_1)] \frac{-i\hbar\Gamma - [\varepsilon^*(\vec{p}_2) - \varepsilon^*(\vec{p}_1)]}{(\hbar\Gamma)^2 + [\varepsilon^*(\vec{p}_2) - \varepsilon^*(\vec{p}_1)]^2} \\
& + \gamma \int \frac{d^3 p}{(2\pi\hbar)^3} \xi_{\mathrm{b}}^{+-} \xi_{\mathrm{s}}^{+-} n_{a+}(\vec{p}_2) \frac{-i\hbar\Gamma - [\varepsilon^*(\vec{p}_2) + \varepsilon^*(\vec{p}_1)]}{(\hbar\Gamma)^2 + [\varepsilon^*(\vec{p}_2) + \varepsilon^*(\vec{p}_1)]^2} \\
& + \gamma \int \frac{d^3 p}{(2\pi\hbar)^3} \xi_{\mathrm{b}}^{-+} \xi_{\mathrm{s}}^{-+} [-n_{a+}(\vec{p}_1)] \frac{-i\hbar\Gamma - [-\varepsilon^*(\vec{p}_2) - \varepsilon^*(\vec{p}_1)]}{(\hbar\Gamma)^2 + [-\varepsilon^*(\vec{p}_2) - \varepsilon^*(\vec{p}_1)]^2} \,,
\end{aligned}
$$
(F.8)

$$
\begin{aligned}
\chi_a^{\mathrm{v}}(\vec{k}, i\Gamma) = {} & \gamma \int \frac{d^3 p}{(2\pi\hbar)^3} \xi_{\mathrm{b}}^{++} \xi_{\mathrm{v}}^{++} [n_{a+}(\vec{p}_2) - n_{a+}(\vec{p}_1] \frac{-i\hbar\Gamma - [\varepsilon^*(\vec{p}_2) - \varepsilon^*(\vec{p}_1)]}{(\hbar\Gamma)^2 + [\varepsilon^*(\vec{p}_2) - \varepsilon^*(\vec{p}_1)]^2} \\
& + \gamma \int \frac{d^3 p}{(2\pi\hbar)^3} \xi_{\mathrm{b}}^{+-} \xi_{\mathrm{v}}^{+-} n_{a+}(\vec{p}_2) \frac{-i\hbar\Gamma - [\varepsilon^*(\vec{p}_2) + \varepsilon^*(\vec{p}_1)]}{(\hbar\Gamma)^2 + [\varepsilon^*(\vec{p}_2) + \varepsilon^*(\vec{p}_1)]^2} \\
& + \gamma \int \frac{d^3 p}{(2\pi\hbar)^3} \xi_{\mathrm{b}}^{-+} \xi_{\mathrm{v}}^{-+} [-n_{a+}(\vec{p}_1)] \frac{-i\hbar\Gamma - [-\varepsilon^*(\vec{p}_2) - \varepsilon^*(\vec{p}_1)]}{(\hbar\Gamma)^2 + [-\varepsilon^*(\vec{p}_2) - \varepsilon^*(\vec{p}_1)]^2} \,,
\end{aligned}
$$
(F.9)

$$
\begin{aligned}
\tilde{\chi}_a^{\mathrm{b}}(\vec{k}, i\Gamma) = {} & \gamma \int \frac{d^3 p}{(2\pi\hbar)^3} \xi_{\mathrm{v}}^{++} \xi_{\mathrm{v}}^{++} [n_{a+}(\vec{p}_2) - n_{a+}(\vec{p}_1] \frac{-i\hbar\Gamma - [\varepsilon^*(\vec{p}_2) - \varepsilon^*(\vec{p}_1)]}{(\hbar\Gamma)^2 + [\varepsilon^*(\vec{p}_2) - \varepsilon^*(\vec{p}_1)]^2} \\
& + \gamma \int \frac{d^3 p}{(2\pi\hbar)^3} \xi_{\mathrm{v}}^{+-} \xi_{\mathrm{v}}^{+-} n_{a+}(\vec{p}_2) \frac{-i\hbar\Gamma - [\varepsilon^*(\vec{p}_2) + \varepsilon^*(\vec{p}_1)]}{(\hbar\Gamma)^2 + [\varepsilon^*(\vec{p}_2) + \varepsilon^*(\vec{p}_1)]^2} \\
& + \gamma \int \frac{d^3 p}{(2\pi\hbar)^3} \xi_{\mathrm{v}}^{-+} \xi_{\mathrm{v}}^{-+} [-n_{a+}(\vec{p}_1)] \frac{-i\hbar\Gamma - [-\varepsilon^*(\vec{p}_2) - \varepsilon^*(\vec{p}_1)]}{(\hbar\Gamma)^2 + [-\varepsilon^*(\vec{p}_2) - \varepsilon^*(\vec{p}_1)]^2} \,,
\end{aligned}
$$
(F.10)

123

$$\tilde{\chi}_a^{\mathrm{s}}(\vec{k},i\Gamma) = \gamma \int \frac{d^3p}{(2\pi\hbar)^3}\xi_{\mathrm{s}}^{++}\xi_{\mathrm{s}}^{++}[n_{a+}(\vec{p}_2)-n_{a+}(\vec{p}_1)]\frac{-i\hbar\Gamma-[\varepsilon^*(\vec{p}_2)-\varepsilon^*(\vec{p}_1)]}{(\hbar\Gamma)^2+[\varepsilon^*(\vec{p}_2)-\varepsilon^*(\vec{p}_1)]^2}$$
$$+ \gamma \int \frac{d^3p}{(2\pi\hbar)^3}\xi_{\mathrm{s}}^{+-}\xi_{\mathrm{s}}^{+-}n_{a+}(\vec{p}_2)\frac{-i\hbar\Gamma-[\varepsilon^*(\vec{p}_2)+\varepsilon^*(\vec{p}_1)]}{(\hbar\Gamma)^2+[\varepsilon^*(\vec{p}_2)+\varepsilon^*(\vec{p}_1)]^2}$$
$$+ \gamma \int \frac{d^3p}{(2\pi\hbar)^3}\xi_{\mathrm{s}}^{-+}\xi_{\mathrm{s}}^{-+}[-n_{a+}(\vec{p}_1)]\frac{-i\hbar\Gamma-[-\varepsilon^*(\vec{p}_2)-\varepsilon^*(\vec{p}_1)]}{(\hbar\Gamma)^2+[-\varepsilon^*(\vec{p}_2)-\varepsilon^*(\vec{p}_1)]^2}\;,$$

(F.11)

and

$$\tilde{\chi}_a^{\mathrm{v}}(\vec{k},i\Gamma) = \gamma \int \frac{d^3p}{(2\pi\hbar)^3}\xi_{\mathrm{s}}^{++}\xi_{\mathrm{v}}^{++}[n_{a+}(\vec{p}_2)-n_{a+}(\vec{p}_1)]\frac{-i\hbar\Gamma-[\varepsilon^*(\vec{p}_2)-\varepsilon^*(\vec{p}_1)]}{(\hbar\Gamma)^2+[\varepsilon^*(\vec{p}_2)-\varepsilon^*(\vec{p}_1)]^2}$$
$$+ \gamma \int \frac{d^3p}{(2\pi\hbar)^3}\xi_{\mathrm{s}}^{+-}\xi_{\mathrm{v}}^{+-}n_{a+}(\vec{p}_2)\frac{-i\hbar\Gamma-[\varepsilon^*(\vec{p}_2)+\varepsilon^*(\vec{p}_1)]}{(\hbar\Gamma)^2+[\varepsilon^*(\vec{p}_2)+\varepsilon^*(\vec{p}_1)]^2}$$
$$+ \gamma \int \frac{d^3p}{(2\pi\hbar)^3}\xi_{\mathrm{s}}^{-+}\xi_{\mathrm{v}}^{-+}[-n_{a+}(\vec{p}_1)]\frac{-i\hbar\Gamma-[-\varepsilon^*(\vec{p}_2)-\varepsilon^*(\vec{p}_1)]}{(\hbar\Gamma)^2+[-\varepsilon^*(\vec{p}_2)-\varepsilon^*(\vec{p}_1)]^2}\;.$$

(F.12)

Here, we use the momentum vectors as $\vec{p}_2 = \vec{p}+\hbar\vec{k}/2$ and $\vec{p}_1 = \vec{p}-\hbar\vec{k}/2$.

The definition of the susceptibility is given in Eq. (4.64) as the determinant of a 6×6 matrix. The elements of this matrix depend on the Linhard functions. Thus, we should obtain the derivative of the Linhard functions in order to find the derivative of the susceptibility. According to definition of the Linhard functions given in Eqs.(4.56) and (4.57), only the term $\frac{1}{\hbar\omega-[\lambda'\varepsilon^*(\vec{p}_2)-\lambda\varepsilon^*(\vec{p}_1)]}$ depends on ω and the derivative of this term is calculated as

$$\frac{\partial}{\partial\omega}\frac{1}{\hbar\omega-[\lambda'\varepsilon^*(\vec{p}_2)-\lambda\varepsilon^*(\vec{p}_1)]} = \frac{-\hbar}{\hbar\omega-[\lambda'\varepsilon^*(\vec{p}_2)-\lambda\varepsilon^*(\vec{p}_1)]^2} \equiv \frac{-\hbar}{[\hbar\omega-\Delta\varepsilon^*_{\lambda\lambda'}]^2}$$

(F.13)

where we use $\Delta\varepsilon^*_{\lambda\lambda'} \equiv [\lambda'\varepsilon^*(\vec{p}_2)-\lambda\varepsilon^*(\vec{p}_1)]$. Then the derivative of the Linhard functions at $\omega = \pm i\Gamma$ can be calculated as

$$\left[\frac{\partial}{\partial\omega}\begin{pmatrix}\chi_a^{\mathrm{v}}(\vec{k},\omega)\\\chi_a^{\mathrm{s}}(\vec{k},\omega)\\\chi_a^{\mathrm{b}}(\vec{k},\omega)\end{pmatrix}\right]_{\omega=\pm i\Gamma} = \gamma\sum_{\lambda\lambda'}\int\frac{d^3p}{(2\pi\hbar)^3}\begin{pmatrix}\xi_{\lambda'\lambda}^{\mathrm{b}}\xi_{\lambda'\lambda}^{\mathrm{v}}\\\xi_{\lambda'\lambda}^{\mathrm{b}}\xi_{\lambda'\lambda}^{\mathrm{s}}\\\xi_{\lambda'\lambda}^{\mathrm{b}}\xi_{\lambda'\lambda}^{\mathrm{b}}\end{pmatrix}[n_{a,\lambda'}(\vec{p}_2)-n_{a,\lambda}(\vec{p}_1)]$$
$$\times\hbar\frac{\Gamma^2\mp 2i\Gamma\Delta\varepsilon^*_{\lambda\lambda'}-(\Delta\varepsilon^*_{\lambda\lambda'})^2}{[\Gamma^2+(\Delta\varepsilon^*_{\lambda\lambda'})^2]^2}$$

(F.14)

124

and

$$
\left[\frac{\partial}{\partial \omega} \begin{pmatrix} \tilde{\chi}_a^{\mathrm{v}}(\vec{k}, \omega) \\ \tilde{\chi}_a^{\mathrm{s}}(\vec{k}, \omega) \\ \tilde{\chi}_a^{\mathrm{b}}(\vec{k}, \omega) \end{pmatrix} \right]_{\omega = \pm i\Gamma} = \gamma \sum_{\lambda\lambda'} \int \frac{d^3p}{(2\pi\hbar)^3} \begin{pmatrix} \xi_{\lambda'\lambda}^{\mathrm{s}} \xi_{\lambda'\lambda}^{\mathrm{v}} \\ \xi_{\lambda'\lambda}^{\mathrm{s}} \xi_{\lambda'\lambda}^{\mathrm{s}} \\ \xi_{\lambda'\lambda}^{\mathrm{v}} \xi_{\lambda'\lambda}^{\mathrm{v}} \end{pmatrix} [n_{a,\lambda'}(\vec{p}_2) - n_{a,\lambda}(\vec{p}_1)]
$$

$$
\times \hbar \frac{\Gamma^2 \mp 2i\Gamma \Delta\varepsilon_{\lambda\lambda'}^* - (\Delta\varepsilon_{\lambda\lambda'}^*)^2}{[\Gamma^2 + (\Delta\varepsilon_{\lambda\lambda'}^*)^2]^2} \ . \qquad \text{(F.15)}
$$

In order to obtain the derivative of the susceptibility, $\partial\varepsilon(\vec{k}, \omega)$, we use the following method:

If the entries $A_{n\times n} = [a_{ij}(t)]$ are differentiable functions of t, then

$\frac{d(det(A))}{dt} = det(D_1) + det(D_2) + ... + det(D_n)$

where D_i is identical to $A_{n\times n}$ except that the entries in the ith row are replaced by their derivatives. By this way, the derivative of the susceptibility becomes

$$
\frac{\partial \varepsilon(\vec{k}, \omega)}{\partial \omega} = \begin{vmatrix} \frac{\partial A_1^p}{\partial \omega} & \frac{\partial A_2^p}{\partial \omega} & \frac{\partial A_3^p}{\partial \omega} & \frac{\partial A_1^n}{\partial \omega} & \frac{\partial A_2^n}{\partial \omega} & \frac{\partial A_3^n}{\partial \omega} \\ B_1^p & B_2^p & B_3^p & B_1^n & B_2^n & B_3^n \\ C_1^p & C_2^p & C_3^p & C_1^n & C_2^n & C_3^n \\ D_1^p & D_2^p & D_3^p & D_1^n & D_2^n & D_3^n \\ E_1^p & E_2^p & E_3^p & E_1^n & E_2^n & E_3^n \\ F_1^p & F_2^p & F_3^p & F_1^n & F_2^n & F_3^n \end{vmatrix}
$$

$$
+ \begin{vmatrix} A_1^p & A_2^p & A_3^p & A_1^n & A_2^n & A_3^n \\ \frac{\partial B_1^p}{\partial \omega} & \frac{\partial B_2^p}{\partial \omega} & \frac{\partial B_3^p}{\partial \omega} & \frac{\partial B_1^n}{\partial \omega} & \frac{\partial B_2^n}{\partial \omega} & \frac{\partial B_3^n}{\partial \omega} \\ C_1^p & C_2^p & C_3^p & C_1^n & C_2^n & C_3^n \\ D_1^p & D_2^p & D_3^p & D_1^n & D_2^n & D_3^n \\ E_1^p & E_2^p & E_3^p & E_1^n & E_2^n & E_3^n \\ F_1^p & F_2^p & F_3^p & F_1^n & F_2^n & F_3^n \end{vmatrix}
$$

$$
+ \begin{vmatrix} A_1^p & A_2^p & A_3^p & A_1^n & A_2^n & A_3^n \\ B_1^p & B_2^p & B_3^p & B_1^n & B_2^n & B_3^n \\ \frac{\partial C_1^p}{\partial \omega} & \frac{\partial C_2^p}{\partial \omega} & \frac{\partial C_3^p}{\partial \omega} & \frac{\partial C_1^n}{\partial \omega} & \frac{\partial C_2^n}{\partial \omega} & \frac{\partial C_3^n}{\partial \omega} \\ D_1^p & D_2^p & D_3^p & D_1^n & D_2^n & D_3^n \\ E_1^p & E_2^p & E_3^p & E_1^n & E_2^n & E_3^n \\ F_1^p & F_2^p & F_3^p & F_1^n & F_2^n & F_3^n \end{vmatrix} + ...
$$

$$
\text{(F.16)}
$$

APPENDIX G

BARYON DENSITY CORRELATION FUNCTIONS

The total spectral intensity of the baryon density correlation function is given as $\tilde{\sigma}(\vec{k},t) = \tilde{\sigma}_{pp}(\vec{k},t) + \tilde{\sigma}_{np}(\vec{k},t) + \tilde{\sigma}_{pn}(\vec{k},t) + \tilde{\sigma}_{nn}(\vec{k},t)$. The spectral intensity functions for proton-proton, neutron-neutron and mixed terms can be calculated separately by using the growing and decaying parts of the density fluctuations given in Eqs. (4.66) and (4.67). The spectral intensity for proton-proton is written as

$$\tilde{\sigma}_{pp}^{BB}(\vec{k},t)(2\pi)^3\delta^3(\vec{k}-\vec{k}') = \overline{\delta\rho_p^{B+}(\vec{k})(\delta\rho_p^{B+}(\vec{k}))^*}e^{2\Gamma_k t} + \overline{\delta\rho_p^{B-}(\vec{k})(\delta\rho_p^{B-}(\vec{k}))^*}e^{-2\Gamma_k t}$$
$$+\overline{\delta\rho_p^{B+}(\vec{k})(\delta\rho_p^{B-}(\vec{k}))^*} + \overline{\delta\rho_p^{B-}(\vec{k})(\delta\rho_p^{B+}(\vec{k}))^*}. \quad \text{(G.1)}$$

Here, the correlation of the growing modes can be written as a function of source terms as

$$\overline{\delta\rho_p^{B+}(\vec{k})(\delta\rho_p^{B+}(\vec{k}))^*}\frac{d_\varepsilon^+ d_\varepsilon^{+*}}{\hbar^2} =$$
$$\overline{\tilde{S}_p^{B+}(\vec{k})\tilde{S}_p^{B+}(\vec{k}')^*}|N_{1p}^+|^2 - \overline{\tilde{S}_p^{B+}(\vec{k})\tilde{S}_p^{S+}(\vec{k}')^*}N_{1p}^+N_{2p}^{+*} + \overline{\tilde{S}_p^{B+}(\vec{k})\tilde{S}_p^{V+}(\vec{k}')^*}N_{1p}^+N_{3p}^{+*}$$
$$- \overline{\tilde{S}_p^{S+}(\vec{k})\tilde{S}_p^{B+}(\vec{k}')^*}N_{2p}^+N_{1p}^{+*} + \overline{\tilde{S}_p^{S+}(\vec{k})\tilde{S}_p^{S+}(\vec{k}')^*}|N_{2p}^+|^2 - \overline{\tilde{S}_p^{S+}(\vec{k})\tilde{S}_p^{V+}(\vec{k}')^*}N_{2p}^+N_{3p}^{+*}$$
$$+ \overline{\tilde{S}_p^{B+}(\vec{k})\tilde{S}_p^{B+}(\vec{k}')^*}N_{3p}^+N_{1p}^{+*} - \overline{\tilde{S}_p^{V+}(\vec{k})\tilde{S}_p^{S+}(\vec{k}')^*}N_{3p}^+N_{2p}^{+*} + \overline{\tilde{S}_p^{V+}(\vec{k})\tilde{S}_p^{V+}(\vec{k}')^*}|N_3^+|^2$$
$$+ \overline{\tilde{S}_n^{B+}(\vec{k})\tilde{S}_n^{B+}(\vec{k}')^*}|N_{4p}^+|^2 - \overline{\tilde{S}_n^{B+}(\vec{k})\tilde{S}_n^{S+}(\vec{k}')^*}N_{4p}^+N_{5p}^{+*} + \overline{\tilde{S}_n^{B+}(\vec{k},)\tilde{S}_n^{V+}(\vec{k}')^*}N_{4p}^+N_{6p}^{+*}$$
$$- \overline{\tilde{S}_n^{S+}(\vec{k})\tilde{S}_n^{B+}(\vec{k}')^*}N_{5p}^+N_{4p}^{+*} + \overline{\tilde{S}_n^{S+}(\vec{k})\tilde{S}_n^{S+}(\vec{k}')^*}|N_{5p}^+|^2 - \overline{\tilde{S}_n^{S+}(\vec{k})\tilde{S}_n^{V+}(\vec{k}')^*}N_{5p}^+N_{6p}^{+*}$$
$$+ \overline{\tilde{S}_n^{B+}(\vec{k})\tilde{S}_n^{B+}(\vec{k}')^*}N_{6p}^+N_{4p}^{+*} - \overline{\tilde{S}_n^{V+}(\vec{k})\tilde{S}_n^{S+}(\vec{k}')^*}N_{6p}^+N_{5p}^{+*} + \overline{\tilde{S}_n^{V+}(\vec{k})\tilde{S}_n^{V+}(\vec{k}')^*}|N_{6p}^+|^2$$
$$\text{(G.2)}$$

where we use the short-hand $d_\epsilon^+ = \frac{\partial\varepsilon(\vec{k},\omega)}{\partial\omega}|_{\omega=i\Gamma}$ and $d_\epsilon^- = \frac{\partial\varepsilon(\vec{k},\omega)}{\partial\omega}|_{\omega=-i\Gamma}$ for the growing and decaying modes respectively and we write $\tilde{S}_a^\pm(\vec{k})$ instead of $\tilde{S}_a^\pm(\vec{k},\omega)$.

Similarly, the correlation of decaying modes can be written as

$$
\overline{\delta\rho_p^{B-}(\vec{k})(\delta\rho_p^{B-}(\vec{k}))^*}\frac{d_\varepsilon^- d_\varepsilon^{-*}}{\hbar^2} =
$$

$$
\overline{\tilde{S}_p^{B-}(\vec{k})\tilde{S}_p^{B-}(\vec{k'})^*}|N_{1p}^-|^2 - \overline{\tilde{S}_p^{B-}(\vec{k})\tilde{S}_p^{S-}(\vec{k'})^*}N_{1p}^- N_{2p}^{-*} + \overline{\tilde{S}_p^{B-}(\vec{k})\tilde{S}_p^{V-}(\vec{k'})^*}N_{1p}^- N_{3p}^{-*}
$$

$$
-\overline{\tilde{S}_p^{S-}(\vec{k})\tilde{S}_p^{B-}(\vec{k'})^*}N_{2p}^- N_{1p}^{-*} + \overline{\tilde{S}_p^{S-}(\vec{k})\tilde{S}_p^{S-}(\vec{k'})^*}|N_{2p}^-|^2 - \overline{\tilde{S}_p^{S-}(\vec{k})\tilde{S}_p^{V-}(\vec{k'})^*}N_{2p}^- N_{3p}^{-*}
$$

$$
+\overline{\tilde{S}_p^{B-}(\vec{k})\tilde{S}_p^{B-}(\vec{k'})^*}N_{3p}^- N_{1p}^{-*} - \overline{\tilde{S}_p^{V-}(\vec{k})\tilde{S}_p^{S-}(\vec{k'})^*}N_{3p}^- N_{2p}^{-*} + \overline{\tilde{S}_p^{V-}(\vec{k})\tilde{S}_p^{V-}(\vec{k'})^*}|N_{3p}^-|^2
$$

$$
+\overline{\tilde{S}_n^{B-}(\vec{k})\tilde{S}_n^{B-}(\vec{k'})^*}|N_{4p}^-|^2 - \overline{\tilde{S}_n^{B-}(\vec{k})\tilde{S}_n^{S-}(\vec{k'})^*}N_{4p}^- N_{5p}^{-*} + \overline{\tilde{S}_n^{B-}(\vec{k})\tilde{S}_n^{V-}(\vec{k'})^*}N_{4p}^- N_{6p}^{-*}
$$

$$
-\overline{\tilde{S}_n^{S-}(\vec{k})\tilde{S}_n^{B-}(\vec{k'})^*}N_{5p}^- N_{4p}^{-*} + \overline{\tilde{S}_n^{S-}(\vec{k})\tilde{S}_n^{S-}(\vec{k'})^*}|N_{5p}^-|^2 - \overline{\tilde{S}_n^{S-}(\vec{k})\tilde{S}_n^{V-}(\vec{k'})^*}N_{5p}^- N_{6p}^{-*}
$$

$$
+\overline{\tilde{S}_n^{B-}(\vec{k})\tilde{S}_n^{B-}(\vec{k'})^*}N_{6p}^- N_{4p}^{-*} - \overline{\tilde{S}_n^{V-}(\vec{k},)\tilde{S}_n^{S-}(\vec{k'})^*}N_{6p}^- N_{5p}^{-*} + \overline{\tilde{S}_n^{V-}(\vec{k})\tilde{S}_n^{V-}(\vec{k'})^*}|N_{6p}^-|^2 .
$$

$$(\text{G.3})$$

The correlations for the cross terms become

$$
\overline{\delta\rho_p^{B+}(\vec{k})(\delta\rho_p^{B-}(\vec{k}))^*}\frac{d_\varepsilon^+ d_\varepsilon^{-*}}{\hbar^2} =
$$

$$
\overline{\tilde{S}_p^{B+}(\vec{k})\tilde{S}_p^{B-}(\vec{k'})^*}N_{1p}^+ N_{1p}^{-*} - \overline{\tilde{S}_p^{B+}(\vec{k})\tilde{S}_p^{S-}(\vec{k'})^*}N_{1p}^+ N_{2p}^{-*} + \overline{\tilde{S}_p^{B+}(\vec{k})\tilde{S}_p^{V-}(\vec{k'})^*}N_{1p}^+ N_{3p}^{-*}
$$

$$
-\overline{\tilde{S}_p^{S+}(\vec{k})\tilde{S}_p^{B-}(\vec{k'})^*}N_{2p}^+ N_{1p}^{-*} + \overline{\tilde{S}_p^{S+}(\vec{k})\tilde{S}_p^{S-}(\vec{k'})^*}N_{2p}^+ N_{2p}^{-*} - \overline{\tilde{S}_p^{S+}(\vec{k})\tilde{S}_p^{V-}(\vec{k'})^*}N_{2p}^+ N_{3p}^{-*}
$$

$$
+\overline{\tilde{S}_p^{B+}(\vec{k})\tilde{S}_p^{B-}(\vec{k'})^*}N_{3p}^+ N_{1p}^{-*} - \overline{\tilde{S}_p^{V+}(\vec{k})\tilde{S}_p^{S-}(\vec{k'})^*}N_{3p}^+ N_{2p}^{-*} + \overline{\tilde{S}_p^{V+}(\vec{k})\tilde{S}_p^{V-}(\vec{k'})^*}N_{3p}^+ N_{3p}^{-*}
$$

$$
+\overline{\tilde{S}_n^{B+}(\vec{k})\tilde{S}_n^{B-}(\vec{k'})^*}N_{4p}^+ N_{4p}^{-*} - \overline{\tilde{S}_n^{B+}(\vec{k})\tilde{S}_n^{S-}(\vec{k'})^*}N_{4p}^+ N_{5p}^{-*} + \overline{\tilde{S}_n^{B+}(\vec{k})\tilde{S}_n^{V-}(\vec{k'})^*}N_{4p}^+ N_{6p}^{-*}
$$

$$
-\overline{\tilde{S}_n^{S+}(\vec{k})\tilde{S}_n^{B-}(\vec{k'})^*}N_{5p}^+ N_{4p}^{-*} + \overline{\tilde{S}_n^{S+}(\vec{k}2)\tilde{S}_n^{S-}(\vec{k'})^*}N_{5p}^+ N_{5p}^{-*} - \overline{\tilde{S}_n^{S+}(\vec{k})\tilde{S}_n^{V-}(\vec{k'})^*}N_{5p}^+ N_{6p}^{-*}
$$

$$
+\overline{\tilde{S}_n^{B+}(\vec{k})\tilde{S}_n^{B-}(\vec{k'})^*}N_{6p}^+ N_{4p}^{-*} - \overline{\tilde{S}_n^{V+}(\vec{k})\tilde{S}_n^{S-}(\vec{k'})^*}N_{6p}^+ N_{5p}^{-*} + \overline{\tilde{S}_n^{V+}(\vec{k})\tilde{S}_n^{V-}(\vec{k'})^*}N_{6p}^+ N_{6p}^{-*}
$$

$$(\text{G.4})$$

and

$$
\overline{\delta\rho_p^{B-}(\vec{k})(\delta\rho_p^{B+}(\vec{k}))^*}\frac{d_\varepsilon^- d_\varepsilon^{+*}}{\hbar^2} =
$$

$$
\overline{\tilde{S}_p^{B-}(\vec{k})\tilde{S}_p^{B+}(\vec{k'})^*}N_{1p}^- N_{1p}^{+*} - \overline{\tilde{S}_p^{B-}(\vec{k})\tilde{S}_p^{S+}(\vec{k'})^*}N_{1p}^- N_{2p}^{+*} + \overline{\tilde{S}_p^{B-}(\vec{k})\tilde{S}_p^{V+}(\vec{k'})^*}N_{1p}^- N_{3p}^{+*}
$$

$$
-\overline{\tilde{S}_p^{S-}(\vec{k})\tilde{S}_p^{B+}(\vec{k'})^*}N_{2p}^- N_{1p}^{+*} + \overline{\tilde{S}_p^{S-}(\vec{k})\tilde{S}_p^{S+}(\vec{k'})^*}N_{2p}^- N_{2p}^{+*} - \overline{\tilde{S}_p^{S-}(\vec{k})\tilde{S}_p^{V+}(\vec{k'})^*}N_{2p}^- N_{3p}^{+*}
$$

$$
+\overline{\tilde{S}_p^{B-}(\vec{k})\tilde{S}_p^{B+}(\vec{k'})^*}N_{3p}^- N_{1p}^{+*} - \overline{\tilde{S}_p^{V-}(\vec{k})\tilde{S}_p^{S+}(\vec{k'})^*}N_{3p}^- N_{2p}^{+*} + \overline{\tilde{S}_p^{V-}(\vec{k})\tilde{S}_p^{V+}(\vec{k'}a)^*}N_{3p}^- N_{3p}^{+*}
$$

$$
+\overline{\tilde{S}_n^{B-}(\vec{k})\tilde{S}_n^{B+}(\vec{k'})^*}N_{4p}^- N_{4p}^{+*} - \overline{\tilde{S}_n^{B-}(\vec{k})\tilde{S}_n^{S+}(\vec{k'})^*}N_{4p}^- N_{5p}^{+*} + \overline{\tilde{S}_n^{B-}(\vec{k})\tilde{S}_n^{V+}(\vec{k'})^*}N_{4p}^- N_{6p}^{+*}
$$

$$
-\overline{\tilde{S}_n^{S-}(\vec{k})\tilde{S}_n^{B+}(\vec{k'})^*}N_{5p}^- N_{4p}^{+*} + \overline{\tilde{S}_n^{S-}(\vec{k})\tilde{S}_n^{S+}(\vec{k'})^*}N_{5p}^- N_{5p}^{+*} - \overline{\tilde{S}_n^{S-}(\vec{k})\tilde{S}_n^{V+}(\vec{k'})^*}N_{5p}^- N_{6p}^{+*}
$$

$$
+\overline{\tilde{S}_n^{B-}(\vec{k})\tilde{S}_n^{B+}(\vec{k'})^*}N_{6p}^- N_{4p}^{+*} - \overline{\tilde{S}_n^{V-}(\vec{k})\tilde{S}_n^{S+}(\vec{k'})^*}N_{6p}^- N_{5p}^{+*} + \overline{\tilde{S}_n^{V-}(\vec{k})\tilde{S}_n^{V+}(\vec{k'})^*}N_{6p}^- N_{6p}^{+*} .
$$

$$(\text{G.5})$$

In order to calculate the correlations for the source terms, we use the definitions of the source terms given in Eq. (4.58) and the following relation

$$
\overline{\delta\rho^a_{\lambda\mu}(\vec{p}_2,\vec{p}_1,0)\delta\rho^b_{\lambda'\mu'}(\vec{p}_2,\vec{p}_1,0)} = \delta_{ab}\delta_{\lambda\lambda'}\delta_{\mu\mu'}(2\pi\hbar)^6\delta(\vec{p}_1-\vec{p}_1')\delta(\vec{p}_2-\vec{p}_2')
$$
$$
\times\frac{1}{2}\left[n_\lambda(\vec{p}_2)(1-n_\mu(\vec{p}_1))+n_\mu(\vec{p}_1)(1-n_\lambda(\vec{p}_2))\right].
$$
(G.6)

According to this relation, proton-neutron and neutron-proton correlations are obtained as zero, $\overline{\tilde{S}_p(\vec{k})\tilde{S}_n(\vec{k}')^*} = \overline{\tilde{S}_n(\vec{k})\tilde{S}_p(\vec{k}')^*} = 0$. The other correlations are defined as follows

$$
\begin{pmatrix} K^{+a}_{\mathrm{BB}} \\ K^{+a}_{\mathrm{ss}} \\ K^{+a}_{\mathrm{vv}} \\ K^{+a}_{\mathrm{Bs}} \\ K^{+a}_{\mathrm{Bv}} \\ K^{+a}_{\mathrm{sv}} \end{pmatrix} = \begin{pmatrix} \overline{\tilde{S}^{B+}_a(\vec{k})\tilde{S}^{B+}_a(\vec{k}')^*} \\ \overline{\tilde{S}^{s+}_a(\vec{k})\tilde{S}^{s+}_a(\vec{k}')^*} \\ \overline{\tilde{S}^{s+}_a(\vec{k})\tilde{S}^{v+}_a(\vec{k}')^*} \\ \overline{\tilde{S}^{B+}_a(\vec{k})\tilde{S}^{s+}_a(\vec{k}')^*} \\ \overline{\tilde{S}^{B+}_a(\vec{k})\tilde{S}^{v+}_a(\vec{k}')^*} \\ \overline{\tilde{S}^{s+}_a(\vec{k})\tilde{S}^{v+}_a(\vec{k}')^*} \end{pmatrix} = \begin{pmatrix} \overline{\tilde{S}^{B-}_a(\vec{k})\tilde{S}^{B-}_a(\vec{k}')^*} \\ \overline{\tilde{S}^{s-}_a(\vec{k})\tilde{S}^{s-}_a(\vec{k}')^*} \\ \overline{\tilde{S}^{s-}_a(\vec{k})\tilde{S}^{v-}_a(\vec{k}')^*} \\ \overline{\tilde{S}^{B-}_a(\vec{k})\tilde{S}^{s-}_a(\vec{k}')^*} \\ \overline{\tilde{S}^{B-}_a(\vec{k})\tilde{S}^{v-}_a(\vec{k}')^*} \\ \overline{\tilde{S}^{s-}_a(\vec{k})\tilde{S}^{v-}_a(\vec{k}')^*} \end{pmatrix}
$$

$$
= \gamma^2 \sum_{\lambda\lambda'} \int \frac{d^3p}{(2\pi\hbar)^3} \begin{pmatrix} \xi^{\mathrm{B}}_{\lambda'\lambda}\xi^{\mathrm{B}}_{\lambda'\lambda} \\ \xi^{\mathrm{s}}_{\lambda'\lambda}\xi^{\mathrm{s}}_{\lambda'\lambda} \\ \xi^{\mathrm{v}}_{\lambda'\lambda}\xi^{\mathrm{v}}_{\lambda'\lambda} \\ \xi^{\mathrm{B}}_{\lambda'\lambda}\xi^{\mathrm{s}}_{\lambda'\lambda} \\ \xi^{\mathrm{B}}_{\lambda'\lambda}\xi^{\mathrm{v}}_{\lambda'\lambda} \\ \xi^{\mathrm{s}}_{\lambda'\lambda}\xi^{\mathrm{v}}_{\lambda'\lambda} \end{pmatrix}
$$
$$
\times\frac{(\hbar\Gamma_k)^2+[\lambda'\varepsilon^*(\vec{p}_2)-\lambda\varepsilon^*(\vec{p}_1)]^2}{\{(\hbar\Gamma_k)^2+[\lambda'\varepsilon^*(\vec{p}_2)-\lambda\varepsilon^*(\vec{p}_1)]^2\}^2}n_{a\lambda'}(\vec{p}_2)[1-n_{a\lambda}(\vec{p}_1)]
$$
(G.7)

and

$$
\begin{pmatrix}
K_{\mathrm{BB}}^{-a} \\
K_{\mathrm{ss}}^{-a} \\
K_{\mathrm{vv}}^{-a} \\
K_{\mathrm{Bs}}^{-a} \\
K_{\mathrm{Bv}}^{-a} \\
K_{\mathrm{sv}}^{-a}
\end{pmatrix}
=
\begin{pmatrix}
\overline{\tilde{S}_a^{B+}(\vec{k})\tilde{S}_a^{B-}(\vec{k}')^*} \\
\overline{\tilde{S}_a^{s+}(\vec{k})\tilde{S}_a^{s-}(\vec{k}')^*} \\
\overline{\tilde{S}_a^{s+}(\vec{k})\tilde{S}_a^{v-}(\vec{k}')^*} \\
\overline{\tilde{S}_a^{B+}(\vec{k})\tilde{S}_a^{s-}(\vec{k}')^*} \\
\overline{\tilde{S}_a^{B+}(\vec{k})\tilde{S}_a^{v-}(\vec{k}')^*} \\
\overline{\tilde{S}_a^{s+}(\vec{k})\tilde{S}_a^{v-}(\vec{k}')^*}
\end{pmatrix}
$$

$$
= -\gamma^2 \sum_{\lambda\lambda'} \int \frac{d^3p}{(2\pi\hbar)^3}
\begin{pmatrix}
\xi_{\lambda'\lambda}^{\mathrm{B}}\xi_{\lambda'\lambda}^{\mathrm{B}} \\
\xi_{\lambda'\lambda}^{\mathrm{s}}\xi_{\lambda'\lambda}^{\mathrm{s}} \\
\xi_{\lambda'\lambda}^{\mathrm{v}}\xi_{\lambda'\lambda}^{\mathrm{v}} \\
\xi_{\lambda'\lambda}^{\mathrm{B}}\xi_{\lambda'\lambda}^{\mathrm{s}} \\
\xi_{\lambda'\lambda}^{\mathrm{B}}\xi_{\lambda'\lambda}^{\mathrm{v}} \\
\xi_{\lambda'\lambda}^{\mathrm{s}}\xi_{\lambda'\lambda}^{\mathrm{v}}
\end{pmatrix}
$$

$$
\times \frac{(\hbar\Gamma_k)^2 - [\lambda'\varepsilon^*(\vec{p}_2) - \lambda\varepsilon^*(\vec{p}_1)]^2}{\{(\hbar\Gamma_k)^2 + [\lambda'\varepsilon^*(\vec{p}_2) - \lambda\varepsilon^*(\vec{p}_1)]^2\}^2} n_{a\lambda'}(\vec{p}_2)[1 - n_{a\lambda}(\vec{p}_1)] .
\tag{G.8}
$$

By using these definitions, we can obtain the correlations for growing and decaying parts of the proton-proton spectral intensity function as

$$
\overline{\left(\delta\rho_p^B(\vec{k})\right)^+ \left[\left(\delta\rho_p^B(\vec{k})\right)^+\right]^*} = \frac{(2\pi)^3\delta(\vec{k}-\vec{k}')\hbar^2}{\left|\left(\frac{\partial\varepsilon(k,\omega)}{\partial\omega}\right)_{\omega=i\Gamma}\right|^2}
$$

$$
\times \left\{ K_{BB}^{+p}|N_{1p}^+|^2 - K_{BS}^{+p}(N_{1p}^+N_{2p}^{+*} + N_{2p}^+N_{1p}^{+*}) + K_{SS}^{+p}|N_{2p}^+|^2 + K_{VV}^{+p}|N_{3p}^+|^2 \right.
$$

$$
+ K_{BB}^{+n}|N_{4p}^+|^2 - K_{BS}^{+n}(N_{4p}^+N_{5p}^{+*} + N_{5p}^+N_{4p}^{+*}) + K_{SS}^{+n}|N_{5p}^+|^2 + K_{VV}^{+n}|N_{6p}^+|^2
$$

$$
+ K_{BV}^{+p}(N_{1p}^+N_{3p}^{+*} + N_{3p}^+N_{1p}^{+*}) - K_{SV}^{+p}(N_{2p}^+N_{3p}^{+*} + N_{3p}^+N_{2p}^{+*})
$$

$$
\left. + K_{BV}^{+n}(N_{4p}^+N_{6p}^{+*} + N_{6p}^+N_{4p}^{+*}) - K_{SV}^{+n}(N_{5p}^+N_{6p}^{+*} + N_{6p}^+N_{5p}^{+*}) \right\}
\tag{G.9}
$$

and

$$
\overline{\left(\delta\rho_p^B(\vec{k})\right)^- \left[\left(\delta\rho_p^B(\vec{k})\right)^-\right]^*} = \frac{(2\pi)^3\delta(\vec{k}-\vec{k}')\hbar^2}{\left|\left(\frac{\partial\varepsilon(k,\omega)}{\partial\omega}\right)_{\omega=-i\Gamma}\right|^2}
$$

$$
\times \left\{ K_{BB}^{+p}|N_{1p}^-|^2 - K_{BS}^{+p}(N_{1p}^-N_{2p}^{-*} + N_{2p}^-N_{1p}^{-*}) + K_{SS}^{+p}|N_{2p}^-|^2 + K_{VV}^{+p}|N_{3p}^-|^2 \right.
$$

$$
+ K_{BB}^{+n}|N_{4p}^-|^2 - K_{BS}^{+n}(N_{4p}^-N_{5p}^{-*} + N_{5p}^-N_{4p}^{-*}) + K_{SS}^{+n}|N_{5p}^-|^2 + K_{VV}^{+n}|N_{6p}^-|^2
$$

$$
+ K_{BV}^{+p}(N_{1p}^-N_{3p}^{-*} + N_{3p}^-N_{1p}^{-*}) - K_{SV}^{+p}(N_{2p}^-N_{3p}^{-*} + N_{3p}^-N_{2p}^{-*})
$$

$$
\left. + K_{BV}^{+n}(N_{4p}^-N_{6p}^{-*} + N_{6p}^-N_{4p}^{-*}) - K_{SV}^{+n}(N_{5p}^-N_{6p}^{-*} + N_{6p}^-N_{5p}^{-*}) \right\} .
\tag{G.10}
$$

The correlations for the mixed terms are obtained as

$$\overline{\left(\delta\rho_p^B(\vec{k})\right)^+\left[\left(\delta\rho_p^B(\vec{k})\right)^-\right]^*} = \frac{(2\pi)^3\delta(\vec{k}-\vec{k}')\hbar^2}{\left[\left(\frac{\partial\varepsilon(k,\omega)}{\partial\omega}\right)_{\omega=i\Gamma}\right]\left[\left(\frac{\partial\varepsilon(k,\omega)}{\partial\omega}\right)_{\omega=-i\Gamma}\right]^*}$$

$$\times\left\{K_{BB}^{-p}N_{1p}^+N_{1p}^{-*} - K_{BS}^{-p}(N_{1p}^+N_{2p}^{-*}+N_{2p}^+N_{1p}^{-*}) + K_{SS}^{-p}N_{2p}^+N_{2p}^{-*} + K_{VV}^{-p}N_{3p}^+N_{3p}^{-*}\right.$$

$$+K_{BB}^{-n}N_{4p}^+N_{4p}^{-*} - K_{BS}^{-n}(N_{4p}^+N_{5p}^{-*}+N_{5p}^+N_{4p}^{-*}) + K_{SS}^{-n}N_{5p}^+N_{5p}^{-*} + K_{VV}^{-n}N_{6p}^+N_{6p}^{-*}$$

$$+K_{BV}^{-p}(N_{1p}^+N_{3p}^{-*}+N_{3p}^+N_{1p}^{-*}) - K_{SV}^{-p}(N_{2p}^+N_{3p}^{-*}+N_{3p}^+N_{2p}^{-*})$$

$$\left.+ K_{BV}^{-n}(N_{4p}^+N_{6p}^{-*}+N_{6p}^+N_{4p}^{-*}) - K_{SV}^{-n}(N_{5p}^+N_{6p}^{-*}+N_{6p}^+N_{5p}^{-*})\right\} , \qquad\text{(G.11)}$$

and

$$\overline{\left(\delta\rho_p^B(\vec{k})\right)^-\left[\left(\delta\rho_p^B(\vec{k})\right)^+\right]^*} = \frac{(2\pi)^3\delta(\vec{k}-\vec{k}')\hbar^2}{\left[\left(\frac{\partial\varepsilon(k,\omega)}{\partial\omega}\right)_{\omega=-i\Gamma}\right]\left[\left(\frac{\partial\varepsilon(k,\omega)}{\partial\omega}\right)_{\omega=i\Gamma}\right]^*}$$

$$\times\left\{K_{BB}^{-p}N_{1p}^-N_{1p}^{+*} - K_{BS}^{-p}(N_{1p}^-N_{2p}^{+*}+N_{2p}^-N_{1p}^{+*}) + K_{SS}^{-p}N_{2p}^-N_{2p}^{+*} + K_{VV}^{-p}N_{3p}^-N_{3p}^{+*}\right.$$

$$+K_{BB}^{-n}N_{4p}^-N_{4p}^{+*} - K_{BS}^{-n}(N_{4p}^-N_{5p}^{+*}+N_{5p}^-N_{4p}^{+*}) + K_{SS}^{-n}N_{5p}^-N_{5p}^{+*} + K_{VV}^{-n}N_{6p}^-N_{6p}^{+*}$$

$$+K_{BV}^{-p}(N_{1p}^-N_{3p}^{+*}+N_{3p}^-N_{1p}^{+*}) - K_{SV}^{-p}(N_{2p}^-N_{3p}^{+*}+N_{3p}^-N_{2p}^{+*})$$

$$\left.+ K_{BV}^{-n}(N_{4p}^-N_{6p}^{+*}+N_{6p}^-N_{4p}^{+*}) - K_{SV}^{-n}(N_{5p}^-N_{6p}^{+*}+N_{6p}^-N_{5p}^{+*})\right\} . \qquad\text{(G.12)}$$

In the above expressions, N_{ia}^+ factors are evaluated at $\omega = +i\Gamma_k$ and N_{ia}^- factors are evaluated at $\omega = -i\Gamma_k$ for $i = 1,...,6$. According to the numerical calculations, $N_{1a}^\pm$, $N_{2a}^\pm$, $N_{4a}^\pm$ and $N_{5a}^\pm$ are found as real and $N_{3a}^\pm$, $N_{6a}^\pm$ are imaginary. There is a relation between them, that can be written as $N_{ia}^- = N_{ia}^+$ for $i = 1,2,4,5$ and $N_{ia}^- = -N_{ia}^+$ for $i = 3,6$. Consequently, we find the correlations of growing and decaying parts equal to each other, $\overline{\left(\delta\rho_p^B(\vec{k})\right)^+\left[\left(\delta\rho_p^B(\vec{k})\right)^+\right]^*} = \overline{\left(\delta\rho_p^B(\vec{k})\right)^-\left[\left(\delta\rho_p^B(\vec{k})\right)^-\right]^*}$. In the calculations of the cross terms, the contributions coming from K_{BV}^{-a} and K_{SV}^{-a} terms cancelled each other. Finally, if we employ the above equations in Eq. (G.1), we get

$$\tilde{\sigma}_{pp}(\vec{k},t) = \hbar^2\frac{E_{pp}^+}{\left|\left(\frac{\partial\varepsilon(k,\omega)}{\partial\omega}\right)_{\omega=i\Gamma}\right|^2}(e^{2\Gamma t}+e^{-2\Gamma t})+\hbar^2\frac{E_{pp}^{+-}+E_{pp}^{-+}}{\left[\left(\frac{\partial\varepsilon(k,\omega)}{\partial\omega}\right)_{\omega=i\Gamma}\right]\left[\left(\frac{\partial\varepsilon(k,\omega)}{\partial\omega}\right)_{\omega=-i\Gamma}\right]^*}$$

$$\text{(G.13)}$$

where the short-hand notations are used for

$$E_{pp}^+ = E_{pp}^- = K_{BB}^{+p}|N_{1p}^+|^2 - K_{BS}^{+p}(N_{1p}^+N_{2p}^- + N_{2p}^+N_{1p}^-) + K_{SS}^{+p}|N_{2p}^+|^2 + K_{VV}^{+p}|N_{3p}^+|^2$$
$$+ K_{BB}^{+n}|N_{4p}^+|^2 - K_{BS}^{+n}(N_{4p}^+N_{5p}^- + N_{5p}^+N_{4p}^-) + K_{SS}^{+n}|N_{5p}^+|^2 + K_{VV}^{+n}|N_{6p}^+|^2$$

$$E_{pp}^{+-} + E_{pp}^{-+} = 2\left\{ K_{BB}^{-p}|N_{1p}^+|^2 - 2K_{BS}^{-p}(N_{1p}^+N_{2p}^+) + K_{SS}^{-p}|N_{2p}^+|^2 + K_{VV}^{-p}|N_{3p}^+|^2 \right.$$
$$\left. + K_{BB}^{-n}|N_{4p}^+|^2 - 2K_{BS}^{-n}(N_{4p}^+N_{5p}^+) + K_{SS}^{-n}|N_{5p}^+|^2 + K_{VV}^{-n}|N_{6p}^+|^2 \right\}$$

$$(G.14)$$

Similarly, we can write the spectral intensity for $\tilde{\sigma}_{nn}^{BB}(\vec{k}, t)$ as

$$\tilde{\sigma}_{nn}^{BB}(\vec{k}, t)(2\pi)^3\delta^3(\vec{k} - \vec{k}') = \overline{\delta\rho_n^{B+}(\vec{k})(\delta\rho_n^{B+}(\vec{k}))^*}e^{2\Gamma_k t} + \overline{\delta\rho_n^{B-}(\vec{k})(\delta\rho_n^{B-}(\vec{k}))^*}e^{-2\Gamma_k t}$$
$$+ \overline{\delta\rho_n^{B+}(\vec{k})(\delta\rho_n^{B-}(\vec{k}))^*} + \overline{\delta\rho_n^{B-}(\vec{k})(\delta\rho_n^{B+}(\vec{k}))^*} \quad (G.15)$$

The correlations are found for the growing, decaying and the mixed terms respectively as,

$$\overline{\left(\delta\rho_n^B(\vec{k})\right)^{\pm}\left[\left(\delta\rho_n^B(\vec{k})\right)^{\pm}\right]^*} = \frac{(2\pi)^3\delta(\vec{k} - \vec{k}')\hbar^2}{\left|\left(\frac{\partial\varepsilon(k,\omega)}{\partial\omega}\right)_{\omega=i\Gamma}\right|^2}$$
$$\times \left\{ K_{BB}^{+p}|N_{1n}^+|^2 - K_{BS}^{+p}(N_{1n}^{+*}N_{2n}^+ + N_{2n}^+N_{1n}^{+*}) + K_{SS}^{+p}|N_{2n}^+|^2 + K_{VV}^{+p}|N_{3n}^+|^2 \right.$$
$$+ K_{BB}^{+n}|N_{4n}^+|^2 - K_{BS}^{+n}(N_{4n}^+N_{5n}^{+*} + N_{5n}^+N_{4n}^{+*}) + K_{SS}^{+n}|N_{5n}^+|^2 + K_{VV}^{+n}|N_{6n}^+|^2$$
$$+ K_{BV}^{+p}(N_{1n}^+N_{3n}^{+*} + N_{3n}^+N_{1n}^{+*}) - K_{SV}^{+p}(N_{2n}^+N_{3n}^{+*} + N_{3n}^+N_{2n}^{+*})$$
$$\left. + K_{BV}^{+n}(N_{4n}^+N_{6n}^{+*} + N_{6n}^+N_{4n}^{+*}) - K_{SV}^{+n}(N_{5n}^+N_{6n}^{+*} + N_{6n}^+N_{5n}^{+*}) \right\}, \quad (G.16)$$

$$\overline{\left(\delta\rho_n^B(\vec{k})\right)^+\left[\left(\delta\rho_n^B(\vec{k})\right)^-\right]^*} = \frac{(2\pi)^3\delta(\vec{k} - \vec{k}')\hbar^2}{\left[\left(\frac{\partial\varepsilon(k,\omega)}{\partial\omega}\right)_{\omega=i\Gamma}\right]\left[\left(\frac{\partial\varepsilon(k,\omega)}{\partial\omega}\right)_{\omega=-i\Gamma}\right]^*}$$
$$\times \left\{ K_{BB}^{-p}N_{1n}^+N_{1n}^{-*} - K_{BS}^{-p}(N_{1n}^+N_{2n}^{-*} + N_{2n}^+N_{1n}^{-*}) + K_{SS}^{-p}N_{2n}^+N_{2n}^{-*} + K_{VV}^{-p}N_{3n}^+N_{3n}^{-*} \right.$$
$$+ K_{BB}^{-n}N_{4n}^+N_{4n}^{-*} - K_{BS}^{-n}(N_{4n}^+N_{5n}^{-*} + N_{5n}^+N_{4n}^{-*}) + K_{SS}^{-n}N_{5n}^+N_{5n}^{-*} + K_{VV}^{-n}N_{6n}^+N_{6n}^{-*}$$
$$+ K_{BV}^{-p}(N_{1n}^+N_{3n}^{-*} + N_{3n}^+N_{1n}^{-*}) - K_{SV}^{-p}(N_{2n}^+N_{3n}^{-*} + N_{3n}^+N_{2n}^{-*})$$
$$\left. + K_{BV}^{-n}(N_{4n}^+N_{6n}^{-*} + N_{6n}^+N_{4n}^{-*}) - K_{SV}^{-n}(N_{5n}^+N_{6n}^{-*} + N_{6n}^+N_{5n}^{-*}) \right\}, \quad (G.17)$$

and

$$
\overline{\left(\delta\rho_n^B(\vec{k})\right)^- \left[\left(\delta\rho_n^B(\vec{k})\right)^+\right]^*} = \frac{(2\pi)^3\delta(\vec{k}-\vec{k}')\hbar^2}{\left[\left(\frac{\partial\varepsilon(k,\omega)}{\partial\omega}\right)_{\omega=-i\Gamma}\right]\left[\left(\frac{\partial\varepsilon(k,\omega)}{\partial\omega}\right)_{\omega=i\Gamma}\right]^*}
$$

$$
\times \left\{ K_{BB}^{-p}N_{1n}^-N_{1n}^{+*} - K_{BS}^{-p}(N_{1n}^-N_{2n}^{+*} + N_{2n}^-N_{1n}^{+*}) + K_{SS}^{-p}N_{2n}^-N_{2n}^{+*} + K_{VV}^{-p}N_{3n}^-N_{3n}^{+*} \right.
$$

$$
+ K_{BB}^{-n}N_{4n}^-N_{4n}^{+*} - K_{BS}^{-n}(N_{4n}^-N_{5n}^{+*} + N_{5n}^-N_{4n}^{+*}) + K_{SS}^{-n}N_{5n}^-N_{5n}^{+*} + K_{VV}^{-n}N_{6n}^-N_{6n}^{+*}
$$

$$
+ K_{BV}^{-p}(N_{1n}^-N_{3n}^{+*} + N_{3n}^-N_{1n}^{+*}) - K_{SV}^{-p}(N_{2n}^-N_{3n}^{+*} + N_{3n}^-N_{2n}^{+*})
$$

$$
\left. + K_{BV}^{-n}(N_{4n}^-N_{6n}^{+*} + N_{6n}^-N_{4n}^{+*}) - K_{SV}^{-n}(N_{5n}^-N_{6n}^{+*} + N_{6n}^-N_{5n}^{+*}) \right\} . \tag{G.18}
$$

Then, the neutron-neutron spectral intensity function, $\tilde{\sigma}_{nn}(\vec{k},t)$, can be written as

$$
\tilde{\sigma}_{nn}(\vec{k},t) = \hbar^2 \frac{E_{nn}^+}{\left|\left(\frac{\partial\varepsilon(k,\omega)}{\partial\omega}\right)_{\omega=i\Gamma}\right|^2}(e^{2\Gamma t}+e^{-2\Gamma t}) + \hbar^2 \frac{E_{nn}^{+-}+E_{nn}^{-+}}{\left[\left(\frac{\partial\varepsilon(k,\omega)}{\partial\omega}\right)_{\omega=i\Gamma}\right]\left[\left(\frac{\partial\varepsilon(k,\omega)}{\partial\omega}\right)_{\omega=-i\Gamma}\right]^*}
$$
(G.19)

where we use

$$
E_{nn}^+ = E_{nn}^- = K_{BB}^{+p}|N_{1n}^+|^2 - K_{BS}^{+p}(N_{1n}^+N_{2n}^- + N_{2n}^+N_{1n}^-) + K_{SS}^{+p}|N_{2n}^+|^2 + K_{VV}^{+p}|N_{3n}^+|^2
$$

$$
+ K_{BB}^{+n}|N_{4n}^+|^2 - K_{BS}^{+n}(N_{4n}^+N_{5n}^- + N_{5n}^+N_{4n}^-) + K_{SS}^{+n}|N_{5n}^+|^2 + K_{VV}^{+n}|N_{6n}^+|^2
$$

$$
E_{nn}^{+-} + E_{nn}^{-+} = 2\left\{ K_{BB}^{-p}|N_{1n}^+|^2 - 2K_{BS}^{-p}(N_{1n}^+N_{2n}^+) + K_{SS}^{-p}|N_{2n}^+|^2 + K_{VV}^{-p}|N_{3n}^+|^2 \right.
$$

$$
\left. + K_{BB}^{-n}|N_{4n}^+|^2 - 2K_{BS}^{-n}(N_{4n}^+N_{5n}^+) + K_{SS}^{-n}|N_{5n}^+|^2 + K_{VV}^{-n}|N_{6n}^+|^2 \right\} .
$$
(G.20)

Finally, the spectral intensity for the cross terms are given by

$$
\tilde{\sigma}_{np}^{BB}(\vec{k},t)(2\pi)^3\delta^3(\vec{k}-\vec{k}') = \overline{\delta\rho_n^{B+}(\vec{k})(\delta\rho_p^{B+}(\vec{k}))^*}e^{2\Gamma_k t} + \overline{\delta\rho_n^{B-}(\vec{k})(\delta\rho_p^{B-}(\vec{k}))^*}e^{-2\Gamma_k t}
$$

$$
+ \overline{\delta\rho_n^{B+}(\vec{k})(\delta\rho_p^{B-}(\vec{k}))^*} + \overline{\delta\rho_n^{B-}(\vec{k})(\delta\rho_p^{B+}(\vec{k}))^*} \tag{G.21}
$$

The correlations for growing and decaying parts of the neutron-proton spectral intensity function as

$$
\overline{\left(\delta\rho_n^B(\vec{k})\right)^+ \left[\left(\delta\rho_p^B(\vec{k})\right)^+\right]^*} = -\frac{(2\pi)^3\delta(\vec{k}-\vec{k}')\hbar^2}{\left|\left(\frac{\partial\varepsilon(k,\omega)}{\partial\omega}\right)_{\omega=i\Gamma}\right|^2}
$$

$$
\times \left\{ K_{BB}^{+p}N_{1n}^+N_{1p}^+ - K_{BS}^{+p}(N_{1n}^+N_{2p}^+ + N_{2n}^+N_{1p}^+) + K_{SS}^{+p}N_{2n}^+N_{2p}^+ + K_{VV}^{+p}N_{3n}^+N_{3p}^+ \right.
$$

$$
+ K_{BB}^{+n}N_{4n}^+N_{4p}^+ - K_{BS}^{+n}(N_{4n}^+N_{5p}^+ + N_{5n}^+N_{4p}^+) + K_{SS}^{+n}N_{5n}^+N_{5p}^+ + K_{VV}^{+n}N_{6n}^+N_{6p}^+
$$

$$
+ K_{BV}^{+p}(-iN_{1n}^+N_{3p}^+ + iN_{3n}^+N_{1p}^+) - K_{SV}^{+p}(-iN_{2n}^+N_{3p}^+ + iN_{3n}^+N_{2p}^+)
$$

$$
\left. + K_{BV}^{+n}(-iN_{4n}^+N_{6p}^+ + iN_{6n}^+N_{4p}^+) - K_{SV}^{+n}(-iN_{5n}^+N_{6p}^+ + iN_{6n}^+N_{5p}^+) \right\} \tag{G.22}
$$

133

and

$$\overline{\left(\delta\rho_n^B(\vec{k})\right)^- \left[\left(\delta\rho_p^B(\vec{k})\right)^-\right]^*} = -\frac{(2\pi)^3 \delta(\vec{k}-\vec{k}')\hbar^2}{\left|\left(\frac{\partial\varepsilon(k,\omega)}{\partial\omega}\right)_{\omega=-i\Gamma}\right|^2}$$

$$\times \left\{ K_{BB}^{+p} N_{1n}^+ N_{1p}^+ - K_{BS}^{+p}(N_{1n}^+ N_{2p}^+ + N_{2n}^+ N_{1p}^+) + K_{SS}^{+p} N_{2n}^+ N_{2p}^+ + K_{VV}^{+p} N_{3n}^+ N_{3p}^+ \right.$$

$$+ K_{BB}^{+n} N_{4n}^+ N_{4p}^+ - K_{BS}^{+n}(N_{4n}^+ N_{5p}^+ + N_{5n}^+ N_{4p}^+) + K_{SS}^{+n} N_{5n}^+ N_{5p}^+ + K_{VV}^{+n} N_{6n}^+ N_{6p}^+$$

$$+ K_{BV}^{+p}(iN_{1n}^+ N_{3p}^+ - iN_{3n}^+ N_{1p}^+) - K_{SV}^{+p}(iN_{2n}^+ N_{3p}^+ - iN_{3n}^+ N_{2p}^+)$$

$$\left. + K_{BV}^{+n}(iN_{4n}^+ N_{6p}^+ - iN_{6n}^+ N_{4p}^+) - K_{SV}^{+n}(iN_{5n}^+ N_{6p}^+ - iN_{6n}^+ N_{5p}^+) \right\} \qquad \text{(G.23)}$$

The correlations for the mixed terms are obtained as

$$\overline{\left(\delta\rho_n^B(\vec{k})\right)^+ \left[\left(\delta\rho_p^B(\vec{k})\right)^-\right]^*} = -\frac{(2\pi)^3 \delta(\vec{k}-\vec{k}')\hbar^2}{\left[\left(\frac{\partial\varepsilon(k,\omega)}{\partial\omega}\right)_{\omega=i\Gamma}\right]\left[\left(\frac{\partial\varepsilon(k,\omega)}{\partial\omega}\right)_{\omega=-i\Gamma}\right]^*}$$

$$\times \left\{ K_{BB}^{-p} N_{1n}^+ N_{1p}^+ - K_{BS}^{-p}(N_{1n}^+ N_{2p}^+ + N_{2n}^+ N_{1p}^+) + K_{SS}^{-p} N_{2n}^+ N_{2p}^+ + K_{VV}^{-p} N_{3n}^+ N_{3p}^+ \right.$$

$$+ K_{BB}^{-n} N_{4n}^+ N_{4p}^+ - K_{BS}^{-n}(N_{4n}^+ N_{5p}^+ + N_{5n}^+ N_{4p}^+) + K_{SS}^{-n} N_{5n}^+ N_{5p}^+ + K_{VV}^{-n} N_{6n}^+ N_{6p}^+$$

$$+ K_{BV}^{-p}(iN_{1n}^+ N_{3p}^+ + iN_{3n}^+ N_{1p}^+) - K_{SV}^{-p}(iN_{2n}^+ N_{3p}^+ + iN_{3n}^+ N_{2p}^+)$$

$$\left. + K_{BV}^{-n}(iN_{4n}^+ N_{6p}^+ + iN_{6n}^+ N_{4p}^+) - K_{SV}^{-n}(iN_{5n}^+ N_{6p}^+ + iN_{6n}^+ N_{5p}^+) \right\} \qquad \text{(G.24)}$$

and

$$\overline{\left(\delta\rho_n^B(\vec{k})\right)^- \left[\left(\delta\rho_p^B(\vec{k})\right)^+\right]^*} = -\frac{(2\pi)^3 \delta(\vec{k}-\vec{k}')\hbar^2}{\left[\left(\frac{\partial\varepsilon(k,\omega)}{\partial\omega}\right)_{\omega=-i\Gamma}\right]\left[\left(\frac{\partial\varepsilon(k,\omega)}{\partial\omega}\right)_{\omega=i\Gamma}\right]^*}$$

$$\times \left\{ K_{BB}^{-p} N_{1n}^+ N_{1p}^+ - K_{BS}^{-p}(N_{1n}^+ N_{2p}^+ + N_{2n}^+ N_{1p}^+) + K_{SS}^{-p} N_{2n}^+ N_{2p}^+ + K_{VV}^{-p} N_{3n}^+ N_{3p}^+ \right.$$

$$+ K_{BB}^{-n} N_{4n}^+ N_{4p}^+ - K_{BS}^{-n}(N_{4n}^+ N_{5p}^+ + N_{5n}^+ N_{4p}^+) + K_{SS}^{-n} N_{5n}^+ N_{5p}^+ + K_{VV}^{-n} N_{6n}^+ N_{6p}^+$$

$$+ K_{BV}^{-p}(-iN_{1n}^+ N_{3p}^+ - iN_{3n}^+ N_{1p}^+) - K_{SV}^{-p}(-iN_{2n}^+ N_{3p}^+ - iN_{3n}^+ N_{2p}^+)$$

$$\left. + K_{BV}^{-n}(-iN_{4n}^+ N_{6p}^+ - iN_{6n}^+ N_{4p}^+) - K_{SV}^{-n}(-iN_{5n}^+ N_{6p}^+ - iN_{6n}^+ N_{5p}^+) \right\} \qquad \text{(G.25)}$$

When we calculate $\tilde{\sigma}_{pn}^{BB}(\vec{k},t) + \tilde{\sigma}_{np}^{BB}(\vec{k},t)$, the terms including K_{BV}^{-a} and K_{SV}^{-a} cancelled each other. Finally, we obtain

$$\tilde{\sigma}_{np}(\vec{k},t) + \tilde{\sigma}_{pn}(\vec{k},t) = \frac{2\hbar^2 E_{np}^+}{\left|\left(\frac{\partial\varepsilon(k,\omega)}{\partial\omega}\right)_{\omega=i\Gamma}\right|^2}(e^{2\Gamma t} + e^{-2\Gamma t}) + \frac{2\hbar^2(E_{np}^{+-} + E_{np}^{-+})}{\left[\left(\frac{\partial\varepsilon(k,\omega)}{\partial\omega}\right)_{\omega=i\Gamma}\right]\left[\left(\frac{\partial\varepsilon(k,\omega)}{\partial\omega}\right)_{\omega=-i\Gamma}\right]^*}$$

$$\text{(G.26)}$$

where

$$E_{np}^+ = E_{np}^- = -K_{BB}^{+p}N_{1n}^+N_{1p}^+ + K_{BS}^{+p}(N_{1n}^+N_{2p}^+ + N_{2n}^+N_{1p}^+) - K_{SS}^{+p}N_{2n}^+N_{2p}^+$$

$$- K_{VV}^{+p}N_{3n}^+N_{3p}^+ - K_{BB}^{+n}N_{4n}^+N_{4p}^+ + K_{BS}^{+n}(N_{4n}^+N_{5p}^+ + N_{5n}^+N_{4p}^+)$$

$$- K_{SS}^{+n}N_{5n}^+N_{5p}^+ - K_{VV}^{+n}N_{6n}^+N_{6p}^+$$

$$E_{np}^{+-} + E_{np}^{-+} = 2\left\{ -K_{BB}^{-p}N_{1n}^+N_{1p}^+ + K_{BS}^{-p}(N_{1n}^+N_{2p}^+ + N_{2n}^+N_{1p}^+) - K_{SS}^{-p}N_{2n}^+N_{2p}^+ \right.$$

$$- K_{VV}^{-p}N_{3n}^+N_{3p}^+ - K_{BB}^{-n}N_{4n}^+N_{4p}^+ + K_{BS}^{-n}(N_{4n}^+N_{5p}^+ + N_{5n}^+N_{4p}^+)$$

$$\left. -K_{SS}^{-n}N_{5n}^+N_{5p}^+ - K_{VV}^{-n}N_{6n}^+N_{6p}^+ \right\}.$$

$$(G.27)$$

In the numerical calculations, the derivative of the susceptibility is found as a complex number, then the denominator of the second term becomes

$$\left[\left(\frac{\partial\varepsilon(k,\omega)}{\partial\omega}\right)_{\omega=i\Gamma}\right]\left[\left(\frac{\partial\varepsilon(k,\omega)}{\partial\omega}\right)_{\omega=-i\Gamma}\right]^* = i^2 \left|\left(\frac{\partial\varepsilon(k,\omega)}{\partial\omega}\right)_{\omega=i\Gamma}\right|^2. \quad (G.28)$$

Therefore, if we define the K^{-a} integrals positive as in Eq. (4.78), we can obtain the spectral intensity of density correlations for all cases as follows

$$\tilde{\sigma}_{ab}(\vec{k},t) = \hbar^2 \frac{E_{ab}^+(\vec{k})}{|[\partial\varepsilon(\vec{k},\omega)/\partial\omega]_{\omega=i\Gamma_k}|^2}(e^{+2\Gamma_k t} + e^{-2\Gamma_k t}) + \frac{2\hbar^2 E_{ab}^-(\vec{k})}{|[\partial\varepsilon(\vec{k},\omega)/\partial\omega]_{\omega=i\Gamma_k}|^2}$$

$$(G.29)$$

where we use the following quantities,

$$E_{pp}^{\pm} = K_{BB}^{\pm p}|N_{1p}^+|^2 - 2K_{BS}^{\pm p}(N_{1p}^+N_{2p}^+) + K_{SS}^{\pm p}|N_{2p}^+|^2 + K_{VV}^{\pm p}|N_{3p}^+|^2$$

$$+ K_{BB}^{\pm n}|N_{4p}^+|^2 - 2K_{BS}^{\pm n}(N_{4p}^+N_{5p}^+) + K_{SS}^{\pm n}|N_{5p}^+|^2 + K_{VV}^{\pm n}|N_{6p}^+|^2$$

$$E_{nn}^{\pm} = K_{BB}^{\pm p}|N_{1n}^+|^2 - 2K_{BS}^{\pm p}(N_{1n}^+N_{2n}^+) + K_{SS}^{\pm p}|N_{2n}^+|^2 + K_{VV}^{\pm p}|N_{3n}^+|^2$$

$$+ K_{BB}^{\pm n}|N_{4n}^+|^2 - 2K_{BS}^{\pm n}(N_{4n}^+N_{5n}^+) + K_{SS}^{\pm n}|N_{5n}^+|^2 + K_{VV}^{\pm n}|N_{6n}^+|^2$$

$$E_{pn}^{\pm} = E_{np}^{\pm} = -K_{BB}^{\pm p}(N_{1p}^+N_{1n}^+) + K_{BS}^{\pm p}(N_{2p}^+N_{1n}^+ + N_{1p}^+N_{2n}^+) - K_{SS}^{\pm p}(N_{2p}^+N_{2n}^+)$$

$$- K_{VV}^{\pm p}(N_{3p}^+N_{3n}^+) - K_{BB}^{\pm n}(N_{4p}^+N_{4n}^+) + K_{BS}^{\pm n}(N_{4p}^+N_{5n}^+ + N_{5p}^+N_{4n}^+)$$

$$- K_{SS}^{\pm n}(N_{5p}^+N_{5n}^+) - K_{VV}^{\pm n}(N_{6p}^+N_{6n}^+). \quad (G.30)$$

CURRICULUM VITAE

PERSONAL INFORMATION

Surname, Name: Acar Çakırca, Fatma
Nationality: Turkish (TC)
Date and Place of Birth: 23.11.1985, Bursa
Phone: 0 312 210 4331
e-mail: fatmacar@gmail.com

EDUCATION

Degree	Institution	Year of Graduation
M.S.	METU Physics	2011
B.S.	METU Physics Education	2009
High School	Ulubatlı Hasan Anatolian High School	2003

WORK EXPERIENCE

Year	Place	Enrollment
2011-2017	METU Department of Physics	Research Assistant

PUBLICATIONS

1. F. Acar, S. Ayik, O. Yilmaz and A. Gokalp, Phys. Rev. **C 92** (2015) 034605.
2. O. Yilmaz, S. Ayik, F. Acar and A. Gokalp, Phys. Rev. **C 91** (2015) 014605.
3. O. Yilmaz, S. Ayik, F. Acar, S. Saatci, A. Gokalp, Eur. Phys. J. **A 49** (2013) 33.

4. S. Ayik, O. Yilmaz, F. Acar, B. Danisman, N. Er and A. Gokalp, Nucl. Phys. **A** **859** (2011) 73.